UNIVERSITAT DE BARCELONA

New immunotherapeutic strategies in acute leukemia

Néstor Tirado Cabrera

Programa de Doctorat en Biomedicina

Universitat de Barcelona

New immunotherapeutic strategies in acute leukemia

Néstor Tirado Cabrera

Director
Pablo Menéndez Buján

Director
Diego Sánchez Martínez

Tutora
Neus Agell i Jané

Josep Carreras
LEUKAEMIA
Research Institute

UNIVERSITAT DE BARCELONA

2024

Aquesta tesi s'ha realitzat a l'Institut Josep Carreras
sota la supervisió dels Drs. Pablo Menéndez Buján i Diego Sánchez Martínez

Finançada per una ajuda de Formació de Profesorat Universitari (FPU19/00039)
del Ministerio de Ciencia, Innovación, y Universidades

Gracias a Pablo, a Diego,
a todo el Menéndez lab.
Gracias a las amigas.
Gràcies al Patxi i al seu llimoner, als falciots.
Gracias a Paco y Ani, por todo.

Abbreviations

ALL	Acute lymphoblastic leukemia
alloHSCT	Allogeneic hematopoietic stem cell transplantation
AML	Acute myeloid leukemia
APC	Antigen-presenting cell
BCR	B cell receptor
BiTE	Bispecific T cell engager
BM	Bone marrow
CAR	Chimeric antigen receptor
CCL25	C-C chemokine ligand 25
CCR9	C-C chemokine receptor 9
CD	Cluster of differentiation
CD4ISP	$CD4^+$ immature single positive (T cells)
CD4SP	$CD4^+$ single positive (T cells)
CD8SP	$CD8^+$ single positive (T cells)
CDR	Complementarity-determining region
CLP	Common lymphoid progenitor
CTL	Cytotoxic T lymphocyte
DN	$CD4^-$ $CD8^-$ double negative (T cells)
DOT	Delta One T cell
DP	$CD4^+$ $CD8^+$ double positive (T cells)
EGIL	European Group for the Immunological Characterization of Leukemias
ETP-ALL	Early T cell precursor acute lymphoblastic leukemia
Fab	(Immunoglobulin) antigen-binding fragment
Fc	(Immunoglobulin) constant fragment
FcR	Fc receptor
GvHD	Graft vs. host disease
GvL	Graft vs. leukemia
HSCT	Hematopoietic stem cell transplantation
HLA	Human leukocyte antigen
HSCs	Hematopoietic stem cells
HSPCs	Hematopoietic stem and progenitor cells
IFN	Interferon
Ig	Immunoglobulin
IL	Interleukin
mAb	Monoclonal antibody

MHC	Major histocompatibility complex
NK cell	Natural killer cell
PB	Peripheral blood
PBMCs	Peripheral blood mononuclear cells
pMHC	Peptide-MHC complex
scFv	Single chain variable fragment
TAA	Tumor-associated antigen
T-ALL	T cell acute lymphoblastic leukemia
TCE	T cell engager
TCR	T cell receptor
T-LBL	T lymphoblastic lymphoma
TRAC	T cell receptor alpha constant
V_H and **V_L**	(Immunoglobulin) heavy (V_H) and light (V_L) chain regions

Table of contents

1. Introduction

1.1. The immune system

The immune system is constituted by different cell types and molecules that mediate the immune response, a highly coordinated response to the introduction of foreign agents and substances. This response is mediated by the sequential and coordinated action of innate and adaptive immunities, respectively. In recent years, the widely-accepted classical division of innate vs. adaptive immunity has been revised, since there is a strong interplay between the two, and some immune cell types (as γδ T cells) serve a role in both of them[1].

Innate immunity is mediated by rapid and non-specific mechanisms in place before lesions occurs. Its main components include (i) physical/chemical barriers (e.g. epithelia), (ii) some immune cells (e.g. macrophages, dendritic cells, granulocytes, and natural killer (NK) cells), and (iii) proteins and other molecules orchestrating the immune response (e.g. the complement system and interferons).

Adaptive immunity, on the other hand, is comprised of B and T lymphocytes and their products, and confers an extraordinarily specific and potent response, stimulated by successive exposure to a particular antigen in a process known as immunologic memory.

Adaptive immunity can be in its turn divided into humoral and cell-mediated immunity, mediated by different types of lymphocytes to neutralize and eliminate different types of foreign agents. Humoral immunity is mediated by antibodies, produced by B cells, that recognize and bind to extracellular microbes and toxins to neutralize them and assist in their elimination. B lymphocytes that recognize antigens proliferate and differentiate into plasma cells, producing different immunoglobulin classes. Cell-mediated immunity or simply cellular immunity is mediated by T cells, capable of recognizing cells infected by intracellular microbes, like viruses, and can kill the host cell to eliminate the parasite or help orchestrate the immune response from other cell types[2].

1.2. Lymphocytes

Lymphocytes are the unique cells responsible for adaptive immunity[3,4]. Lymphocytes can recognize a wide variety of antigens with extreme specificity. This recognition is clonally distributed, meaning that each lymphocyte and its daughter cells (i.e. clones) can only recognize one antigen, and the bulk of all lymphocytes in the body that constitutes the diverse repertoire[5,6].

The are two major types of lymphocytes: B cells and T cells. Although they may serve very different functions in the immune response, they are morphologically very similar, and their development shows genetic parallels behind their extreme diversity of antigen specificity[1].

Hematopoietic stem cells (HSCs) in the bone marrow give rise to all blood cells, including the cells of the immune system. HSCs differentiate into common lymphoid progenitors (CLPs), which can in turn develop into B cells, T cells, and NK cells, among others (**Figure 1**). CLPs then go into their respective primary lymphoid organs (bone marrow and thymus for B and T cells, respectively)[7,8]. Mature naïve lymphocytes leave their maturation niches through the blood and migrate to secondary lymphoid organs and tissues, where they may be exposed to their cognate antigens and further differentiate into effector lymphocytes to perform their immune function[9,10].

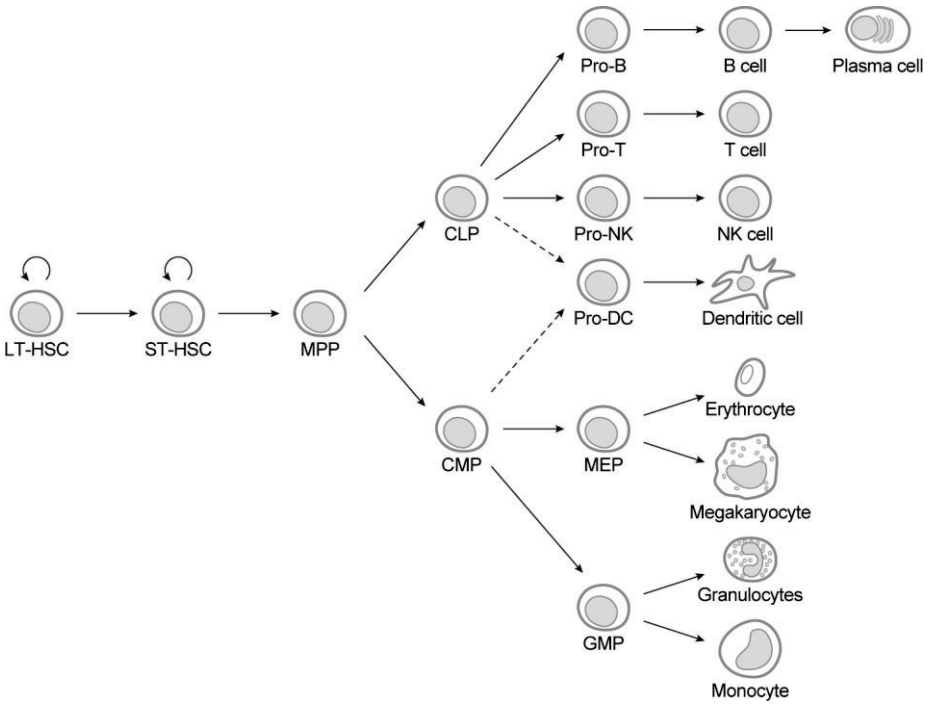

Figure 1. Hematopoietic cellular hierarchy. Hematopoiesis originates from hematopoietic stem cells (both long-term, LT; and short-term, ST). HSCs self-renew and give rise to multipotent progenitors (MPPs), which in turn differentiate into common lymphoid and myeloid progenitors (CLPs, CMPs). CLPs generate all lymphoid lineage cells, while CMPs generate myeloid cells through intermediary megakaryocyte/erythrocyte (MEPs) and granulocyte/monocyte progenitors (GMPs).

A fundamental event during lymphocyte development is the rearrangement of the antigen receptor genes: the immunoglobulin (Ig) and the T cell receptor (TCR) genes for B and T cells, respectively. In any individual there are up to 10^9 different B and T cell clones, each with a unique receptor and specificity. This extremely diverse repertoire is not explained through somatic (germline) genes, but through combinatorial selection of a small set of genes, organized in different loci and clusters[11].

Antigen receptors are generated by the recombination of different variable region (V) gene segments with diversity (D) and joining (J) gene segments, in a process known as V(D)J recombination (**Figure 2**). Rearrangement is irreversible, as unused segments are excised from genomic DNA. To increase the diversity even more, a lymphoid-specific enzyme called terminal deoxynucleotidyl transferase (TdT) adds random nucleotides to the DNA breakpoints during recombination[12,13].

After V(D)J recombination the pool of immature lymphocytes is positively and negatively selected. Positive selection occurs for lymphocytes with productive V(D)J rearrangements, and in the case of T cells, with TCRs capable of interacting with major histocompatibility complex (MHC) molecules. Negative selection occurs for lymphocytes with self-antigen reactivity or too-high avidity receptors, which will undergo apoptosis to prevent autoimmunity.

Lymphocytes are continuously circulating through the blood and lymphatic vessels to secondary lymphoid organs and other tissues. When a mature naïve (non-antigen-exposed) lymphocyte leaves its primary lymphoid organ it homes to the spleen, lymph nodes, and mucosal lymphoid patches. If the lymphocyte does not recognize its cognate antigen, it will leave through the lymphatic system and back into the bloodstream, to repeat the cycle again. This phenomenon, known as lymphocyte recirculation, maximizes the chances that a small number of lymphocytes with specificity to one

particular antigen will encounter it wherever in the body it may be. Once the lymphocytes encounter their antigen they will proliferate and differentiate into their effector and memory phenotypes[14–17].

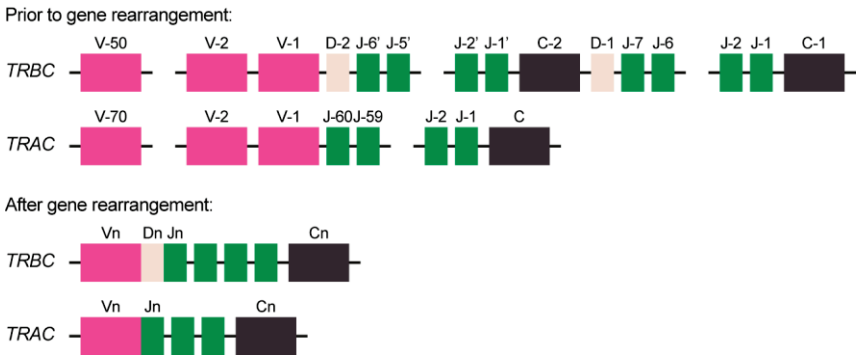

Figure 2. Somatic rearrangement of variable (V), diversity (D) and joining (J) genes encoding antigen receptors. To generate the repertoire diversity needed for adaptive immunity, the loci encoding for the T cell receptor and immunoglobulins undergo multiple rearrangements to form the mature chains. For the TCRβ and γ and immunoglobulin heavy chains, DNA recombination occurs between a V, a D, and a J gene segment to create, along with a constant fragment, the final mature antigen receptor. For the TCRα and δ and immunoglobulin light chains, recombination takes place only between a V segment and a J segment. In successfully recombined lymphocytes, additional J segments are removed during transcription and the different chains of the TCR/Igs assembled after translation.

1.2.1. B lymphocytes

The antigen receptor of B lymphocytes is the B cell receptor (BCR): a variable, specific, and clonally distributed antigen receptor. The BCR consists of a transmembrane antibody molecule (either IgM or IgG) associated with invariant signaling proteins to activate the B cell upon antigen binding and receptor cross-linking[18,19].

When naïve B cells are activated, they proliferate and differentiate into antibody-secreting plasma cells, which produce and release large amounts of soluble immunoglobulins to initiate the humoral immune response, neutralizing their antigen and facilitating their elimination. Some activated B cells live on as memory lymphocytes in secondary lymphoid organs (e.g. lymph nodes and spleen), thus expanding the clone of antigen-reactive lymphocytes and contributing to immunologic memory for future exposures[20].

1.2.2. Antibodies

Antibodies, also commonly known as immunoglobulins (Ig), are circulating proteins with extremely high affinities to their cognate antigens. There are several Ig classes or isotypes, but they all share a common structure. Antibodies are composed of two identical heavy chains and two identical light chains, bound by several disulfide bonds. Both the heavy and light chains consist of a series of repeated independent conserved structural domains known as Ig domains[21].

Two regions may be distinguished within immunoglobulin chains: the constant (C) and variable (V) regions. The constant region is relatively conserved among isotypes, whereas the variable region contains three hypervariable sequences known as complementarity-determining regions (CDR1-3).

These CDRs, surrounded by the conserved sequences of the framework regions, form loops that interact directly with their epitope (the part of the antigen that is recognized by the immune system), and are responsible for antibody specificity[22,23].

The V region of a heavy chain (V_H) and its associated light chain (V_L) form an antigen-binding site. Because of the symmetric structure of antibodies, each antibody molecule contains two identical antigen-binding sites. The C region of the immunoglobulin heavy chains form the constant fragment (Fc), involved in effector functions, capable of recruiting other agents of the immune system like the complement proteins or phagocytes through their Fc receptors (FcRs)[24] (**Figure 3**).

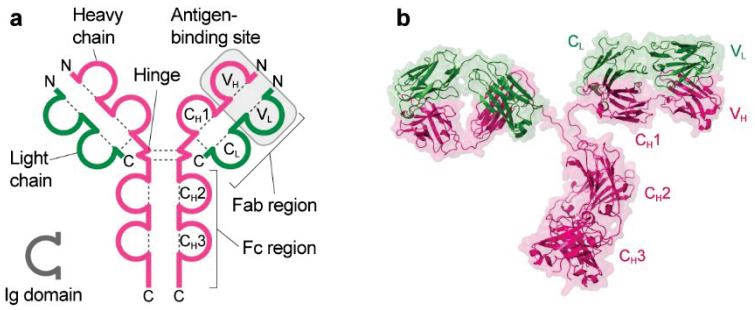

Figure 3. Structure of an antibody molecule**.** (**a**) Schematic diagram of a secreted immunoglobulin G (IgG) molecule. The antigen binding sites are formed by the pairing of the V_H and V_L domains. (**b**) Protein structure of a murine IgG2a molecule as revealed by X-ray crystallography (PDB 1IGT).

The different Ig isotypes present in humans are IgA, IgD, IgE, IgG, and IgM, where IgA and IgG may be subdivided into further subclasses (IgA1-2, IgG1-4). These isotypes differ in the heavy chain of their constant region (C_H), named after the Greek letter corresponding to the isotype, the length of which varies among isotypes. Furthermore, some Ig classes are secreted in a multimeric form: IgA mainly as a dimer and IgM as a pentamer[23].

There are also two classes of light chains, κ and λ, with different constant regions. In humans, about 60% of antibody molecules bear κ chains and 40% λ chains. Although there are no known functional differences among these two subtypes they may be used to detect B cell malignancies as the clonal nature of the tumor will lead to marked changes in this ratio[25].

Different isotypes differ on their Fc regions, and as most of the effector functions of antibodies are mediated by their binding to their corresponding FcRs, they will differ in what receptors they bind to and what effector functions they will perform[26].

Monoclonal antibodies (mAbs) are all antibodies derived from a single B cell clone, meaning they share the same specificity. mAbs were first identified in the serum of myeloma (plasma cell tumors) patients. A technique to obtain mAbs was developed by Köhler and Milstein in 1975, proving to be one of the most valuable and versatile tools in biomedical sciences and earning them the medicine Nobel prize. This method consists of the fusion of splenocytes (B cells) from a previously immunized animal (typically a mouse or a rabbit) with an immortal myeloma cell line, maintained in a selective media that only allows for the growth of fused hybridoma cells. Hybridoma cells are then subcloned and each clone is tested for reactivity to the immunogen of interest[27].

1.2.3. T lymphocytes

Thymus-derived (T) lymphocytes play an essential role in the elimination of intracellular pathogens and cells that have undergone malignant transformation. Two major subsets can be defined based on their expression of cluster of differentiation (CD) markers CD4 and CD8[28].

$CD4^+$ T cells, also known as helper T cells, act as orchestrators of the immune response, secreting a number of cytokines and factors that act on various other cells of the immune system, including other T cells, B cells, and macrophages. $CD4^+$ T cells may be further divided into subsets, including Th1, Th2, and Th17, depending on their cytokine production profile. On the other hand, $CD8^+$ T cells or cytotoxic T lymphocytes (CTLs) can recognize and kill cells infected with viruses and intracellular parasites, as well as cells that have undergone malignant transformation. Finally, another type of T cells are $CD4^+$ regulatory T cells (Tregs, with a $CD4^+FOXP3^+CD25^{high}$ phenotype), cells with potent immunosuppressive functions to modulate the immune response and to avoid autoimmunity[28,29].

During T cell development, the thymus provides all sorts of stimuli required for the proliferation and maturation of developing T cells, also known as thymocytes. CLPs get into the thymus through the thymic cortex, progressively committing to the T lymphoid lineage and finally undergoing V(D)J TCR rearrangements and positive and negative selection. The migration of these T cell progenitors into and through the thymus is driven by the chemokine receptor CCR9, which provides tropism for its ligand CCL25, strongly expressed in the thymic epithelia[8,30].

Unlike the BCR and antibodies, which recognize antigens in their natural 3D conformation, the TCR can only recognize antigens, usually peptides, presented by highly polymorphic MHC molecules. The association of a peptide and its presenting MHC molecule is referred to as a pMHC complex[31].

There are two classes of MHC molecules: class I and II (or MHC-I and MHC-II, respectively). Under normal conditions, all cells express MHC-I, which presents peptides originating from proteasomal degradation of intracellular proteins. MHC-I may present "non-self" viral peptides, or neo-antigenic peptides (antigens that arise after malignant transformation and aberrant protein expression), thus eliciting a cytotoxic $CD8^+$ response[31–33].

MHC-II, on the other hand, is only expressed by antigen-presenting cells (APCs), a group of cells that includes dendritic cells, B cells, macrophages, thymic epithelial cells, and a few other cell types. APCs' MHC-II can present peptides from the extracellular milieu that are internalized and processed via lysosomal degradation. This presentation can activate a $CD4^+$ T cell response to orchestrate an immune response against extracellular microbes[31,34].

The TCR is a heterodimer of two transmembrane chains, designated TCR α and β (or less commonly γ and δ), covalently linked by disulfide bonds. Each chain consists of an Ig-like N-terminal V domain, an Ig-like C domain, a hydrophobic transmembrane region, and a short intracellular tail. The V region of both TCR chains contain the three hypervariable CDRs, recognizing pMHC complexes[35,36].

Similar to the naïve BCR, the TCR requires additional molecules to transduce the signal cascade leading to T cell activation. The TCR complex is composed of the TCR chains themselves and a series of CD3 proteins: one heterodimer of CD3 γε, one heterodimer of CD3 δε, and one homodimer of CD3 ζζ, all of which contain sites available for tyrosine phosphorylation by coreceptors CD4/CD8-associated SRC-family kinases (**Figure 4**).

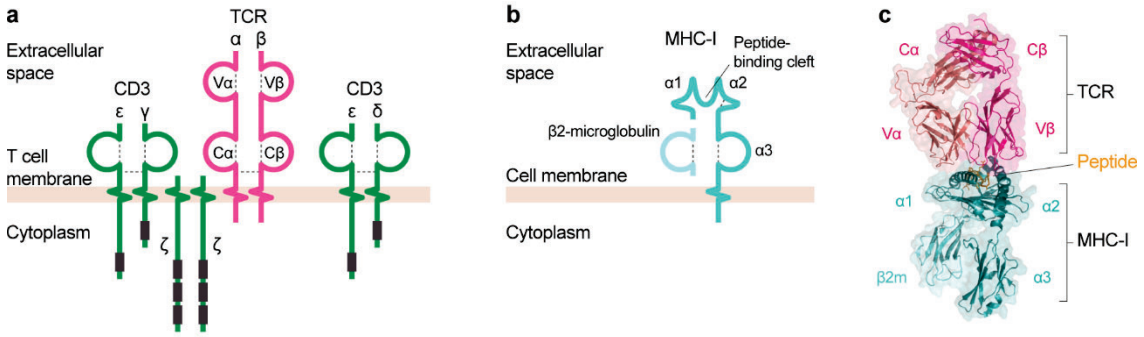

Figure 4. Structure of the T cell receptor and the major histocompatibility complexes. (**a**) Schematic diagram of the TCR complex. Activating phosphorylation sites are indicated in dark. (**b**) Schematic diagram of an MHC class I molecule. Peptides are presented in a cleft between α helixes 1 and 2. MHC-I consists of one polypeptide chain stabilized by β-microglobulin. (**c**) X-ray crystallography of a TCR-pMHC-I interaction (PDB 3RGV).

CD4 and CD8 coreceptors, like the TCR and CD3 proteins, belong to the Ig superfamily. They bind to invariable regions of MHC molecules and facilitate signaling by the TCR complex. Mature (αβ) T cells express either CD4 or CD8, not both. CD4, a monomeric protein expressed on a subset of T cells and also at lower levels by monocytes and some dendritic cells, is a coreceptor for MHC-II. CD8, expressed in some T cells and some NK cells, can exist as CD8αβ heterodimers or the rarer CD8αα homodimers, and is a coreceptor for MHC-I.

When the TCR complex recognizes MHC-presented peptides, be it an antigen-presenting cells or any other cells presenting intracellular peptides through MHC-I, several other T cell proteins are rapidly recruited to the site of contact, forming a bullseye-shaped supramolecular activation cluster known as the immune synapse, enriched in costimulatory proteins such as CD28 or 4-1BB, as well as enzymes, adaptor molecules, and integrins on the periphery that stabilize the synapse[37,38].

The immune synapse enhances the binding of the TCR to MHC molecules and allows the assembly of all the signaling machinery of the T cells. It also maintains the contact between the effector T cell and the target cell in the case of cytotoxic $CD8^+$ T cells, ensuring the delivery of secretory granules containing perforin and granzymes into the target cell for its elimination. The synapse is a region of high protein turnover, with the degradation of the signaling molecules contributing to the termination of T cell activation[39,40].

1.2.3.1. αβ T cells

Thymocytes follow a precise order for TCR rearrangement and CD4 and CD8 coreceptor expression during T lymphopoiesis. The most immature thymocytes, early T cell progenitors (ETPs) are not fully committed to the T lineage and still retain myeloid potential. These earlier cells do not express CD4 or CD8, and are aptly known as double negative (DN) thymocytes[41,42].

As cells move through the thymic cortex towards the medulla, at the pro-T stage, they commit to the T lineage and start expressing the recombinases (recombination activating genes, RAG1 and RAG2) needed for TCR gene rearrangement. Most of these thymocytes develop into αβ T cells. The TCRβ chain is the first to recombine, but because of random nucleotide addition and removal during rearrangement, many of the thymocytes will have a frameshift and non-productive protein, leading to negative selection and cell death, in a process known as β selection[42].

At the pre-T stage, the newly formed TCRβ in DN T cells couples with pre-Tα chain, an invariant surrogate chain that along with the β chain and CD3 molecules forms the pre-TCR complex. The pre-TCR signaling promotes massive proliferation and survival of developing thymocytes, as well as blocking the rearrangement of the TCRβ on the unrearranged locus. At this point, thymocytes gain the sequential expression of CD4 ($CD4^+$ immature single positive, CD4ISP) and CD8, becoming double positive (DP) T cells[43,44].

A second wave of recombinase expression in DP T cells promotes TCRα locus recombination and the formation of the final TCRαβ. Because the TCRδ locus is located within the α locus, after T cells successfully rearrange the α genes, δ genes are excised, and they can no longer become γδ[44].

DP cells enter the medulla and encounter medullary thymic epithelial cells (mTECs), dendritic cells, and macrophages, all of which express MHC class I and II molecules. The movement of thymocytes into the medulla is mediated by the chemokines CCL21 and CCL19, which bind to CCR7, expressed in immature and naïve T cells. Thymocytes whose TCRs are able to weakly interact with self MHC molecules will be stimulated, survive and differentiate into single positive $CD4^+$ and $CD8^+$ T cells (CD4SP, CD8SP) for MHC-II and -I, respectively[45,46]. Thymocytes whose TCRs do not recognize any MHC will die by apoptosis[44] (**Figure 5**).

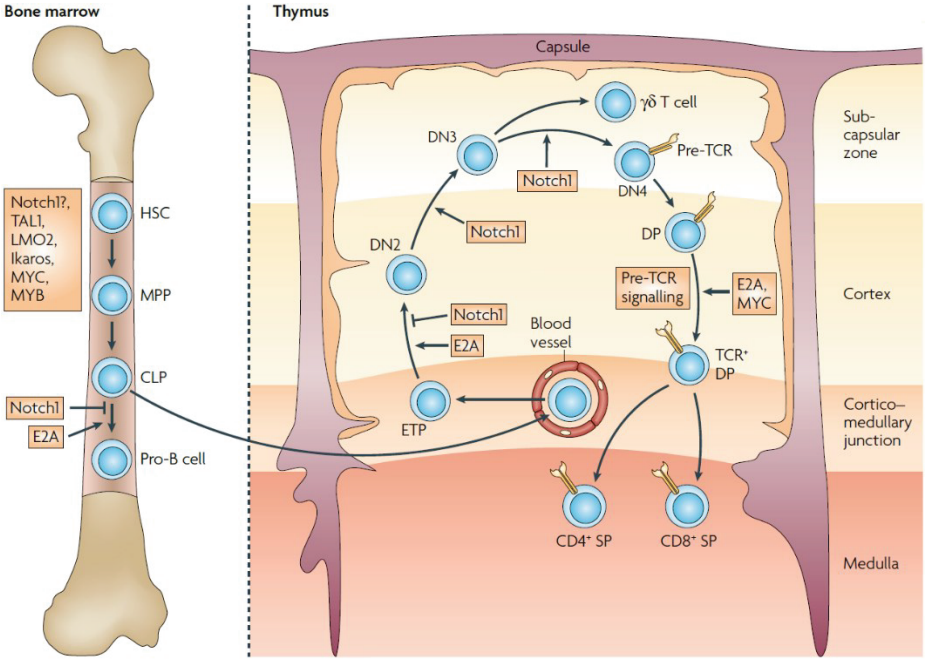

Figure 5. Stages of T cell development. Bone marrow hematopoietic stem cells (HSCs) exit the niche and differentiate into multipotent progenitors (MPPs), which further commit to the lymphoid lineage generating common lymphoid progenitors (CLPs). These migrate into the thymus as early T cell progenitors (ETPs) and irreversibly commit to the T lineage, progressing through several double negative (DN; $CD4^-CD8^-$) stages. After a successful recombination of the TCRβ locus, pre-T cells acquire surface expression of the pre-TCR, promoting differentiation to a double positive (DP) stage, at which point they undergo processes of positive and negative selection. Mature selected cells exit the thymus as single positive (SP) $CD4^+$ or $CD8^+$ T cells. Major signaling pathways and transcription factors at each step are indicated. Adapted from Aifantis *et al.*, 2008[47].

mTECs participate in negative selection through the low level expression of self-antigens that would not be present in the thymus otherwise, to eliminate self-reactive TCRs and prevent autoimmunity. Some of these self-reactive $CD4^+$ T cells may survive apoptosis and become Tregs[48,49].

Finally, mature naïve single positive T cells are able to leave the thymus and go into the bloodstream to start the lymphocyte (re)circulation process[10,50].The life cycle of T cells begins with mature naïve T cells. Naïve T cell responses to an antigen result in the generation of memory T cells specific to that same antigen, which survive for longer periods of time (they can last for years or even a lifetime) and are able to respond more rapidly to repeated antigen exposures. These undifferentiated T cells are characterized by CCR7 and CD62L (adhesion molecule L-selectin) expression, homing to lymph nodes. The effector capabilities of memory cells are limited, but they proliferate greatly and generate many effector cells upon activation.

Effector phenotype T cells lose CCR7 and CD62L, lacking lymph node tropism and remaining in the site of antigen stimulation instead. Effector T cells or terminally differentiated T cells readily produce cytokines like IFN-γ and become greatly cytotoxic[51,52] (**Figure 6**).

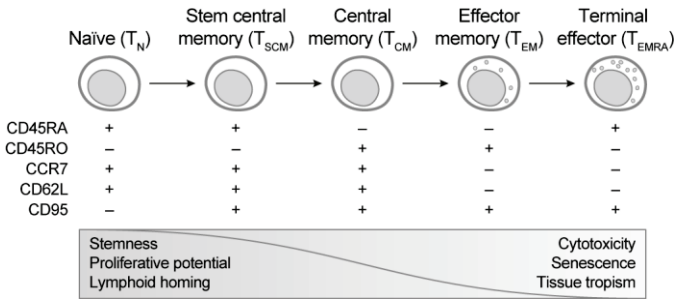

Figure 6. Model of T cell differentiation. After antigen priming naïve T cells progressively differentiate into diverse memory subpopulations, and ultimately into terminally differentiated effector T cells. T cell subsets may be distinguished by the combinatorial expression of the indicated surface markers. Along differentiation, T cells gain and lose several functional attributes. Adapted from Gattinoni *et al.*, 2017[52].

Strong, persistent T cell activations, like those elicited by chronic viral infections, lead to exhaustion, characterized by the gradual extinguishing of effector responses: decreased proliferative capacity, cytokine production, cytotoxic activity, etc. Exhaustion is associated with an increased expression of immune checkpoints like PD-1, CTLA-4, TIM-3, LAG-3, and others[53,54].

1.2.3.2. γδ T cells

γδ T cells, often termed “innate-like”, display properties of both the innate and the adaptive immune systems, and play critical roles in immune regulation, tumor surveillance, and primary responses.

Because γδ thymocytes are not positively selected for MHC recognition, they are MHC-unrestricted (and mostly negative for CD4 and CD8 coreceptors), meaning they recognize their cognate antigens regardless of MHC haplotype. Furthermore, the TCRγδ recognizes non-canonical antigens, often lipidic in nature, presented by MHC-analogue proteins[33,55].

γδ T cells amount to 1-5% of circulating T cells in humans, although the numbers are much greater in other species[56]. Although they serve different functions than their αβ counterparts, they originate

from the same common DN precursors. TCRγδ loci rearrangements do not follow a rigid order like for αβ thymocytes: If a thymocyte can successfully rearrange both γ and δ loci before a productive TCRβ rearrangement, it will commit to the γδ lineage[44,57].

There are fewer gene segments in the TCRγ and δ loci than in the a and b counterparts, leading to a relatively less diverse TCR repertoire. There are three V gene segments in the human δ locus: Vδ1 through Vδ3, and γδ T cells are often classified based on their V gene usage[58,59].

Vδ1$^+$ T cells are mostly tissue-resident and tumor-infiltrating, and can be found in epithelia, dermis, spleen, and liver. They have a very potent antitumor activity. Vδ2$^+$ (most commonly paired with Vγ9) T cells, on the other hand, are the most abundant γδ subtype in the blood. Vδ3$^+$ T cells have been less studied, and their functions are not well defined[58,60].

Tumor cell recognition by γδ T cells is attributed not only to TCR engagement but also on natural cytotoxicity receptors (NCRs), invariant receptors of stress ligands upregulated in transformed cells, typically present in NK cells, and the direct killing of the tumor cells. γδ T cells also produce high levels of interferon γ (IFN-γ) and tumoral necrosis factor α (TNF-α), promoting MHC-I expression by cancer cells and facilitating bystander T cell engagement[58,59,61].

Because of their MHC-unrestriction, they can be used in an allogeneic manner and do not need to be haplotype-matched, making them very attractive for immunotherapies. It is paradoxical that most clinical applications of therapeutic γδ T cells have been focused on Vδ2$^+$ T cells, surely given how easily they can be expanded by phosphoantigen stimulation (usually with zoledronate), as Vδ1$^+$ T cells often outperform them in antitumoral capacity[61].

Recently, protocols to grow Vδ1$^+$ T (Delta One T, DOT) cells from peripheral blood under two-week cytokine stimulation have been developed[62,63]. Due to their potent antitumor activity and allogeneic promise, they are being tested in relapse/refractory (R/R) acute myeloid leukemia (NCT05886491).

1.3. Acute leukemias

Leukemias develop from serial acquisition of somatic mutations in hematopoietic progenitor cells, known as blasts, with the capacity to self-renew and propagate the clone. Acute leukemias include a very heterogeneous group of hematological malignancies that infiltrate the bone marrow, blood, and other secondary organs, leading to the displacement of healthy hematopoiesis and subsequent cytopenias. Three broad types of acute leukemias may be distinguished, based on the morphologic and phenotypic assessment of the blasts: acute myeloid leukemia (AML), B cell acute lymphoblastic leukemia (B-ALL), and T cell acute lymphoblastic leukemia (T-ALL)[64,65].

Leukemic blasts often present with an aberrant phenotype that permits their distinction from normal precursors. Such abnormalities include the expression of markers from a different lineage[66] and the asynchronous expression of markers, not following the well-defined ordered maturation pattern of their healthy counterparts[67]. Immunophenotyping can, in some cases, be informative of the genetic lesions driving the leukemia: for instance, t(8;21) AML typically presents aberrant CD19 expression, whereas CD10$^-$ B-ALL blasts are often indicative of t(4;11)[63–70].

The European Group for the Immunological Characterization of Leukemias (EGIL) first proposed a scoring system based on marker expression for acute leukemia standardized diagnosis (**Table 1**)[71],

which accounts for mixed-phenotype acute leukemias (MPAL). A score of >2 points in more than one lineage must be obtained for MPAL diagnosis.

	2 Points	1 Point	0.5 Points
Myeloid lineage	Myeloperoxidase (MPO)	CD13 CD33 CD65a	CD14 CD15 CD64 CD117
B lymphoid lineage	CD79a cIgM cCD22	CD10 CD19 CD20	TdT CD24
T lymphoid lineage	cCD3 / sCD3 TCRαβ TCRγδ	CD2 CD5 CD8 CD10	TdT CD1a CD7

Table 1. EGIL criteria for the diagnosis of mixed phenotype acute leukemia. A marker is considered positive if more than 20% of blasts stain, and a lower threshold of 10% is set for MPO, CD3, CD79a, and TdT. Adapted from Bene *et al.*, 1995.[71]

1.3.1. Acute myeloid leukemia

Acute myeloid leukemia includes a heterogenous group of genetically distinct disorders, originating from the acquisition of cytogenetic, genetic, and/or epigenetic alterations by a myeloid progenitor. AML is a hierarchical disease, where certain cells termed leukemic stem cells (LSCs) lay at the top of a clonal hierarchy and are able to give rise to bulk AML blasts invading the bone marrow and to self-renew the stem cell population. LSCs are mostly quiescent, making them intrinsically resistant to most forms of chemotherapy, and responsible for the common relapses. Parallel to healthy HSCs, LSCs represent a minority of total leukemic blasts, but they are the ones responsible for initiating a secondary AML when transplanted into immune-deficient mice[72–74].

AML is the most frequent form of leukemia, with a 4.3/100,000 incidence. It is slightly more frequent in men, and the median onset age is 68 years old, with approximately 75% of the patients being older than 65 years old. Global AML incidence has been on the rise for the last decades, probably due to the global increase in life expectancy. Many chemotherapeutic agents and ionizing radiation used in oncology can also lead to the development of therapy related AML (t-AML)[75,76].

AML diagnosis requires the identification of myeloid blasts in peripheral blood (PB) or bone marrow (BM), or less commonly in non-hematological tissues. AML is defined by having ≥20% of blasts in the BM, or ≥10% if recurrent hallmark genetic abnormalities are detected. Otherwise, lower levels of blasts are classified as myelodysplastic syndromes[76].

Because of their clear, overriding impact on disease outcome, genetic alterations are given priority in AML classification. Besides conventional cytogenetics and fluorescence *in situ* hybridization for the detection of recurrent genetic abnormalities, next generation molecular testing for mutations and rearrangements are recommended for proper risk assessment[64].

Although cytogenetics and other factors allow for risk stratification, on the whole AML has a dismal prognosis, with cure rates of around 40% in patients under 60 years and only 15% in older patients. Although the general therapeutic strategy has barely changed in the past three decades, some new drugs and combinations (like midostaurin and novel FLT3 inhibitors) have recently been introduced. Younger fit patients usually receive intensive chemotherapy regimens and allogeneic hematopoietic stem cell transplantation (alloHSCT) after disease remission[77].

AlloHSCT is a major cornerstone of AML treatment: its effects rely not only on the ability to administer higher doses of chemotherapy without bone marrow toxicity being a limiting factor, but also on the immune rejection from grafted allogeneic T cells of residual AML blasts[78]. However, alloHSCT comes with high morbi-mortality: the leading causes of death after alloHSCT are disease relapse, infections, and graft vs. host disease[79]. Despite this, relapse occurs in most patients with AML within 3 years after initial diagnosis, and achieving durable responses remains a challenge[75].

1.3.2. B cell acute lymphoblastic leukemia

Acute lymphoblastic leukemia comprises multiple entities with a wide range of genetic alterations, including aneuploidy (most common alteration), chromosomal rearrangements that deregulate gene expression or produce chimeric fusion proteins, deletions and gains of DNA, and mutations. Many of these alterations affect processes like the transcriptional regulation of lymphoid development and differentiation, cell-cycle regulation, and signaling pathways. Based on the cell of origin, it can be broadly classified into B-ALL or T-ALL, originating from B and T cell precursors, respectively[65].

ALL is the most common pediatric cancer, accounting for nearly a quarter of total cases of pediatric cancer. It is a predominantly pediatric disease, with an incidence of about 3 in 100,000 (depending on ethnicity) and a peak occurring at 3-to-5 years of age. Just like AML, it is slightly more common in males, and some genetic predispositions (most prominently Down's syndrome) are associated with an increased risk of developing ALL. B-ALL is the most common form of ALL, comprising up to 85% and 75% of total pediatric and adult ALL cases, respectively[65,81].

In B-ALL, the existence and relevance of LSCs is not clear: several works describe subpopulations of more immature ($CD34^+CD19^-$) phenotypes in primary samples, but it has also been suggested that most leukemic subfractions are able to propagate leukemia in the appropriate experimental setting, questioning the existence of a strict hierarchy in ALL[82–84].

Chromosomal rearrangements are considered to be early initiating events in leukemogenesis. Some of these translocations can be detected in pre-leukemic stages, sometimes years before the start of the clinical manifestations. There are two types of rearrangements. In the first class, oncogenes are relocated near actively transcribed genes, like the immunoglobulin genes in B-ALL and the TCR genes in T-ALL. In the second class, two genes are fused creating chimeric proteins with distinct functions and regulation than the initial proteins. This is the case of t(12;21)/*ETV6::RUNX1*, a fusion of two hematopoietic transcription factors, which is the most common translocation in B-ALL. Other significant cases are t(9;22) resulting in the formation of the Philadelphia (Ph) chromosome and the *BCR::ABL1* fusion gene, and the multiple examples of rearrangements involving the 11q23 *KMT2A* gene, formerly known as mixed-lineage leukemia (*MLL*). MLL is an epigenetic modulator involved in blood cell development, and more than 70 fusion partners have been described. *MLL*-rearranged leukemias (MLLr) make up most cases of infant ALL, before 1 year of age, and have a particularly bad outcome[65].

B-ALL survival has drastically increased in the past 50 years. The Berlin-Frankfurt-Münster regimen, introduced in the 1970s, became the backbone of most contemporary ALL therapies, which have increased the event-free and overall survivals up to 85% and 90%, respectively. Treatment schemes are based on different phases of glucocorticoids (potent immune suppressors), vincristine (mitosis inhibitor), peg-asparaginase (toxic enzyme), and anthracyclines (antitumoral antibiotics). Triple intrathecal chemotherapy, consisting of methotrexate (antifolate), cytarabine (DNA synthesis inhibitor), and hydrocortisone (glucocorticoid), is administered as a prophylaxis of central nervous system involvement[65,81]. In Ph^+ B-ALL, considered an extremely high-risk subgroup, precision therapy with tyrosine kinase inhibitors (TKis) like dasatinib that target the BCR-ABL1 oncoprotein, have increased event-free survival while reducing the need for alloHSCT[85].

Despite significant improvements in overall and disease-free survival over the last decades, there are still many cases or relapse or refractory disease, for which the most recent immunotherapeutic approaches have provided an unprecedented therapeutic opportunity[86–90], as discussed in a later section.

1.3.3. T cell acute lymphoblastic leukemia

T cell acute lymphoblastic leukemia arises from malignant transformation of thymocytes at defined crucial steps of T cell development, and the expression of certain oncogenes is linked to arrest at particular stages of normal T cell ontogeny. Attempts to characterize and isolate proper T-ALL LSC populations have failed, and different groups have reported different phenotypes of their putative leukemic-initiating cells[91–93].

Although leukemic lymphoblasts can show asynchronous gene expression with subtle variations to their healthy counterparts, likely a result of aberrant gene expression regulation, leukemic cells are often classified according to the developmental stage. T-ALL subtypes based on immunophenotype corresponding to thymocyte developmental stages were created from pro-T (T-I) up to mature (T-IV) subgroups[71,94] (**Table 2**). Cortical T-ALL (coT-ALL, T-III), defined by expression of CD1a, constitutes a distinct subgroup with improved outcome and better response[95–99].

T-ALL	cCD3	sCD3	CD7	CD1a	TdT	CD2	CD5	CD4	CD8
ETP-ALL	+	–	+	–	+/–	–	–	–	–
Pro-T (T-I)	+	–	+	–	+/–	–	–	–	–
Pre-T (T-II)	+	–	+	–	+	+	+	–/+	–
Cortical (T-III)	+	–/+	+	+	+	+	+	+	+
Mature (T-IV)	+	+	+	–	+/–	+	+	+/–	–/+

Table 2. T-ALL subtype classification based on immunophenotype, as proposed by the EGIL, also including the later described ETP-ALL entity. Adapted from Bayón-Calderón *et al.* 2020[94].

Some of the most common genetic alterations in T-ALL include tumor suppressor genes *CDKN2A/B* loss and subsequent cell cycle deregulation, and mutations in *NOTCH1* and *FBXW7*, with abnormal

signaling in a critical pathway during T cell development, present in over 60% of patients[100–102]. The chromosomal translocations occurring in T-ALL frequently juxtapose the strong regulatory elements of TCR genes with transcription factors involved in hematopoietic and T cell development. Some of these transcription factors have been associated with particular differentiation stages: *LYL1/LMO2* are commonly affected in immature leukemias, cortical leukemias express aberrant *TLX1/TLX3* and *HOXA* genes, and mature leukemias have *TAL1* activation. However, functional information on many of these alterations is lacking, and further studies are needed to assess their clinical impact[102–104].

Historically, T cell acute lymphoblastic leukemia has been less well studied than B-ALL, and it has had worse outcomes, although recently due to risk-directed intensive chemotherapy, this difference has narrowed substantially[65,105]. Compared to B-ALL patients, T-ALL patients tend to be older (peak incidence is 20-39 years old), more likely to be male (75% of patients are male, likely due to specific mutations on X chromosome tumor suppressor genes[106,107]) and black, and present with higher white blood cell counts, extramedullary and central nervous system involvement[105].

Age at diagnosis is a major prognosis factor, with pediatric and young adult patients benefiting from intensive chemotherapy achieving survival rates of around 70-80%. Many studies have shown that treatment protocols based on intensive pediatric schemes yield better outcomes for adult patients, whereas with traditional non-intensive chemotherapy survival is only around 40%[95,105,108–111].

Early T cell precursor (ETP)-ALL, a very high risk subtype, was identified in 2009[112]. ETP-ALL, arising from early T precursors that just colonized the thymus, is characterized by cCD3^{+}CD7^{+} T lineage immunophenotype, but being CD5^{low}CD1a^{-}CD8^{-} and retaining some myeloid and stem cell marker expression (CD34, CD117, CD13). Initial ETP-ALL outcome was dismal, with an even poorer overall survival than with typical T-ALL and a higher risk of remission failure or relapse[112]. Rearrangements involving the 14q32/*BCL11B* locus are a hallmark of immature myeloid/T lymphoid acute leukemias, highly sensitive to tyrosine kinase and JAK/STAT inhibition, leading to better outcomes[113,114].

T-ALL cases with ETP-like phenotypes but CD5 positivity are known as near-ETP-ALL, but whether these two entities have different clinical outcomes remains to be elucidated[115].

Current treatments regimens follow the same schemes as Ph-negative B-ALL, and the only T-ALL-specific chemotherapeutic agent available is nelarabine, a T cell-specific nucleoside analogue[116]. In ETP-ALL, recent protocols (NCT04179929) have proposed treatment schemes commonly used in AML, namely FLAG-Ida (fludarabine, ara-C, G-CSF, and idarubicin)[117]. The standard treatment for R/R T-ALL is re-induction chemotherapy and alloHSCT (for eligible patients), both of which carry high toxicities[95,118,119]. Still, long-term survival is only around 20%, highlighting the need for new effective therapies able to induce minimal residual disease responses and bridge patients to a potentially curative alloHSCT[111,120,121].

Some of the promising therapeutic strategies being evaluated in T-ALL include BH3 mimetics (pro-apoptotic agents) like venetoclax or navitoclax[122,123], epigenetic modulators like decitabine[124], tyrosine kinase inhibitors like dasatinib[125,126], and other immunotherapeutic strategies like anti-CD38 antibody daratumumab[127] or CAR-T cells.

1.4. Immunotherapy

Immunotherapy is the use of resources from the immune system to selectively treat disease, usually cancer. Although we tend to think about the immune system as a barrier to foreign, non-self agents, Ehrlich first formulated in 1909 the hypothesis that host defense may also prevent neoplastic cells

from developing into tumors[128,129]. The hypothesis could not be proven experimentally until 1957 by Burnet, who coined the concept of immune surveillance, after experiments using immunodeficient mice[130,131].

Tumor cells, especially those of high mutational burdens, often express tumor-associated antigens (TAAs). TAAs arise from genetic fusions or mutations, generating non-naturally-occurring epitopes (also called neoantigens); or from overexpression of "natural" antigens expressed only in immune-privileged tissues (e.g. the testes) or during embryonic development, and thus no immune tolerance is generated against them. Other TAAs include proteins expressed at abnormally high levels due to gene amplification (HER2 in many breast cancers), or aberrant glycoproteins due to dysregulated glycosylation in tumor cells[132–135].

Tumor antigens stimulate immune responses that prevent or limit tumor growth. The most clinically relevant immune response against tumors comes from $CD8^+$ cytotoxic T cells. Solid tumors can be classified as immunologically "hot" or "cold" based on the level of leukocyte infiltration, correlating with disease prognosis.

The cancer immunosurveillance hypothesis was later refined into the concept of cancer immune-editing, a process comprised of three phases: elimination, equilibrium, and escape. The elimination phase corresponds to the original concept of immunosurveillance: if the tumor cells are successfully eliminated, the entire process ends here[136].

In the equilibrium phase, the host immune system and the surviving tumor cells reach a dynamic equilibrium, where the immune system's suppressive action is enough to contain but not fully extinguish the neoplastic cells. This is a period of intense selective pressure on the tumor, in which highly immunogenic cancer clones are rapidly detected and eliminated by the immune system, leaving behind less immunogenic clones[136–139].

Finally, in the escape phase, these selected cancer clones outgrow the immune pressure and fully develop into a tumor. Immune evasion is, in fact, one of the hallmarks of cancer[140]. Some of the mechanisms by which cancer cells escape the immune system include:

(i) Expression of immune checkpoints (ICs): Many tumors evade antitumoral T cell responses by upregulating inhibitory molecules, that normally function to prevent autoimmunity and to modulate the immune response. Tumor cells often express PD-1 ligands in response to IFN-γ produced by T cells. Another inhibitory molecule is CTLA-4, which binds with higher affinity to the same ligands as T cell costimulatory receptor CD28 and thus acting as a competitive inhibitor. Other common ICs include LAG-3, TIM-3, and TIGIT[141,142].

(ii) Immunosuppressive tumor microenvironment: Tumoral production of transforming growth factor (TGF)-β and the presence of suppressive cell types like Tregs, M2 macrophages, and myeloid-derived suppressor cells strongly inhibit T cell activation and differentiation into pro-inflammatory phenotypes[143,144].

(iii) Failure to present tumor antigens: Downregulation of MHC-I as a result of selective pressure by $CD8^+$ T cells in the tumor microenvironment leads to lack of antigen recognition of tumor cells. However, MHC-I also acts as an inhibitory molecule to NK cell activation, so this MHC-I loss makes tumor cells good targets for NK cytotoxicity. In addition, many tumors express ligands for natural cytotoxicity ligands present in NK cells and γδ T cells[145,146].

(iv) Failure to produce tumor antigens: The strong selective pressure against one single antigen, especially common in engineered immunotherapies, can result in the survival and outgrowth

of tumor clones with reduced immunogenicity. Given the high proliferation rate of tumor cells and their genetic instability, mutations or deletions in genes encoding for target antigens are common[138,147].

Despite tumor mechanisms to evade immune responses, immunotherapeutic strategies, in all their forms, have proven to be of extreme clinical usefulness, especially (although not only) in the field of hemato-oncology. The main advantage of immunotherapy relies on harnessing the highly specificity of adaptive immunity to selectively target and eliminate the cell of interest.

1.4.1. Monoclonal antibodies

Some monoclonal antibodies directed against tumor-associated antigens have been used in cancer treatment for 20 years, and many more have been approved since or are in advanced development. Different mechanisms of action exist for therapeutic mAbs and mAb-like molecules:

(i) Simple mAbs bind to surface molecules of tumor cells, and recruit innate immune effector mechanisms through their Fc fraction. Antibody-covered tumor cells can be eliminated by complement-mediated cytotoxicity (CDC) or antibody-dependent cell cytotoxicity (ADCC), in which NK cells, macrophages and other types of leukocytes recognize tumor cells through their FcRs. This is the case of rituximab (anti-CD20) or daratumumab (anti-CD38), commonly used in the treatment of different B cell malignancies[127,148,149].

(ii) Antibody-drug conjugates (ADCs) are TAA-specific mAbs linked to a chemotherapy drug or radioisotope, allowing the targeted delivery of these therapeutic agents to tumor cells. This is the case of gemtuzumab (anti-CD33) and inotuzumab ozogamicin (anti-CD22), linked to antitumoral antibiotic calicheamicin and used for AML and B-ALL, respectively[150,151].

(iii) Neutralizing mAbs that target and block mutated or amplified signaling receptors tumor cells rely on, interfering with tumor growth and survival. Trastuzumab is a neutralizing antibody used for the treatment of HER2-positive malignancies[152].

(iv) Immune checkpoint inhibitors are neutralizing mAbs against immune checkpoint receptors or ligands, dampening immunosuppressive signals from the tumor microenvironment. mAbs like pembrolizumab and nivolumab block PD-1 in T cells, and are extensively used in many types of solid cancers[153,154].

(v) Bispecific T cell engagers (BiTEs) combine two single chain variable fragments (scFvs) with different specificities: one end is a TAA-directed antibody, whereas the other recognizes a T cell surface antigen, usually CD3. BiTEs act as immune bridges, facilitating bystander T cell engagement and the formation of immune synapses. Blinatumomab is a CD19xCD3 BiTE commonly used in B-ALL treatment, and many more, with different specificities, have been approved since or are in advanced development[155,156].

Although monoclonal antibodies have great clinical versatility, a major hindrance is that they do not create long-lasting immunity.

1.4.1.1. Antibody humanization

A limitation of the use of mAb-derived therapeutics is the animal source of the antibody itself. Most of them come from mouse immunization with the human protein of interest, but due to differences

in the protein sequence of human and murine Igs they are immunogenic, and patients may develop antibodies against the mouse antibodies known as human anti-mouse antibodies (HAMAs). HAMAs can neutralize therapeutic mAbs, blocking their function and enhancing their clearance, dampening or even completely ablating their effects and rendering patients treatment-refractory[157].

A solution to HAMAs generation is antibody humanization, which entails genetic engineering of the original murine cDNA encoding the Ig to make it more human-like. As discussed earlier, only some parts of the antibody are responsible for antigen-binding, and the rest of the polypeptide sequence simply acts as a scaffold or framework. This structural organization allows for the complementarity-determining regions of the murine Ig to be cloned or grafted into human Ig frameworks, generating a murine-human hybrid antibody that retains the antigen specificity of the original mAb but with the reduced immunogenicity of a human protein[158]. Many mAb-derived products currently being used in the clinic have been humanized, including gemtuzumab, inotuzumab, trastuzumab, and even the scFv regions of different CAR-T therapies currently in advanced development[159,88,160].

1.4.2. Adoptive cell therapy

Adoptive cell therapy (ACT) is the administration of tumor-reactive immune cells into a patient. The source of the cells can come either from the same patient (autologous), an identical twin (syngeneic), or a healthy donor with a different MHC haplotype (allogeneic).

1.4.2.1. Hematopoietic cell transplantation

Hematopoietic cell transplantation is a common procedure in the treatment of many hematological diseases, consisting on the ablation of the patient's hematopoietic system (myeloablation) and its replacement with new, healthy HSCs to repopulate the bone marrow and hematological tissues and differentiate into all blood lineages[161].

HSCs from a healthy donor can be obtained by bone marrow aspiration or from blood apheresis, after mobilizing BM-resident HSCs with colony-stimulating factors (more common nowadays, as it is less invasive). Patients receive a conditioning treatment that may include total body irradiation, chemotherapy, cyclophosphamide, and even immunotherapy to increase immunosuppression and achieve myeloablation, freeing up the bone marrow and facilitating the colonization of transplanted HSCs[162].

Because mismatches in MHC molecule haplotypes will lead to immune activation and rejection, it is important for donors and recipients to be matched. For leukemia patients, however, alloHSCT with only partial haplotype matching is usually preferred, so that there will be some immune rejection of residual leukemic (and non-leukemic) cells in the host from the transferred T cells. This is known as the graft-versus-leukemia (GvL) effect[163,164].

A common limitation to all adoptive cell therapies, and a reason for the toxicities associated with HSCT, is graft-versus-host disease (GvHD). GvHD, which courses with multi-organ failure, is caused by the immune reaction of grafted T cells with alloantigens from the host, and, if untreated, is fatal. Based on the histologic patterns of inflammation, GvHD may be classified into acute GvHD (with massive epithelial cell death and liver and gastrointestinal toxicity) or chronic GvHD (with fibrosis and atrophy of one or more organs, but without acute cell death). T cell depletion in the transferred product can prevent the development of GvHD, but it also decreases GvL effect and can affect the efficiency of engraftment[165].

HSCT is also accompanied by partial immune deficiencies and temporary cytopenias, so patients become susceptible to infections. Transplanted patients receive prophylactic antibiotics, antivirals, and antifungals, as well as immunization vaccines to create immune memory from scratch[79,166,167].

1.4.2.2. Autologous tumor-specific T cells

T cells present within solid tumors, known as tumor-infiltrating lymphocytes (TILs), often possess tumor antigen-specific TCRs, as evidenced by the pioneering works of Rosenberg and colleagues. These TILs can be harvested from a patient (usually by tumor biopsy), expanded and activated *in vitro* under cytokine stimulation, selected for tumor reactivity, and infused back into the patient[168,169].

TCR-engineered T cells (TCR-Ts) suppose a similar adoptive cell therapy currently in development. TCR-Ts are T cells that have been genetically engineered to express, instead of their natural TCR, a different TCR that is specific for a tumor antigen commonly presented by a known HLA molecule. This therapy, although effective, requires previous knowledge on individual TCR reactivities and that a tumor expresses not only the TCRs cognate antigens but also the appropriate HLA haplotype for TCR-pMHC interaction. These restrictions make TCR-T therapies extremely personalized, so that the logistics and economic cost of producing such a therapy present an obstacle for widespread accessibility[170].

Recent work has been made towards identifying public neoantigens, driver mutations in oncogenes or tumor suppressor genes that are recurrent among patients. Identification of public neoantigens along with the most frequent HLA alleles in the population will allow the creation of a library of well-documented tumor-reactive TCR for more patients, and facilitate its implementation in the clinic[134].

1.4.2.3. Chimeric antigen receptors

Chimeric antigen receptors (CARs) are genetically engineered surface membrane antigen receptors comprising an antigen recognition domain, a transmembrane domain, and a series of intracellular stimulating domains, so that transgenic effector cells (usually CAR-T cells) get activated upon target antigen recognition.

Eshhar and co. first described, in the early 1990s, chimeric T cell receptors fusing the variable region (scFv) of an anti-tumor antibody with the signaling motifs of the TCR complex, particularly the CD3ζ chain[171,172]. Further iterations and improvements to CAR design were made by the work of Sadelain, Brentjens, June, and many others, until the first FDA approval of CAR-T cells in 2017: CD19-directed CAR-T cells for the treatment of R/R B-ALL[86,88,173]. Additional CAR-T therapies have been approved since, all for B cell malignancies (B-ALL, multiple myeloma, B cell lymphomas) targeting either CD19 or B cell maturation antigen (BCMA).

Despite fantastic initial responses of CAR-T therapies, with a complete response rate of 85%, half of the patients show disease progression after just one year[89]. Many cases of disease relapse occur because of low CAR-T cell persistence, or antigen down-regulation/loss in leukemic blasts[174]. For instance, loss of the CD19 antigen has been observed in 30-70% of patients with disease relapse after CD19 immunotherapy[175]. Besides the desired tumor cell elimination, these therapies cause B cell aplasia, and patients have to receive periodical immunoglobulin transfusions from healthy donor plasma to restore humoral immunity[176].

No CAR-T therapies have been approved as a first line of treatment. Instead, they are currently used as a second or even third line, in relapse/refractory disease. T cells from patients are harvested by

leukapheresis, modified using viral vectors to express the CAR, expanded *ex vivo*, and after passing a quality control are administered back into the patients.

Before CAR-T infusion, patients receive a lymphodepleting conditioning therapy, usually fludarabine and cyclophosphamide or bendamustine, to enable better *in vivo* expansion and engraftment of the transferred T cells[177,178].

One of the major adverse effects in CAR-T therapy is cytokine release syndrome (CRS), also known as cytokine storm. This adverse reaction occurs soon after adoptive cell transfer, especially in those patients with a high tumor burden, due to a massive CAR-T cell activation upon encountering tumor cells in the patient. CAR-T cells release large amounts of pro-inflammatory cytokines, which in turn cause further cytokine release from bystander immune cells in the patient.

Another common toxicity observed after CAR-T therapy, appearing a bit later than CRS, is immune effector cell-associated neurotoxicity (ICANS), which may manifest as a wide range of neurological symptoms such as delirium, encephalopathy, or aphasia. CRS and ICANS are commonly treated with corticosteroids and tocilizumab (interleukin (IL)-6 blocking mAb)[179–181]. Fractionated administration of CAR-T cells over several days has also been proposed by some hospital centers as a measure to reduce their incidence[89,90,160].

The antigen recognition domain is usually based on an Ig-derived scFv, although the recombinant ectodomain of the natural ligand/receptor of the target molecule may be used as well in some cases. CAR-redirection of T cell effector functions avoids the problem of TCR MHC restriction, so the same CAR construct may be used for a particular tumor type in any patients, regardless of their haplotype. In addition, CAR-T cells may recognize tumor cells even upon MHC-I downregulation, a common mechanism of immune escape as seen before.

Different intracellular stimulatory domains have been used for CAR design. First generation CARs only contained CD3ζ signaling domains (signal 1), whereas second generation CARs also included additional domains from co-stimulatory molecules involved in T cell activation (providing signal 2), most commonly CD28 and 4-1BB (other less common co-stimulatory molecules under exploration include ICOS, OX40, and CD27). Newer generation CARs are in development, although all approved CAR-T cells are 2nd generation. 3rd gen CARs include both CD28 and 4-1BB domains, while 4th gen or “armored” CAR include additional cytokine production and/or signaling circuits upon stimulation to potentiate the effector function in immunosuppressive environments (**Figure 7**).

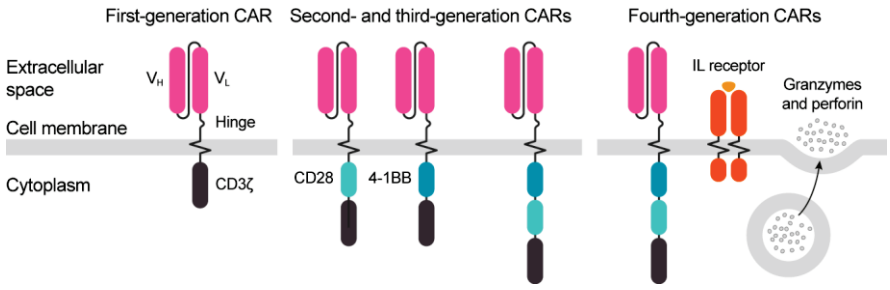

Figure 7. Schematic design of different generations of chimeric antigen receptors. The first chimeric antigen receptors were composed of an scFv and a CD3ζ signaling domain. Their poor functionality and expansion led to the incorporation of additional co-stimulatory domains, usually CD28/4-1BB, in second and third-generation CARs. Subsequent generations, like armored CAR-T cells, have been engineered to potentiate cytokine circuits and overcome immunosuppression.

The choice of co-stimulating molecule is not banal: every domain favors different effector kinetics, and the appropriate one should be selected depending on the goal. CD28 provides a very potent T cell short-lived activation, whereas 4-1BB promotes more long-lived activations, with T cells being less susceptible to exhaustion[182].

1.4.2.3.1. CAR-Ts for AML

The most commonly targeted antigens for AML treatment are CD33 and CD123, both of which are expressed at high levels by most AMLs[183–186]. However, and this remains true for most targetable antigens in AML, they are also expressed by healthy HSCs, and their targeting will inevitably lead to myeloablation[187].

Despite this, CD33- and CD123-directed immunotherapies still have a place in the clinic (anti-CD33 gemtuzumab is also used) as they can be used to reduce tumor burden, hopefully achieving minimal residual disease negativity, bridging to a potentially curative alloHSCT to restitute the hematopoietic system. In these cases, CD28 co-stimulating domains are favored, as a long-lasting disease control is not required[186]. Other CAR-T therapies proposed for AML include targeting of CLL-1, CD13, TIM3, folate receptor (FR)-β, and FLT3[188–191].

The repurposing of CAR-T therapies initially designed for other malignancies has been proposed in some AML cases. As mentioned earlier, t(8;21) AML is characterized by aberrant CD19 expression[70], and CD19 CAR-T immunotherapy has been applied[192]. Furthermore, around 30% of AML patients present with ectopic CD7[193], and CD7 CAR-Ts have been indicated for their treatment[194,195].

Current trends propose genetic editing of the pan-myeloid targeted antigens in transplanted HSCs, either knocking them out or base-editing them to alter the recognized epitope, so that the restituted hematopoietic system is immunotherapy-resistant[196,197]. Some groups even propose the targeting of pan-hematological antigen CD45, and base-edited HSCs for bridging HSCT, as a treatment for all blood cancers[198]. Albeit very elegant, the clinical implementation of this latter work might not be easy.

1.4.2.3.2. CAR-Ts for T-ALL

CAR-T immunotherapy for T-ALL has three major limitations that must be overcome, arising from the phenotypical similarities between effector T cells and leukemic T lymphoblasts, and the lack of safe, actionable tumor-specific antigens. These challenges are:

(i) Leukapheresis blast contamination: A key step during CAR-T manufacturing is the depletion of contaminant blast cells in the starting product, as accidental blast transduction with the CAR can lead to antigen-positive, immunotherapy-resistant leukemia due to cis “shielding” of the target epitope by CAR molecules on the surface of blasts. Cases of this happening have been reported in B-ALL[199], although blast depletion in T-ALL is even more complicated as T lymphoblasts often express CD4, CD8, or CD3, commonly used for T cell selection[200].

(ii) CAR-T fratricide: Expression of the target antigen on CAR-T cells results in fratricide, where CAR-T cells kill each other, leading to limited expansion during the manufacturing process or even an altogether failure to manufacture. Various approaches can be used to overcome fratricide, namely genetic editing to eliminate the antigen in effector T cells, the use of protein

expression blockers (PEBL) to avoid surface antigen expression, or the targeting of tumor-restricted antigens, not expressed in healthy T cells[201–203].

(iii) T cell aplasia: Unlike B cell toxicity, which is well tolerated, T cell aplasia leads to severe life-threatening immune depression, and patients must undergo HSCT to restore T cell immunity. T cell aplasia can be avoided through the use of safety switches to eliminate CAR-Ts after tumor regression (although long term disease control would be lost) or by targeting tumor-restricted antigens not expressed by mature T cells.

Most CAR-T therapies for T-ALL are focused on pan-T antigens CD7 and CD5. These two molecules are expressed by up to 95% of all T-ALL cases (CD5 is negative in ETP-ALL), but they require some additional genetic engineering to prevent CAR-T fratricide, and the unavoidable T cell aplasia must be reverted via alloHSCT[201–203]. Thus, many efforts are being made towards the identification of safe and targetable T-ALL antigens.

A very attractive approach is the targeting of TRBC1, the constant region of the TCRβ chain. During TCR recombination, two genes encoding for the constant region of the TCRβ chain may be used, *TRBC1* and *TRBC2*, in a mutually exclusive manner. The repertoire of healthy T cells is composed of a mix of TRBC1$^+$ and TRBC2$^+$ lymphocytes, whereas leukemic blasts, due to their clonality, can only express one of them (if malignant transformation occurred after β rearrangement). This was the rationale for the development of TRBC1- (and later TRBC2-) directed CAR-T cells, targeting a large number of T-ALL cases while only causing partial T cell aplasia[204,205].

Our group has identified CD1a as a safe immunotherapeutic target for the treatment of R/R cortical T-ALL, a major subtype accounting for ~40% of all T-ALL cases[71,206–208], and accordingly generated CD1a-directed CAR-T cells[209], now part of a phase I clinical trial (NCT05679895). CD1a expression is limited to a subset of skin-resident dendritic cells (known as Langerhans cells) and thymocytes during normal T cell development, while absent in both HSCs and mature T cells and circumventing the limitations of CAR-T fratricide and T cell aplasia. However, the targeting of CD1a only covers cortical T-ALL cases, excluding other subtypes with a worse prognosis[95,96,98,210], highlighting the need to identify further safe T-ALL antigens for its immunotherapy.

In that sense, we propose the chemokine receptor CCR9 as a novel immunotherapeutic antigen in the treatment of T-ALL. CCR9 is the G protein-coupled receptor for the ligand CCL25[211–213], and its CCR9 expression in healthy cells is restricted to thymocytes, some intestine-resident lymphocytes, a subset of IgA-producing B cells and plasmacytoid dendritic cells[212,214–216], all relatively expendable tissues. CCL25, on the other hand, is produced by the thymic and small intestine epithelia, mediating the migration of CCR9$^+$ cells to the tissues. During normal T cell ontogeny, early thymic precursors (ETPs) from the bone marrow gain CCR9 and migrate to the thymus, where T cell development takes place[50].

CCR9 has been reported to negatively correlate with the prognosis of a number of different solid tumors and contribute to their progression[217–224], as well as being involved in T-ALL proliferation and a predictor of its relapses[225,226]. Accordingly, CCR9-directed immunotherapies including mAbs and even CAR-T cells have been developed against CCR9[227–229].

1.4.2.4. Improvements to CAR-T therapies

1.4.2.4.1. Allogeneic effector cells

The obtention of autologous effector cells for immunotherapy is oftentimes a critical step in adoptive cell immunotherapies. The timing of leukapheresis and patients' lymphocyte counts are important questions, and the reasons are twofold:

(i) Patients receiving CAR-T cells are multi-treated, in second or even third lines of treatment, and their T cells commonly show signs of exhaustion and impaired effector functions[230–232].

(ii) Similarly, and due to the lymphodepleting effects of chemotherapeutic regimens, many trials and centers require a treatment-free period following certain procedures prior to apheresis, particularly after HSCT (ideally >100 days), immunosuppressive therapies for GvHD (1 month), and immune-targeted therapies (1 month)[233–235].

Because of these reasons, plus to avoid the problem of contaminating blasts in the starting product, there is great interest in finding allogeneic-safe, universal effector cells, which can be manufactured beforehand, quality checked, and stored for an off-the-shelf use for any patient needing them.

NK cells have been proposed as effector cells, as they possess intrinsic antitumoral activity and are MHC-unrestricted, being able to be used in an allogeneic manner. However, NK cells are short-lived and their ability to form immune memory and prevent disease recurrence is limited[236].

MHC-unrestricted γδ T cells have emerged as a promising, very attractive alternative based on their potent cytotoxic activity and release of cytokines stimulating and recruiting other immune cells to the tumor site[61,59,237,238]. While their relatively low abundance in peripheral blood has hindered their implementation in the clinical practice, recent protocol developments have enabled their large-scale *ex vivo* expansion[63,239,240].

Finally, some groups have opted for genetic editing of the TCRα chain (TRAC) locus to prevent the formation of the TCR complex, making these T cells MHC-unrestricted and avoiding GvHD[241,242]. A few elegant works have already been published using this strategy, showing great promise[243–247]. However, even if this strategy circumvents the need for a large-scale expansion of γδ T cells, it has been reported that TCR elimination in CAR-T cells leads to decreased persistence[248]. Furthermore, CRISPR/Cas9 genome editing still has to solve additional regulatory requirements.

1.4.2.4.2. STAb-T cells

Secreting T cell-redirecting antibodies (STAb) immunotherapy is an emerging strategy that involves the genetic engineering of T cells to produce and secrete BiTEs. In contrast to CAR-T therapies, in which genetically manipulated T cells are the only ones performing antitumor effector functions, the paracrine secretion of BiTEs by edited STAb-T cells is able to recruit bystander non-edited T cells, boosting the antitumor response[249]. Several groups have shown the promising therapeutic potential of STAb-T cells in $CD19^+$ B cell malignancies[250–252].

STAb therapy combines the best of CAR-Ts and systemic administration of BiTEs: as they exhibit active trafficking to the tumor site, provide long-lasting BiTE release, and can recruit bystander T cells (**Figure 8**).

Another difference between CAR-T and STAb-T therapy regards the immune synapse: it has been reported that the immune synapse initiated by CARs differs from the canonical, TCR-mediated one, conforming disorganized multifocal clusters leading to shorter effector-tumor cell interactions[253–255].

As in STAb-T therapy, T cell engagement is dependent on CD3 recruitment, the immune synapse formed is identical in structure and composition to that induced by canonical TCR engagement[256–258], possibly leading to more physiological signaling and regulation of the synapse, although the full extent of the functional implications remains to be elucidated.

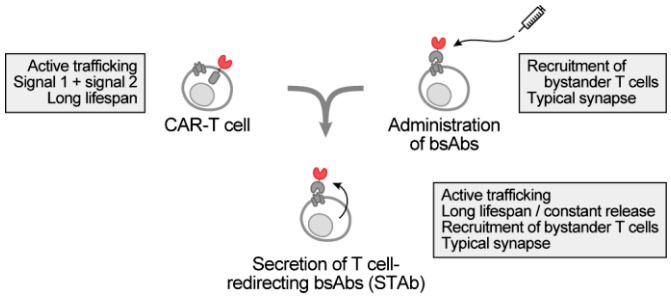

Figure 8. Schematic summary of the advantages of classical T cell-redirecting strategies: chimeric antigen receptor (CAR)-engineered T cells and systemic administration of bispecific antibodies (bsAbs), and a next-generation strategy based on the *in situ* secretion of bsAbs by engineered T cells. Adapted from Blanco *et al*. 2019.

1.4.2.4.3. Dual targeting

As mentioned before, a common mechanism of tumor escape to antigen-directed immunotherapies is antigen escape, where strong selective pressure on a single antigen facilitates the appearance of antigen-negative clones that escape the immunotherapy. Antigen escape has been well described in B-ALL: up to 30% of relapses after blinatumomab and 60% after CD19 CAR-Ts are characterized by CD19 loss, rendering malignant cells invisible to CD19 immunotherapies[86,259–261]. In the case of T-ALL, CD7 escape has been reported in as many as 25% of CD7 CAR-T-treated patients[262].

The simultaneous targeting of multiple tumor-associated antigens can help prevent antigen escape, as selective pressure is distributed among the different molecules. Several clinicals exploring the combinatorial targeting of CD19 and CD22 for B-ALL are underway, to optimize response rates and reduce the risk of leukemic cell escape[263–268].

Dual targeting strategies include the use of bicistronic constructs (a single viral vector, two separate CAR molecules), tandem CARs (two antigen recognition in a single CAR molecule), co-transduced CAR-Ts (transduction of T cells with two different single CAR constructs), or even the administration of two independently manufactured, single-targeting CAR-T cell populations (**Figure 9**).

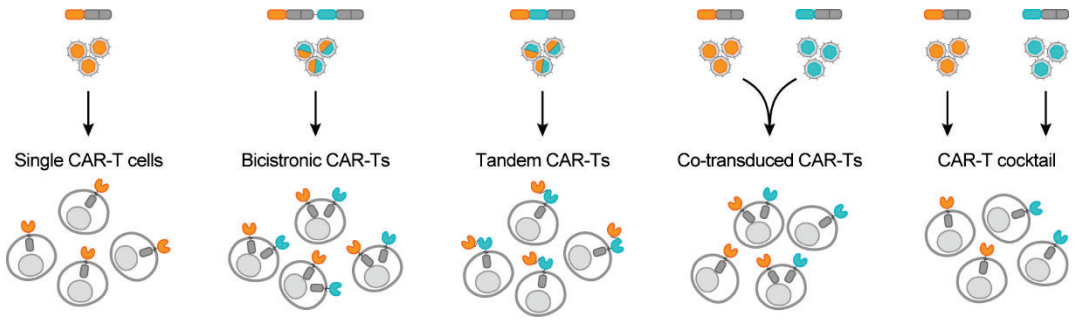

Figure 9. Schematic of types of dual-targeting CAR-T cells generated by different methods.

Bicistronic and tandem CAR designs allow for cheaper manufacturing, as only one viral vector must be produced for T cell transduction. However, these larger constructs usually come at the cost of lower transduction efficiencies. Using co-transduction, not all T cells have the ability to target both antigens, as there is a mix of single and double targeting cells (as well as untransduced). Finally, the administration of two (or more) single-targeting CAR-T products is the most expensive option, as independent viral productions and CAR-T manufactures are required[269].

These dual products get activated by the expression of either target antigen (logic "OR" gating), but other logic gates can be engineered. Molecules that are expressed by both tumor and healthy cells can be safely targeted using combinatorial antigen recognition, where engagement of two different antigens is required for full T cell activation. "AND" gated CAR-T cells can be engineered by splitting the stimulatory and co-stimulatory domains into two separate CAR molecules, with different antigen specificities[270,271]. However, this system is a bit leaky, and toxicities are to be expected, so systems with inducible CAR expression have been designed[272,273]

2. Aims

The general aim of this doctoral thesis is to improve current CAR-T immunotherapeutic strategies in the treatment of acute leukemias. The specific aims of this doctoral thesis are:

1. To develop and characterize CD123-directed CAR-DOT cells as an allogeneic-safe, off-the-shelf therapy for the treatment of R/R AML.

2. To engineer CD1axCD3 BiTE-secreting STAb-T cells and compare their effectiveness against conventional CD1a-directed CAR-T cells against coT-ALL.

3. To generate a CCR9-directed immunotherapy for the safe treatment of R/R T-ALL.
   (i) To validate CCR9 as an immunotherapeutic target for T-ALL.
   (ii) To generate CCR9-directed CAR-T cells.
   (iii) To generate dual CCR9/CD1a-directed CAR-T cells for increased targeting of T-ALL.

3. Results

Informe de los directores

Barcelona, junio de 2024

Los doctores Pablo Menéndez Buján y Diego Sánchez Martínez certifican que los artículos científicos* que forman parte de la defensa de la tesis titulada "New immunotherapeutic strategies in acute leukemia", presentada por Néstor Tirado Cabrera, estudiante del programa de doctorado en Biomedicina, formaran parte exclusivamente de esta tesis doctoral.

*

Generation and proof-of-concept for allogeneic CD123 CAR-Delta One T (DOT) cells in acute myeloid leukemia

J Immunother Cancer 2022 Sep;10(9):e005400

DOI: 10.1136/jitc-2022-005400

El alumno puso a punto la tecnología DOT en el laboratorio, optimizó la infección de estas células, y participó activamente en toda la caracterización funcional, tanto *in vitro* como *in vivo*, incluida en el artículo.

Efficient preclinical treatment of cortical T cell acute lymphoblastic leukemia with T lymphocytes secreting anti-CD1a T cell engagers

J Immunother Cancer 2022 Dec;10(12):e005333

DOI: 10.1136/jitc-2022-005333

El alumno participó en la concepción y diseño del estudio, y realizó la caracterización funcional *in vitro* e *in vivo* de la inmunoterapia descrita.

CAR-T cells targeting CCR9 and CD1a for the treatment of T cell acute lymphoblastic leukemia

In preparation

Pablo Menéndez Buján
10892394P

Diego Sánchez Martínez
72992698J

3.1. Generation and proof-of-concept for allogeneic CD123 CAR-Delta One T (DOT) cells in acute myeloid leukemia

Diego Sánchez Martínez, **Néstor Tirado**, Sofia Mensurado, Alba Martínez-Moreno, Paola Romecín, Francisco Gutiérrez-Agüera, Daniel V Correia, Bruno Silva-Santos, Pablo Menéndez

Journal for ImmunoTherapy of Cancer. 2022, 10(9):e005400

2022 Impact Factor: 12.485

Quartile 1 (Oncology, Immunology)

Journal for ImmunoTherapy of Cancer

Generation and proof-of-concept for allogeneic CD123 CAR-Delta One T (DOT) cells in acute myeloid leukemia

Diego Sánchez Martínez ,[1,2] Néstor Tirado,[1,2] Sofia Mensurado,[3] Alba Martínez-Moreno,[1,2] Paola Romecín,[1,2] Francisco Gutiérrez Agüera,[1,2] Daniel V Correia,[3] Bruno Silva-Santos,[3] Pablo Menéndez[1,2,4,5]

To cite: Sánchez Martínez D, Tirado N, Mensurado S, *et al*. Generation and proof-of-concept for allogeneic CD123 CAR-Delta One T (DOT) cells in acute myeloid leukemia. *Journal for ImmunoTherapy of Cancer* 2022;**10**:e005400. doi:10.1136/jitc-2022-005400

► Additional supplemental material is published online only. To view, please visit the journal online (http://dx.doi.org/10.1136/jitc-2022-005400).

Accepted 26 August 2022

For numbered affiliations see end of article.

Correspondence to
Dr Diego Sánchez Martínez; dsanchez@carrerasresearch.org

Dr Bruno Silva-Santos; bssantos@medicina.ulisboa.pt

Dr Pablo Menéndez; pmenendez@carrerasresearch.org

ABSTRACT

Background Chimeric antigen receptor (CAR)-T cells have emerged as a breakthrough treatment for relapse/refractory hematological tumors, showing impressive complete remission rates. However, around 50% of the patients relapse before 1-year post-treatment. T-cell 'fitness' is critical to prolong CAR-T persistence and activity. Allogeneic T cells from healthy donors are less dysfunctional or exhausted than autologous patient-derived T cells; in this context, Delta One T cells (DOTs), a recently described cellular product based on MHC/HLA-independent Vδ1$^+$γδ T cells, represent a promising allogeneic platform.

Methods Here we generated and preclinically validated, for the first time, 4-1BB-based CAR-DOTs directed against the interleukin-3α chain receptor (CD123), a target antigen widely expressed on acute myeloid leukemia (AML) blasts.

Results CD123CAR-DOTs showed vigorous, superior to control DOTs, cytotoxicity against AML cell lines and primary samples both *in vitro* and *in vivo*, even on tumor rechallenge.

Conclusions Our results provide the proof-of-concept for a DOT-based next-generation allogeneic CAR-T therapy for AML.

WHAT IS ALREADY KNOWN ON THIS TOPIC

⇒ Allogeneic cytotoxic cells obtained from healthy donors are a very interesting alternative for next-generation 'off-the-shelf' chimeric antigen receptor (CAR)-T cell therapies. In particular, MHC/HLA-independent γδ T cells have emerged as a promising candidate based on their high cytotoxic activity, stimulatory cytokine release and recruitment of other immune cells to the tumor site.

WHAT THIS STUDY ADDS

⇒ Our data demonstrate the capacity of CAR-Delta One T cells (DOTs) to be a disruptive 'off-the-shelf' allogeneic cellular immunotherapy for acute myeloid leukemia.

HOW THIS STUDY MIGHT AFFECT RESEARCH, PRACTICE OR POLICY

⇒ CAR-DOTs exhibit a combination of properties that may change allogeneic cell immunotherapy of hematological (and probably solid) tumors in the future.

INTRODUCTION

Immunotherapy has promoted marked improvements in cancer treatment over the last decade. The immune system offers a wide range of alternatives, including cytotoxic lymphocytes—native or engineered—to eliminate treatment-resistant tumors. In this context, CD19-directed chimeric antigen receptor (CAR)-transduced T cell (CAR-T) therapies have shown impressive rates of complete remissions (CR) in relapse/refractory (r/r) B-cell malignancies, especially in B-cell acute lymphoblastic leukemia (ALL).[1 2] However, 1 year progression-free survival remains ~50% due to frequent relapses.[3 4] Antigen loss and phenotypic escape as well as CAR-T cell disappearance, dysfunctionality or exhaustion are commonly responsible for such failures.[5 6] Thus, new therapeutic options based on 'fitter' effector T cells are being actively investigated in order to increase T-cell persistence and efficacy.

Allogeneic cytotoxic cells obtained from healthy donors (HD) are an especially attractive avenue for 'off-the-shelf' next-generation CAR-T cell therapies. In particular, MHC/HLA-independent γδ T cells have emerged as a promising candidate based on their potent cytotoxic activity and release of cytokines stimulating and recruiting other immune cells to the tumor site.[7–9] While the low abundance of γδ T cells in the human peripheral blood (PB) has hindered their clinical application, recent advances in protocol development have enabled their *ex vivo* expansion to large numbers.[10–13] In particular, we have characterized Delta One T (DOT) cells, a Vδ1 T cell-enriched cellular product expressing enhanced levels of natural cytotoxicity receptors, and demonstrated that they constitute a safe and efficient effector platform to eliminate cancer cells in *in vitro* and *in vivo*

preclinical models of solid and hematological malignancies,[10] most notably acute myeloid leukemia (AML).[14]

AML, the most common acute leukemia in adults, is characterized by the accumulation of differentiation-defective immature and proliferative myeloid blasts in the bone marrow (BM) and PB.[15] Unfortunately, patient overall survival has not improved significantly over the last decades, with relapses being frequent and presenting poor outcome, thus requiring hematopoietic stem cell transplantation as rescue therapy.[16] Despite its molecular enormous heterogeneity,[15 17 18] CD123, the α chain of the interleukin (IL)-3 receptor, is consistently expressed in >90% of AML blasts, in similar levels to leukemic stem cells, and its expression is maintained at relapse.[19 20] Based on this rational, we previously showed robust efficacy of second generation (4-1BB-based) CD123-directed CAR-T cells in preclinical AML models.[21]

Clinically implemented CAR-T cell approaches are based on abundant αβ T cells[22–24] which have limited applicability in the allogeneic setting due to their MHC/HLA restriction and graft-versus-host potential.[25] Importantly, immunological BM dysfunction and T-cell exhaustion has been reported in intensively chemotherapy-treated r/r AMLs.[26] Thus, safety allowing, allogeneic T cells from HDs would represent an 'off-the-shelf' cost-efficient therapy to eliminate r/r AML. Building on these foundations, we prompted to explore the potential of MHC/HLA-independent DOT cells as vehicle for our second generation CD123CAR in preclinical AML models.

Here we describe, for the first time, the generation of CAR-expressing DOT cells (CAR-DOTs) and provide the proof-of-concept for their application in AML treatment. Retrovirally-transfected CD123CAR-DOTs potently eliminated AML cell lines and primary samples both *in vitro* and *in vivo*, increasing the efficacy of 'naked' (mock-transduced) DOTs in different models and conditions, without phenotypic alterations. Moreover, CD123CAR-DOTs released type 1 (antitumor) cytokines and chemokines on exposure to primary AML cells. In *in vivo* rechallenge experiments, CD123CAR-DOTs persisted and remained functional against AML, 9 weeks after their infusion into mice. IL-15 significantly improved their *in vivo* efficacy by sustaining longer action and enabling one-single-dose treatment. Our data demonstrate the potential of CAR-DOTs to represent a disruptive 'off-the-shelf' allogeneic cellular immunotherapy for AML.

METHODS

DOT cell generation

PB mononuclear cells (PBMCs) were isolated from buffy coats from HDs by Ficoll-Hypaque gradient centrifugation. Buffy coats were obtained from the Barcelona Blood and Tissue Bank on Institutional Review Board-approval (HCB/2018/0030). PBMCs were incubated with anti-αβTCR Biotin mAb (Miltenyi Biotec) followed by incubation with anti-Biotin mAb microbeads to deplete αβ T cells by magnetic separation using autoMACS under depleteS protocol (Miltenyi Biotec, Biergisch Gladbach, Germany). DOT cells were generated from αβ-depleted PBMCs cultured in either 96-well plates or G-REX platform (Wilson Wolf Manufacturing), based on an adaptation from our previous protocol.[10 14] Briefly, αβ-depleted PBMCs were resuspended in OpTmizer-CTS medium supplemented with 2.5% heat-inactivated human plasma (LifeSciences), 2 mmol/L L-glutamine (Thermo Fisher) and 50 U/mL/50 µg/mL of penicillin/streptomycin (Thermo Fisher) and cultured for 16–20 days. Animal-free human cytokines rIL-4 (100 ng/mL), rIFN-γ (70 ng/mL), rIL-21 (7 ng/mL), and rIL-1β (15 ng/mL; all from PeproTech), and a soluble mAb anti-CD3 (clone OKT-3, 140 ng/mL; BioLegend), were added to the medium at day 0. At day 7, cultures were supplemented with anti-CD3 (clone OKT-3, 1 µg/mL or 2 µg/mL for 96-well plate protocol), rIL-21 (13 ng/mL) and rIL-15 (70 ng/mL; also from PrepoTech). On day 11, new medium was added to cultures, supplemented with anti-CD3 (1 µg/mL) and rIL-15 (100 ng/mL). Cells were incubated at 37°C and 5% CO_2. DOT cells were harvested at the end of the culture and either used fresh (for *in vitro* assays) of cryopreserved (for *in vivo* experiments) in OpTmizer media+20% human plasma+10% DMSO, and stored in liquid nitrogen.

CD123-CAR retroviral production and transduction

To construct the retroviral transfer vector, the complete CD123-directed CAR (including CSL362 scFv, CD8 transmembrane domain, 4-1BB costimulatory domain, CD3z endodomain, and a T2A-eGFP cassette) previously described[21] was cloned into an SFG retroviral backbone. The SFG vector expressing eGFP alone (mock vector) was used as a control. Viral particles pseudotyped with RD114 were generated using 293 T cells with GeneJuice transfection reagent (Sigma-Aldrich, Saint Louis, Missouri, USA) following manufacturer's instructions with a 1.5:1.5:1 µg ratio of the SFG:Peq-Pam:RD114 DNA plasmids and concentrated using Retro-X Concentrator (Takara, Kusatsu, Japan) following manufacturer's instructions. DOT cells were expanded for 7 days prior to viral transduction. Proper CAR transduction was checked by flow cytometry by eGFP expression and by using AffiniPure $F(ab')_2$ Fragment Goat Anti-Human IgG (H+L) (Jackson ImmunoResearch Laboratories). Other conditions tested during transduction optimization of DOT cells included the use of lentiviral particles as previously reported[27] at multiplicities of infection between 10 and 50, as well as with retroviral particles with RetroNectin (Takara) following manufacturer's instructions. All lentiviral transduction conditions were tested at days 7 and 11 of the DOT cell expansion protocol.

Immunophenotyping of DOT cells, cell lines and primary AML samples

Proper differentiation and activation of DOT cells was confirmed by surface staining with CD3-PB (UCHT1), CD3-APCCy7 (UCHT1), TCRγδ-PE (B1), TCRαβ-APC

(IP26), CD4-APCCy7 (RPA-T4), CD8-BV510 (RPA-T8), CD25-APCCy7 (BC96), CD69-BV510 (FN50), NKp30-BV421 (P30-15), NKG2D-BV510 (1D11), CD45RA-APC (HI100), CD27-PB (O323), CD62L-BV510 (DREG-56), DNAM-1-BV510 (11A8) from BioLegend (San Diego, California, USA) and TCR Vδ1-PE (REA173), TCR Vδ2-APC (123R3) and NKp44-APC (2.29) from Miltenyi Biotec. Briefly, 2.5×10^5 cells were incubated with the antibodies for 30 min at 4°C and then washed. For intracellular staining, DOT cells were incubated after membrane labeling with anti-perforin-BV241 (dG9) and anti-granzyme B-BV510 (GB11) from BD Biosciences, and anti-granzyme A-APC (CB9) from BioLegend (San Diego, California, USA), using FIX&PERM Sample Kit (Nordic MUbio) under manufacturer's instructions. Non-reactive, isotype-matched fluorochrome-conjugated mAbs were systematically used to set the gates. Dead cells were discarded by 7-AAD staining.

The immunophenotyping of AML cell lines and primary samples (obtained from Hospital Clínic of Barcelona) was done by surface staining with CD45-PE (HI30), CD33-BV421 (HIM3-4) and CD123-APC (7G3) (BD Biosciences, Franklin Lakes, New Jersey, USA). A FACS-Canto-II flow cytometer equipped with FACSDiva software (BD Biosciences) was used for the analysis.[27]

In vitro cytotoxicity assays and cytokine release determination

The cell lines MOLM13, THP-1 and Jurkat were purchased from DSMZ (Germany) and expanded according to DSMZ recommendations. Target cells (cell lines and primary AML blasts) were labeled with 3 µM eFluor 670 (eBioscience) and incubated with CAR-DOTs or mock-DOTs at different Effector:Target (E:T) ratios for the indicated time periods in complete DOT media. CAR-DOT-mediated cytotoxicity was determined by analyzing the residual alive (7-AAD$^-$) eFluor 670$^+$ target cells at each time point and E:T ratio. Absolute cell counts were determined using Trucount absolute count beads (BD Biosciences).[28] Cytokine production was measured by G-Series Human Cytokine Antibody Array 4000 from RayBiotech in supernatants harvested after 48 hours-incubation CAR-DOT/mock-DOT (four donors) with two primary AML samples.

In vivo AML patient-derived xenograft models

The 7–12 weeks old non-obese diabetic Cg-*Prkdc*^{scid} *Il2rg*^{tm1Wjl}/SzJ (NSG) mice (Jackson Laboratory) were bred and housed under pathogen-free conditions in the animal facility of the Barcelona Biomedical Research Park (PRBB). Mice were intravenously transplanted in the tail with 2.5×10^5 Luc-GFP-expressing primary CD123$^+$ AML blasts (primograft-expanded) (579AML-patient-derived xenograft (PDX)^{LUC}).[29] CAR-DOTs or mock-DOTs were thawed and resuspended in complete media and mice were intravenously infused in the tail vein with 10×10^6 cells once, two times or three times 7, 14 and 21 days post-tumor inoculation, respectively. Where indicated, mice were injected intraperitoneally with 1 µg of hrIL-15 every 3–4 days or daily from day 7 to the end of the experiment, as a strategy to support DOT-cell persistence *in vivo*. Tumor burden was followed by bioluminescence (BLI) using the Xenogen IVIS 50 Imaging System (PerkinElmer). To measure luminescence, mice received 150 mg/kg of D-luciferin intraperitoneally, and tumor burden was monitored at the indicated time points as we previously described.[27 30] Living Image software (PerkinElmer) was used to visualize and calculate total luminescence. Besides, tumor burden was followed-up at different time points by bleeding and BM aspirate using fluorescence activated cell sorting (FACS) analysis. Mice were sacrificed when control and/or mock-DOT-treated animals were leukemic, and tumor burden (hHLA-ABC$^+$hCD45$^+$hCD33$^+$hCD123$^+$ graft) and effector DOT persistence (hHLA-ABC$^+$hCD45$^+$hCD3$^+$Vδ1$^+$Vd2$^+$) were analyzed in BM and PB by FACS. In rechallenge experiments, leukemia-free animals were reinfused with 2.5×10^5 CD123+AML primary cells, and disease reappearance was followed-up by BLI and FACS as above. All procedures were performed in compliance with the institutional animal care committee of the PRBB (DAAM9624).

Statistical analysis

Data from at least three individual donors are shown in all figures. All p values were calculated by unpaired two-tailed or one-tailed Student's *t*-test using Prism software (GraphPad). A p value *<0.05/**<0.01/***<0.001/****<0.0001 was considered statistically significant.

RESULTS

CD123-directed DOT cells (CD123CAR-DOTs) expand robustly while preserving DOT phenotype

We set out to generate, for the first time, CAR-DOT cells, and purpose them for AML targeting. DOT cells were expanded and activated as described,[10 14] and transduction was tested at days 7 and 11 using different retroviral (PeqPam/RD114) and lentiviral (VSV-G/psPAX2) conditions (online supplemental figure S1). Retro-X Concentrator at day 7 showed the highest rate of anti-CD123CAR expression and was chosen for downstream generation of CD123CAR-DOTs (figure 1A). CD123CAR transduction/expression did not impact γδ TCR$^+$ and Vδ1$^+$ T cell percentages, which were ~97% and ~70%, respectively, as in the original 'naked' DOT product.[10 14] Likewise, total and Vδ1$^+$ T-cell numbers at the end of the process were similar for mock-DOTs and CAR-DOTs (figure 1C). Retroviral particles infected the Vδ1$^+$ and Vδ1$^-$γδ T-cell populations in similar proportions, and the CD123CAR expression as determined by GFP positivity correlated well with anti-ScFv labeling (figure 1B,C). CAR$^+$ DOTs (n=14) presented a similar T-cell differentiation stage to CAR$^-$ DOTs, as demonstrated by CD62L/CD45RA staining by FACS. The majority of DOTs were effector T cells (T_{EFF}), with an expected degree of variability between donors, followed by effector memory (T_{EM}) DOTs,

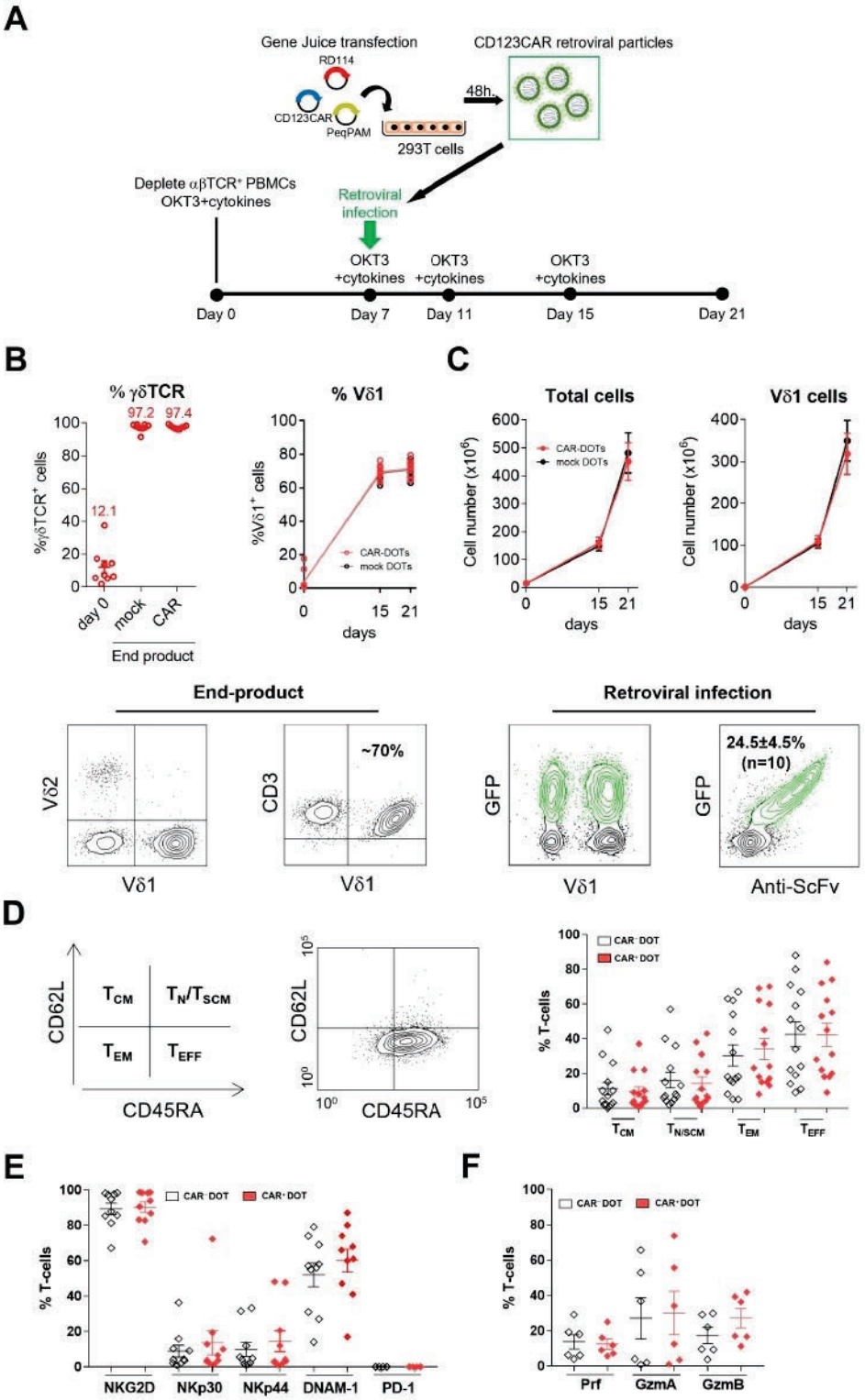

Figure 1 CD123CAR-DOT cell generation and phenotypic characterization. (A) CD123CAR-DOT cell production scheme. αβ-depleted PBMCs were cultured under OKT3 antibody and cytokine stimulation for 3 weeks and transduced with γ-retroviruses at day 7. (B) Upper panels, γδ-TCR+ and Vδ1+T cell percentages evolution from day 0 to end-product for mock DOTs and CAR-DOTs. Lower panels, representative FACS dot plots depicting the expression of Vδ1/Vδ2 and Vδ1/CD3 in end-products. (C) Upper panels, cell number for total cells and Vδ1+T cells along the CAR-DOT generation process. Lower panels, representative FACS dot plot for Vδ1/GFP and anti-ScFv/GFP expression. (D) Left-middle panels, scheme and representative FACS plot depicting T_{CM}, $T_{N/SCM}$, T_{EM}, T_{EFF} T-cell subsets as defined by CD62L versus CD45RA staining. Right panel, percentage of T_{CM}, $T_{N/SCM}$, T_{EM}, T_{EFF} T-cell subsets for CAR^+DOT and CAR^-DOT subpopulations (n=14). (E) NKG2D, NKp30, NKp44, DNAM-1 and PD-1 expression (n=10), and (F) perforin (Prf), granzyme A (GzmA) and granzyme B (GzmB) expression (n=6) in CAR^-DOT versus CAR^+DOT cells. CAR, chimeric antigen receptor; DOT, Delta One T cells; PBMCs, peripheral blood mononuclear cells; T_{CM}, central memory; T_{EFF} effector T cells; T_{EM}, effector memory; $T_{N/SCM}$, naïve/stem central memory.

and lower contributions of central memory (T_{CM}) and naïve/stem central memory ($T_{N/SCM}$) DOTs (figure 1D). Furthermore, both CAR^+ and CAR^- DOTs expressed their natural killer (NK) cell receptor signature according to the published[10] hierarchy: NKG2D (>90%) > DNAM-1 (~60%) > NKp30 and NKp44. By contrast, the immune checkpoint programmed cell death protein-1 (PD-1) was strikingly absent from both DOT populations (figure 1E). The expression of the key components of cytotoxic granules, perforin, granzyme (Gzm) A and GzmB, was also not affected by CAR transduction (figure 1F). Collectively, these data demonstrate the feasibility of CAR-DOT generation, and further show that retroviral infection and CD123CAR expression on the cell surface does not modify DOT expansion properties or phenotype, thus generating NK-like cytotoxic effector γδ T cells highly enriched in $V\delta1^+$ T cells.

CD123CAR-DOTs specifically augment cytotoxicity against AML cell lines and primary blasts *in vitro*

In order to test the anti-AML activity of CAR-DOTs, we performed *in vitro* cytotoxicity assays against the $CD123^+$ AML cell lines MOLM13 and THP-1, and the $CD123^-$ T-cell ALL line Jurkat, as negative control. CD123CAR-DOTs specifically eliminated $CD123^+$ AML cells in an E:T ratio-dependent manner, with substantially increased cytotoxic activity compared with mock-DOTs. Even at low E:T ratios (1:16, 1:8, 1:4) we achieved 20–60% more AML cell lysis than with mock-DOTs in 48 hours and 24 hours assays (figure 2, online supplemental figure S2). Importantly, CD123CAR-DOTs showed similar potency to conventional CD123CAR-Ts (online supplemental figure S3), thus allowing us to concentrate on the allogeneic advantages of CD123CAR-DOTs. Next, to evaluate their capacity to kill primary tumors, CD123CAR-DOTs were co-cultured with primary $CD123^+$ AML samples, with different percentages of $CD123^+CD33^+$ blasts (figure 2B). CD123CAR-DOTs showed enhanced cytotoxicity over mock-DOTs against $CD123^+$ AML primary blasts in 48 hours assays (figure 2C). Moreover, compared with mock-DOTs, CD123CAR-DOTs produced significantly higher levels of master antitumor mediators, namely the cytokines tumor necrosis factor-α and interferon-γ, as well as IL-13, recently implicated in orchestrating tumor surveillance in mice[31]; the T-cell costimulator 4-1BB, a major determinant of γδ T-cell-mediated tissue surveillance[32]; the signal transducer Axl, shown to maximize IL-15R signaling in human NK cell differentiation[33]; the myeloid differentiation factor, granulocyte-macrophage colony-stimulating factor (GM-CSF); and the chemokines MIP-1a (CCL3), CCL5, CXCL13 and lymphotactin (XCL1), all important in mobilizing multiple leukocyte subsets in cancer immunity.[34] While not significantly augmented, IL-2 and FasL, key mediators of T-cell proliferation and cytotoxicity, respectively, also showed a tendency for higher expression in CD123CAR-DOT cells (figure 2D). These data demonstrate an enhanced effector potential of CD123CAR-DOT cells in direct comparison with naked/mock-DOT cells.

Serial infusions of CD123CAR-DOTs exhibit robust anti-leukemic effect *in vivo*

CD123CAR-DOT function was evaluated *in vivo* by employing Luc-expressing AML-PDX^{LUC}. NSG mice were transplanted with 2.5×10^5 AML-PDX^{LUC} cells and, based on our previous extensive experience with DOTs in AML xenograft models,[14] infused with 10×10^6 (CAR-DOTs or mock-DOTs) DOTs in three serial infusions (one injection per week (day 7, 14, 20), starting 1 week post-tumor injection), and leukemia progression was followed by BLI (figure 3A). CD123CAR-DOTs controlled AML tumor burden between days 20 and 47 significantly better than mock-DOTs which only managed to delay tumor growth and could not prevent an eventual logarithmic tumor growth from day 47 onwards (figure 3B). At this point, we decided to provide an additional fourth infusion at day 53, which resulted in complete control of leukemia in CD123CAR-DOT mice, in stark contrast with continued tumor growth in mock DOT-treated mice (figure 3B). Furthermore, FACS analyses of PB and BM samples collected at days 47 and 67 confirmed the BLI data. Leukemic burden, as determined by HLA-ABC/CD45/CD123/CD33 expression, showed high, intermediate and absent blast cells in untreated, mock-DOT and CAR-DOT-treated mice, respectively (figure 3C). These data highlight the therapeutic advantage over 12 weeks of CD123CAR-DOTs over mock-DOTs in *in vivo* AML-PDX models.

Provision of IL-15 supports single-dose CD123CAR-DOT activity *in vivo*

Having achieved the initial proof-of-concept for CD123CAR-DOT activity in AML xenografts, we next aimed to maximize it through provision of key DOT survival factors, particularly since the murine milieu lacks human cytokines. Given that the DOT protocol relies on IL-15 as the critical cytokine in the second stage of expansion/differentation,[10 14] we combined CD123CAR-DOTs with intraperitoneal IL-15 administration every 3–4 days. In this set of experiments, NSG mice were transplanted with 2.5×10^5 AML-PDX^{LUC} cells, and starting 1 week later, they received one, two or three doses of 10×10^6 CD123CAR-DOTs, with or without IL-15 injection (figure 4A). Leukemia engraftment was followed weekly by BLI and by flow cytometry analysis of BM and PB samples. In the absence of exogenous IL-15, three doses of CD123CAR-DOT (CAR3) were clearly more efficacious than one (CAR1) or two (CAR2) doses, since these only managed to delay tumor burden (compared with untreated control mice) (figure 4B,C). Strikingly, the provision of IL-15 every 3–4 days overrode all such differences, thus allowing complete leukemia control 60 days after even with a single CD123CAR-DOT infusion (figure 4B,C). These results demonstrate a critical

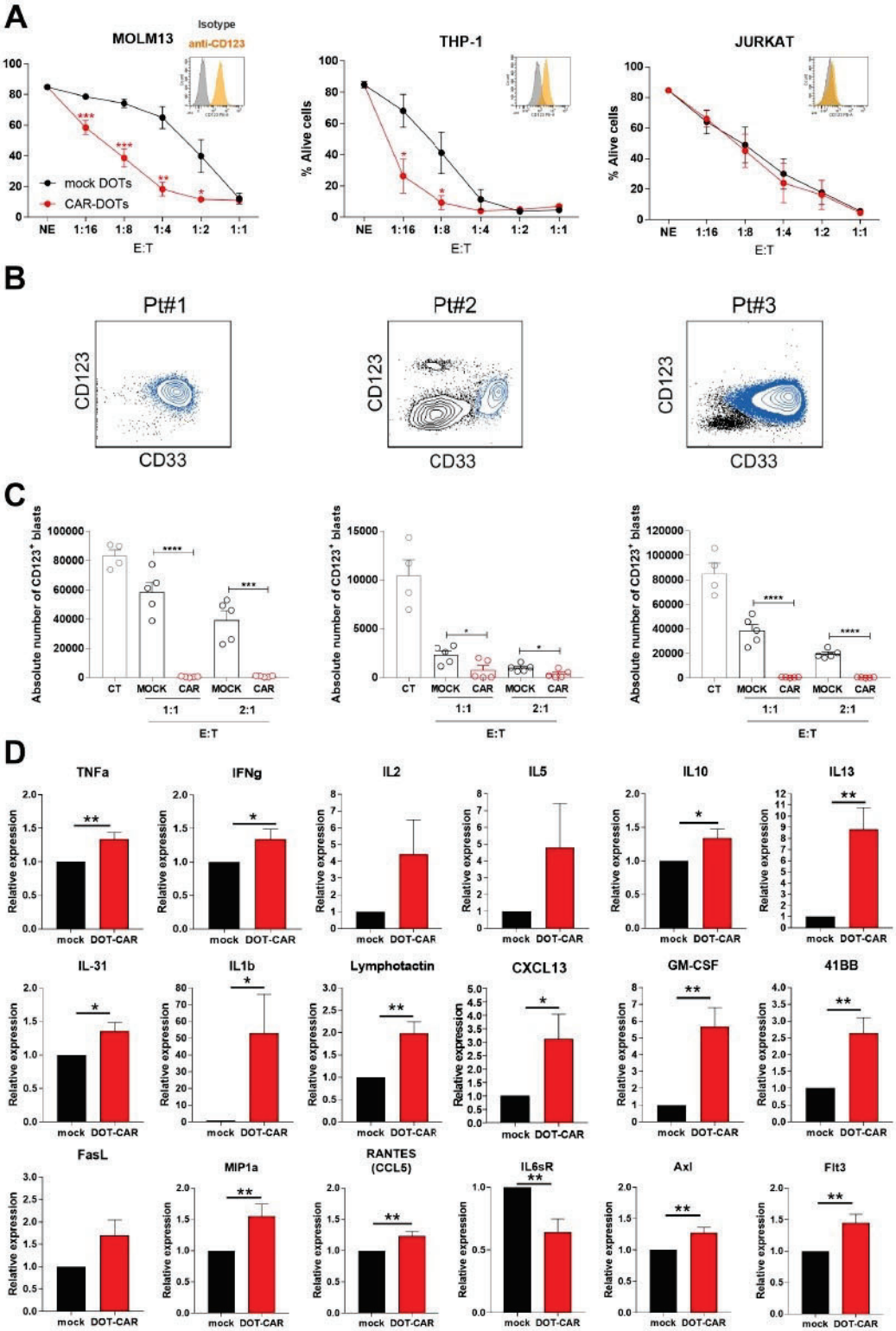

Figure 2 CD123CAR-DOT cells specifically target and eliminate CD123+AML cell lines and primary samples *in vitro*. (A) Cytotoxicity of CAR-DOTs and mock-DOTs against CD123+ AML (MOLM13 and THP-1) and CD123– T-ALL (Jurkat, negative control) cell lines at the indicated E:T ratios in 48 hours assays (n=5). Small insets, CD123 expression in each cell line. (B) AML primary sample (Pt, patient) phenotype showing CD33/CD123 analysis by FACS. AML blasts are highlighted in blue. (C) Absolute counts of alive eFluor+CD123+ AML blasts measured by FACS in 48-hour cytotoxicity assays at 1:1/2:1 E:T ratios. (D) Cytokine array determination in supernatants obtained from four donors of CAR-DOTs/mock-DOTs exposed to two different AML primary samples for 48 hours. Relative expression was normalized to mock-DOT levels. *p<0.05, **p<0.01, ***p<0.001. ALL, acute lymphoblastic leukemia; AML, acute myeloid leukemia; CAR, chimeric antigen receptor; DOTs, Delta One T cells; E:T, Effector:Target.

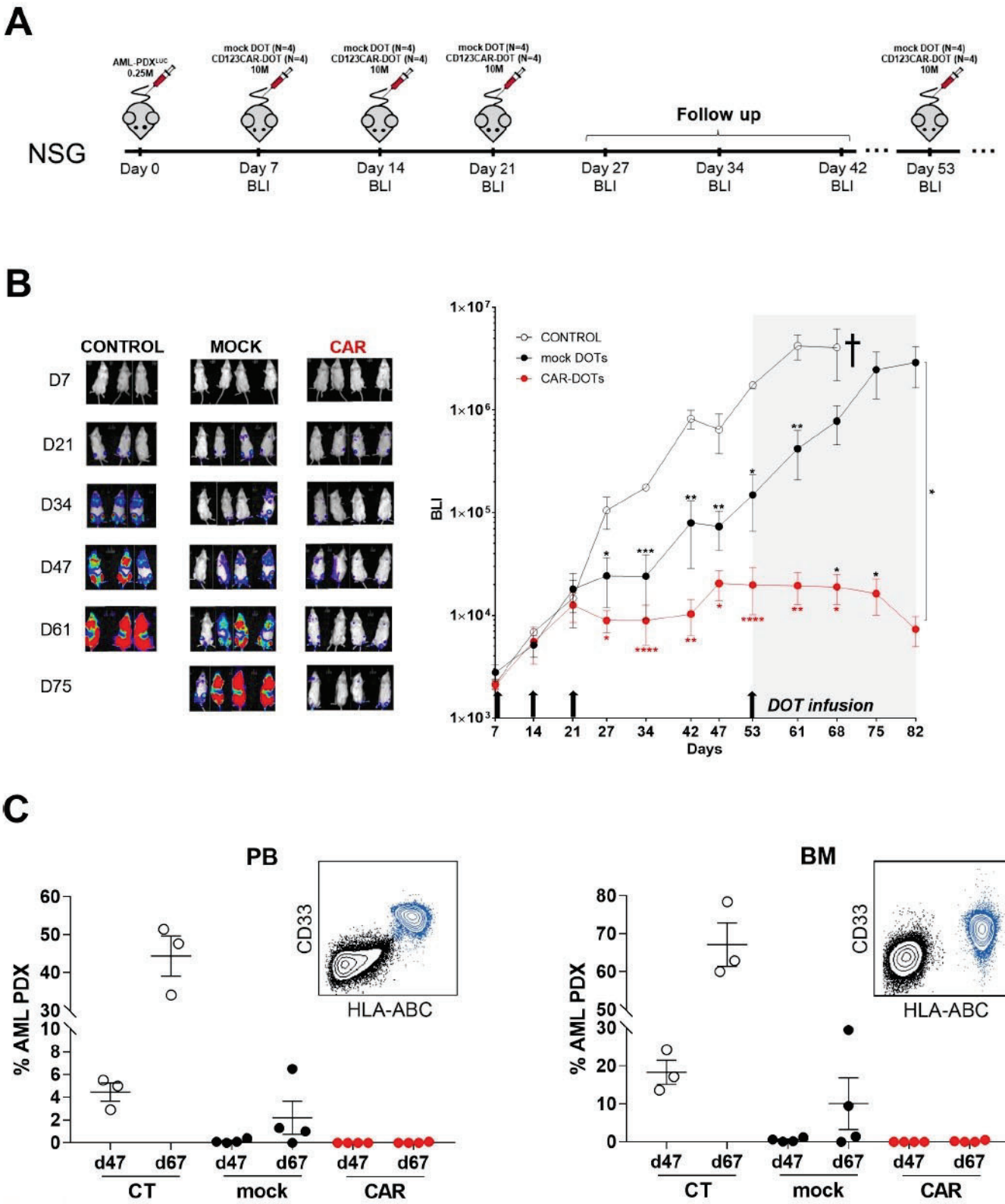

Figure 3 CD123CAR-DOT cells fully control growth of primary CD123+AML blasts in a PDX model. (A) Schematic of the AML-PDX model. NSG mice (n=4/group) were intravenously injected with 2.5×105 AML-PDX^{LUC} cells and then received three intravenous injections (one per week, starting 7 days after tumor injection) of 10×10^6 CAR-DOT or mock-DOT cells. Tumor burden was monitored weekly by BLI using IVIS imaging. At day 53, mock-treated and DOT-treated mice received an extra infusion of 10×10^6 mock-DOTs or CAR-DOTs, respectively. (B) IVIS imaging of tumor burden monitored by BLI at the indicated time points(escale: 5x10^4-1x10^6). Right panel shows the total radiance quantification (p/sec/cm^2/sr) at the indicated time points. †: sacrifice. (C) Tumor burden analyzed by FACS in PB and BM at days 47 and 67. Primary AML blasts are shown in blue. Mouse cells are shown in black. *p<0.05, **p<0.01, ***p<0.001. AML, acute myeloid leukemia; BLI, bioluminescence; BM, bone marrow; CAR, chimeric antigen receptor; DOTs, Delta One T cells; PB, peripheral blood; PDX, patient-derived xenograft.

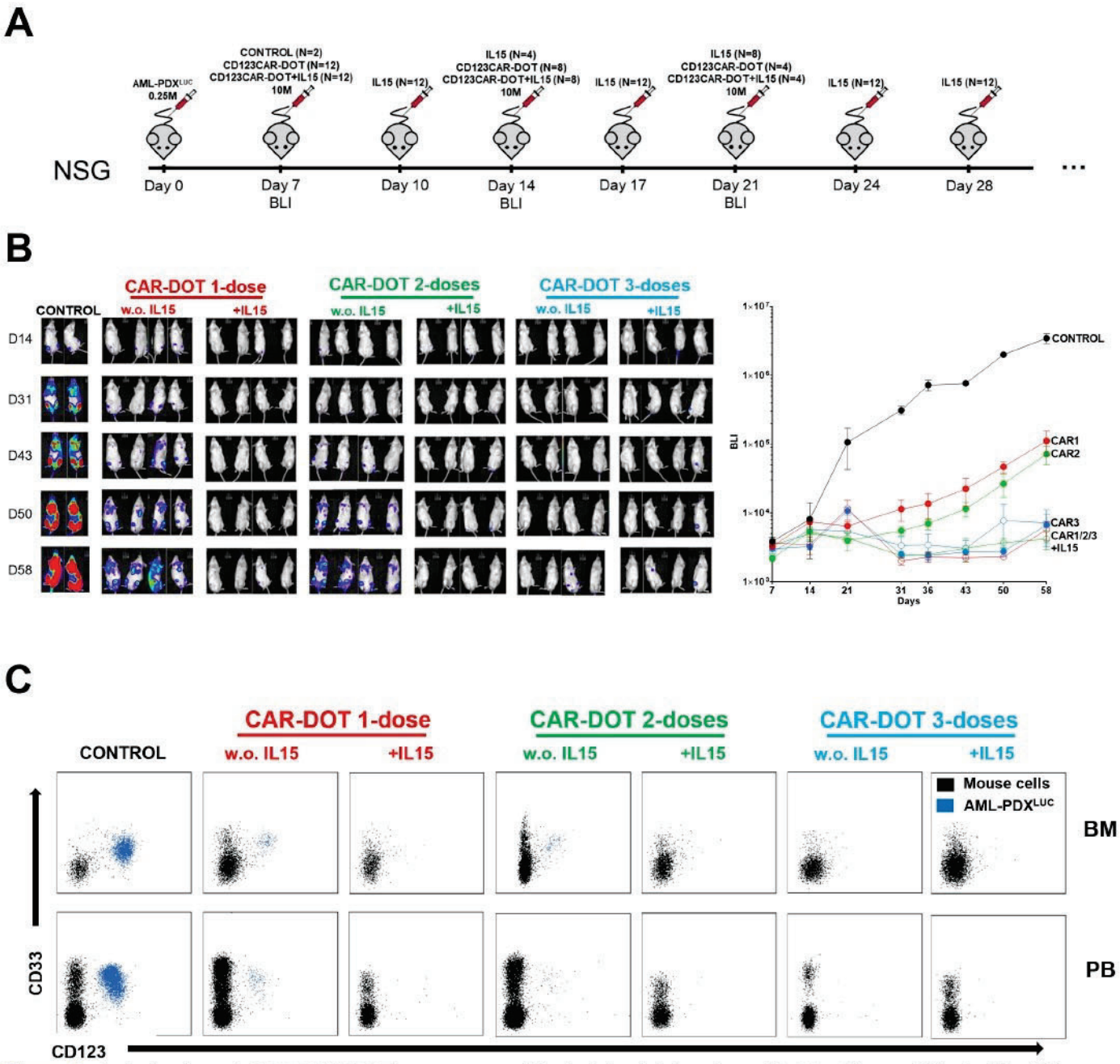

Figure 4 A single-dose of CD123CAR-DOT treatment combined with administration of IL-15 suffices to fully abolish AML progression in a PDX model. (A) Schematic of the AML-PDX model. NSG mice (n=4/group) were intravenously injected with 2.5×105 AML-PDX^{LUC} cells followed 7 days after by one, two or three intravenous injections (one per week) of 10×106 CAR-DOT cells, with or without administration of IL-15 intraperitoneally. (B) IVIS imaging of tumor burden monitored by BLI at the indicated time points(scale: 5x10^4-1x10^6). Right panel shows the total radiance quantification (p/sec/cm^2/sr) at the indicated time points. (C) Tumor burden analyzed by FACS in PB and BM at the end of the experiment. AML blasts are highlighted in blue. AML, acute myeloid leukemia; BLI, bioluminescence; BM, bone marrow; CAR, chimeric antigen receptor; DOTs, Delta One T cells; IL, interleukin; PB, peripheral blood; PDX, patient-derived xenograft.

adjuvant effect of exogenous IL-15 on CD123CAR-DOT therapy in AML-PDX *in vivo*.

Daily provision of IL-15 maximizes DOT-cell therapeutic efficacy *in vivo*

Building on the observed major impact of IL-15 on CD123CAR-DOT activity, we decided to evaluate side-by-side how IL-15 provision, in various regiments, would boost single-dose CD123CAR-DOT versus mock-DOT activities *in vivo*. In this experimental design, CD123CAR-DOTs or mock-DOTs were infused (in a single-one dose) 1 week after intravenous injection of 2.5×10^5 AML-PDX^{LUC} cells, followed by three different IL-15 administration regimens: daily, every 3–4 days, or none at all (figure 5A). Strikingly, mock-DOTs plus daily IL-15 showed similar leukemia

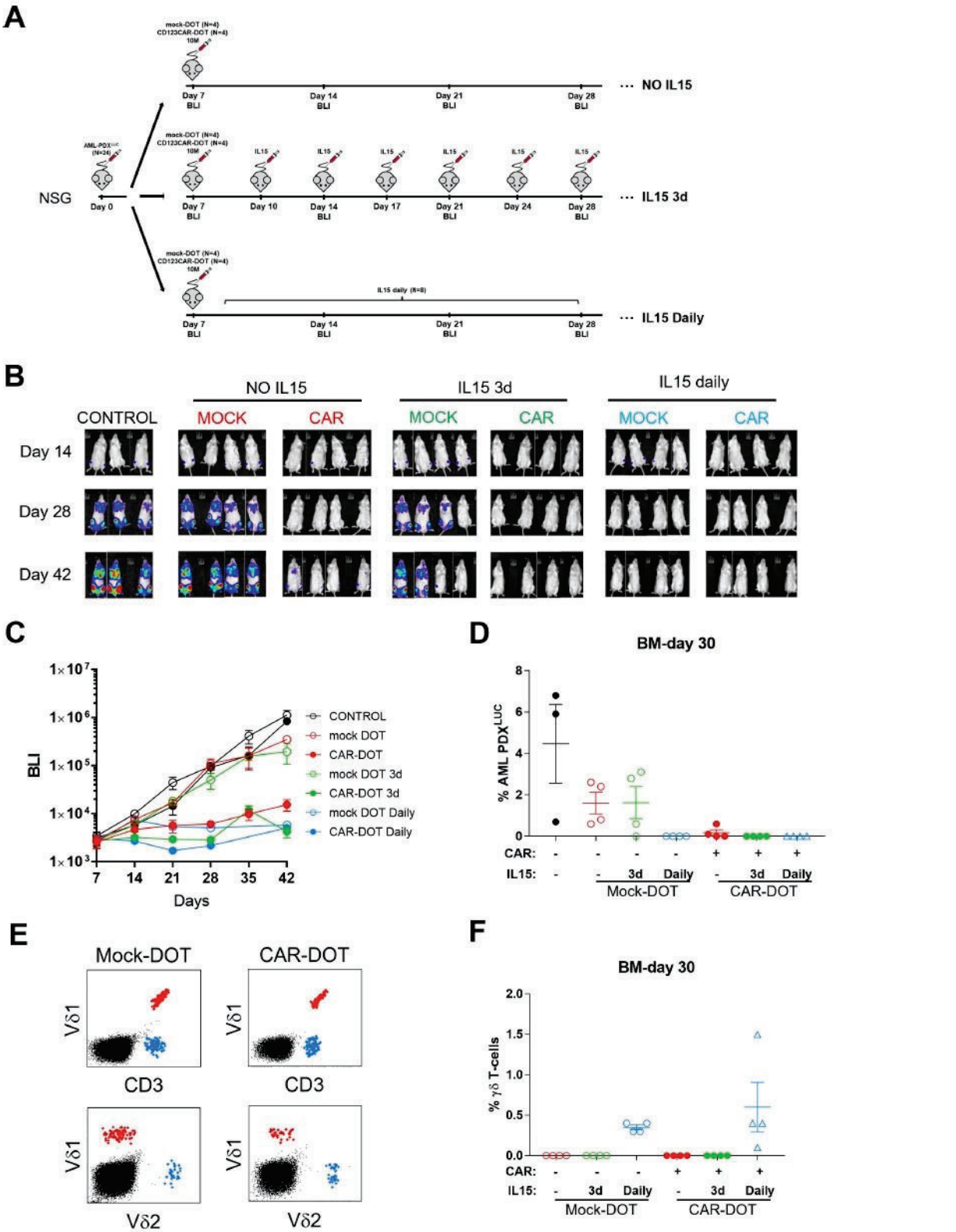

Figure 5 Daily-infused IL-15 increases DOT cell persistence and enables elimination of primary CD123+AML blasts in a PDX model. (A) Schematic of the AML-PDX model. NSG mice (n=4/group) were intravenously injected with 2.5×105 AML-PDX^{LUC} cells followed 7 days after by a one-single dose intravenous injection of 10×106 CAR-DOTs or mock-DOTs. Mock-DOT and CAR-DOT-treated mice were followed in the absence or presence of IL-15, intraperitoneal administered either daily or every 3–4 days. (B) IVIS imaging of tumor burden monitored weekly by BLI at the indicated time points (scale: 5x10^4-1x10^6). (C) Total radiance quantification (p/sec/cm^2/sr) at the indicated time points. (D) Tumor burden was monitored by FACS in BM at day 30. (E) Dot plots of representative Vδ1+ and Vδ2+T cells determined in CAR-DOT/ mock-DOT-treated mice in BM at day 30. (F) Total γδ T cells were monitored by FACS in BM at day 30. AML, acute myeloid leukemia; BLI, bioluminescence; BM, bone marrow; CAR, chimeric antigen receptor; DOTs, Delta One T cells; IL, interleukin; PB, peripheral blood; PDX, patient-derived xenograft.

control to all groups of CD123CAR-DOT-treated mice, as evaluated by BLI up to day 42 (figure 5B,C). The daily provision of IL-15 was critical to enhance mock-DOT cell activity, since the 3–4 day IL-15 regimen barely reduced tumor burden compared with control groups (figure 5B,C). These data were consolidated by flow cytometry analysis of BM aspirates, which showed that AML cell engraftment correlated with IVIS imaging (figure 5D). Importantly, the infused (CAR- or mock-) DOTs were only detected in the BM at the endpoint of the experiment when daily IL-15 was administered, thus highlighting the importance of *in vivo* persistence of the T_{EFF} (figure 5E,F). These data unveil the importance of *in vivo* IL-15 administration regimens on DOT-based therapies in AML.

Optimized CD123CAR-DOT treatment controls AML growth on *in vivo* rechallenge

Persistence is a key goal and a major challenge of adoptive cellular immunotherapy. Aiming to determine the sustained functionality and potency of (CAR- or mock-) DOTs after >40 days of controlling AML progression, we then performed a tumor rechallenge experiment. Disease-free mice that eliminated the previous AML graft (figure 5), either under all CD123CAR-DOT treatments or under mock-DOTs+daily IL-15, were rechallenged with an additional AML-PDX^{LUC} intravenous infusion at day 47 (figure 6A). In stark contrast to the other groups, CD123CAR-DOTs plus daily IL-15 was the only condition in which tumor growth kept controlled; in fact, AML cells were barely detectable by BLI or FACS analysis of PB and BM samples (figure 6B–E). These results firmly demonstrate a vigorous and persistent anti-leukemia effect of CD123CAR-DOTs plus daily IL-15, sustained over 70 days and even on tumor rechallenge, thus providing seminal proof-of-concept for their application for adoptive cellular immunotherapy in AML.

DISCUSSION

In the last few years, treatments for hematological neoplasias have undergone a revolution due to immunotherapy. In B-cell malignancies, autologous CAR-T cell therapies have rescued r/r patients on the path to palliative care, obtaining very impressive CR rates.[1 2] The number of CAR-T clinical trials keeps increasing, aiming to implement alternatives for bad prognosis tumors and expanding their horizons to other types of diseases (HIV, COVID-19, autoimmune diseases, cardiac damage, etc).[35–37] However, CAR-T cells are still at the beginning of their clinical implementation, and a significant fraction (around 50%) of the patients relapse after treatment in a relative short period of time.[3 4] Factors like the low number of T cells retrieved from the patient's leukapheresis, tumor blast contamination in the starting material, or T-cell exhaustion in multitreated patients, can all explain autologous CAR-T failures stemming from the manufacturing process.[38]

The BM of patients with leukemia is exposed to several cycles of chemotherapy and immunosuppressants, which alter the status of normal T cells.[5 39 40] Particularly in patients with AML, T cells have been characterized with an exhausted phenotype at relapse.[26] In this context, allogeneic T cells represent an attractive alternative, since circulating T cells from HDs have not suffered disease-induced or therapy-induced dysfunction. While various groups have reported the generation of allogeneic αβ T cells, these cells must undergo genetic manipulation, generally CRISPR/Cas9 editing, to eliminate the endogenous T-cell receptor (TCR) since it would otherwise drive a (potentially severe) graft-versus-host reaction. Elegant studies have reported the feasibility of these TCR^{KO} CAR-T cells in preclinical models and even in pediatric patients.[41–43] However, a relevant recent paper has reported that TCR elimination in CAR-T cells leads to a decrease in persistence.[44] Furthermore, from a clinical point-of-view, CRISPR/Cas9 handling would still have to solve complex regulatory requirements.

Since the vast majority of γδ T cells are HLA-independent,[45] they do not require genetic manipulation to be used as allogeneic therapies. It was with this purpose that we previously developed DOT cells, a Vδ1 T-cell-enriched cell product characterized by the upregulation of multiple activating/cytotoxicity-associated NK-cell receptors (NKG2D, DNAM-1, NKp30, NKp44), and showed their anti-leukemic potential.[10 14] However, our previous data in AML xenograft models left a significant margin for improvement in terms of control of tumor burden.[15] Here we investigated whether DOT transduction with a CD123-directed CAR would improve efficacy and lead to complete and durable leukemia remissions. We show that, compared (side-by-side) with control (mock-)DOTs, CAR123-DOTs are substantially more potent at eliminating AML blasts (both cell lines and primary samples) *in vitro*; release increased levels of key cytokines involved in immune orchestration and amplification of the antitumor response; and are more efficient at controlling tumor growth *in vivo*, in AML-PDX experiments conducted over 70 days.

We also found that on administration of IL-15 in our AML-PDX models, CD123CAR-DOTs (and also mock-DOTs) persisted better, thus allowing a single dose to maintain mice free of leukemia. Critically, daily-infused IL-15 enabled CD123CAR-DOTs to sustain their anti-leukemic activity for more than 70 days, even after AML rechallenge. These results are in agreement with recent elegant publications showing CAR-Vδ1 T-cell efficacy and the adjuvant effect of IL-15 in B-cell lymphoma and hepatocellular carcinoma models.[12 46] Of note, our study is the first to compare CAR-transduced with mock-transduced Vδ1 T cells, thus being able to ascertain the increased potency provided by CAR targeting. Only the clinical setting can establish the real benefit of IL-15 co-administration (potentially with an inducible 'switch off' system) with DOTs or CD123CAR-DOTs. Obviously, our (and other) preclinical mouse xenograft models lack

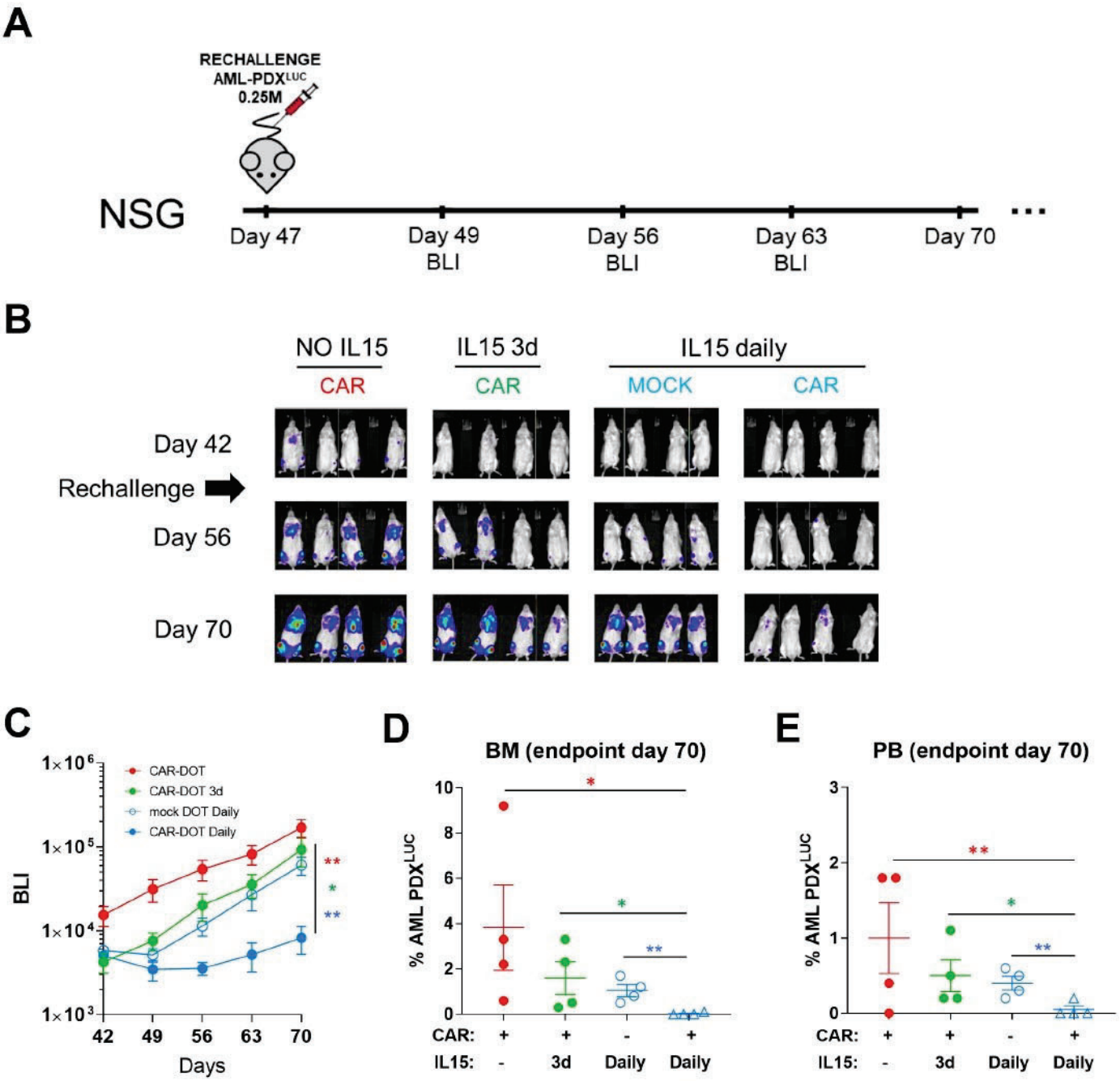

Figure 6 A single-dose of CD123CAR-DOT cells plus daily IL-15 sustain the ability to control AML progression on rechallenge in a PDX model. (A) Schematic of the tumor rechallenge AML-PDX^{LUC} experiments. Mock-DOTs plus daily IL-15-treated mice and CAR-DOTs-treated mice (regardless of IL-15 regiment) were rechallenged with 2.5×105 primary CD123+AML, 47 days after initial (CAR- or mock-) DOT cell infusion. (B) IVIS imaging of tumor burden monitored by BLI at the indicated time points (scale: 5x10^4-1x10^6). (C) Total radiance quantification (p/sec/cm^2/sr) over time in mice rechallenged with AML-PDX^{LUC}. Tumor burden was monitored at endpoint analysis (day 70) by FACS in BM (D) and PB (E). *p<0.05, **p<0.01, ***p<0.001 with one-tailed Student's t-test. AML, acute myeloid leukemia; BLI, bioluminescence; BM, bone marrow; CAR, chimeric antigen receptor; DOTs, Delta One T cells; IL, interleukin; PB, peripheral blood; PDX, patient-derived xenograft.

endogenous human IL-15; thus, basal circulating IL-15 levels in patients could suffice to sustain (CD123CAR-) DOT persistence and activity/efficacy in the clinical setting. Importantly, lymphodepletion regimens that are used prior to CAR T-cell infusions were shown to increase the levels of IL-15 in patients.[47] Therefore, although described as safe in non-human primates,[48] the need for exogenous (adjuvant) IL-15 should be carefully examined since it caused some toxicities in a recent clinical trial in patients with cancer.[49] This notwithstanding, this clinical trial employed a continuous bolus of IL-15 as single therapy, and thus, lower and/or intermittent IL-15 dosing may be a promising solutions.[50 51]

An important final aspect to discuss is the potential advantage of using DOTs as effector cells for CAR transduction. Compared with conventional αβ-dominated T-cell products, DOTs offer several advantages: first and foremost, the previously mentioned suitability for allogeneic use, without any need for additional genetic engineering,[52] and without any loss in potency (online supplemental figure S3). Additionally, the immune checkpoint PD-1 is absent in DOTs[10] and CD123CAR-DOTs (figure 1E), whereas the upregulated NK-associated cytotoxicity machinery (including DNAM-1, NKp30 and NKp44)[10 14] may be critical on CAR antigen loss as observed with CD19 in B-ALL.[6] Importantly, this enhanced NK-like cytotoxicity is also an advantage over other γδ T cell-based products being developed for adoptive immunotherapy of cancer.[7–9 12 46] On the other hand, in comparison with NK cells, which obviously share such activating NK-cell receptors, DOTs offer as key advantages[7 8 53] the previously documented[10] absence of inhibitory KIRs, namely KIR2DL1, KIR2DL2, KIR2DL4, KIR2DL5A and KIR3DL1, and the additional input of TCR-dependent activation and expansion (up to very high yields as reported).[10 14] In fact, the presence of a stochastically recombined and highly polyclonal TCR repertoire,[14] allowing HLA-unrestricted recognition of stress-induced molecules,[7] may also counteracts tumor immune evasion (via CAR antigen loss or HLA downregulation, eg). Moreover, the 'trophic' (homeostatic) signals received through γδ TCR binding to butyrophilins constitutively expressed in multiple tissues[54] may be beneficial for *in vivo* persistence, and may underlie the recent description of a striking Vδ1$^+$ T cell-associated CD19CAR-T cell expansion (from a very low initial frequency), over 10 years in a patient with disease-free Chronic Lymphocytic Leukemia (CLL).[55] Furthermore, although allogeneic CD19-directed CAR-NK cells have recently shown promising clinical results,[56] their 'off-the-shelf' implementation may be difficult due to the reported substantial decrease in viability after the freezing/thawing process,[57 58] which contrasts with the robustness we observed with CD123CAR-DOTs. We therefore strongly believe that CAR-DOTs combine a set of properties that may revolutionize allogeneic cell immunotherapy of hematological (and possibly also solid) cancers in the near future.

Author affiliations
[1]Josep Carreras Leukaemia Research Institute, Department of Biomedicine, School of Medicine, University of Barcelona, Barcelona, Spain
[2]Red Española de Terapias Avanzadas (TERAV) - Instituto de Salud Carlos III (ISCII) (RICORS, RD21/0017/0029)
[3]Instituto de Medicina Molecular João Lobo Antunes, Faculdade de Medicina, Universidade de Lisboa, Portugal
[4]Centro de Investigación Biomédica en Red-Oncología (CIBERONC), Instituto de Salud Carlos III, Barcelona, Spain
[5]Institució Catalana de Recerca i Estudis Avançats (ICREA), Barcelona, Spain

Acknowledgements We are indebted with Dr Talía Velasco-Hernández for technical support with interleukin-15 infusions, Dr Matteo Libero Baroni for retroviral cloning, Professor Irmela Jeremias for the Luc+ acute myeloid leukemia primografts, Dr Maksim Mamonkin for retroviral generation protocol kindly provided, Dr Clara Bueno and Dr Virginia Rodríguez for laboratory maintenance, Dr Pedro Roda for technical support, and Natacha Gonçalves-Sousa for administrative help.

Contributors Conception and design of the study: DSM, BS-S, PM. Acquisition of data: DSM, NT, SM, AM-M, PR, FGA, DVC. Analysis and interpretation of data: DSM, NT, SM, AM-M, PR, FGA, DVC. Writing original draft: DSM, BS-S, PM. Review and editing: DSM, NT, SM, BS-S, PM. Guarantors: PM, BS-S.

Funding "la Caixa" Foundation (ID 100010434) under the agreement LCF/PR/HR19/52160011 (BS-S, PM) ISCIII-RICORS within the Next Generation EU program (plan de recuperación, transformación y resilencia) (PM). CERCA/Generalitat de Catalunya (PM) Fundació Josep Carreras-Obra Social la Caixa (PM). Sara Borrell fellowship from the Instituto de Salud Carlos III (DS-M). FPU PhD Scholarship form MINECO (NT).

Competing interests BS-S and DVC were co-founders and shareholders of Lymphact/Gamma Delta Therapeutics. PM is co-founder of OneChain ImmunoTherapeutics, a spin-off from the Josep Carreras Leukemia Research Institute.

Patient consent for publication Not applicable.

Ethics approval Not applicable.

Provenance and peer review Not commissioned; externally peer reviewed.

Data availability statement All data relevant to the study are included in the article or uploaded as supplementary information.

ORCID iD
Diego Sánchez Martínez http://orcid.org/0000-0003-4605-5325

REFERENCES

1 Maude SL, Frey N, Shaw PA, *et al*. Chimeric antigen receptor T cells for sustained remissions in leukemia. *N Engl J Med* 2014;371:1507–17.
2 Ortíz-Maldonado V, Rives S, Castellà M, *et al*. CART19-BE-01: A Multicenter Trial of ARI-0001 Cell Therapy in Patients with CD19$^+$ Relapsed/Refractory Malignancies. *Mol Ther* 2021;29:636–44.
3 Gardner RA, Finney O, Annesley C, *et al*. Intent-to-treat leukemia remission by CD19 CAR T cells of defined formulation and dose in children and young adults. *Blood* 2017;129:3322–31.
4 Maude SL, Laetsch TW, Buechner J, *et al*. Tisagenlecleucel in children and young adults with B-cell lymphoblastic leukemia. *N Engl J Med* 2018;378:439–48.
5 Finney OC, Brakke HM, Rawlings-Rhea S, *et al*. CD19 CAR T cell product and disease attributes predict leukemia remission durability. *J Clin Invest* 2019;129:2123–32.
6 Xu X, Sun Q, Liang X, *et al*. Mechanisms of relapse after CD19 CAR T-cell therapy for acute lymphoblastic leukemia and its prevention and treatment strategies. *Front Immunol* 2019;10:1–15.
7 Sebestyen Z, Prinz I, Déchanet-Merville J, *et al*. Translating gammadelta (γδ) T cells and their receptors into cancer cell therapies. *Nat Rev Drug Discov* 2020;19:169–84.
8 Silva-Santos B, Mensurado S, Coffelt SB. γδ T cells: pleiotropic immune effectors with therapeutic potential in cancer. *Nat Rev Cancer* 2019;19:392–404.
9 Kabelitz D, Serrano R, Kouakanou L, *et al*. Cancer immunotherapy with γδ T cells: many paths ahead of US. *Cell Mol Immunol* 2020;17:925–39.

10 Almeida AR, Correia DV, Fernandes-Platzgummer A, *et al*. Delta one T cells for immunotherapy of chronic lymphocytic leukemia: clinical-grade expansion/differentiation and preclinical proof of concept. *Clin Cancer Res* 2016;22:5795–804.
11 Wang H, Chen H, Liu S, *et al*. Costimulation of γδTCR and TLR7/8 promotes Vδ2 T-cell antitumor activity by modulating mTOR pathway and APC function. *J Immunother Cancer* 2021;9:e003339–15.
12 Nishimoto KP, Barca T, Azameera A, *et al*. Allogeneic CD20-targeted γδ T cells exhibit innate and adaptive antitumor activities in preclinical B-cell lymphoma models. *Clin Transl Immunology* 2022;11:1–23.
13 Weng RR, Lu H-H, Lin C-T, *et al*. Epigenetic modulation of immune synaptic-cytoskeletal networks potentiates γδ T cell-mediated cytotoxicity in lung cancer. *Nat Commun* 2021;12:1–18.
14 Di Lorenzo B, Simões AE, Caiado F, *et al*. Broad cytotoxic targeting of acute myeloid leukemia by polyclonal delta one T cells. *Cancer Immunol Res* 2019;7:552–8.
15 Döhner H, Estey E, Grimwade D, *et al*. Diagnosis and management of AML in adults: 2017 ELN recommendations from an international expert panel. *Blood* 2017;129:424–47.
16 Kantarjian H, Kadia T, DiNardo C, *et al*. Acute myeloid leukemia: current progress and future directions. *Blood Cancer J* 2021;11:41.
17 DiNardo CD, Wei AH. How I treat acute myeloid leukemia in the era of new drugs. *Blood* 2020;135:85–96.
18 Johansson B, Harrison CJ. Acute myeloid leukemia. *Cancer Cytogenet* 2010:45–139.
19 Bras AE, de Haas V, van Stigt A, *et al*. CD123 expression levels in 846 acute leukemia patients based on standardized immunophenotyping. *Cytometry B Clin Cytom* 2019;96:134–42.
20 Haubner S, Perna F, Köhnke T, *et al*. Coexpression profile of leukemic stem cell markers for combinatorial targeted therapy in AML. *Leukemia* 2019;33:64–74.
21 Baroni ML, Sanchez Martinez D, Gutierrez Aguera F, *et al*. 41BB-based and CD28-based CD123-redirected T-cells ablate human normal hematopoiesis in vivo. *J Immunother Cancer* 2020;8:e000845.
22 Mardiana S, Gill S. Car T cells for acute myeloid leukemia: state of the art and future directions. *Front Oncol* 2020;10:1–12.
23 Gill S, Tasian SK, Ruella M, *et al*. Preclinical targeting of human acute myeloid leukemia and myeloablation using chimeric antigen receptor-modified T cells. *Blood* 2014;123:2343–54.
24 Kenderian SS, Ruella M, Shestova O, *et al*. CD33-specific chimeric antigen receptor T cells exhibit potent preclinical activity against human acute myeloid leukemia. *Leukemia* 2015;29:1637–47.
25 Liu P, Liu M, Lyu C, *et al*. Acute graft-versus-host disease after humanized Anti-CD19-CAR T therapy in relapsed B-ALL patients after allogeneic hematopoietic stem cell transplant. *Front Oncol* 2020;10:573822.
26 Noviello M, Manfredi F, Ruggiero E, *et al*. Bone marrow central memory and memory stem T-cell exhaustion in AML patients relapsing after HSCT. *Nat Commun* 2019;10:1–15.
27 Sánchez-Martínez D, Baroni ML, Gutierrez-Agüera F, *et al*. Fratricide-resistant CD1a-specific CAR T cells for the treatment of cortical T-cell acute lymphoblastic leukemia. *Blood* 2019;133:2291–304.
28 Menendez P, Redondo O, Rodriguez A, *et al*. Comparison between a lyse-and-then-wash method and a lyse-non-wash technique for the enumeration of CD34+ hematopoietic progenitor cells. *Cytometry* 1998;34:264–71.
29 Ebinger S, Zeller C, Carlet M, *et al*. Plasticity in growth behavior of patients' acute myeloid leukemia stem cells growing in mice. *Haematologica* 2020;105:2855–60.
30 Sánchez-Martínez D, Gutiérrez-Agüera F, Romecin P, *et al*. Enforced sialyl-Lewis-X (SLex) display in E-selectin ligands by exofucosylation is dispensable for CD19-CAR T-cell activity and bone marrow homing. *Clin Transl Med* 2021;11:e280.
31 Dalessandri T, Crawford G, Hayes M, *et al*. Il-13 from intraepithelial lymphocytes regulates tissue homeostasis and protects against carcinogenesis in the skin. *Nat Commun* 2016;7:12080.
32 McKenzie DR, Hart R, Bah N, *et al*. Normality sensing licenses local T cells for innate-like tissue surveillance. *Nat Immunol* 2022;23:411–22.
33 Park I-K, Giovenzana C, Hughes TL, *et al*. The Axl/Gas6 pathway is required for optimal cytokine signaling during human natural killer cell development. *Blood* 2009;113:2470–7.
34 Nagarsheth N, Wicha MS, Zou W. Chemokines in the cancer microenvironment and their relevance in cancer immunotherapy. *Nat Rev Immunol* 2017;17:559–72.
35 Aghajanian H, Kimura T, Rurik JG, *et al*. Targeting cardiac fibrosis with engineered T cells. *Nature* 2019;573:430–3.
36 Rurik JG, Tombácz I, Yadegari A, *et al*. CAR T cells produced in vivo to treat cardiac injury. *Science* 2022;375:91–6.
37 Maldini CR, Ellis GI, Riley JL. CAR T cells for infection, autoimmunity and allotransplantation. *Nat Rev Immunol* 2018;18:605–16.
38 Abou-El-Enein M, Elsallab M, Feldman SA, *et al*. Scalable manufacturing of CAR T cells for cancer immunotherapy. *Blood Cancer Discov* 2021;2:408–22.
39 Das RK, Vernau L, Grupp SA, *et al*. Naïve T-cell deficits at diagnosis and after chemotherapy impair cell therapy potential in pediatric cancers. *Cancer Discov* 2019;9:492–9.
40 Das RK, O'Connor RS, Grupp SA, *et al*. Lingering effects of chemotherapy on mature T cells impair proliferation. *Blood Adv* 2020;4:4653–64.
41 Qasim W, Zhan H, Samarasinghe S, *et al*. Molecular remission of infant B-ALL after infusion of universal TALEN gene-edited CAR T cells. *Sci Transl Med* 2017;9:1–9.
42 Rasaiyaah J, Georgiadis C, Preece R, *et al*. TCRαβ/CD3 disruption enables CD3-specific antileukemic T cell immunotherapy. *JCI Insight* 2018;3. doi:10.1172/jci.insight.99442. [Epub ahead of print: 12 07 2018].
43 Eyquem J, Mansilla-Soto J, Giavridis T, *et al*. Targeting a CAR to the TRAC locus with CRISPR/Cas9 enhances tumour rejection. *Nature* 2017;543:113–7.
44 Stenger D, Stief TA, Kaeuferle T, *et al*. Endogenous TCR promotes in vivo persistence of CD19-CAR-T cells compared to a CRISPR/Cas9-mediated TCR knockout CAR. *Blood* 2020;136:1407–18.
45 Vantourout P, Hayday A. Six-of-the-best: unique contributions of γδ T cells to immunology. *Nat Rev Immunol* 2013;13:88–100.
46 Makkouk A, Yang XC, Barca T, *et al*. Off-the-shelf Vδ1 gamma delta T cells engineered with glypican-3 (GPC-3)-specific chimeric antigen receptor (CAR) and soluble IL-15 display robust antitumor efficacy against hepatocellular carcinoma. *J Immunother Cancer* 2021;9.
47 Dudley ME, Yang JC, Sherry R, *et al*. Adoptive cell therapy for patients with metastatic melanoma: evaluation of intensive myeloablative chemoradiation preparative regimens. *J Clin Oncol* 2008;26:5233–9.
48 Berger C, Berger M, Hackman RC, *et al*. Safety and immunologic effects of IL-15 administration in nonhuman primates. *Blood* 2009;114:2417–26.
49 Conlon KC, Potter EL, Pittaluga S, *et al*. Il15 by continuous intravenous infusion to adult patients with solid tumors in a phase I trial induced dramatic NK-cell subset expansion. *Clin Cancer Res* 2019;25:4945–54.
50 Waldmann TA, Dubois S, Miljkovic MD, *et al*. Il-15 in the combination immunotherapy of cancer. *Front Immunol* 2020;11.
51 Dubois SP, Miljkovic MD, Fleisher TA, *et al*. Short-course IL-15 given as a continuous infusion led to a massive expansion of effective NK cells: implications for combination therapy with antitumor antibodies. *J Immunother Cancer* 2021;9.
52 Handgretinger R, Schilbach K. The potential role of γδ T cells after allogeneic HCT for leukemia. *Blood* 2018;131:1063–72.
53 Morandi F, Yazdanifar M, Cocco C, *et al*. Engineering the bridge between innate and adaptive immunity for cancer immunotherapy: focus on γδ T and NK cells. *Cells* 2020;9:1757.
54 Hayday AC, Vantourout P. The innate biologies of adaptive antigen receptors. *Annu Rev Immunol* 2020;38:487–510.
55 Melenhorst JJ, Chen GM, Wang M, *et al*. Decade-long leukaemia remissions with persistence of CD4$^+$ CAR T cells. *Nature* 2022;602:503–9.
56 Liu E, Marin D, Banerjee P, *et al*. Use of CAR-Transduced natural killer cells in CD19-Positive lymphoid tumors. *N Engl J Med* 2020;382:545–53.
57 Mark C, Czerwinski T, Roessner S, *et al*. Cryopreservation impairs 3-D migration and cytotoxicity of natural killer cells. *Nat Commun* 2020;11:1–8.
58 Liu S, Galat V, Galat Y, *et al*. Nk cell-based cancer immunotherapy: from basic biology to clinical development. *J Hematol Oncol* 2021;14:7.

SUPPLEMENTARY FIGURES

Sánchez-Martínez, D. et al. Figure S1

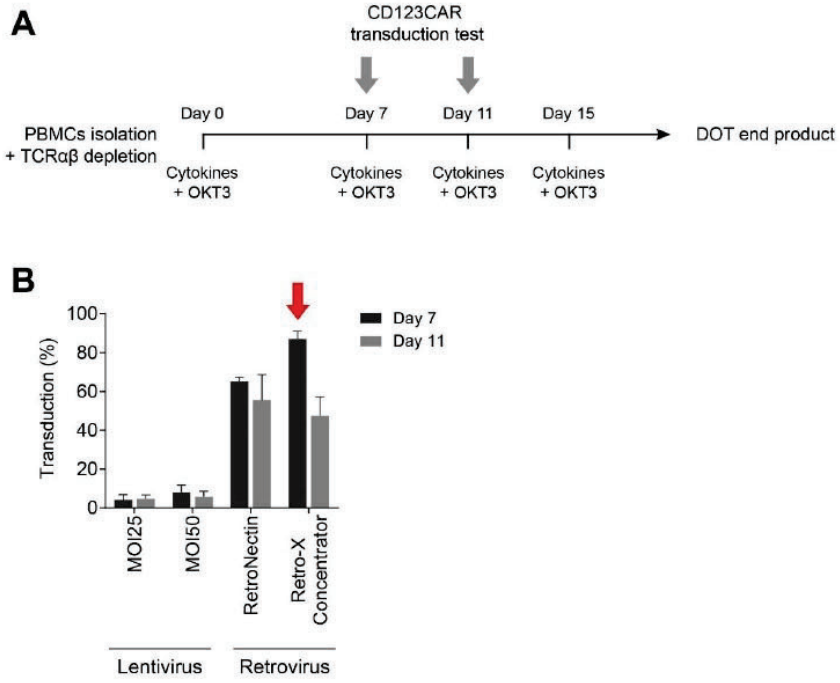

Figure S1. CD123CAR-DOT transduction protocol establishment. (A) CD123CAR-DOT transduction scheme. The cells were transfected at days 7 or 11 of the DOT protocol. **(B)** MOI (Multiplicity of infection) 25 and 50 for lentiviruses, RetroNectin and Retro-X Concentrator for retroviruses, were tested at day 7 or 11 to transfect DOT cells.

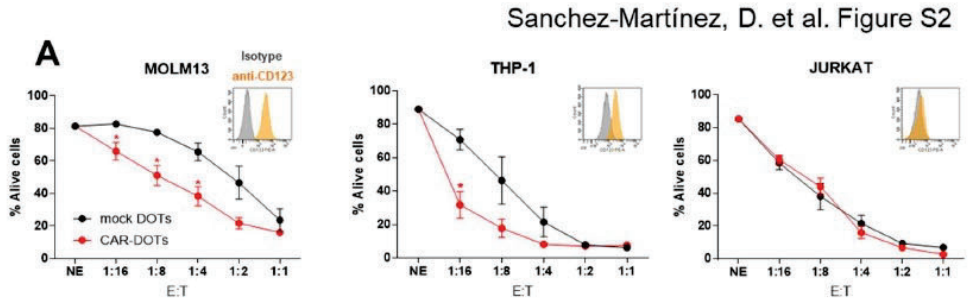

Figure S2. CD123CAR-DOTs specifically target and eliminate CD123+ AML cell lines *in vitro*. (A) Cytotoxicity of CAR-DOTs and mock-DOTs against $CD123^{+}$ AML (MOLM13 and THP-1) and $CD123^{-}$ T-ALL (Jurkat, negative control) cell lines at the indicated E:T ratios in 24-hour assays (n=5). *Small insets*, CD123 antigen density in each cell line. *p<0.05, **p<0.01, ***p<0.001.

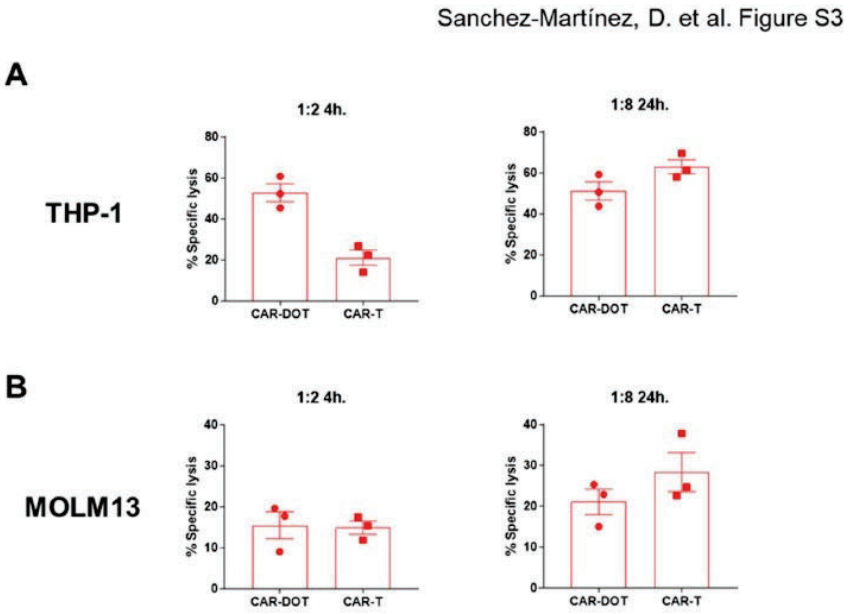

Figure S3. CD123 CAR-DOT cells show similar potency to CD123 CAR-T cells against CD123+ AML cells *in vitro*. Two cell lines were used as targets cells. Cytotoxicity assays were performed at E:T of 1:2 and 1:8 with readouts at 4h and 24h.

Sánchez-Martínez, D. et al. Figure S4

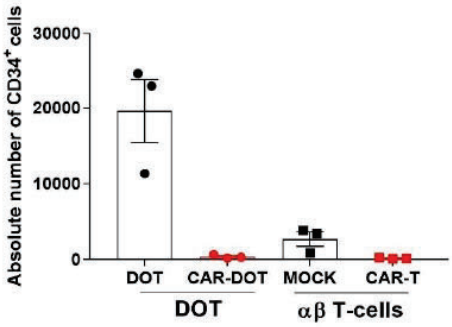

Figure S4. CD123 CAR-DOT cells eliminate CD34+ hematopoietic stem/progenitor cells *in vitro*. Alive CD34+ cells were quantified with Trucount tubes after 24h of incubation at 2:1 E:T.

Sánchez-Martínez, D. et al. Figure S5

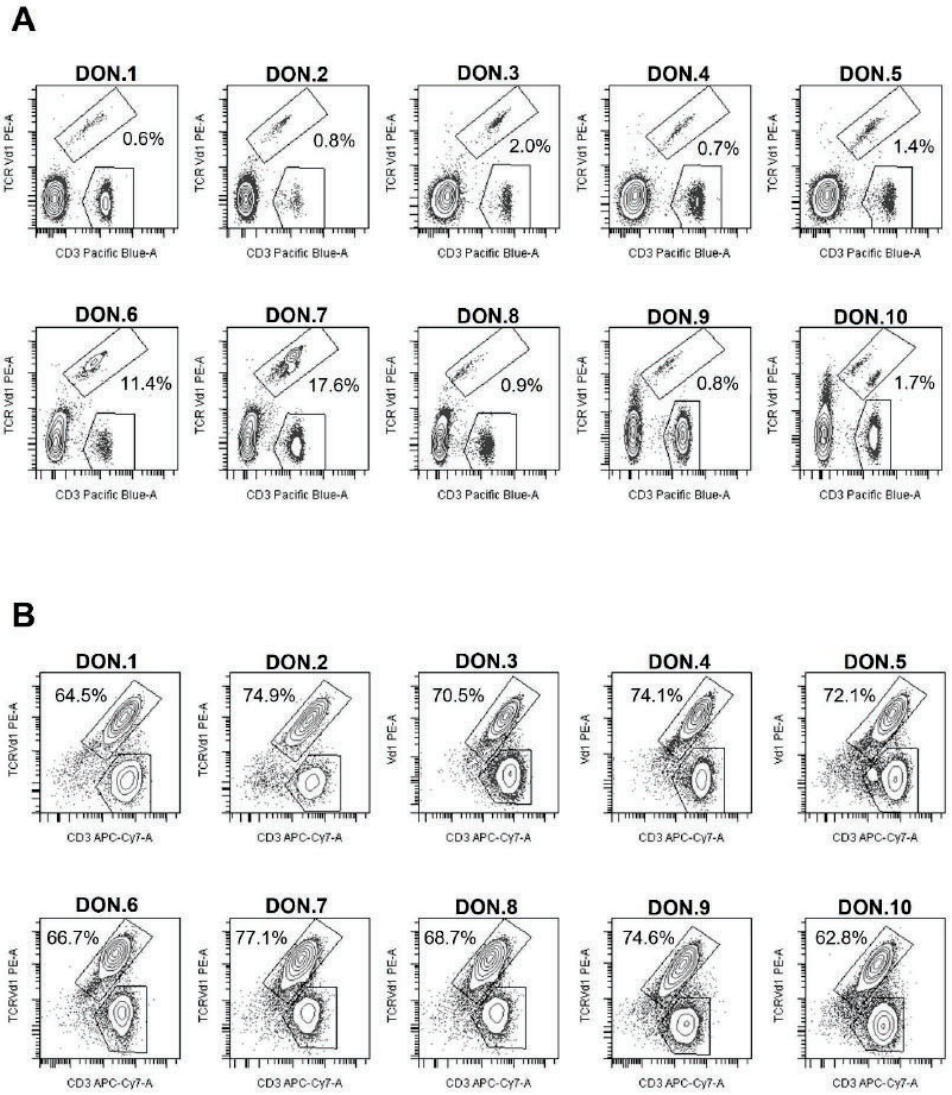

Figure S5. FACS analysis of Vδ1 γδT cells in each independent PB donor before and after DOT expansion. Vδ1 vs CD3 labeling at day 0 (A) and day 21 (B) of DOT protocol expansion (Fig 1B).

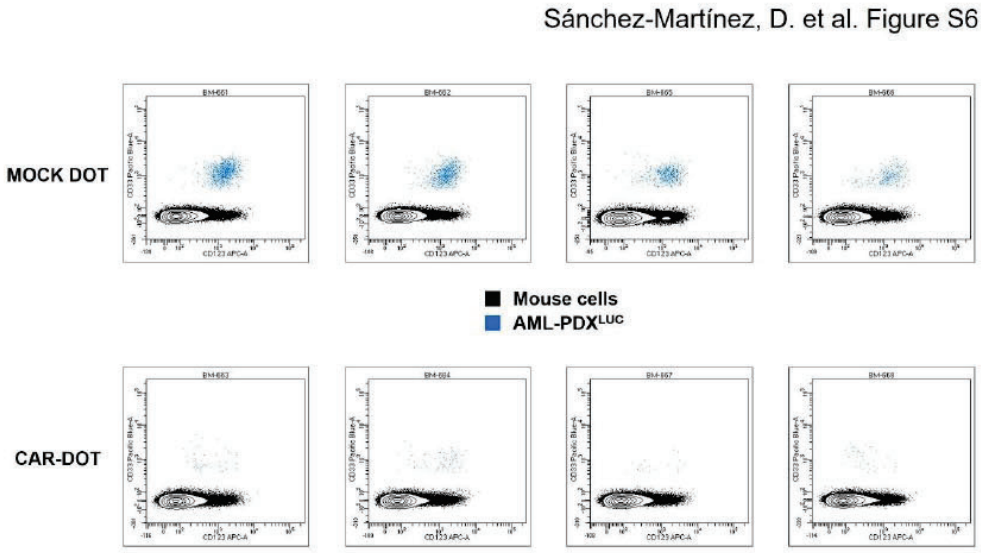

Figure S6. FACS determination of AML-PDX^{LUC} cells in mock/CAR-DOT-treated mice. Representative FACS dot plots at the time of sacrifice of four independent mice treated with mock-DOTs or CAR-DOTs + daily IL15. AML-PDX^{LUC} cells were identified as hHLA-ABC^{+}hCD45^{+}hCD33^{+}hCD123^{+} (blue). Black cells are hHLA-ABC^{-}hCD45^{-} mouse cells.

3.2. Efficient preclinical treatment of cortical T cell acute lymphoblastic leukemia with T lymphocytes secreting anti-CD1a T cell engagers

Anaïs Jiménez-Reinoso*, **Néstor Tirado***, Alba Martínez-Moreno, Víctor M Diaz, Marina García-Peydró, Oana Hangiu, Laura Díez-Alonso, Ángela Albitre, Petronila Penela, María L Toribio Pablo Menéndez, Luis Álvarez-Vallina, Diego Sánchez Martínez

* These authors contributed equally.

Journal for ImmunoTherapy of Cancer. 2022, 10(12):e005333

2022 Impact Factor: 12.485

Quartile 1 (Oncology, Immunology)

Journal for ImmunoTherapy of Cancer

Efficient preclinical treatment of cortical T cell acute lymphoblastic leukemia with T lymphocytes secreting anti-CD1a T cell engagers

Anaïs Jiménez-Reinoso ,[1,2,3] Néstor Tirado ,[4] Alba Martinez-Moreno,[4] Víctor M Díaz ,[5] Marina García-Peydró ,[6] Oana Hangiu,[1,2] Laura Díez-Alonso ,[1,2,3] Ángela Albitre,[6,7] Petronila Penela ,[6,7] Maria L Toribio ,[6] Pablo Menéndez ,[4,8,9,10,11] Luis Álvarez-Vallina ,[1,2,3,12] Diego Sánchez Martínez [4]

To cite: Jiménez-Reinoso A, Tirado N, Martinez-Moreno A, *et al*. Efficient preclinical treatment of cortical T cell acute lymphoblastic leukemia with T lymphocytes secreting anti-CD1a T cell engagers. *Journal for ImmunoTherapy of Cancer* 2022;**10**:e005333. doi:10.1136/jitc-2022-005333

► Additional supplemental material is published online only. To view, please visit the journal online (http://dx.doi.org/10.1136/jitc-2022-005333).

AJ-R and NT contributed equally.

Accepted 19 October 2022

For numbered affiliations see end of article.

Correspondence to
Dr Diego Sánchez Martínez; dsanchez@carrerasresearch.org

Dr Pablo Menéndez; pmenendez@carrerasresearch.org

Dr Luis Álvarez-Vallina; lav.imas12@h12o.es

ABSTRACT

Background The dismal clinical outcome of relapsed/refractory (R/R) T cell acute lymphoblastic leukemia (T-ALL) highlights the need for innovative targeted therapies. Although chimeric antigen receptor (CAR)-engineered T cells have revolutionized the treatment of B cell malignancies, their clinical implementation in T-ALL is in its infancy. CD1a represents a safe target for cortical T-ALL (coT-ALL) patients, and fratricide-resistant CD1a-directed CAR T cells have been preclinically validated as an immunotherapeutic strategy for R/R coT-ALL. Nonetheless, T-ALL relapses are commonly very aggressive and hyperleukocytic, posing a challenge to recover sufficient non-leukemic effector T cells from leukapheresis in R/R T-ALL patients.

Methods We carried out a comprehensive study using robust *in vitro* and *in vivo* assays comparing the efficacy of engineered T cells either expressing a second-generation CD1a-CAR or secreting CD1a x CD3 T cell-engaging Antibodies (CD1a-STAb).

Results We show that CD1a-T cell engagers bind to cell surface expressed CD1a and CD3 and induce specific T cell activation. Recruitment of bystander T cells endows CD1a-STAbs with an enhanced *in vitro* cytotoxicity than CD1a-CAR T cells at lower effector:target ratios. CD1a-STAb T cells are as effective as CD1a-CAR T cells in cutting-edge *in vivo* T-ALL patient-derived xenograft models.

Conclusions Our data suggest that CD1a-STAb T cells could be an alternative to CD1a-CAR T cells in coT-ALL patients with aggressive and hyperleukocytic relapses with limited numbers of non-leukemic effector T cells.

WHAT IS ALREADY KNOWN ON THIS TOPIC

⇒ Relapsed/refractory coT-acute lymphoblastic leukemia (ALL) displays a poor outcome and CD1a has recently been proposed as a specific and safe target for chimeric antigen receptor (CAR) T cell redirecting strategies in coT-ALL.

WHAT THIS STUDY ADDS

⇒ Secreted CD1a x CD3 T cell engaging antibodies (CD1a-STAb) show robust efficacy *in vitro* in recruiting bystander T cells and are as effective as CD1a-CAR T cells in *in vivo* cutting-edge patient-derived xenograft models.

HOW THIS STUDY MIGHT AFFECT RESEARCH, PRACTICE OR POLICY

⇒ This study validates the efficacy of T cell redirecting strategies targeting CD1a for coT-ALL and supports the therapeutic use of CD1a-STAbs as alternative to CD1a-CAR T cells in coT-ALL patients with limited numbers of non-leukemic effector T cells.

INTRODUCTION

T cell acute lymphoblastic leukemia (T-ALL) is a hematological malignancy resulting from the transformation and accumulation of T lineage precursor cells.[1] T-ALL is phenotypically and genetically very heterogeneous, with frequent genetic mutations in transcription factors and signaling pathways involved in hematopoietic homeostasis and T cell development.[2 3] T-ALL accounts for around 10%–15% and 20%–25% of all acute leukemias diagnosed in children and adults, respectively, with a median age at presentation of 9 years.[4] Although intensive chemotherapy regimens developed over the last two decades have allowed improved clinical management and survival rates, the 5-year event-free and overall survival rates are still low, especially in adult patients. More importantly, relapse/refractory (R/R) T-ALL remains a challenge with a particularly dismal outcome and lack of approved potentially curative options beyond hematopoietic stem cell transplantation and conventional chemotherapy, thus highlighting the need for novel targeted therapies.[5 6]

Immunotherapeutic strategies based on the redirection of the immune effector cells to

efficiently recognize and eliminate tumor cells has revolutionized cancer treatment.[7 8] In recent years, adoptive cell immunotherapies based on T cells bearing chimeric antigen receptors (CAR T) or systemic administration of bispecific T cell-engaging (TCE) antibodies have shown outstanding response rates in B cell malignancies, mainly B-ALL.[9–13] However, T cell-redirecting strategies for T cell malignancies raise additional challenges such as fratricide of effector T cells and potential life-threatening T cell aplasia due to shared antigen expression between effector T cells and T cell blasts,[14 15] reinforcing the need of both complex genome editing approaches of uncertain safety/efficacy and novel target antigens differentially expressed between normal T cells and T cell blasts.[16–21] In this sense, we have previously identified CD1a as a surface antigen with barely expression across human cells/tissues but highly and consistently expressed in blasts from patients suffering from cortical T-ALL (coT-ALL), a major subgroup of T-ALL, thus representing a therapeutic target for R/R coT-ALL patients while preventing effector T cell fratricide and T cell aplasia. We consequently generated and characterized CD1a-directed CAR T cells for the treatment of coT-ALL with robust and specific cytotoxicity against CD1a$^+$ T-ALL samples both *in vitro* and *in vivo* model.[22]

An emerging strategy which combines advantages of antibody-based and T cell-based therapies, termed Secreting T cell-redirecting Antibodies (STAb)-T immunotherapy,[23] involves the use of engineered T cells secreting small-sized bispecific anti-TAA (tumor-associated antigen) x anti-CD3 antibodies, such as diabodies[24–26] or tandem scFvs.[27] In contrast to CAR T cell therapies, T cell recruitment is not restricted to engineered T cells when using STAb T strategies. The polyclonal recruitment by secreted TCEs of both engineered and unmodified bystander T cells present at the tumor site might boost the antitumor T cell response. In fact, several groups have shown promising therapeutic effects of STAb T cells in CD19$^+$ B cell malignancies.[28–30]

Here, we report for the first time the generation of STAb T cells secreting an anti-CD1a x anti-CD3 TCE (CD1a-STAb T cells) and demonstrate their efficacy in several *in vitro* and *in vivo* cutting-edge models of coT-ALL. Our results indicate that STAb T therapy controls tumor progression similar to CD1a-CAR T therapy and exhibits slightly higher persistence of T cells *in vivo*. Our study suggests that CD1a-STAb T cells represent an alternative to CD1a-CAR T cells in coT-ALL, especially in R/R patients with leukapheresis products showing limited numbers of non-tumoral effector T cells.

METHODS

Cell lines and culture conditions

HEK293T (CRL-3216), MOLT4 (CRL-1582, ACC 362), NALM6 (CRL-3273), and K562 (CCL-243) cell lines were purchased either from the American Type Culture Collection (Rockville, Maryland, USA) or the DSMZ (Braunschweig, Germany). Target cells expressing the firefly luciferase gene were either produced in house (NALM6^{Luc}, K562^{Luc}) or a gift from Jan Cools Laboratory (MOLT4^{Luc}). HEK293T cells stably expressing extracellular CD1a (HEK293T^{CD1a}) were generated in house by transduction with pCCL lentiviral vectors encoding CD1a cDNA and cell sorting with anti-CD1a antibodies. HEK293T (WT and CD1a) cells were cultured in Dulbecco's modified Eagle's medium (DMEM) (Lonza, Walkersville, Maryland, USA) supplemented with 2mM L-glutamine (Life Technologies, Paisley, UK), 10% (vol/vol) heat inactivated fetal bovine serum (FBS) and antibiotics (100 units/mL penicillin, 100 µg/mL streptomycin) (both from Sigma-Aldrich, St. Louis, Missouri, USA), referred to as DMEM complete medium. MOLT4, NALM6, and K562 cells were cultured in RPMI-1640 (Lonza) supplemented with 2mM L-glutamine, 10% heat-inactivated FBS and antibiotics, referred to as RPMI complete medium (RCM). All the cell lines were grown at 37°C in 5% CO_2 and routinely screened for mycoplasma contamination by PCR using the Mycoplasma Gel Detection Kit (Biotools, Madrid, Spain).

Vector construction

The pCDNA3.1-CD1a-scFv expression vector encoding the human kappa (κ) light chain signal peptide L1,[31] followed by the NA1/34.HLK clone-derived CD1a scFv (V_H–V_L)[22] and a C-terminal polyHis tag was synthesized by GeneArt AG (ThermoFisher Scientific, Regensburg, Germany). To generate the CD1a-TCE-encoding lentiviral transfer vector, a synthetic gene encoding the L1-CD1a-scFv flanked by *Mlu*I and *Afe*I was synthesized by GeneArt AG and cloned into the vector pCCL-EF1α-LiTE-T2A-EGFP (unpublished), obtaining the plasmid pCCL-EF1α-CD1a-TCE-T2A-EGFP. The lentiviral transfer vector pCCL-EF1α-CD1a-CAR-T2A-EGFP encoding the CD1a-CAR was previously described.[22] pCCL lentiviral vectors encoding CD1a cDNA were obtained by blunt-*Xho*I and *Bam*HI subcloning from CD1A_OHu13436C_pcDNA3.1(+) (GenScript) into blunt-*Bsp*EI and *Bam*HI pCCL.

Cell transfection, T cell binding and activation assays

HEK293T^{WT} cells were transfected with the appropriate expression vectors using Lipofectamine 3000 Reagent (ThermoFisher Scientific, Waltham, Massachusetts, USA) according to the manufacturer's protocol. After 48 hours, transiently transfected HEK293T^{WT} cells were analyzed by flow cytometry and conditioned media were collected and stored at −20°C for western blotting, TCE binding assays and T cell activation studies. For CD1a-TCE binding assay, conditioned media from transiently transfected HEK293T^{WT} cells were incubated with CD1a-negative and CD1a-positive cells and analyzed with an APC-conjugated anti-His mAb (Miltenyi Biotec, Auburn, CA, USA) by flow cytometry. For T cell activation assays, CD1a-negative and CD1a-positive cells were cocultured with freshly isolated T cells at a 1:1 effector:target (E:T) ratio in the presence of conditioned media from transiently transfected HEK293T^{WT} cells. After 24 hours, T cell activation was

analyzed by flow cytometry using PE-conjugated anti-CD69 mAb.

Western blotting

Samples were separated under reducing conditions on 10%–20% Tris-glycine gels (Life Technologies, Carlsbad, California, USA), transferred onto PVDF membranes (Merck Millipore, Tullagreen, Carrigtwohill, Ireland) and probed with 200 ng/mL anti-His mAb (Qiagen, Hilden Germany), followed by incubation with 1.6 µg/mL horseradish peroxidase (HRP)-conjugated goat anti-mouse IgG, Fc specific (Sigma-Aldrich). Visualization of protein bands was performed with Pierce ECL Western Blotting substrate (Rockford, IL, USA) and ChemiDoc MP Imaging System machine (Bio-Rad Laboratories, Hercules, California, USA).

Lentivirus production and titration

CD1a, CD1a-CAR- or CD1a-TCE-encoding viral particles pseudotyped with vesicular stomatitis virus G glycoprotein were generated in HEK293T cells by using standard polyethylenimine transfection protocols and concentrated by ultracentrifugation, as previously described.[22] Viral titers were consistently in the range of 1×10^8 transducing units/mL. Functional titers of CD1a-CAR- and CD1a-TCE-encoding lentiviruses were determined by limiting dilution in HEK293T cells and analyzed using green fluorescent protein (EGFP) expression by flow cytometry.

T cell transduction and culture conditions

Peripheral blood mononuclear cells (PBMC) were isolated from volunteer healthy donors' peripheral blood (PB) or buffy coats by density-gradient centrifugation using Lymphoprep (Axis-Shield, Oslo, Norway) or Ficoll Paque Plus (GE Healthcare, Little Chalfont, UK). PBMC were plate-coated activated with 1 µg/mL anti-CD3 (OKT3) and 1 µg/mL anti-CD28 (CD28.2) mAbs (BD Biosciences) for 2 days and transduced (MOI of 10) with CD1a-CAR- or CD1a-STAb-encoding lentiviruses in the presence of 10 ng/mL interleukin (IL)-7 and 10 ng/mL IL-15 (Miltenyi Biotec, Bergisch Gladbach, Germany). As negative controls, non-transduced or GFP-transduced T cells were used (NT). T cells were expanded in RCM supplemented with IL-7 and IL-15 (10 ng/mL) (Miltenyi Biotec).[22 32]

Cytotoxicity assays

For cytotoxicity assays, target cells (cell lines and primary T-ALL blasts, 1×10^5 cells/well in a 96-well plate for cell lines and 2×10^5 for primary blasts) were labeled with 3 µM cell proliferation dye eFluor 670 (ThermoFisher Scientific) following manufacturer's instructions and co-cultured with NT, CD1a-CAR, or CD1a-STAb T cells at different E:T ratios for the indicated time periods. Effector cell-mediated cytotoxicity was assessed by flow cytometry analyzing the residual alive, non-apoptotic (7-aminoactinomycin D$^-$, AnnexinV$^-$) eFluor 670-positive target cells in each condition. For primary T-ALL blasts, absolute counts of target cells were also determined by using Trucount absolute counting tubes (BD Biosciences).[22] Additional wells with only target cells were always plated as controls. For bystander cytotoxicity assays, CD1a-CAR or CD1a-STAb T cells were co-cultured with or without non-transduced activated T cells (NT) and luciferase-expressing target cells ($K562^{Luc}$ or $MOLT4^{Luc}$) at the indicated E:T ratios. As controls, NT cells were cultured with target cells. After 48 hours, supernatants were collected and stored at −20°C for cytokine secretion analysis, and 20 µg/mL D-luciferin (Promega) was added before bioluminescence quantification using a Victor luminometer (PerkinElmer, Waltham, Massachusetts, USA). Percent-specific cytotoxicity was calculated using the formula: 100 – [(bioluminescence of each sample*100) / mean bioluminescence of NT-target cells]. Specific lysis was established as 100% of cell viability, and 100% lysis was established by adding 5% Triton X-100 into target cells. For cytotoxic studies using transwell non-contacting system, 5×10^4 $K562^{Luc}$ or $MOLT4^{Luc}$ cells and 1×10^5 NT cells were plated on bottom wells, and CD1a-CAR, CD1a-STAb or NT T cells were added at the indicated ratios into 0.4 µm-pore polycarbonate insert wells (Corning, Kennebunk, Maine, USA). Bioluminescence was quantified after 48 hours. For real-time cytotoxicity assays, the xCELLigence RTCA DP system (Acea BioSciences, San Diego, California, USA) was used. At day 0 1×10^4, $HEK293T^{WT}$ or $HEK293T^{CD1a}$ cells were plated in an E-Plate 16 (Acea Biosciences) and cultured at 37°C and 5% CO_2. After 24 hours, NT, CD1a-CAR or CD1a-STAb T cells were added at different E:T ratios and cell index values were measured every 15 min for 80 hours using RTCA Software 2.0 (Acea Biosciences). Specific lysis was established as 100% of cell viability of target cells, and 100% lysis was established by adding 10-fold diluted (in RCM) Cytolysis Reagent (Acea Biosciences) instead of effector cells.

Cytokine secretion analysis

IFN-γ, TNFα, and IL-2 secretion was analyzed by ELISA (Diaclone, Besancon Cedex, France; BD Biosciences), following manufacturer's instructions.

Flow cytometry

Antibodies used for flow cytometry analysis are detailed in online supplemental table S1. Cell surface expression of CD1a-CAR and cell surface-bound CD1a-TCE were detected using a biotin-SP goat anti-mouse IgG, $F(ab')_2$ (Jackson ImmunoResearch, West Grove, Pennsylvania, USA) and PE-conjugated streptavidin (ThermoFisher Scientific). Cell acquisition was performed in a BD FACSCanto II flow cytometer using BD FACSDiva software (BD Biosciences). Analysis was performed using FlowJo V10 software (Tree Star, Ashland, Oregon, USA).

In vivo T-ALL xenograft models

Seven to twelve-week-old NOD.Cγ-*Prkdc*^{scid} *Il2rg*^{tm1Wjl}/SzJ mice (NSG; The Jackson Laboratory, USA) were bred and housed under pathogen-free conditions. Mice were

infused intravenously with 3×10^6 MOLT4^{Luc} cells and 3 days later received 5×10^6 NT, CD1a-CAR, or CD1a-STAb T cells. Tumor growth was evaluated twice a week by bioluminescence imaging as previously described.[22 32] Tumor burden and T cell persistence was evaluated by flow cytometry in PB, and bone marrow (BM) after sacrifice at week 3. For T-ALL patient-derived xenograft (PDX) models, seven-to twelve-week-old NSG mice were sublethal irradiated (2 Gy) and intravenously transplanted with 1×10^6 CD1a$^+$ T-ALL PDX blasts. Two weeks later, mice were intravenously infused with $3–4\times10^6$ NT, CAR-CD1a, or STAb-CD1a T cells. Tumor burden and effector T cell persistence was followed up every 2 weeks by bleeding and by BM analysis at different time points, and subsequent flow cytometry analysis. *In vivo* studies were carried out at the Barcelona Biomedical Research Park (PRBB) in accordance with the guidelines of the Animal Experimentation Ethics Committee. All procedures were performed in compliance with the institutional animal care committee of the PRBB (DAAM9624).

Statistical analysis

Results of experiments are expressed as mean or mean±SE of the mean (SEM). Statistical tests indicated in figure legends were performed using Prism V.6 (GraphPad Software, La Jolla, California, USA). Significance was considered only when p values were less than 0.05 (*p<0.05; **p<0.01; ***p<0.001, ****p<0.0001).

RESULTS

The CD1a-TCE binds to cell surface expressed CD1a and CD3 and induces specific T cell activation

To generate a small-sized Fc-free CD1a-directed TCE, the NA1/34.HLK scFv and the OKT3 scFv were fused in tandem via a G_4S peptide linker[27] and cloned under the control of the EF1α promoter in a T2A-based bicistronic lentiviral vector (pCCL-EF1α-CD1a-TCE-T2A-EGFP, figure 1A,B). The vector encoding an anti-CD1a second-generation (4-1BB-based) CAR (pCCL-EF1α-CD1a-CAR-T2A-EGFP, figure 1C,D) has been described previously.[22] The CD1a-TCE was efficiently secreted by transfected HEK293T^{WT} cells with the expected molecular weight of 58 kDa (online supplemental figure S1A). Binding assays using CD1a$^-$CD3$^-$ K562 cells, CD1a$^+$CD3$^-$ MOLT4 cells, and CD1a$^-$CD3$^+$ primary PB lymphocytes (online supplemental figure S2) demonstrated the bispecificity of the secreted CD1a-TCE (online supplemental figure S1B). To study the biological activity of the secreted CD1a-TCE on T cell activation, primary T cells were co-cultured with K562 or MOLT4 cells in the presence of cell-free conditioned medium (CM) derived from non-transfected (NT) or transiently transfected (CD1a-CAR or CD1a-TCE) HEK293T^{WT} cells. High expression of CD69 was detected only when T cells were co-cultured with CD1a-positive cells in the presence of CD1a-TCE CM. T cell activation was not detected when CM from NT or CD1a-CAR-transfected HEK293T^{WT} cells were used (online supplemental figure S1C).

Generation of human primary CD1a-STAb T cells

We next transduced primary T cells with CD1a-CAR- or CD1a-TCE-encoding lentiviruses. Transduction efficiencies were determined by flow cytometry after 4–8 days according to the percentage of GFP$^+$CD3$^+$ cells (figure 1E). CD1a-CAR surface expression as well as CD1a-TCE decoration in CD1a-STAb T cells were successfully detected using a polyclonal anti-F(ab')$_2$ antibody (figure 1F) recognizing the scFv domains of both CD1a-CAR and CD1a-TCE constructs. Transduction efficiencies were 40%–50% and 20%–30% for CD1a-CAR- and CD1a-TCE-transduced T cells, respectively. While in CD1a-CAR-transduced T cells the expression of EGFP and F(ab')$_2$ mainly identifies a single transduced population (figure 1F, upper panel), in CD1a-TCE-transduced T cells several subpopulations are distinguished: transduced/decorated T cells (GFP$^+$F(ab')$_2^+$), non-transduced/decorated T cells (GFP$^-$F(ab')$_2^+$), and transduced/non-decorated T cells (GFP$^+$F(ab')$_2^-$) (figure 1F, lower panel). Transduced CD1a-CAR T cells and CD1a-STAb T cells exhibited a similar proportion of CD4$^+$ and CD8$^+$ cells (figure 1G). The relative distribution of naïve, central memory, effector memory, and effector T cell subsets was similar in NT, CD1a-CAR$^{+/-}$ and CD1a-STAb$^{+/-}$ T cells, with the most prevalent subset being effector memory T cells (figure 1H).

STAb-CD1a T cells induce a more potent and rapid cytotoxic responses than CAR-CD1a T cells

To test the ability of CD1a-CAR and CD1a-STAb T cells to kill CD1a$^+$ T-ALL cells, several cytotoxicity assays were conducted. First, we studied the killing capacity of non-transduced (NT), CD1a-CAR, and CD1a-STAb transduced T cells at different E:T ratios after 24 hour co-culture with CD1a$^-$ (NALM6) or CD1a$^+$ (MOLT4) cells (online supplemental figure S2). CD1a-STAb T cells were able to significantly eliminate CD1a$^+$ cells even at a 1:16 E:T ratio and induce ~90% cytotoxicity at a 1:1 E:T ratio. In contrast, CD1a-CAR T cells only exhibited significant cytotoxicity at high E:T ratios (figure 1I). Similar results were obtained using primary T-ALL samples in 24 hour assays, where co-culture with CD1a-STAb T cells induced a slight increase in target cell death compared with CD1a-CAR T cells (figure 1J, online supplemental figure S2). In short-time co-culture systems with CD1a$^-$ or CD1a$^+$ target cells at a 1:4 E:T ratio, CD1a-STAb T cells killed, in clear contrast to CD1a-CAR T cells, a significant proportion of leukemic cells after 2 hours (35%) and 4 hours (70%) (figure 1K). Next, using an impedance-based real-time cytotoxicity assay, CD1a-STAb T cells mediated a rapid reduction of CD1a$^+$ target cell viability (online supplemental figure S3A), whereas CD1a-CAR T cells showed a significantly lower cytotoxic effect that required higher E:T ratios (figure 1L). Target cells cultured alone (online

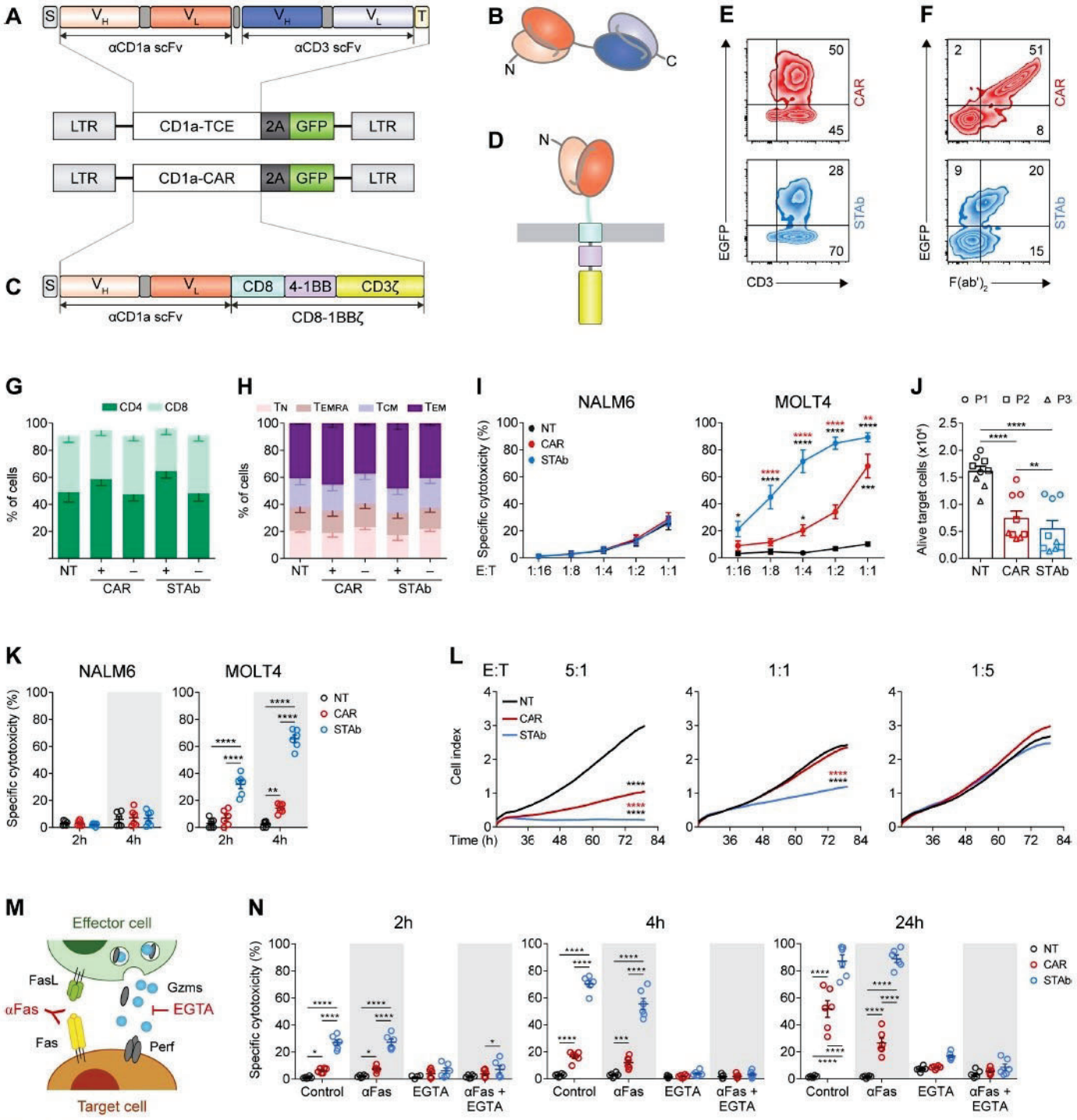

Figure 1 continued on next page

Figure 1 continued

Figure 1 Comparative *in vitro* study of engineered CD1a-STAb and CD1a-CAR T cells. (A, B) Schematic diagrams showing the genetic (A) and domain structure (B) of the CD1a-TCE bearing a signal peptide from the human κ light chain signal peptide (S, gray box), the anti-CD1a scFv gene (orange boxes), the anti-CD3 scFv gene (blue boxes), and the Myc and his tags (light yellow box). (C, D) Schematic diagrams showing the genetic (C) and domain structure (D) of the CD1a-CAR bearing the CD8a signal peptide (S, gray box), the anti-CD1a scFv gene (orange boxes), followed by the human CD8 transmembrane domain and the human 4-1BB and CD3ζ endodomains. CD1a-TCE and CD1a-CAR constructs were cloned into a pCCL lentiviral-based backbone containing a T2A-enhanced green fluorescent protein (GFP) cassette (A, C). (E, F) Percentage of reporter GFP (E) and $F(ab')_2$ (F) expression in CD1a-CAR and CD1a-STAb T cells. One representative transduction out of four independent transductions performed is shown. Numbers represent the percentage of cells staining positive for the indicated marker. (G, H) Percentages of $CD4^+$ and $CD8^+$ T cells (G) and percentages of naïve (T_N), effector memory re-expressing CD45RA (T_{EMRA}), central memory (T_{CM}), and effector (T_{EM}) T cells (H) among non-transduced (NT), or CD1a-CAR and CD1a-STAb transduced T cells. (I) Specific cytotoxicity of NT, CD1a-CAR or CD1a-STAb T cells toward CD1a negative (NALM6) or CD1a positive (MOLT4) cells at the indicated E:T ratios after 24 hours. (J) Alive primary cells from three different coT-ALL patients (P1, P2, P3) after 24 hours co-culture at a 1:1 E:T ratio with NT, CD1a-CAR or CD1a-STAb T cells. (K) Specific cytotoxicity of NT, CD1a-CAR or CD1a-STAb T cells toward NALM6 or MOLT4 cells at 1:4 E:T ratio after 2 and 4 hours. (L) Real-time cell cytotoxicity assay with $HEK293T^{CD1a}$ target cells co-cultured with NT, CD1a-CAR or CD1a-STAb T cells at the indicated E:T ratios. Cell index values were determined every 15 min for 80 hours using an impedance-based method. Data from (G–L) is shown as mean±SEM of at least three independent experiments by triplicates (n=9). (M) Cartoon depicting target cell death induction by FasL and perforin/granzymes, and how these pathways can be blocked using anti-Fas mAb or EGTA, respectively. (N) Cytotoxicity of MOLT4 cells at 2 and 4 hours (E:T ratio 1:1) and at 24 hours (E:T ratio 1:4) in the presence or absence of anti-Fas mAb or EGTA. Plots show mean±SEM of two independent experiments with triplicates (n=6). Statistical significance was calculated by one-way (L) or two-way (G–K, N) ANOVA test corrected with a Tukey's multiple comparisons test (*p<0.05; **p<0.01; ***p<0.001, ****p<0.0001). ALL, acute lymphoblastic leukemia; ANOVA, analysis of variance; CAR, chimeric antigen receptor; E:T, effector:target; STAb, secreting T cell-redirecting antibodies.

supplemental figure S3B) revealed similar viability kinetics to the co-culture of NT cells with $CD1a^+$ cells as well as the co-culture of NT, CD1a-CAR or CD1a-STAb T cells with $CD1a^-$ cells (online supplemental figure S3C).

After 24 hour co-culture at a 1:1 E:T ratio, TNFα was significantly increased only in co-cultures of $CD1a^+$ target cells with CD1a-STAb T cells. However, IL-2 secretion was significantly higher in co-cultures of $CD1a^+$ target cells with CD1a-CAR T cells (online supplemental figure S3D). IFNγ levels were similar in co-cultures of CD1a-CAR or CD1a-STAb T cells with MOLT4 and primary T-ALL cells (online supplemental figure S3D), revealing different proinflammatory cytokine profiles depending on whether the CD1a-specific interaction was triggered by CAR or STAb T cells.

CD1a-STAb T cells eliminate T-ALL cells through the granular exocytosis pathway

To determine the effector mechanisms involved in CD1a-CAR and CD1a-STAb killing of T-ALL cells, we used the Ca^{2+}-chelating agent EGTA to inhibit granular exocytosis and/or a blocking anti-Fas mAb[18 33] (figure 1M). In control (untreated) conditions, CD1a-STAb T cells induce higher cytotoxicity than CD1a-CAR-T cells on MOLT4 cells at the different time points tested (2, 4, and 24 hours). The cytotoxic action of both CD1a-CAR and CD1a-STAb T cells was completely ablated on EGTA treatment, indicating their dependence on the granular exocytosis pathway to induce target cell death (figure 1N). However, Fas blockage did not diminish lysis levels, showing no influence in the cytotoxic process (figure 1N). These data suggest that CD1a-directed CAR and STAb T cells follow a different kinetic profile but share the same cytolytic effector mechanisms.

Recruitment of bystander T cells provides STAb-CD1a T cells with greater *in vitro* tumor cell killing efficiency than CD1a-CAR T cells

To study the ability of CD1a-STAb T cells to recruit non-engineered bystander T cells, direct contacting co-culture systems were performed (figure 2A). Keeping a constant number of 5×10^4 $CD1a^+$ $MOLT4^{Luc}$ cells, decreasing numbers of activated effector T cells (AT: NT, CD1a-CAR or CD1a-STAb T cells) were added to the culture, resulting in different AT:Target ratios (from 1:50 000 to 2:1). Increasing numbers of NT bystander T cells were added to maintain a constant 2:1 E(AT+bystander):T ratio (figure 2C). The bystander recruitment ability of CD1a-STAb T cells was demonstrated by their enhanced specific cytotoxicity achieved at an E:T ratio as low as 1:50 after 48 hour co-culture with $MOLT4^{Luc}$ cells. In contrast, CD1a-CAR T cell-mediated cytotoxicity against $CD1a^+$ cells only reached that shown by CD1a-STAb T cells at the highest E:T ratio (2:1), with significantly reduced cytotoxicity across lower E:T ratios.

Interestingly, the levels of IFNγ secretion by CD1a-CAR T cells were higher than in CD1a-STAb T cells at the highest E:T condition (figure 2C), but these levels rapidly decreased at lower E:T ratios, indicating that the bystander effect mediated from CD1a-STAb T cells offers equal or superior cytotoxicity capacity than CD1a-CAR T cells without an enhanced cytokine release. No cytotoxicity, bystander effect or IFNγ secretion were detected after 48 hours direct co-culture of activated effector cells with $CD1a^-$ ($K562^{Luc}$) cells (online supplemental figure S3E).

To further demonstrate the bystander effect of CD1a-STAb T cells, similar co-cultures were performed in a non-contacting transwell system (figure 2B). Keeping

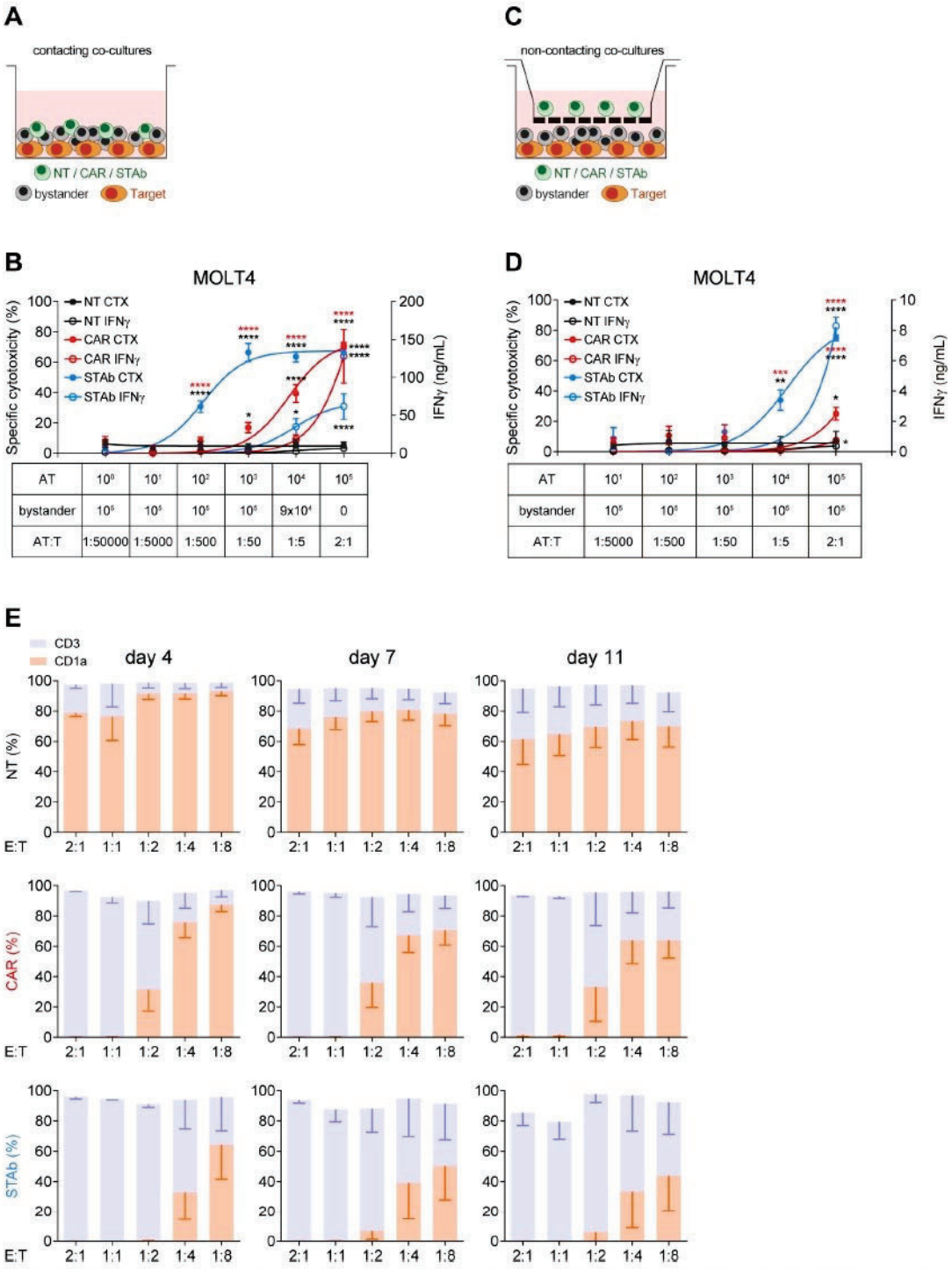

Figure 2 STAb-CD1a T cells display enhanced tumor cell killing by recruiting bystander T cells. (A, B) Schematic representation of the direct contact (A) and the non-contacting Transwell (B) co-culture systems used to study the ability of secreted CD1a-STAb to induce bystander T cell cytotoxicity. (C) Decreasing numbers of activated effector T (AT) cells (NT, CD1a-CAR or CD1a-STAb) were co-cultured with 5×10^4 MOLT4^{Luc} target cells and increasing numbers of NT T cells from the same donor (bystander T cells), resulting in the indicated AT:T ratios but maintaining a constant 2:1 effector (AT+bystander):Target ratio. (D) 5×10^4 MOLT4^{Luc} cells and 1×10^5 bystander T cells were plated in the bottom well and decreasing numbers (from 1×10^5 to 1×10^1) of activated T (AT) cells (NT, CD1a-CAR or CD1a-STAb) in the upper well. After 48 hours, the percentage of specific cytotoxicity was calculated by adding D-luciferin to detect bioluminescence, and IFNγ secretion was determined by ELISA (C, D). (E) MOLT4 cells were co-cultured with NT, CD1a-CAR or CD1a-STAb T cells at the indicated E:T ratios, and the expression of CD3 and CD1a was analyzed by flow cytometry after 4 and 11 days to assess potential leukemia escape. Data represent mean±SEM of at least three independent experiments by triplicates. Significance was calculated by a two-way ANOVA test corrected with a Tukey's multiple comparisons test (*p<0.05; **p<0.01; ***p<0.001, ****p<0.0001). ANOVA, analysis of variance; E:T, effector:target; NT, non-transduced; CAR, chimeric antigen receptor; STAb, secreting T cell-redirecting antibodies.

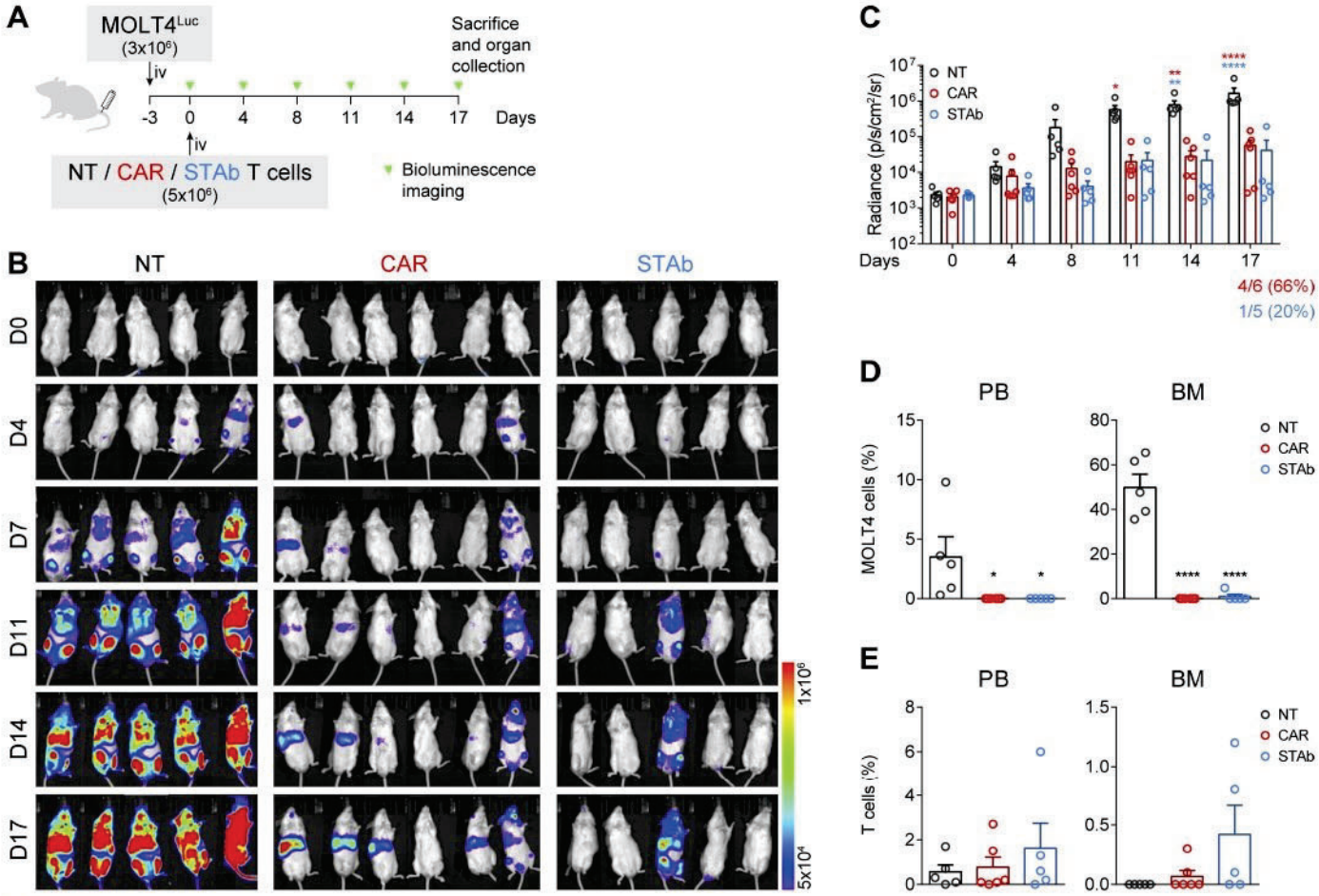

Figure 3 CD1a-STAb T cells control the progression of coT-ALL cells *in vivo*. (A) Experimental design of *in vivo* cytotoxicity in NSG mice intravenously engrafted with MOLT4^{Luc} cells followed by infusion of NT, CD1a-CAR, or CD1a-STAb T cells. (B, C) Bioluminescence images monitoring disease progression (B) and total RADIANCE quantification at the indicated time points (C). (D) Percentage of MOLT4 cells, identified as HLA-ABC$^+$CD45$^+$CD1a$^+$CD3$^-$ by flow cytometry, in peripheral blood (PB) and bone marrow (BM) at sacrifice. (E) Percentage of T cells, identified as HLA-ABC$^+$CD45$^+$CD1a$^-$CD3$^+$ by flow cytometry, in PB, BM and spleen at sacrifice. Plots from (C), D), E) show mean±SEM of at least 5 mice per group. Statistical significance was calculated by an one-way ANOVA test corrected with a Tukey's multiple comparisons test (*p<0.05; **p<0.01; ***p<0.001, ****p<0.0001). ALL, acute lymphoblastic leukemia; ANOVA, analysis of variance; NT, non-transduced; CAR, chimeric antigen receptor; STAb, secreting T cell-redirecting antibodies.

a constant number of 5×10^4 MOLT4^{Luc} cells and 1×10^5 non-engineered bystander T cells both plated in the bottom well, decreasing numbers (from 1×10^5 to 1 x 10^1) of AT (NT, CD1a-CAR or CD1a-STAb T cells) were plated in the insert upper well of the transwell system. After 48 hours, cell killing was only detected when CD1a-STAb T cells were present, indicating that secreted CD1a-TCEs effectively redirected non-engineered bystander T cells toward CD1a$^+$ target cells in the bottom wells (figure 2D). IFNγ secretion was also dependent on the presence of CD1a-STAb T cells in the transwell system (figure 2D). In contrast, no cytotoxicity or IFNγ secretion were detected in the presence of CD1a-CAR T cells, or when the target cells were CD1a$^-$ (online supplemental figure S3F).

In addition, we studied whether cortical T-ALL cells were able to escape from immune control by co-culturing either NT, CD1a-CAR or CD1a-STAb T cells with MOLT4 cells at low E:T ratios. After 4 days coculture, CD1a-STAb T cells completely eliminated leukemic cells at 2:1, 1:1 and 1:2 E:T ratios; even after 11 days, leukemic cell numbers were restrained below 10% of total cells (figure 2E). In contrast, CD1a-CAR T cells were not able to control MOLT4 growth below the 1:1 E:T ratio. No cell surface CD1a down-modulation was detected when MOLT4 cells were co-cultured with CD1a-CAR or CD1a-STAb T cells (online supplemental figure S3G).

CD1a-STAb T cells are as effective as CD1a-CAR T cells in short-term *in vivo* T-ALL models

The antitumor effect of CD1a-STAb T cells was evaluated in a coT-ALL xenograft model. 3×10^6 MOLT4^{Luc} cells were intravenously injected in NSG mice, followed by intravenously administration of 5×10^6 NT, CD1a-CAR, or CD1a-STAb T cells 3 days later (figure 3A). BLI of the mice was done twice per week at the indicated time points to assess leukemia progression (figure 3A). While all NT-treated mice showed unrestricted leukemia development,

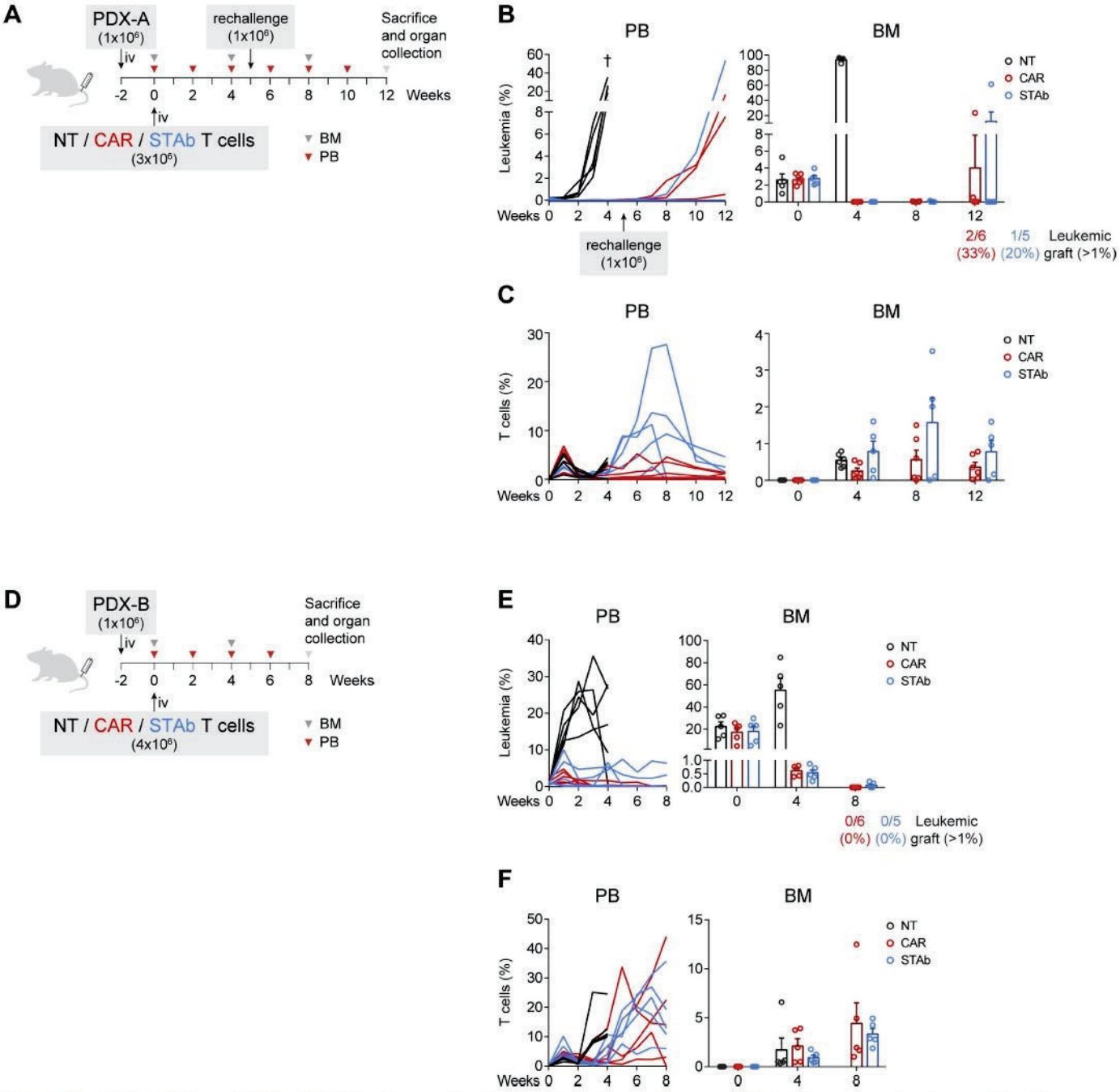

Figure 4 CD1a-STAb and CD1a-CAR T cells are effective in eliminating primary coT-ALL in long-term *in vivo* models. (A, D) Experimental design of *in vivo* cytotoxicity in NSG mice receiving intravenous coT-ALL patient-derived xenograft (PDX-A in a and PDX-B in D) cells (1×10^6) followed by NT, CD1a-CAR or CD1a-STAb T cells 2 weeks later (3×10^6 in a and 4×10^6 in D). In (A), disease-free mice were rechallenged with further 1×10^6 PDX-A cells on week 5. (B, C) Percentage of leukemic (B) and T cells (C) in PB and BM at the indicated time points in the PDX-A model. (E, F) Percentage of leukemic (E) and T cells (F) in PB and BM at the indicated time points in the PDX-B model. Numbers of mice with leukemic graft at endpoint, determined as >1% blasts, are indicated. Leukemic blasts were identified by flow cytometry as HLA-ABC$^+$CD45$^+$CD1a$^+$CD3$^-$ and CD34$^+$ (PDX-A) or CD38$^+$ (PDX-B), and T cells as HLA-ABC$^+$CD45$^+$CD1a$^-$CD3$^+$. BM plots from B, C) and E, F) show mean±SEM of at least 5 mice per group. ALL, acute lymphoblastic leukemia; BM, bone marrow; PB, peripheral blood; NT, non-transduced; CAR, chimeric antigen receptor; STAb, secreting T cell-redirecting antibodies.

both the CD1a-CAR- and CD1a-STAb-treated groups were equally able to control disease progression, as evidenced by BLI (figure 3B,C). Even though bioluminescence analysis showed some tumor burden in 4/6 mice in the CD1a-CAR group and only in 1/5 in the CD1a-STAb group, flow cytometry analysis of PB and BM at sacrifice revealed complete control of the disease in both CD1a-CAR-treated and CD1a-STAb-treated mice (figure 3D). Regarding T cell persistence, we observed similar levels across all treatments in all tissues analyzed,

with a non-statistically significant tendency for higher persistence in the CD1a-STAb group (figure 3E).

CD1a-STAb and CD1a-CAR T cells are effective in eliminating primary T-ALL in long-term *in vivo* models

The effectiveness of CD1a-STAb T cells and CD1a-CAR T cells were also compared side-by-side against primary samples *in vivo*. Two independent CD1a$^+$ coT-ALL PDX models with different aggressiveness were used. We intravenouslyinjected 1×10^6 leukemic blasts for both models in NSG mice, and 2 weeks later, after confirming leukemic engraftment in the BM, 3×10^6 (PDX-A) or 4×10^6 (PDX-B) effector T cells were intravenously injected (figure 4A,D). In the PDX-A model we tested the efficacy of both T cell-redirecting strategies in a setting with relatively low tumor burden, around 2% blasts in the BM at the time of T cells transfer. Both CD1a-CAR and CD1a-STAb T cells were able to ablate leukemic graft in PB and BM in contrast to NT-treated mice, which showed uncontrolled leukemia progression and had to be sacrificed by week 4. To evaluate the effectiveness of the remaining effector cells in the CAR and STAb groups, mice were re-challenged with 1×10^6 PDX-A cells to simulate a relapse in week 5 and followed up until week 12. In the CD1a-CAR group 2/6 (33%) and 1/6 (17%) mice showed significant leukemic graft (>1% blasts) in PB and BM, respectively, whereas in the CD1a-STAb group only 1/5 (20%) mice did (figure 4B). Of note, leukemia relapses in independent mice correlated with decreased numbers of effector T cells in the PB and BM compartments (figure 4C).

In a second PDX model (PDX-B), with higher tumor burden at the time of T cell transfer (engraftment of ~20% in BM), we assessed the effectiveness of CD1a-STAb T cells in a more aggressive, highly active disease setting. Because of its higher aggressiveness (higher leukemic graft at week 0), mice were injected with 4×10^6 rather than 3×10^6 effector T cells. Although CD1a-CAR T cells were slightly more effective than CD1a-STAb T cells in achieving minimal residual disease negative in this aggressive PDX-B, both CD1a-CAR- and CD1a-STAb treatments were similarly effective and able to reduce leukemic burden in the BM to~0.5% by week 4 and further down (<0.02%) by week 8 (figure 4E). Similar T cell persistence levels were observed in CAR- or STAb-treated mice (figure 4F). Taken together, both strategies show robust anti-leukemic activity in long-term cutting-edge in vivo models, and slight differences in the efficacy might be attributed to differential persistence of CD1a-CAR and CD1a-STAb T cells in independent mice.

DISCUSSION

The development of safer and efficacious immunotherapies for T-ALL remains challenging because the shared expression of target antigens between CAR T cells and T-ALL blasts leads to either CAR T cell fratricide or immunodeficiency, but also because of potential T-ALL blast contamination during the manufacturing process.[15] We report the first CD1a x CD3 TCE immunotherapy strategy for the treatment of CD1a$^+$ coT-ALL. We have engineered T cells to express soluble CD1a x CD3 TCEs which successfully bind to cell surface expressed CD1a and CD3, resulting in the specific activation of the T cells. In contrast to membrane-anchored CD1a-CAR-transduced T cells, flow cytometry analysis several subpopulations in the CD1a-TCE-transduced T cell preparation, transduced and decorated T cells ($GFP^+F(ab')_2^+$), non-transduced but decorated T cells ($GFP^-F(ab')_2^+$) and transduced but non-decorated T cells ($GFP^+F(ab')_2^-$), thus confirming the secretion of functional CD1a x CD3 TCE and their ability to decorate surrounding bystander T cells. *In vitro* short-term and long-term co-culture assays revealed that CD1a-STAb T cells induce a more potent and rapid cytotoxic responses than CD1a-CAR T cells. Mechanistically, the CD1a-specific interaction triggered by either CAR or STAb T cells resulted in different proinflammatory cytokine profile whereas both CD1a-CAR and CD1a-STAb T cells use the granular exocytosis pathway as a common cytolytic effector mechanism. Both contacting and non-contacting co-culture systems confirmed the bystander recruitment ability of CD1a-STAb T cells, a major biological feature providing STAb-CD1a T cells with greater *in vitro* tumor cell killing efficiency than CD1a-CAR T cells. Interestingly, the bystander effect mediated from CD1a-STAb T cells offers equal or superior cytotoxicity capacity than CD1a-CAR T cells without an enhanced IFNγ release, thus reducing potential cytokine release-associated side effects and offering a safer therapeutic profile than CD1a-CAR T cells. Finally, CD1a-STAb T cells are as effective as CD1a-CAR T cells in cutting-edge *in vivo* T-ALL cell line and PDX models. Although similar T cell persistence levels were observed in CAR- or STAb-treated mice, leukemia relapses correlated with decreased numbers of effector T cells in the PB and BM. Our data suggest that CD1a-STAb T cells could be an alternative to CD1a-CAR T cells for treating coT-ALL patients.

STAb T cells represent a next-generation T cell-redirecting immunotherapy for B-ALL[30] and coT-ALL, being easily applicable to other cancers for which a suitable immunotherapy target is available.[23] A major advantage for STAb T cells over CAR T cells lies in the fact that an effective treatment with STAb T cells might require lower T cell doses, which could be of particular relevance when an adequate number of mature effector T cells cannot be engineered due to either the lymphopenic status of many multi-treated patients or manufacturing constrains in patients with aggressive and hyperleukocytic relapses.[29 30] In this regard, a reduction in the therapeutically effective effector T cell dose to be transferred into the patients may increase the number of patients benefiting from STAb T cell therapy, and significantly reduce the manufacturing costs.

Immune and phenotypic escape mechanisms to anti-CD19 immunotherapies have been experimentally and clinically demonstrated in B-ALL, and commonly lead

to CD19-resistant leukemias with dismal prognosis.[34–40] Our previous work in B-ALL showed that CD19-STAb T cell therapy could prevent CD19 downregulation and subsequent tumor escape more efficiently and at lower E:T ratios than CD19-CAR T cells.[30 41] In contrast, loss of CD1a expression was not detected on cell surface of target cells co-cultured with either CD1a-CAR or CD1a-STAb T cells. These differences may be attributable to the impact that the density and biology of the targeted antigen plays on T cell activation.[42] In addition, it is worth mentioning that cell fate plasticity and transcription factor-mediated lineage conversion have been extensively reported for the B cell but not the T cell compartment.[43 44] The absence of evident immune escape to either CD1a-CAR or CD1a-STAb T cells may explain the very similar efficacy in controlling leukemia progression in multiple *in vivo* models despite the apparently more potent and rapid *in vitro* cytotoxic responses of CD1a-STAb T cells. In summary, CD1a-STAb T therapy could be an alternative to CD1a-CAR T in T-ALL, especially in R/R patients with leukapheresis products showing limited numbers of non-tumoral effector T cells.

Author affiliations
[1]Cancer Immunotherapy Unit (UNICA), Department of Immunology, Hospital Universitario 12 de Octubre, Madrid, Spain
[2]Immuno-Oncology and Immunotherapy Group, Instituto de Investigación Sanitaria 12 de Octubre (imas12), Madrid, Spain
[3]H12O-CNIO Cancer Immunotherapy Clinical Research Unit, Centro Nacional de Investigaciones Oncológicas (CNIO), Madrid, Spain
[4]Josep Carreras Leukaemia Research Institute (IJC), Barcelona, Catalonia, Spain
[5]OneChain Immunotherapeutics S.L, Barcelona, Spain
[6]Centro de Biología Molecular Severo Ochoa CSIC-UAM, Madrid, Spain
[7]Instituto de Investigación Sanitaria La Princesa, Madrid, Spain
[8]Red Española de Terapias Avanzadas (TERAV) - Instituto de Salud Carlos III (ISCII) (RICORS, RD21/0017/0029-RD21; RD21/0017/0030), Madrid, Spain
[9]Centro de Investigación Biomédica en Red-Oncología (CIBERONC), Instituto de Salud Carlos III, Madrid, Spain
[10]School of Medicine and Health Sciences, University of Barcelona (UB), Barcelona, Catalonia, Spain
[11]Institució Catalana de Recerca i Estudis Avançats (ICREA), Barcelona, Spain
[12]Red Española de Terapias Avanzadas (TERAV) - Instituto de Salud Carlos III (ISCII) (RICORS, RD21/0017/0029-RD21; RD21/0017/0030), Madrid, Spain

Contributors Conception and design of the study: AJ-R, NT, PM, LA-V, DSM; acquisition of data: AJ-R, NT, AM-M, VMD, MG-P, OH, AA, PP, DSM; analysis and interpretation of data: AJ-R, NT, MLT, PM, LA-V, DSM; writing original draft: AJ-R, NT, PM, LA-V, DSM; review and editing: all authors; guarantors: PM, LA-V, DSM.

Funding Research in LA-V laboratory is funded by the Spanish Ministry of Science and Innovation (PID2020-117323RB-100 and PDC2021-121711-100), and the Carlos III Health Institute (DTS20/00089), with European Regional Development Fund (FEDER) cofinancing; the Spanish Association Against Cancer (AECC PROYE19084ALVA) and the CRIS Cancer Foundation (FCRIS-2018-0042 and FCRIS-2021-0090). Research in PM laboratory is supported by CERCA/Generalitat de Catalunya and Fundació Josep Carreras-Obra Social la Caixa for core support; 'la Caixa' Foundation under the agreement LCF/PR/HR19/52160011; the European Research Council grant (ERC-PoC-957466); the Spanish Ministry of Science and Innovation (PID2019-108160RB-I00); and the ISCIII-RICORS within the Next Generation EU program (plan de Recuperación, Transformación y Resilencia). MLT is supported by Spanish Ministry of Science and Innovation (PID2019-105623RB-I00) and the Spanish Association Against Cancer (CICPF18030TORI). PP is supported by Carlos III Health Institute (PI21-01834), with FEDER cofinancing and Fundación Ramón Areces. NT was supported by an FPU PhD fellowship from Spain's Ministerio de Universidades (FPU19/00039). OH was supported by an industrial PhD fellowship from the Comunidad de Madrid (IND2020/BMD-17668). LD-A was supported by a Rio Hortega fellowship from the Carlos III Health Institute (CM20/00004). VMD is supported by the Torres Quevedo subprogram of the State Research Agency of the Ministry of Science, Innovation and Universities (Ref. PTQ2020-011056). DSM is partially founded by a Sara Borrell fellowship from Carlos III Health Institute (CD19/00013).

Competing interests LA-V is cofounder of Leadartis, a spin-off focused on unrelated interest. PM is cofounder of OneChain Immunotherapeutics, a spin-off company from the Josep Carreras Leukemia Research Institute. VMC is current employee of One Chain Immunotherapeutics.

Patient consent for publication Not applicable.

Ethics approval All samples were obtained after written informed consent from the donors and all studies were performed according to the principles expressed in the Declaration of Helsinki and approved by the Institutional Research Ethics Committees of the hospitals and research centers involved (HCB/2019/0450, HCB/2018/0030).

Provenance and peer review Not commissioned; externally peer reviewed.

Data availability statement Data are available on reasonable request.

ORCID iDs
Anaïs Jiménez-Reinoso http://orcid.org/0000-0001-8229-1881
Néstor Tirado http://orcid.org/0000-0001-8352-2194
Víctor M Díaz http://orcid.org/0000-0001-8561-7576
Marina García-Peydró http://orcid.org/0000-0002-8791-132X
Laura Díez-Alonso http://orcid.org/000-0002-9545-6910
Petronila Penela http://orcid.org/0000-0002-0434-4738
Maria L Toribio http://orcid.org/0000-0002-8637-0373
Pablo Menéndez http://orcid.org/0000-0001-9372-1007
Luis Álvarez-Vallina http://orcid.org/0000-0003-3053-6757
Diego Sánchez Martínez http://orcid.org/0000-0003-4605-5325

REFERENCES

1 Karrman K, Johansson B. Pediatric T-cell acute lymphoblastic leukemia. *Genes Chromosomes Cancer* 2017;56:89–116.
2 Belver L, Ferrando A. The genetics and mechanisms of T cell acute lymphoblastic leukaemia. *Nat Rev Cancer* 2016;16:494–507.
3 Liu Y, Easton J, Shao Y, *et al*. The genomic landscape of pediatric and young adult T-lineage acute lymphoblastic leukemia. *Nat Genet* 2017;49:1211–8.
4 Hunger SP, Mullighan CG. Acute lymphoblastic leukemia in children. *N Engl J Med* 2015;373:1541–52.
5 Litzow MR, Ferrando AA. How I treat T-cell acute lymphoblastic leukemia in adults. *Blood* 2015;126:833–41.
6 Pocock R, Farah N, Richardson SE, *et al*. Current and emerging therapeutic approaches for T-cell acute lymphoblastic leukaemia. *Br J Haematol* 2021;194:28–43.
7 Waldman AD, Fritz JM, Lenardo MJ. A guide to cancer immunotherapy: from T cell basic science to clinical practice. *Nat Rev Immunol* 2020;20:651–68.
8 Couzin-Frankel J. Breakthrough of the year 2013. Cancer immunotherapy. *Science* 2013;342:1432–3.
9 Maude SL, Frey N, Shaw PA, *et al*. Chimeric antigen receptor T cells for sustained remissions in leukemia. *N Engl J Med* 2014;371:1507–17.
10 Brentjens RJ, Davila ML, Riviere I, *et al*. CD19-targeted T cells rapidly induce molecular remissions in adults with chemotherapy-refractory acute lymphoblastic leukemia. *Sci Transl Med* 2013;5:177ra38.

11 Gardner RA, Finney O, Annesley C, *et al*. Intent-To-Treat leukemia remission by CD19 CAR T cells of defined formulation and dose in children and young adults. *Blood* 2017;129:3322–31.
12 Fry TJ, Shah NN, Orentas RJ, *et al*. CD22-targeted CAR T cells induce remission in B-ALL that is naive or resistant to CD19-targeted CAR immunotherapy. *Nat Med* 2018;24:20–8.
13 Ortíz-Maldonado V, Rives S, Castellà M, *et al*. CART19-BE-01: A Multicenter Trial of ARI-0001 Cell Therapy in Patients with CD19$^+$ Relapsed/Refractory Malignancies. *Mol Ther* 2021;29:636–44.
14 Scherer LD, Brenner MK, Mamonkin M. Chimeric antigen receptors for T-cell malignancies. *Front Oncol* 2019;9:126.
15 Alcantara M, Tesio M, June CH, *et al*. Car T-cells for T-cell malignancies: challenges in distinguishing between therapeutic, normal, and neoplastic T-cells. *Leukemia* 2018;32:2307–15.
16 Gomes-Silva D, Srinivasan M, Sharma S, *et al*. CD7-edited T cells expressing a CD7-specific CAR for the therapy of T-cell malignancies. *Blood* 2017;130:285–96.
17 Png YT, Vinanica N, Kamiya T, *et al*. Blockade of CD7 expression in T cells for effective chimeric antigen receptor targeting of T-cell malignancies. *Blood Adv* 2017;1:2348–60.
18 Mamonkin M, Rouce RH, Tashiro H, *et al*. A T-cell-directed chimeric antigen receptor for the selective treatment of T-cell malignancies. *Blood* 2015;126:983–92.
19 Rasaiyaah J, Georgiadis C, Preece R, *et al*. TCRαβ/CD3 disruption enables CD3-specific antileukemic T cell immunotherapy. *JCI Insight* 2018;3:e99442.
20 Maciocia PM, Wawrzyniecka PA, Philip B, *et al*. Targeting the T cell receptor β-chain constant region for immunotherapy of T cell malignancies. *Nat Med* 2017;23:1416–23.
21 Pan J, Tan Y, Wang G, *et al*. Donor-Derived CD7 chimeric antigen receptor T cells for T-cell acute lymphoblastic leukemia: first-in-human, phase I trial. *J Clin Oncol* 2021;39:3340–51.
22 Sánchez-Martínez D, Baroni ML, Gutierrez-Agüera F, *et al*. Fratricide-resistant CD1a-specific CAR T cells for the treatment of cortical T-cell acute lymphoblastic leukemia. *Blood* 2019;133:2291–304.
23 Blanco B, Compte M, Lykkemark S, *et al*. T Cell-Redirecting Strategies to 'STAb' Tumors: Beyond CARs and Bispecific Antibodies. *Trends Immunol* 2019;40:243–57.
24 Blanco B, Holliger P, Vile RG, *et al*. Induction of human T lymphocyte cytotoxicity and inhibition of tumor growth by tumor-specific diabody-based molecules secreted from gene-modified bystander cells. *J Immunol* 2003;171:1070–7.
25 Compte M, Blanco B, Serrano F, *et al*. Inhibition of tumor growth in vivo by in situ secretion of bispecific anti-CEA X anti-CD3 diabodies from lentivirally transduced human lymphocytes. *Cancer Gene Ther* 2007;14:380–8.
26 Mølgaard K, Compte M, Nuñez-Prado N, *et al*. Balanced secretion of anti-CEA × anti-CD3 diabody chains using the 2A self-cleaving peptide maximizes diabody assembly and tumor-specific cytotoxicity. *Gene Ther* 2017;24:208–14.
27 Compte M, Alvarez-Cienfuegos A, Nuñez-Prado N, *et al*. Functional comparison of single-chain and two-chain anti-CD3-based bispecific antibodies in gene immunotherapy applications. *Oncoimmunology* 2014;3:e28810.
28 Velasquez MP, Torres D, Iwahori K, *et al*. T cells expressing CD19-specific Engager molecules for the immunotherapy of CD19-positive malignancies. *Sci Rep* 2016;6:27130.
29 Liu X, Barrett DM, Jiang S, *et al*. Improved anti-leukemia activities of adoptively transferred T cells expressing bispecific T-cell engager in mice. *Blood Cancer J* 2016;6:e430.
30 Blanco B, Ramírez-Fernández Ángel, Bueno C, *et al*. Overcoming CAR-mediated CD19 downmodulation and leukemia relapse with T lymphocytes secreting anti-CD19 T-cell Engagers. *Cancer Immunol Res* 2022;10:498–511.
31 Haryadi R, Ho S, Kok YJ, *et al*. Optimization of heavy chain and light chain signal peptides for high level expression of therapeutic antibodies in CHO cells. *PLoS One* 2015;10:e0116878.
32 Sánchez-Martínez D, Gutiérrez-Agüera F, Romecin P, *et al*. Enforced sialyl-Lewis-X (SLex) display in E-selectin ligands by exofucosylation is dispensable for CD19-CAR T-cell activity and bone marrow homing. *Clin Transl Med* 2021;11:e280.
33 Sánchez-Martínez D, Azaceta G, Muntasell A, *et al*. Human NK cells activated by EBV$^+$ lymphoblastoid cells overcome anti-apoptotic mechanisms of drug resistance in haematological cancer cells. *Oncoimmunology* 2015;4:e991613.
34 Bagashev A, Sotillo E, Tang C-HA, *et al*. Cd19 alterations emerging after CD19-Directed immunotherapy cause retention of the misfolded protein in the endoplasmic reticulum. *Mol Cell Biol* 2018;38:e00383–18.
35 Braig F, Brandt A, Goebeler M, *et al*. Resistance to anti-CD19/CD3 bite in acute lymphoblastic leukemia may be mediated by disrupted CD19 membrane trafficking. *Blood* 2017;129:100–4.
36 Fischer J, Paret C, El Malki K, *et al*. Cd19 isoforms enabling resistance to CART-19 immunotherapy are expressed in B-ALL patients at initial diagnosis. *J Immunother* 2017;40:187–95.
37 Gardner R, Wu D, Cherian S, *et al*. Acquisition of a CD19-negative myeloid phenotype allows immune escape of MLL-rearranged B-ALL from CD19 CAR-T-cell therapy. *Blood* 2016;127:2406–10.
38 Jacoby E, Nguyen SM, Fountaine TJ, *et al*. CD19 CAR immune pressure induces B-precursor acute lymphoblastic leukaemia lineage switch exposing inherent leukaemic plasticity. *Nat Commun* 2016;7:12320.
39 Orlando EJ, Han X, Tribouley C, *et al*. Genetic mechanisms of target antigen loss in CAR19 therapy of acute lymphoblastic leukemia. *Nat Med* 2018;24:1504–6.
40 Sotillo E, Barrett DM, Black KL, *et al*. Convergence of acquired mutations and alternative splicing of CD19 enables resistance to CART-19 immunotherapy. *Cancer Discov* 2015;5:1282–95.
41 Ramírez-Fernández Ángel, Aguilar-Sopeña Óscar, Díez-Alonso L, *et al*. Synapse topology and downmodulation events determine the functional outcome of anti-CD19 T cell-redirecting strategies. *Oncoimmunology* 2022;11:2054106.
42 Majzner RG, Mackall CL. Tumor antigen escape from CAR T-cell therapy. *Cancer Discov* 2018;8:1219–26.
43 Laiosa CV, Stadtfeld M, Graf T. Determinants of lymphoid-myeloid lineage diversification. *Annu Rev Immunol* 2006;24:705–38.
44 Graf T, Enver T. Forcing cells to change lineages. *Nature* 2009;462:587–94.

Supplementary Table 1. Flow cytometry antibodies

Target	Fluorophore	Clone	Isotype	Source	Identifier
7-AAD	–	–	–	BD Biosciences	559925
Annexin V	PE	–	–	BD Biosciences	556421
Cell Proliferation Dye eFluor™ 670	–	–	–	ThermoFisher Scientific	65-0840-85
Streptavidin	PE	–	–	ThermoFisher Scientific	12-4317-87
Biotin-SP goat anti-mouse IgG, $F(ab')_2$	–	Polyclonal	–	Jackson ImmunoResearch	115-065-072
CD1a	BV421	HI149	Mouse IgG1, κ	BD Biosciences	563938
CD1a	APC	HI149	Mouse IgG1, κ	BD Biosciences	559775
CD2	PE	S5.2	Mouse IgG2a	BD Biosciences	347405
CD3	V450	UCHT1	Mouse IgG1, κ	BD Biosciences	560365
CD3	FITC	UCHT1	Mouse IgG1, κ	BD Biosciences	555332
CD3	PerCP	SK7	Mouse IgG1, κ	BD Biosciences	345766
CD3	PE-Cy7	UCHT1	Mouse IgG1, κ	BD Biosciences	563423
CD3	APC	UCHT1	Mouse IgG1, κ	BD Biosciences	555335
CD4	PE	SK3	Mouse IgG1, κ	BD Biosciences	555347
CD4	PerCP-Cy5.5	SK3	Mouse IgG1, κ	BD Biosciences	332772
CD7	FITC	M-T701	Mouse IgG1, κ	BD Biosciences	555360
CD8	BV510	SK1	Mouse IgG1, κ	BioLegend	563919
CD8	APC-Cy7	SK1	Mouse IgG1, κ	BioLegend	344714
CD25	APC	M-A251	Mouse IgG1, κ	BD Biosciences	555434
CD34	APC	581	Mouse IgG1, κ	BD Biosciences	555824
CD38	APC	HIT2	Mouse IgG1, κ	BD Biosciences	555462
CD45	APC-H7	2D1	Mouse IgG1, κ	BD Biosciences	560178
CD45 RA	V500	HI100	Mouse IgG2b, κ	BD Biosciences	561640
CD69	PE	L78	Mouse IgG1, κ	BD Biosciences	341652
CD197 (CCR7)	BV421	150503	Mouse IgG2a	BD Biosciences	562555
Fas	APC	DX2	Mouse IgG1	BD Biosciences	558814
His	Unconjugated	Penta·His	Mouse IgG1	QIAGEN	34660
His	APC	GG11-8F3.5.1	Mouse IgG1	Miltenyi Biotec	130-119-782
HLA-ABC	BV510	G45-2.6	Mouse IgG1, κ	BD Biosciences	740172
TCR alpha/beta	PE-Cy7	IP26	Mouse IgG1, κ	ThermoFisher Scientific	25-9986-42

Supplementary Figure Legends

Supplementary Figure 1. Functionality of secreted CD1a-TCE. **(A)** Western blot detection of secreted CD1a-TCE in the conditioned media from transfected HEK293T^{WT} cells. Conditioned media from non-transfected cells (NT) and blinatumomab (Blina) were used as negative and positive controls, respectively. One representative experiment is shown. **(B)** Binding assays of conditioned media from NT- or CD1a-TCE-transfected HEK293T^{WT} cells to K562 cells, primary peripheral blood lymphocytes and MOLT4 cells. Specific binding was detected using anti-His-tag mAb and analyzed by flow cytometry. **(C)** T cell activation assay. Freshly isolated T lymphocytes and CD1a-negative (K562) or CD1a-positive (MOLT4) cells were co-cultured at a 1:1 E:T ratio for 24 hours in the presence of conditioned media from NT, CD1a-CAR- and CD1a-TCE-transfected HEK293T^{WT} cells, and CD69 expression was analyzed by flow cytometry. The inset numbers in **B** and **C** represent the percentage of cells staining positive for the indicated marker.

Supplementary Figure 2. Cells surface expression profiles of CD3 and CD1a from all cell types used in this study. The numbers represent the percentage of cells staining positive for the indicated marker.

Supplementary Figure 3. Comparative in vitro study of engineered CD1a-STAb and CD1a-CAR T cells (cont.). **(A)** CD1a expression on HEK293T^{WT} and HEK293T^{CD1a} cells. **(B)** Cell viability kinetics over time of both cell lines cultured alone. **(C)** Real-time cell cytotoxicity kinetics of HEK293T^{WT} cells co-cultured with activated NT, CD1a-CAR or CD1a-STAb T cells at different E:T ratios (5:1 and 1:1). Cell index values were determined over 80 hours with measurements taken at 15 min intervals after addition of effector cells to target cells. Results from duplicates are shown. **(D)** Cytokine secretion assays from NT, CD1a-CAR or CD1a-STAb T cells co-cultured 24 hours with NALM6, MOLT4 or coT-ALL patient primary cells in a 1:1 E:T ratio. Statistical significance was calculated by a two-way ANOVA test corrected with a Tukey's multiple comparisons test. **(E,F)** Direct contact **(E)** and non-contacting **(F)** bystander T cell cytotoxicity. **(E)** Decreasing numbers of activated effector T (AT) cells (NT, CD1a-CAR or CD1a-STAb) were co-cultured with $5x10^4$ K562^{Luc} target cells and increasing numbers of NT T cells from the same donor (bystander T cells), resulting in the indicated AT:T ratios but maintaining a constant 2:1 Effector (AT+bystander):Target ratio. **(F)**. $5x10^4$ K562^{Luc} cells and $1x10^5$ bystander T cells were plated in the bottom well and decreasing numbers of AT cells (NT, CD1a-CAR or CD1a-STAb) in the upper well; ND, not determined. After 48 hours, the percentage of specific cytotoxicity was calculated by adding D-luciferin to detect bioluminescence **(E,F)**. **(G)** Representative experiment of coT-ALL leukemia escape from immune pressure after 4 days. MOLT4 cells were co-cultured with NT, CD1a-CAR or CD1a-STAb T cells at the indicated E:T ratios, and the expression of CD3 and CD1a was analyzed by flow cytometry. Inset numbers represent the percentage of cells staining positive for the indicated marker. **(H)** Percentage of CD1a-CAR T cells, CD1a-STAb T cells and non-transduced T cells (Non-CAR T and Non-STAb T) within CD1a$^-$CD3$^+$ cells from immune escape assays after 4, 7 and 11 days of co-culture with MOLT4 cells at the indicated E:T ratios.

Supplementary Figure 4. MOLT4 cells express functional Fas receptor (CD95) in the membrane. **(A)** Representative FACS analysis showing cell surface expression of Fas receptor in MOLT4 cells. The inset number represents the percentage of cells staining positive. **(B)** MOLT4 cytotoxicity after 24-hour incubation with the activating anti-Fas clone CH11 with or without the neutralizing anti-Fas clone ZB4. Statistical significance was calculated by a one-way ANOVA test corrected with a Tukey's multiple comparisons test.

Jiménez-Reinoso A, *et al*. *J Immunother Cancer* 2022; 10:e005333. doi: 10.1136/jitc-2022-005333

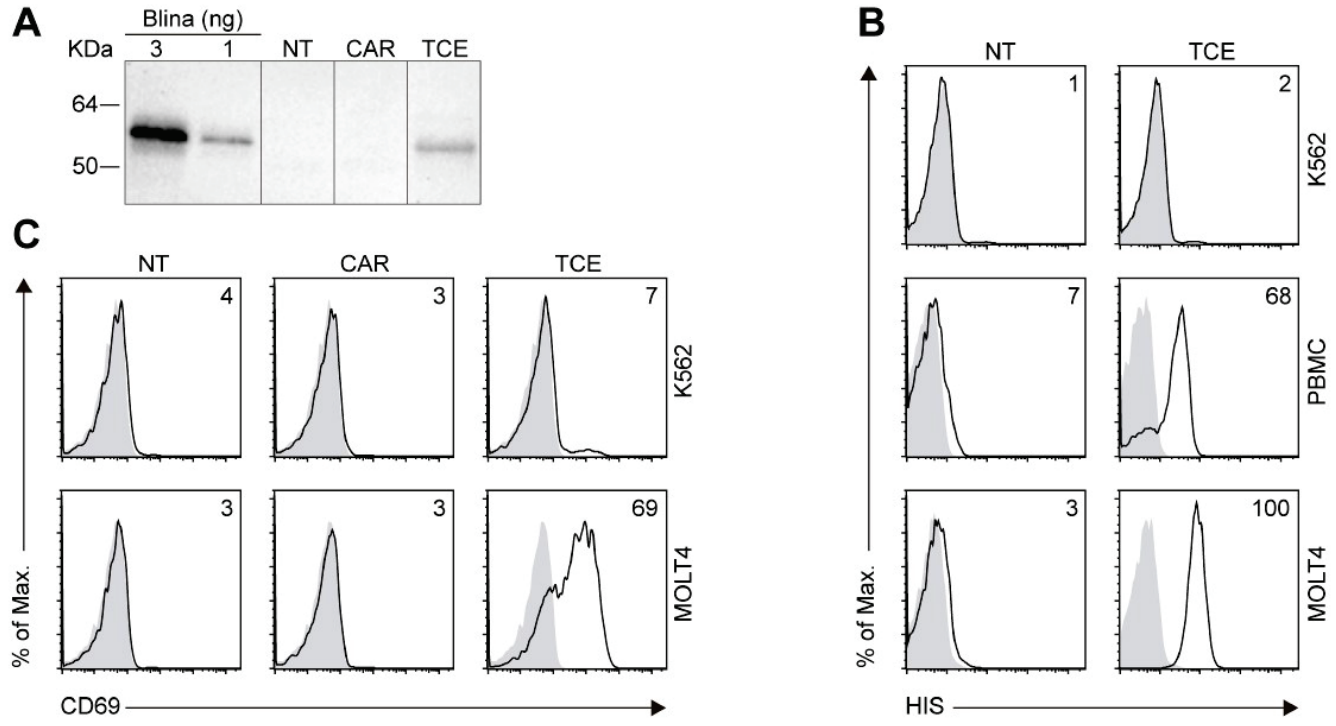
A
Blina (ng)
KDa
3
1
NT
CAR
TCE
64
50
B
NT
TCE
1
2
K562
7
68
PBMC
3
100
MOLT4
% of Max.
HIS
C
NT
CAR
TCE
4
3
7
K562
3
3
69
MOLT4
% of Max.
CD69

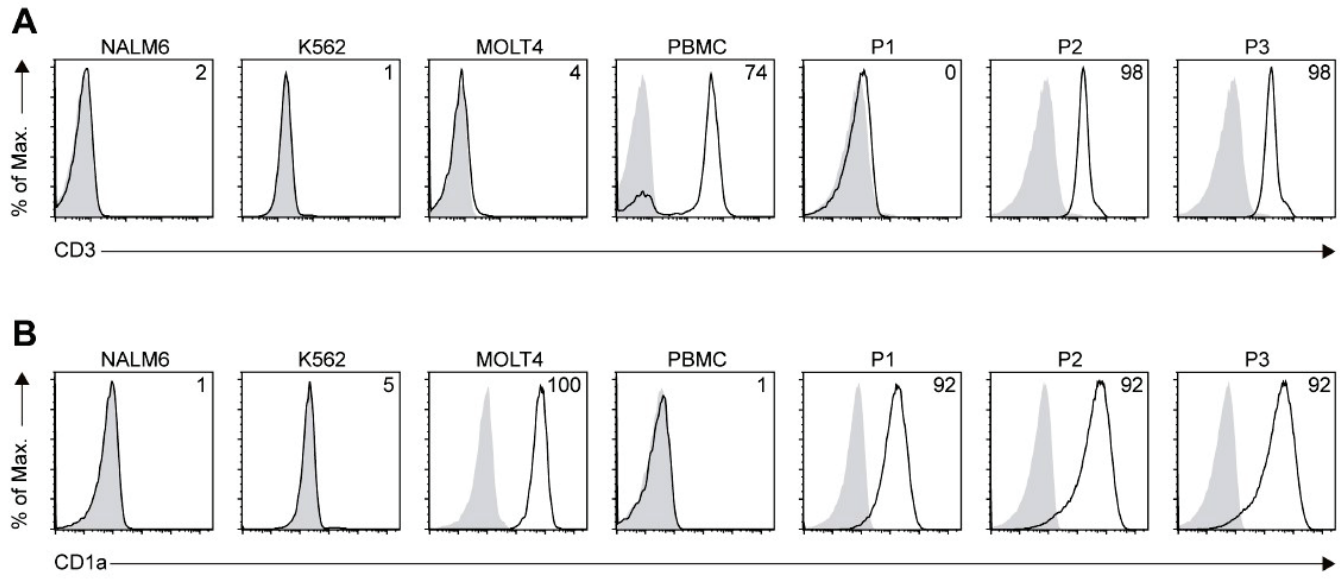
A
NALM6
K562
MOLT4
PBMC
P1
P2
P3
2
1
4
74
0
98
98
% of Max.
CD3
B
NALM6
K562
MOLT4
PBMC
P1
P2
P3
1
5
100
1
92
92
92
% of Max.
CD1a

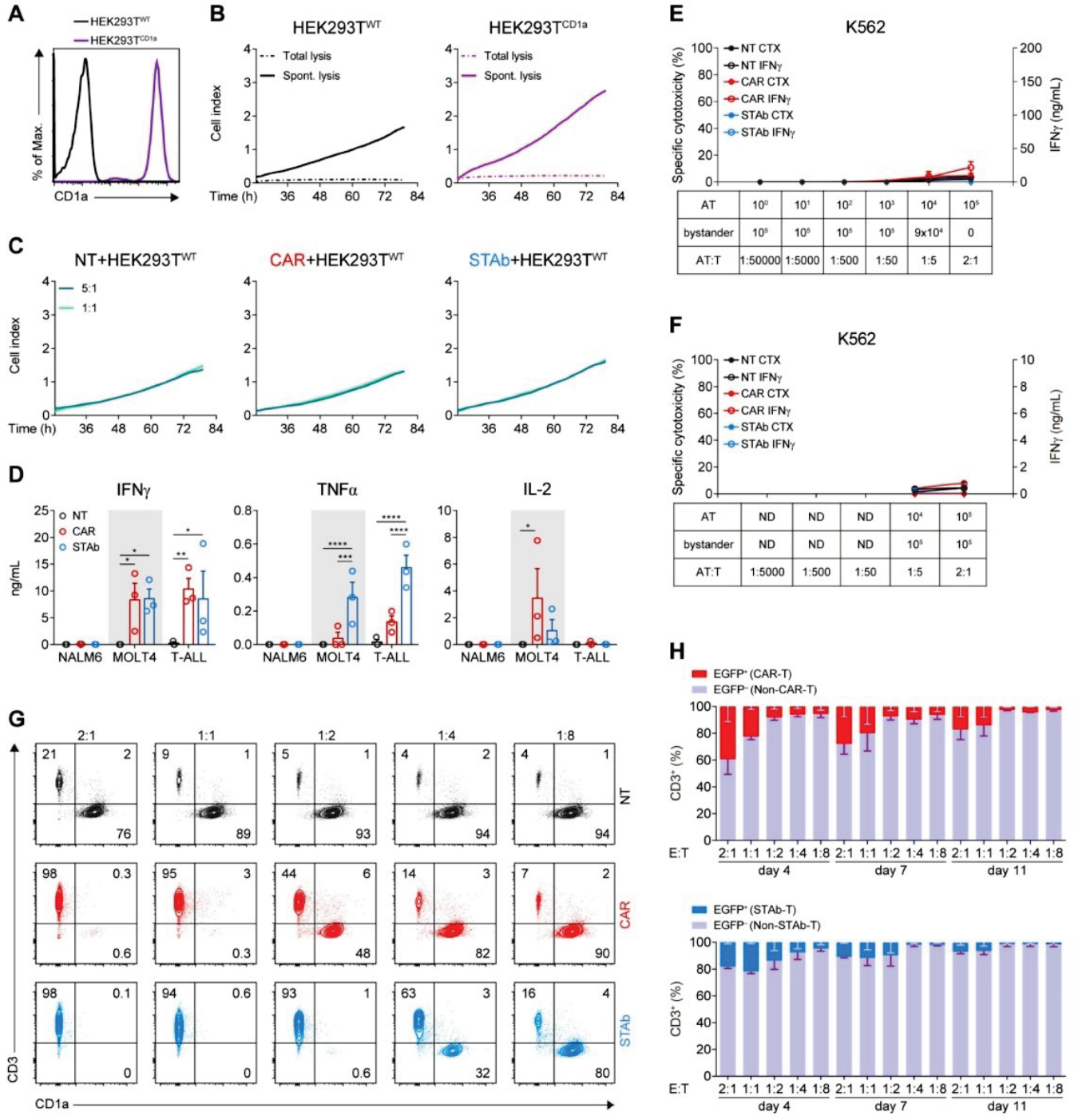
A
HEK293T^WT
HEK293T^CD1a
% of Max.
CD1a
B
HEK293T^WT
HEK293T^CD1a
Total lysis
Spont. lysis
Cell index
Time (h)
C
NT+HEK293T^WT
CAR+HEK293T^WT
STAb+HEK293T^WT
5:1
1:1
D
IFNγ
TNFα
IL-2
NT
CAR
STAb
ng/mL
NALM6 MOLT4 T-ALL
E
K562
NT CTX
NT IFNγ
CAR CTX
CAR IFNγ
STAb CTX
STAb IFNγ
Specific cytotoxicity (%)
IFNγ (ng/mL)
AT 10^0 10^1 10^2 10^3 10^4 10^5
bystander 10^5 10^5 10^5 10^5 9x10^4 0
AT:T 1:50000 1:5000 1:500 1:50 1:5 2:1
F
K562
AT ND ND ND 10^4 10^5
bystander ND ND ND 10^5 10^5
AT:T 1:5000 1:500 1:50 1:5 2:1
G
2:1 1:1 1:2 1:4 1:8
NT
CAR
STAb
CD3
CD1a
H
EGFP+ (CAR-T)
EGFP- (Non-CAR-T)
CD3+ (%)
E:T
2:1 1:1 1:2 1:4 1:8
day 4
day 7
day 11
EGFP+ (STAb-T)
EGFP- (Non-STAb-T)

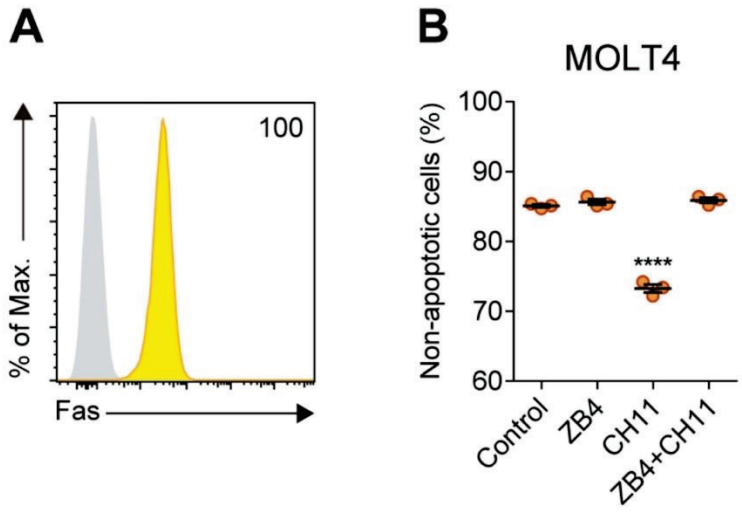
A
100
% of Max.
Fas
B
MOLT4
Non-apoptotic cells (%)
100
90
80
70
60
****
Control
ZB4
CH11
ZB4+CH11

3.3. CAR-T cells targeting CCR9 and CD1a for the treatment of T cell acute lymphoblastic leukemia

Néstor Tirado, María José Mansilla, Alba Martínez-Moreno, Juan Alcaín, Marina García-Peydró, Heleia Roca-Ho, Narcís Fernández-Fuentes, Alba García Pérez, Mercedes Guerrero-Murillo, Aïda Falgàs, Talía Velasco-Hernández, Meritxell Vinyoles, Clara Bueno, Pablo Engel, E Azucena González, Binje Vick, Irmela Jeremias, Aurélie Caye-Eude, André Baruchel, Eulàlia Genescà, Jordi Ribera, Manuel Ramírez-Orellana, Monserrat Torrebadell, Marina Díaz-Beyá, Hélène Cavé, Víctor M Díaz, María L Toribio, Diego Sánchez-Martínez, Pablo Menéndez

Manuscript in preparation

CAR-T cells targeting CCR9 and CD1a for the treatment of T cell acute lymphoblastic leukemia

Néstor Tirado[1,2], María José Mansilla[3], Alba Martínez-Moreno[1,2], Juan Alcain[4], Marina García-Peydró[4], Heleia Roca-Ho[1,2], Narcís Fernández-Fuentes[1,2], Alba García Pérez[3], Mercedes Guerrero-Murillo[1,2], Aïda Falgàs[1,2], Talía Velasco-Hernández[1,2,5], Meritxell Vinyoles[1,2], Clara Bueno[1,2], Pablo Engel[5], E Azucena González[2,6], Binje Vick[7], Irmela Jeremias[7,8], Aurélie Caye-Eude[9], André Baruchel[9], Hélène Cavé[9], Eulàlia Genescà[1], Jordi Ribera[1,10], Marina Díaz-Beyá[11], Manuel Ramírez-Orellana[2,12], Montserrat Torrebadell[13], Víctor M Díaz[3], María L Toribio[4,*], Diego Sánchez-Martínez[1,2,14,15,*], Pablo Menéndez[1,2,5,16,17,*].

1. Josep Carreras Leukaemia Research Institute (IJC), Barcelona, Spain
2. Red Española de Terapias Avanzadas (TERAV), Instituto de Salud Carlos III, Madrid, Spain
3. OneChain Immunotherapeutics S.L, Barcelona, Spain
4. Centro de Biología Molecular Severo Ochoa CSIC-UAM, Madrid, Spain
5. Department of Biomedicine, School of Medicine, University of Barcelona, Barcelona, Spain
6. Department of Immunology, Hospital Clínic de Barcelona, Barcelona, Spain
7. Helmholtz Munich, German Research Center for Environmental Health (HMGU), Munich, Germany
8. Department of Pediatrics, Dr. von Hauner Children's Hospital, LMU University Hospital, LMU Munich, Germany
9. Department of Genetics, University Hospital Robert Debré, Paris, France; INSERM Institut de Recherche Saint Louis, Paris, France
10. Department of Hematology, Institut Català d'Oncologia-Hospital Germans Trias i Pujol, Badalona, Spain
11. Department of Hematology, Hospital Clínic de Barcelona, Barcelona, Spain
12. Department of Pediatric Hematology and Oncology, Hospital Infantil Universitario Niño Jesús, Universidad Autónoma de Madrid, Madrid, Spain
13. Institut de Recerca Pediàtrica Sant Joan de Déu, Barcelona, Spain; Department of Hematology, Hospital Sant Joan de Déu, Barcelona, Spain
14. Aragon Health Research Institute (IIS Aragón), Zaragoza, Spain
15. Aragon Foundation for Research & Development (ARAID), Zaragoza, Spain
16. Institució Catalana de Recerca i Estudis Avançats (ICREA), Barcelona, Spain
17. Centro de Investigación Biomédica en Red de Cáncer (CIBERONC), Madrid, Spain

*** Correspondence should be addressed to**

P.M (pmenendez@carrerasresearch.org)
D.S.M (dsanchez@carrerasresearch.org)
M.L.T (mtoribio@cbm.csic.es)

ABSTRACT

T cell acute lymphoblastic leukemia (T-ALL) is an aggressive malignancy characterized by high rates of induction failure and relapse. Effective targeted immunotherapies for T-ALL are currently lacking. Despite recent clinical advances with genome-edited CD7-directed CAR-T cells, which are difficult-to-implement logistically and regulatory-wise, CAR-T cell therapies remain challenging in T-ALL due to the shared expression of target antigens between malignant and healthy T cells, leading to CAR-T cell fratricide, T cell aplasia, and potential blast contamination in CAR-T cell manufactured products. Recently, CAR-T cells targeting two non-pan-T cell antigens absent in healthy T cells but expressed in specific subgroups of T-ALL, have been described. These antigens are CD1a, expressed in cortical T-ALL patients (phase I trial: NCT05679895), and CCR9. Here, we show that CCR9 is expressed in >70% of T-ALL patients (132/180), and its expression is highly retained at relapse, with a safe expression profile within hematopoietic and non-hematopoietic healthy tissues. Further immunophenotyping analysis revealed that dual targeting of CCR9 and CD1a may benefit more patients (~86%) with a greater blast coverage than treatment with single CAR-T cells. We thus developed, characterized, and preclinically validated a novel humanized CCR9-specific CAR with robust and specific antileukemic activity as monotherapy in *in vitro* and *in vivo* cytotoxicity assays against cell lines, primary T-ALL samples and patient-derived xenografts. Importantly, dual-transduced CAR-T cells targeting both CCR9 and CD1a showed higher efficacy than single CAR-T cells, especially in T-ALL cases with phenotypically heterogeneous leukemic populations. We propose this highly effective CAR-T cell therapy for T-ALL, which could avoid allogenic transplantation, T cell aplasia, and regulatory-challenging genome engineering approaches.

INTRODUCTION

T cell acute lymphoblastic leukemia (T-ALL) is a clonal hematological malignancy characterized by a differentiation blockade and the accumulation of T cell lineage lymphoblasts[1]. T-ALL often presents with leukocytosis or cytopenia, and extramedullary infiltration is common. It is a highly heterogeneous disease both phenotypically and genetically, with recurrent mutations in transcription factors and signaling pathways involved in hematopoietic homeostasis and T cell development[2-4]. T-ALL accounts for ~15% and ~25% of total pediatric and adult ALL cases, respectively. Treatment is based on intensive multi-agent cytotoxic chemotherapy[95]. Despite cure rates of ~85% in children[97,274], long-term survival in adults is <45% for patients who can tolerate intensive chemotherapy[275]. More than half of patients relapse or fail to respond to standard therapy resulting in a very poor prognosis, with a median overall survival of ~8 months[276]. In relapsed/refractory (R/R) T-ALL, the standard approach to achieving remission is with intensive re-induction chemotherapy followed by allogeneic hematopoietic stem cell transplantation, which associates with significant toxicity and high failure rates. This scenario highlights the need for new, targeted, and safe therapeutic strategies for R/R T-ALL patients.

Unlike B cell malignancies, which have effective immunotherapy target antigens such as CD19, CD22, or CD20, no approved immunotherapies are available for T-ALL[16-20]. A major drawback to the development of immunotherapies against T cell malignancies is the lack of safe and actionable tumor-specific antigens[21,22]. The phenotypic similarities between effector T cells and leukemic lymphoblasts not only make autologous CAR-T cells directed against pan-T antigens like CD7 or CD5 difficult to manufacture but also induce fratricide and life-threatening T cell aplasia[23–26]. In fact, recent clinical studies have circumvented these limitations through either genome-edited or expression blocker-engineered CD7-directed CAR-T cells[195,201–203,242,277–279,262,280]. These strategies, although elegant, remain difficult to implement logistically- and regulatory-wise, and are restricted to the use of allogeneic effector T cells and to fit patients with the availability of a donor for rescue therapy with allogeneic transplantation.

Directing CAR-T cells against a non-pan-T antigen, supposedly expressed on blasts but not on healthy T lymphocytes would overcome these limitations. This strategy would not only facilitate the manufacture of autologous CAR-T cells but also circumvent both fratricide and immune toxicity[204,205,209,229,281,282]. In this regard, we previously identified CD1a as an immunotherapeutic target for the treatment of T-ALL with a safe profile within non-hematopoietic and hematopoietic tissues—absent in normal T cells—which led us to generate and validate CD1a-directed CAR-T cells that are now being tested in a phase I clinical trial (NCT05679895)[209,283]. However, CD1a only covers cortical T-ALL cases, a subtype accounting for ~40% of all T-ALL cases, while sparing other T-ALL subtypes associated with higher refractoriness and relapse rates. In addition, the expression of the chemokine receptor CCR9, a G protein-coupled receptor for the ligand CCL25, was recently suggested to be restricted to two-thirds of T-ALL cases, and CAR-T cells targeting CCR9 were resistant to fratricide and had potent antileukemic activity preclinically[225,226,229].

Here, we suggest that dual targeting of CCR9 and CD1a may benefit a large fraction of T-ALL cases, with greater blast coverage than treatment with single-targeting CAR-T cells. We preclinically validate a novel humanized CCR9-specific CAR with robust and specific antileukemic activity as monotherapy in *in vitro* and *in vivo*, and demonstrate the benefits of CCR9- and CD1a-targeting

dual CAR-T cells, especially in T-ALL cases with phenotypically heterogeneous leukemic populations. We propose a highly effective CAR-T cell strategy for T-ALL, which could avoid allogenic transplantation, T cell aplasia, and regulatory-challenging genome engineering approaches.

METHODS

Donor and patient samples

Research involving human samples was approved by the Clinical Research Ethics Committee (HCB/2023/0078, Hospital Clínic, Barcelona, Spain). For immunophenotyping, thymus (*n*=4), peripheral blood (PB, *n*=18), and bone marrow (BM, *n*=13) samples were obtained from healthy individuals. BM samples were leftovers from transplantation harvests, and thymi were sourced from thymectomies from thoracic surgeries in infants. Diagnostic and relapse primary T-ALL samples (*n*=180) were obtained after informed consent from samples collections from the participating hospitals.

Cell lines

MOLT4, SupT1, and MV4;11 cell lines were purchased from the DSMZ cell line bank and cultured in RPMI 1640 supplemented with 10% fetal bovine serum (FBS). CCR9 knockout (KO) and CD1a KO MOLT4 cells were generated by CRISPR-mediated genome editing. Briefly, 500.000 cells were electroporated using the Neon Transfection System (Thermo Fisher Scientific) with a Cas9/crRNA:tracrRNA complex (IDT). A crRNA guide was designed for each gene: *CCR9* 5'-GAAGTTAACGTAGTCTTCCATGG-3' and *CD1A* 5'-TATTCCGTATACGCACCATTCGG-3'. After electroporation, cells were recovered, and the different KO clones were FACS-sorted and purity confirmed (>99%).

CCR9 monoclonal antibody, epitope mapping, generation of a humanized scFv

Monoclonal antibodies (MoAb) reactive with human CCR9 were generated using hybridoma technology as previously reported[284]. Briefly, NS-1 myeloma cells were fused with splenocytes from BALB/c mice pre-immunized with the extracellular N-terminal domain of hCCR9. After hybridoma subcloning, supernatants from individual clones were screened by flow cytometry for reactivity against CCR9-expressing MOLT4 and 300.19-hCCR9 cells, as well as their respective negative controls, MOLT4 CCR9 KO and wild-type 300.19 cells. One hybridoma (clone #115) was selected, and its productive IgG was sequenced and the V_H and V_L regions used to derive the murine single-chain variable fragment (scFv) using the Mouse IgG Library Primer Set (Progen), as previously described[185,209,284].

For humanization, a sequence search was performed in the IMGT database[285] to identify Ig genes with the highest identity to both V_H and V_L domains to the murine #155 antibody. The highest murine-human sequence identities were *IGHV1-3*01* for the V_H (60% identity) and *IGKV2D-29*02* for the V_L (82% identity). The number of differing residues (with different levels of conservation) excluding the complementarity-determining regions (CDRs) were 32 and 13, respectively. The CDRs, including the Vernier regions, were grafted into the human scaffolds. A structural model of the murine scFv was used to identify other structurally important residues in the antibody that differ from the equivalent positions in the humanized versions, which should be retained (e.g., buried residues, residues located at the interface, etc.). Two humanized candidates were generated, each with different degrees of residue substitution at non-conserved positions. The sequence-based humanized candidate #1 (H1) aims to make the minimum changes necessary to achieve

humanization, whereas humanized candidate #2 (H2) allows for more extensive changes to match the human sequence.

CAR design and vectors, lentiviral production, and T cell transduction

Single scFvs (CD1a H and CCR9 M, H1, and H2), all possible configurations of tandem CAR constructs (*n*=8) and four distinct configurations of bicistronic CAR were cloned into the clinically validated pCCL lentiviral backbone containing the human CD8 hinge and transmembrane (TM) domains, 4-1BB and CD3ζ endodomains, and a T2A-eGFP reporter cassette. All constructs contain the signal peptide (SP) derived from CD8α (SP1) upstream (5') the first scFv. Two distinct SPs derived from either human IgG1 (SP2) or murine IgG1 (SP3) were used for the second CAR in bicistronic constructs.

Third-generation lentiviral vectors were generated in 293T cells by co-transfection of the different pCCL expression plasmids, pMD2.G (VSV-G) envelope, and pRSV-Rev and pMDLg/pRRE packaging plasmids using polyethylenimine (Polysciences)[286]. Viral particle-containing supernatants were collected at 48 and 72h after transfection and concentrated by ultracentrifugation.

PBMCs were isolated from healthy donor buffy coats by density-gradient centrifugation using Ficoll Paque Plus (Merck). Buffy coats were sourced from the Catalan Blood and Tissue Bank (BST). T cells were activated in plates coated with anti-CD3 (OKT3) and anti-CD28 (CD28.2) antibodies (BDBiosciences) for two days and transduced with CAR-encoding lentiviral particles at a multiplicity of infection (MOI) of 10. T cells were expanded in RPMI 1640 medium containing 10% heat-inactivated FBS, penicillin-streptomycin, and 10 ng/mL interleukin (IL)-7 and IL-15 (Miltenyi Biotec). The expression of CAR molecules in T cells was detected by flow cytometry using eGFP reporter signal and biotin-SP goat anti-mouse IgG, $F(ab')_2$ (Jackson ImmunoResearch) and PE-conjugated streptavidin (Thermo Fisher Scientific).

In vitro cytotoxicity and cytokine secretion assays

Target cells (100,000 to 300,000 cells/well) were labeled with eFluor 670 (Thermo Fisher Scientific) following the manufacturer's instructions and incubated in a 96-well plate with untransduced or CAR-T cells at the indicated effector:target (E:T) ratios for 24 hours. Cytotoxicity was assessed by flow cytometry analysis of residual live target cells (eFluor 670^+ 7-AAD^-). For primary T-ALL blasts, absolute counts of live target cells were also determined using Trucount beads tubes (BD Biosciences). Additional wells containing only target cells ("no effector"; NE) were always plated as controls. When comparing several CAR-T constructs transduction percentages were matched across conditions. Quantification of the proinflammatory cytokines IFN-γ, TNF-α, and IL-2 was performed by ELISA using BD OptEIA Human ELISA kits (BD Biosciences) on supernatants harvested at 24 hours of target cell exposure.

Flow cytometry

The fluorochrome-conjugated antibodies against CD1a (HI149), CD3 (UCHT1), CD4 (SK3), CD7 (M-T701), CD8 (SK1), CD14 (MφP9), CD19 (HIB19), CD34 (8G12), CD38 (HIT2), CD45 (HI30, 2D1), HLA-ABC (G46-2.6), mouse IgG1, κ isotype control (X40) and the 7-AAD cell viability solution were purchased from BD Bioscience. Antibodies against CCR9 (L053E8), TCRαβ (IP26), TCRγδ (B1), His tag (J095G46), and mouse IgG2a, κ isotype control (MOPC-173) were purchased from BioLegend. Alexa Fluor 647-conjugated anti-mouse IgG (H+L) was purchased from Cell Signaling Technology.

Samples were stained with MoAbs (30 min at 4ºC in the darkness) and erythrocytes lysed (when applicable) using a FACS lysing solution (BD Bioscience). Isotype-matched nonreactive fluorochrome-conjugated antibodies MoAbs were used as controls. Cell acquisition was performed in a FACSCanto-II and analyzed using BDFACSDiva and FlowJo v10 softwares (BD Bioscience). All gating strategies and analysis are shown in **Fig. S1**.

In vivo assessment of CAR-T cell efficacy in T-ALL models

In vivo studies were conducted at the Barcelona Biomedical Research Park (PRBB) following the guidelines of the Animal Experimentation Ethics Committee. All procedures complied with the institutional animal care committee of the PRBB (DAAM11883). All mice were bred and housed under pathogen-free conditions. Seven- to twelve-week-old NOD.Cg-*Prkdc*^{scid} *Il2rg*^{tm1Wjl}/SzJ (NSG) mice (The Jackson Laboratory) were sublethally irradiated (2 Gy) and systemically transplanted with 1×10^6 T-ALL patient-derived xenograft (PDX) cells via the tail vein. Two-to-three weeks later, PB and BM samples were harvested to assess leukemic burden and establish the different treatment groups before CAR-T cell injection ($3\text{-}4\times10^6$) via the tail vein. For *in vivo* experiments using MOLT4 cell lines, phenotypically heterogeneous MOLT4 cells (1:1:1 ratio, 1×10^6 cells) were transplanted three days before CAR-T cell administration. Tumor burden was monitored weekly by flow cytometry of PB samples. For luciferase-expressing T-ALL models, mice were given 60 mg/kg of D-luciferin intraperitoneally, and tumor growth was monitored weekly. Bioluminescence was evaluated using Living Image software (PerkinElmer). Mice were culled when signs of disease or graft-versus-host disease (GvHD) were evident. Spleens were dissected manually, and a single-cell suspension was obtained using 70 μm strainers. Samples were stained and processed for flow cytometry as described above.

Statistical analysis

For CAR-T cell expansion, cytotoxicity, and *in vivo* studies, two-way ANOVA tests with Tukey's adjustment for multiple comparisons were used to compare the different groups, with untransduced T cells serving as controls. For cytokine release assays, a one-way ANOVA test with Dunnett's multiple comparison adjustment was utilized. All statistical tests were performed using Prism 6 (GraphPad Software). The number of biological replicates is indicated in the figure legends. Significance was considered when *p*-values were lower than 0.05 (ns, not significant; *$p<0.05$; **$p<0.01$; ***$p<0.001$).

RESULTS

CCR9 is a safe and specific target for T-ALL

Besides CD1a, there are few non-pan-T therapeutic targets for the immunotherapy of T cell tumors. Immunotherapy targets should ideally be expressed in tumor cells but absent in healthy tissues, including T cells, thus offering unique clinical advantages. We first analyzed CCR9 expression by flow cytometry in a cohort of 180 T-ALL samples (**Fig. 1a**). Consistent with previous reports from the Great Ormond Street Hospital/University College London group[229], we found that 73% (132/180) of T-ALL samples are $CCR9^+$, with variable levels of expression (using a cut-off of ≥20% for positivity) (**Fig. 1a, S1a**). Importantly, non-leukemic $CD4^+$ and $CD8^+$ T cells from the same patients remained $CCR9^-$. This proportion of CCR9 positivity in T-ALL was maintained (64-76%) when patients were stratified into different maturation subtypes following the EGIL immunophenotypic classification[71] (**Fig. 1b**). Notably, the number of $CCR9^+$ T-ALL cases increased considerably in relapse samples (92%, 12/13), with a much higher blast coverage than was observed at diagnosis (**Fig. 1c**).

The implementation of an immunotherapeutic target requires that it meets a safety profile, meaning no expression in other hematopoietic and non-hematopoietic cell types. To assess the safety profile of CCR9, we first examined its expression in the Tabula Sapiens scRNAseq dataset, a human reference atlas comprising 24 different tissues and organs from healthy donors[287], and found a complete absence of CCR9 expression in all tissues except the thymus and a minor subset of small intestine-resident lymphocytes (**Fig. 1d,e**). We confirmed the expression of CCR9 in all thymocyte subpopulations along T cell development by flow cytometry analysis of postnatal thymi (*n*=4, **Fig. 1f, S1b**). However, flow cytometry analysis of healthy pediatric and adult PB (*n*=18) and BM (*n*=13) samples revealed that, except for expression in 10-30% of B cells, CCR9 is minimally expressed in all the major leukocyte subpopulations analyzed, including $CD34^+$ hematopoietic stem/progenitor cells (HSPCs) and resting and CD3/CD28-activated T cells (**Fig. 1g,h; S1c,d**). Collectively, CCR9 was expressed in a high proportion of T-ALL patients, especially upon relapse, while showing a safety profile dictated by its low or absent expression in healthy tissues, $CD34^+$ HSPCs, and T lymphocytes, highlighting its potential as a target for the development of CCR9-directed, fratricide-resistant, safe CAR-T cell therapy.

CCR9 CAR-T cells are highly effective against T-ALL blasts

We next sought to develop a humanized CCR9-directed CAR for the treatment of R/R T-ALL. The highly hydrophobic nature and insolubility of the CCR9 protein prompted us to use the CCR9 N-terminal extracellular domain for mice immunization and subsequent generation of murine CCR9 antibody-producing hybridoma. After hybridoma subcloning and individual testing for CCR9 reactivity one clone (#115) tested positive (**Fig. 2a**). The productive IgG was sequenced and the V_H and V_L regions used to derive the murine scFv for CAR design. Two additional humanized scFvs were generated by structural fitting and modeling of the CDRs and neighboring regions into human IgG scaffolds (**Fig. S2a**). Epitope mapping using overlapping peptides from the CCR9 N-terminus revealed the CCR9 epitope recognized by the clone #115 scFv (**Fig. S2b**). The murine (M) and both humanized (H1 and H2) CCR9 scFvs were cloned into the clinically validated pCCL-based second-generation CAR lentiviral backbone, including a T2A-eGFP reporter cassette (**Fig. 2b**). Primary T

cells were successfully transduced and CAR expression detected using anti-F(ab')$_2$, correlated with eGFP signal (**Fig. 2c**). All CCR9 CAR-T cells showed identical expansion to untransduced T cells, demonstrating a lack of fratricide (**Fig. 2d**).

T-ALL cell lines MOLT4 and SupT1 (with high and dim expression of CCR9, respectively) and control AML cell line MV4;11 (CCR9 negative) (**Fig. 2e**), as well as two independent T-ALL PDX samples (**Fig. 2g**) were used to assess the *in vitro* cytotoxicity of CCR9 CAR-T cells (**Fig. 2f, h**). Cytotoxic activity was assessed in 24-hour co-cultures with untransduced/CAR-T cells at different effector:target (E:T) ratios. CCR9 M and H2 CAR-T cells demonstrated similarly robust and specific cytotoxicity in an antigen density-dependent manner (**Fig. 2f,h**), whereas H1 CAR-T cells exhibited a slightly inferior killing, particularly with the CCR9^{dim} SupT1 cells and, to a lesser extent, with PDX1 blasts (**Fig. 2f,h**). IFN-γ secretion in the co-culture supernatants, used as a proxy for CAR-T cell activation and cytotoxicity, revealed the highest IFN-γ production by CCR9 M and H2 CAR-T cells (**Fig. 2i**).

To test *in vivo* CAR-T function, we used two different T-ALL PDX models. In the first model, we compared untransduced and all three CAR-T groups against slower-growing T-ALL PDX2 cells (**Fig. 2j**). All three treatment groups were able to control leukemia progression, in contrast to untransduced T cells, as evaluated by flow cytometry 10-week follow-up in BM, PB, and spleen (**Fig. 2k**, FACS gating strategies in **Fig. S1e**). However, while all mice treated with either CCR9 M or H2 CAR-T cells achieved complete responses, 2 out of 6 mice treated with CCR9 H1 CAR-T cells showed detectable leukemic burden at the endpoint. This further supported the *in vitro* data demonstrating higher anti-leukemia efficacy of H2 over H1 CAR-T cells. Therefore, CCR9 H2 CAR-T cells were selected for downstream experiments. To further test the robustness of CCR9 H2 CAR-T cells we used a second, highly aggressive CCR9$^+$ luciferase-bearing PDX model (**Fig. 2l**). Bioluminescence follow-up showed disease remission in 4 out of 5 mice (80%) in the CCR9 H2 CAR-T-treated group, in contrast to disease progression in all control mice (**Fig. 2m**). Disease progression was also monitored by flow cytometry analysis of BM, PB, and spleen, confirming leukemia control in the mice treated with CCR9 H2 CAR-T cells relative to control-treated mice (**Fig. 2n**), even in this highly aggressive model. Collectively, the humanized CCR9 H2 CAR is highly effective against T-ALL blasts *in vitro* and *in vivo* using several T-ALL cell lines and different PDX models.

Humanized CCR9 and CD1a dual targeting CAR-T cells for T-ALL

Our group previously proposed a CD1a-directed CAR for the treatment of the cortical T-ALL subtype (CD1a$^+$)[209,283]. al (NCT05679895). Since both CD1a and CCR9 are safe non-pan-T targets (circumventing both fratricide and T cell aplasia), we next immunophenotyped the 180 T-ALL samples for CD1a and CCR9 co-expression (**Fig. 3a**). Using a 20% positivity cut-off for each marker, we observed that 51% and 73% of the patients express either CD1a or CCR9, respectively (**Fig. 3a**). Remarkably, however, there are highly heterogeneous leukemic populations for CCR9 and CD1a, with each patient showing a unique co-expression profile, predominating in either CCR9$^+$ or CD1a$^+$ blasts populations (**Fig. 3a,b**). Strikingly, the sum of all patients with >20% expression of either antigen showed that 86% (155/180) of all cases could benefit from a dual CAR-T cell therapy.

The malleable nature of many markers has been demonstrated in various subtypes of acute leukemias[288,289]. To gain insights into the clinical-biological impact of the intratumoral phenotypic heterogeneity of CD1a and CCR9, we conducted *in vivo* experiments where the $CD1a^{+/-}$ and $CCR9^{-}$ leukemic fractions from primary T-ALLs were FACS-sorted and transplanted into NSG immunodeficient mice to evaluate the phenotype of the resulting engraftment (**Fig. S3**). These experiments revealed that both $CD1a^{-}$ and $CCR9^{-}$ fractions were capable of engrafting and, importantly, the graft reproduced the initial leukemia phenotype, where positive and negative populations for CD1a and CCR9 coexist (**Fig. S3**). This marker plasticity suggests that $CD1a^{low}$ and $CCR9^{low}$ patients could still benefit from dual immunotherapy (**Fig 3a**), thereby increasing not only the number of patients eligible for treatment but also the blast coverage per patient, likely contributing to lower immune escape rates.

We thus set out to generate dual CAR-T cells targeting both CCR9 and CD1a. Several molecular strategies for achieving dual targeting were tested, including eight configurations of tandem CARs (two scFvs in a single CAR molecule), four bicistronic CARs (two independent CAR molecules encoded in one lentiviral vector), and co-transduction with two single CAR-encoding lentiviral vectors simultaneously (**Fig. S4a**). A comparison of the transduction efficiency and cytotoxic efficacy for each strategy revealed that the co-transduction strategy achieved significantly higher transduction levels and specific cytotoxic performance using T-ALL cells with combinatorial CCR9/CD1a phenotypes (wt, CCR9 KO, CD1a KO, and double KO) (**Fig. S4b,c**). Thus, co-transduction with single CCR9 CAR and CD1a CAR viral vectors was selected for downstream experiments as our dual-targeting CAR-T cell strategy of choice (**Fig. 3c**).

Using combinatorial phenotypes for both antigens of T-ALL cells we then demonstrated the specificity and efficiency of dual CCR9/CD1a-directed CAR-T cells generated by co-transduction. In contrast to single CAR-T cells, dual CCR9/CD1a CAR-T cells could eliminate all target cells in 24-hour co-cultures at low E:T ratios as long as one of the antigens remained expressed (**Fig. 3d,e**). We next tested the *in vivo* efficacy of dual CCR9/CD1a CAR-T cells in a stressed model against PDX cells expressing both antigens by injecting fewer therapeutic T cells (**Fig. 3f, S1e**). Weekly flow cytometry follow-up in PB revealed that all CAR-T cell treatments controlled the disease for up to weeks 4-5. However, when mice were allowed to relapse the dual CAR-T therapy offered slightly higher rates of complete responses (defined as <1% of blasts) in PB and spleen (**Fig. 3g**). Furthermore, immunophenotyping of the CAR-resistant T-ALL blasts analyzed at the endpoint (week 8) revealed a partial down-regulation of CD1a in the mice treated with CD1a-directed CAR-T therapies (both with CD1a H CAR-Ts and with dual CAR-Ts), but no down-regulation was observed under CCR9 targeting (**Fig. 3h**). Overall, the immunophenotyping data together with the *in vitro* and *in vivo* experimental results support the potential for treating R/R T-ALL with CAR-T cells targeting both CCR9 and CD1a, generated by co-transduction with two separate CARs.

CCR9 and CD1a dual targeting CAR-T cells efficiently eliminate T-ALL with phenotypically heterogeneous leukemic populations

We next set out to assess the efficiency of co-transduced dual CCR9/CD1a CAR-T cells in the context of phenotypically heterogeneous leukemias. Intratumor phenotypic heterogeneity was recreated by mixing CCR9/CD1a combinatorial phenotypes ($CCR9^{+}CD1a^{+}$, $CCR9^{+}CD1a^{-}$, and $CCR9^{-}CD1a^{+}$) of MOLT4 T-ALL cells at a ratio 1:1:1 (**Fig. 4a**). Time-course cytotoxicity assays

revealed complete ablation of all leukemic population with dual CAR-T cells, whereas, as expected, single CAR-T cells were not able to eliminate those T-ALL cells negative for their corresponding target antigen, leading to leukemic escape (**Fig. 4b**). Identical results were obtained with a MOI of 5+5 and 10+10 for each individual CAR vector for the dual strategy (**Fig. S4d**). Similar levels were observed in terms of pro-inflammatory cytokines IFN-γ, TNF-α, and IL-2 production (**Fig. 4c**).

Finally, we tested the efficacy of dual CCR9/CD1a CAR-T cells in an *in vivo* setting using mixed phenotypes of MOLT4 target cells (**Fig. 4d**). Bioluminescence imaging and BM flow cytometry analysis revealed massive disease control of the highly aggressive heterogeneous MOLT4 cells, as opposed to both single CAR-T treatments (**Fig. 4e,f**). Taken together, our data highlights a superior efficacy of dual CCR9/CD1a CAR-T cells over single-targeting CAR-T cells in the treatment of T-ALL cases with phenotypically heterogeneous leukemic populations.

DISCUSSION

The clinical management of relapsed or refractory T cell leukemias and lymphomas represents an unmet clinical need. Although various immunotherapy strategies such as bispecific antibodies and CAR-T cells have revolutionized the treatment of B cell leukemias, lymphomas, and multiple myeloma, with several products approved by the FDA/EMA, these immunotherapies are much less advanced and have not been approved for T cell malignancies[290]. The primary challenge for the implementation of adoptive immunotherapies in T cell tumors is the shared expression of surface membrane antigens between tumoral cells and healthy/non-leukemic T cells. This implies that the expression of a CAR targeting any pan-T antigen would very likely generate toxicities such as CAR-T fratricide and T cell aplasia[290,291]. Additionally, the shared antigen expression between effector and tumor T cells can hinder the manufacturing process of autologous T cell therapies due to blast contamination of the leukapheresis products[200]. This leads to many clinical trials with pan-T antigen-directed CAR-T cells establishing a maximum blast threshold to ensure blast-free production, thus avoiding accidental CAR transduction of tumoral T cells and potential blast interference during the activation and expansion of the CAR-T product (NCT06064903).

To avoid these drawbacks, the current trend is to use allogeneic T lymphocytes, circumventing potential blast contamination. However, this allogeneic strategy requires multiple CRISPR/Cas9-mediated gene editing to eliminate molecules such as the target antigen and the TCR, thereby preventing fratricide and graft-vs.-host disease[242,243]. This strategy is only feasible with “off-the-shelf” effector cells given that the technical and regulatory complexity of CRISPR/Cas9-mediated genomic editing makes it difficult to implement with autologous T cells harvested from patients in critical clinical conditions. Importantly, previous studies have demonstrated the negative impact that the elimination of the TCR and genomic manipulation of T cells have on the persistence of CAR-T cells and their genomic/chromosomal stability[248].

With the goal of circumventing the limitations of adoptive cell therapies for T cell malignancies, it would be ideal to redirect effector cells against non-pan-T targets present in the tumor but absent in healthy tissues. This approach facilitates the manufacture of autologous CAR-T cells and circumvents both fratricide and immune toxicity[204,281,209,282,229,205]. In this regard, we previously identified CD1a as a *bona fide* immunotherapeutic target for the treatment of T-ALL with a safe profile within non-hematopoietic and hematopoietic tissues[209,283]. This led us to generate and preclinically validate CD1a-directed CAR-T cells, which are now being tested in a phase I clinical trial (NCT05679895). However, CD1a only covers cases of cortical T-ALL, a subtype accounting for ~40% of all diagnosed T-ALL cases, while sparing other T-ALL subtypes associated with higher refractoriness and relapse rates[95,96,98,229].

Here, we identify CCR9 as a target expressed in ~72% of diagnostic T-ALL cases and, importantly, in ~92% of relapses. Of note, Maciocia and colleagues have previously suggested CCR9 as a target for T-ALL and elegantly reported similar expression and safety data[229]. It is important to highlight that these expression rates are maintained in subtypes with dismal prognosis and very high rates of refractoriness and relapse, such as early T cell progenitor ALL (ETP-ALL), an entity with unmet clinical needs[112]. Crucially, CCR9 is not expressed is not expressed in normal circulating T cells or other hematopoietic or non-hematopoietic tissues, except for a subset of B cells, thymocytes, and a small fraction of small intestine-resident lymphocytes. This is to be expected, as CCR9 expression plays a key role in the homing of certain immune cells to the thymus and small intestine[211–213].

Thymic toxicity is not critical, as many studies in non-oncological pediatric and adult patients who have undergone thymectomy have demonstrated immune memory and a complete T cell repertoire[292,293]. In addition, the CCL25-CCR9 axis has been shown to play a role in inflammatory bowel disease, and previous clinical trials have used CCR9 small molecule inhibitors without therapy-related severe toxicities reported, reinforcing the safety of CCR9 as a therapeutic target[294–297]. Collectively, these data support CCR9 as a safe target with promising potential for a large proportion of R/R T-ALL cases.

A major strength of our work lies in the immunophenotypic characterization of CCR9 and CD1a expression in a cohort of 180 primary T-ALL cases. This analysis revealed the existence of significant intratumoral phenotypic heterogeneity, with double positive, single positive, and double negative fractions co-existing within a same sample. This indicates that a dual CAR-T cell therapy targeting both antigens expressed in heterogeneous leukemias, as is the case of a large percentage of R/R T-ALL cases, would increase the number of patients eligible for treatment and offer greater blast coverage, and possibly reduce the likelihood of phenotypic/antigen escape. In addition, the transplantation of CCR9- and CD1a-negative fractions into immunodeficient mice showed that leukemic engraftment reproduces the phenotypic heterogeneity of the original leukemia regardless of the input. This provides unequivocal proof of the plasticity of these antigens, extending the applicability of such dual-targeting immunotherapy to patients without the need for high antigen positivity rates to achieve deep responses. Overall, these results highlight the benefit of a dual targeting strategy, even in patients with leukemic populations only partially positive for one of the markers.

Based on these clinical-biological data, we generated a CCR9-specific hybridoma and derived the scFv sequence that was used to generate a second-generation CAR. The murine scFv was humanized by CDR grafting, and one of the humanized CAR candidates (H2) proved to be as effective as the murine CAR, finally being selected to minimize potential immunogenicity in humans. We next leveraged our humanized CD1a H CAR (NCT05679895) and CCR9 H2 CAR to generate dual-targeting strategies. Of the different possible molecular strategies to direct T cells against two molecules[269] we focused on three: co-transduction with two lentiviral vectors each encoding a different single-targeting CAR, multiple configurations of tandem CARs (two scFvs within the same CAR molecule), and bicistronic CARs (two separate CAR molecules with different specificities encoded in one lentiviral vector). Despite our lab's previous experience in generating tandem CARs targeting other antigens[298], none of the possible tandem CAR configurations worked properly, possibly due to biochemical properties and steric hindrance associated with these specific scFvs. Both co-transduction and bicistronic CAR strategies demonstrated efficacy, but we chose co-transduction for further experiments based on the higher rates of transduction achieved. We then demonstrated the functional advantage of dual-targeting CAR-T cells generated by co-transduction with CCR9- and CD1a-directed CARs over single-targeting CAR-T cells for the treatment of phenotypically heterogeneous T-ALL cases. To the best of our knowledge, this work provides an exhaustive molecular comparative study of all dual targeting CAR-T cell strategies, confirming that the development of dual strategies is not trivial, and generating a unique foundation and knowledge for the applicability of our strategy and that of future constructs.

Taken together, the proposed CAR-T cell strategy directed against two non-pan-T antigens absent in normal T cells and barely expressed in other healthy tissues will achieve a large blast coverage

and benefit a very significant proportion of R/R T-ALL patients, while circumventing T cell fratricide and aplasia, regulatory-challenging genome engineering approaches, and the clinical need for an allogeneic transplantation of patients after CAR-T therapy to rescue T cell aplasia. The fact that CCR9 is also highly expressed in various subtypes of solid tumors with poor prognosis[217–224], along with the fact that CCR9 is the only canonical receptor of the chemokine CCL25, opens enormous possibilities for cancer adoptive immunotherapy beyond T-ALL using either antibody scFv-based or CCL25 zetakine-based CARs[299,300].

ACKNOWLEDGMENTS AND FUNDING

The authors wish to acknowledge Virginia C Rodríguez-Cortez, Pau Ximeno-Parpal, Carla Panisello, Ángela Messeguer Girón, Patrizio Panelli, Alex Bataller, and Patricia Fuentes for their technical support. Research in PM laboratory is supported by CERCA/Generalitat de Catalunya and Fundació Josep Carreras-Obra Social la Caixa for core support, the European Research Council grants (ERC-PoC-957466 IT4B-TALL, ERC-PoC-101100665 BiTE-CAR); H2020 (101057250-CANCERNA), the Spanish Research Agency (AEI) (PID2022-142966OB-I00 funded by MCIN/AEI/10.13039/501100011033 and Feder Funds, and CPP2021-008508, CPP2021-008676 CPP2022-009759 funded by MICIU/AEI/10.13039/501100011033 and the "European Union NextGenerationEU/PRTR); the Spanish Association Against Cancer (AECC, PRYGN234975MENE, PRYGN211192BUEN), the Uno Entre Cien Mil Foundation to CB, and the ISCIII-RICORS within the Next Generation EU program (plan de Recuperación, Transformación y Resilencia). AF was supported by a Juan de la Cierva postdoctoral fellowship (FJC2021-046789-I) and NT by a PhD fellowship (FPU19/00039) from the Spanish Ministry of Science and Innovation.

AUTHOR CONTRIBUTION

Conception and design of the study: NT, DSM, PM; sample acquisition of data: NT, MJM, AM-M, JA, MG-P, HR-H, NF-F, AGP, AF, TV-H, MV, CB, PE, EAG; analysis and interpretation of data: NT, MJM, NF-F, MG-G, PE, VMD, MLT, DS-M, PM; sample preparation and clinical data: AC-E, AB, HC, EG, JR, MD-B, MR-O, MT ; writing: NT, DS-M, PM; review and editing: all authors; guarantors: MLT, VMD, PM.

CONFLICTS OF INTEREST

PM is a cofounder of OneChain Immunotherapeutics, a spin-off company from the Josep Carreras Leukemia Research Institute which has licenced in the CCR9 binder (PCT/EP2024/053734). The remaining authors report no conflicts of interest in this work.

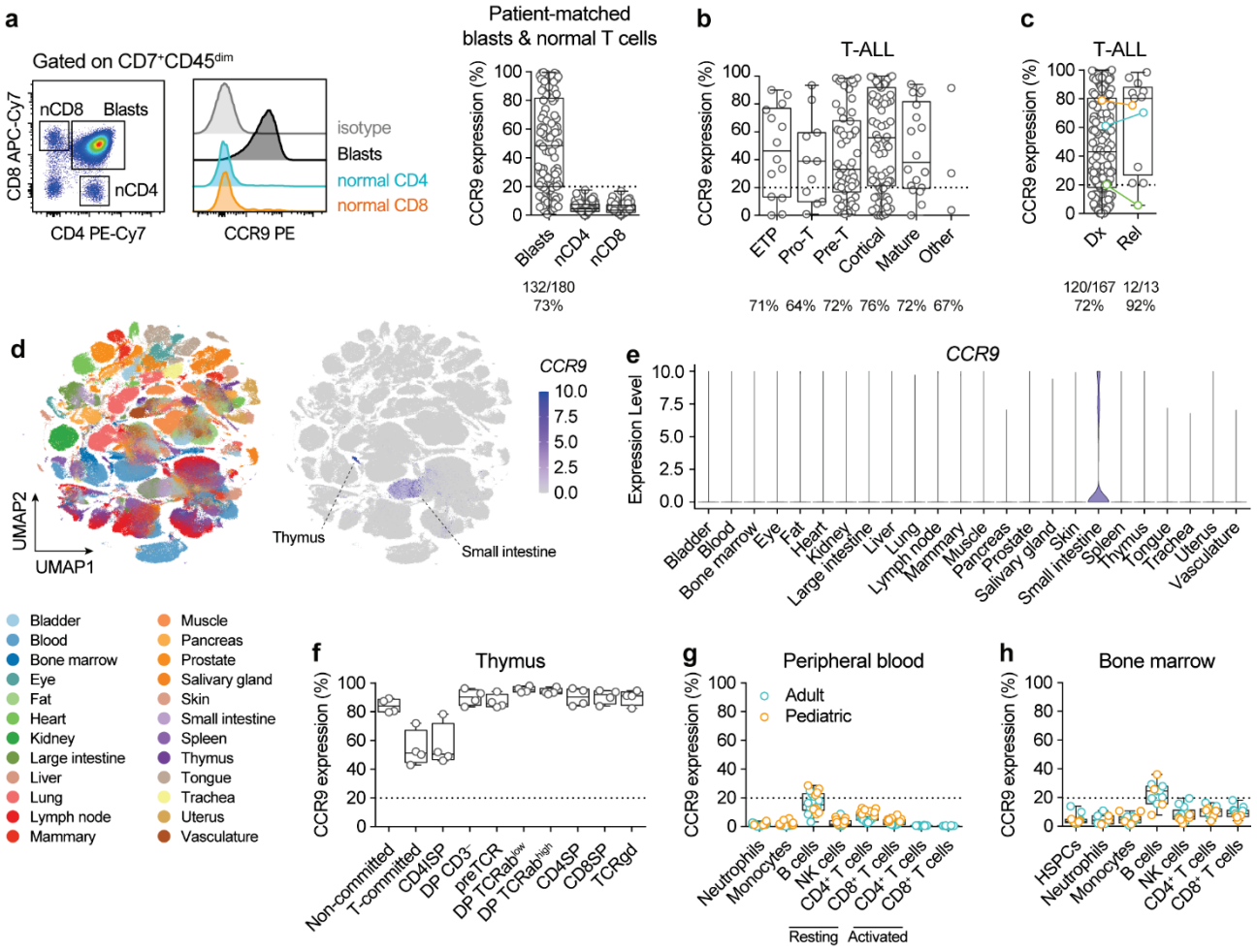

Figure 1. CCR9 is a safe and specific target for T-ALL. (**a**) Flow cytometry analysis of CCR9 in patient-matched leukemic blasts and normal (n) CD4+ and CD8+ T cells in 180 T-ALL patients. Left panels, representative flow cytometry. (**b,c**) Expression of CCR9 in the same cohort of 180 T-ALL primary samples classified by developmental stage (**b**) or disease stage, at diagnosis (Dx) or relapse (Rel) (**c**). Three cases with Dx-Rel matched samples are color-coded. (**d**) UMAP representation showing organ annotation and *CCR9* expression levels in 483,152 cells from human healthy tissues (Tabula Sapiens scRNAseq dataset). (**e**) Violin plots for *CCR9* expression levels across tissues identified in (d). (**f-h**) CCR9 expression in the indicated leukocyte populations in relevant hematological tissues: thymus (**f**, *n*=4), PB (**g**, *n* =18), and BM (**h**, *n*=13).

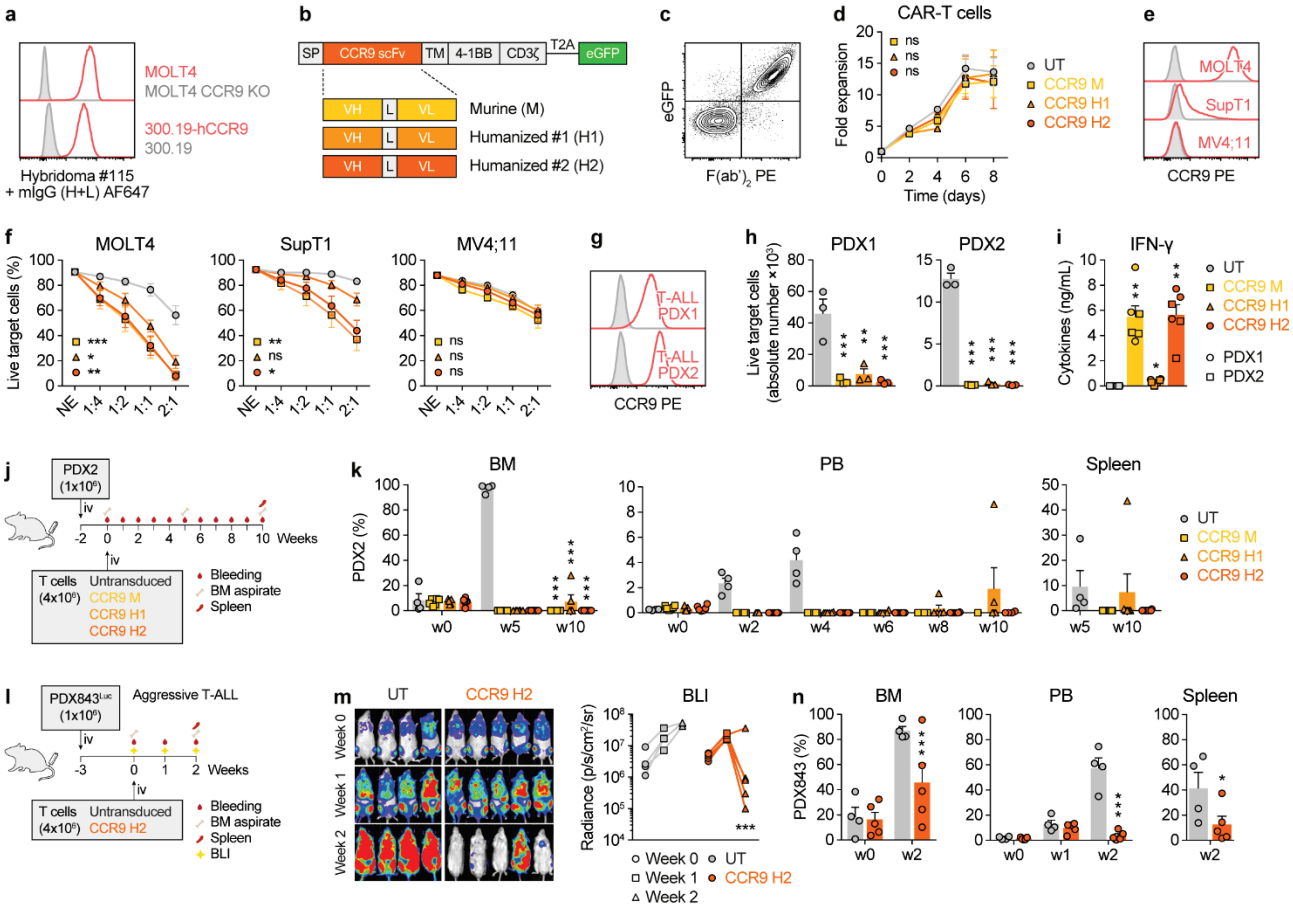

Figure 2. CCR9 CAR-T cells are highly effective against T-ALL. (**a**) In-house developed anti-CCR9 hybridoma specifically stains CCR9-expressing cells. (**b**) Cartoon of second-generation CAR constructs. Three scFv versions were generated: scFv derived from the murine (M) hybridoma, and two humanized candidates (H1 and H2). SP, signal peptide; L, linker. TM, CD8 transmembrane domain. (**c**) Representative flow cytometry plot showing successful detection of transduced CAR-T cells as measured by co-expression of surface F(ab')$_2$ (scFv) and eGFP reporter. (**d**) Proliferation curves for untransduced and the indicated CCR9 CAR-transduced T cells (*n*=3). (**e**) CCR9 expression in the target T-ALL cell lines MOLT4 (CCR9^{high}) and SupT1 (CCR9^{dim}) and the AML cell line MV4;11 (CCR9^{neg}). (**f**) 24-hour cytotoxicity mediated by the different murine and humanized CCR9 CAR-T cells against the indicated cell lines at different effector:target (E:T) ratios (*n*=5). NE, no effector T cells. (**g**) CCR9 expression in two T-ALL PDXs. (**h**) Absolute numbers of live target PDX cells after co-culture with untransduced (UT) or the indicated CCR9 CAR-T cells for 24h at an E:T ratio of 1:1 (*n*=3). (**i**) IFN-γ production by the indicated CCR9 CAR-T cells upon 24h co-culture with PDXs. (**j**) *In vivo* experimental design for the assessment of the efficacy of the three indicated CCR9 CAR-T cells against a T-ALL PDX (PDX2, *n*=4-6 mice/group). (**k**) Flow cytometry follow-up of tumor burden in BM, PB, and spleen in the different treatment groups indicated in (j). (**l**) *In vivo* experimental design for the assessment of the efficacy of the selected CCR9 H2 CAR-T cells against a highly aggressive Luciferase-bearing T-ALL PDX (PDX843, *n*=4-5 mice/group). (**m**) Weekly bioluminescence imaging of mice. Left panel, bioluminescence images. Right panel, bioluminescence quantification. (**n**) Flow cytometry follow-up of tumor burden in BM, PB, and spleen after treatment with untransduced or CCR9 H2 CAR-T cells. Plots show mean ± SEM.

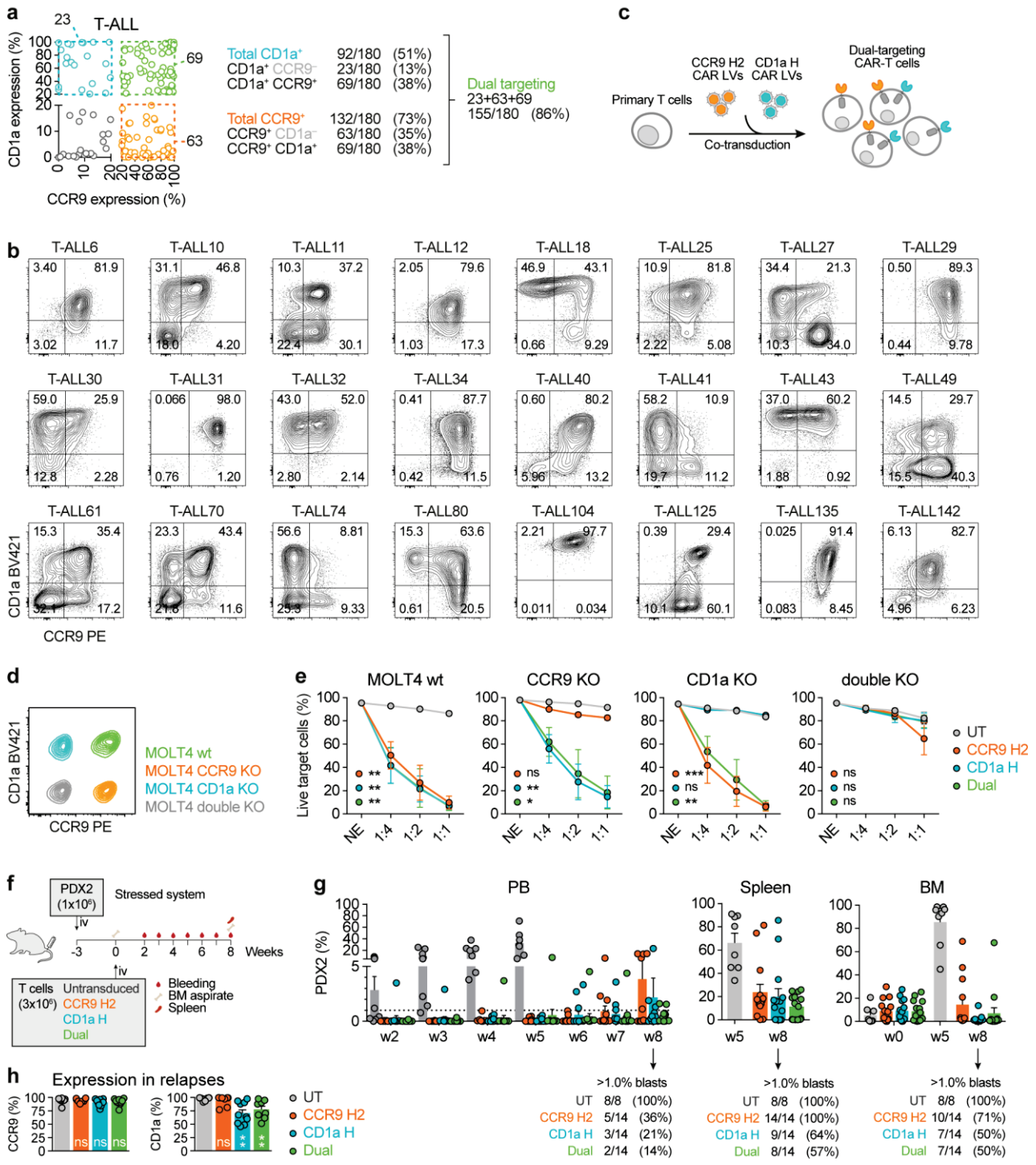

Figure 3. Development of dual CAR-T cells targeting CCR9 and CD1a to cover a broader spectrum of patients T-ALL patients. (**a**) Flow cytometry analysis of CCR9 and CD1a expression in blasts from 180 T-ALL primary samples. 20% expression cut-off was set to define positivity for each marker. (**b**) CCR9 and CD1a immunophenotypes in 24 representative T-ALL patient samples. Cut-off thresholds for antigen positivity were determined using isotype controls. (**c**) Scheme depicting the generation of dual-targeting CAR-T cells through lentiviral co-transduction of single CARs. (**d**) Flow cytometry analysis of the MOLT4 cells CRISPR/Cas9-engineered to express combinatorial CCR9/CD1a phenotypes (+/+, –/+, +/–, –/–). (**e**) *In vitro* cytotoxicity assays demonstrating specific and efficient killing of the different phenotypes of MOLT4 cells with UT T

cells, single CAR (CD1a H or CCR9 H2) T cells and CCR9/CD1a dual-targeting CAR-T cells at different E:T ratios after 24h of co-culture (*n*=3). (**f**) *In vivo* experimental design for the assessment of the efficacy of CCR9- and CD1a-targeting CAR-T cells against a $CCR9^{+}CD1a^{+}$ T-ALL PDX (PDX2) (*n*=8-14 mice/group). (**g**) Flow cytometry follow-up of tumor burden in PB, spleen, and BM after treatment with the indicated CAR treatments. Frequencies of relapsing mice (>1% blasts) for each tissue are indicated. (**h**) Expression of CCR9 and CD1a in CAR-T-resistant blasts.

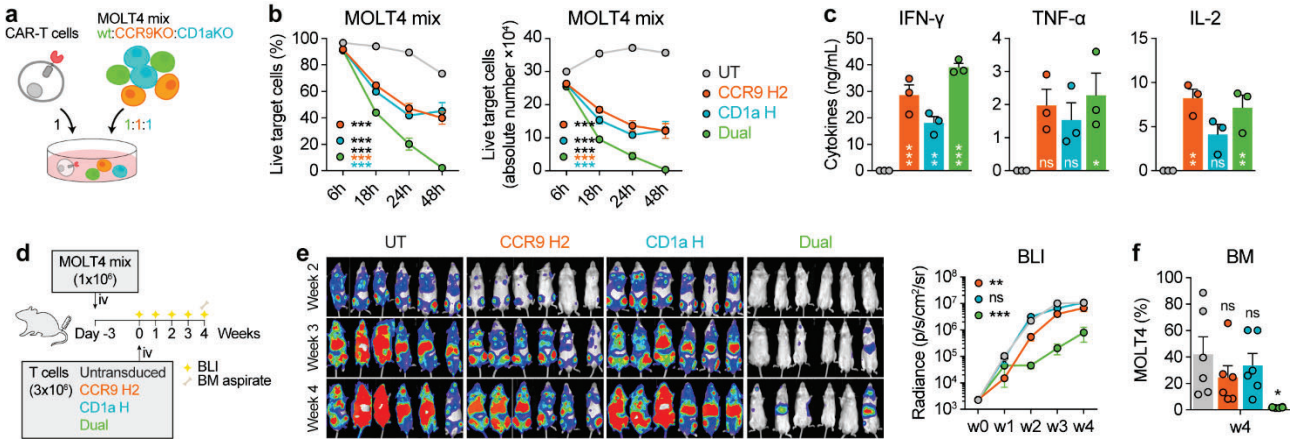

Figure 4. Superior efficacy of dual CCR9 and CD1a CAR-T cells for the treatment of T-ALL cases with phenotypically heterogeneous leukemic populations. (**a**) Combinatorial phenotypes ($CCR9^{+}CD1a^{+}$, $CCR9^{+}CD1a^{-}$, $CCR9^{-}CD1a^{+}$) of T-ALL cells were mixed at a 1:1:1 ratio to reproduce phenotypically heterogenous leukemic samples. (**b**) Relative (left) and absolute (right) numbers of live mixed target cells after a time-course cytotoxicity with UT, single CAR (CCR9 H2 or CD1a H) or CCR9/CD1a dual-targeting CAR-T cells at a 1:1 E:T ratio (*n*=3). (**c**) Cytokine production by the indicated CAR-T cells upon 24h co-culture with target cells (*n*=3). (**d**) *In vivo* experimental design for the assessment of CCR9- and CD1a-targeting dual CAR-T cells against phenotypically heterogeneous Luc-bearing T-ALL target cells (*n*=6 mice/group). (**e**) Weekly bioluminescence imaging of mice (*n*=6 mice/group). Left panel, bioluminescence images. Right panel, bioluminescence quantification. (**f**) Flow cytometry analysis of BM tumor burden at the endpoint. Plots show mean ± SEM.

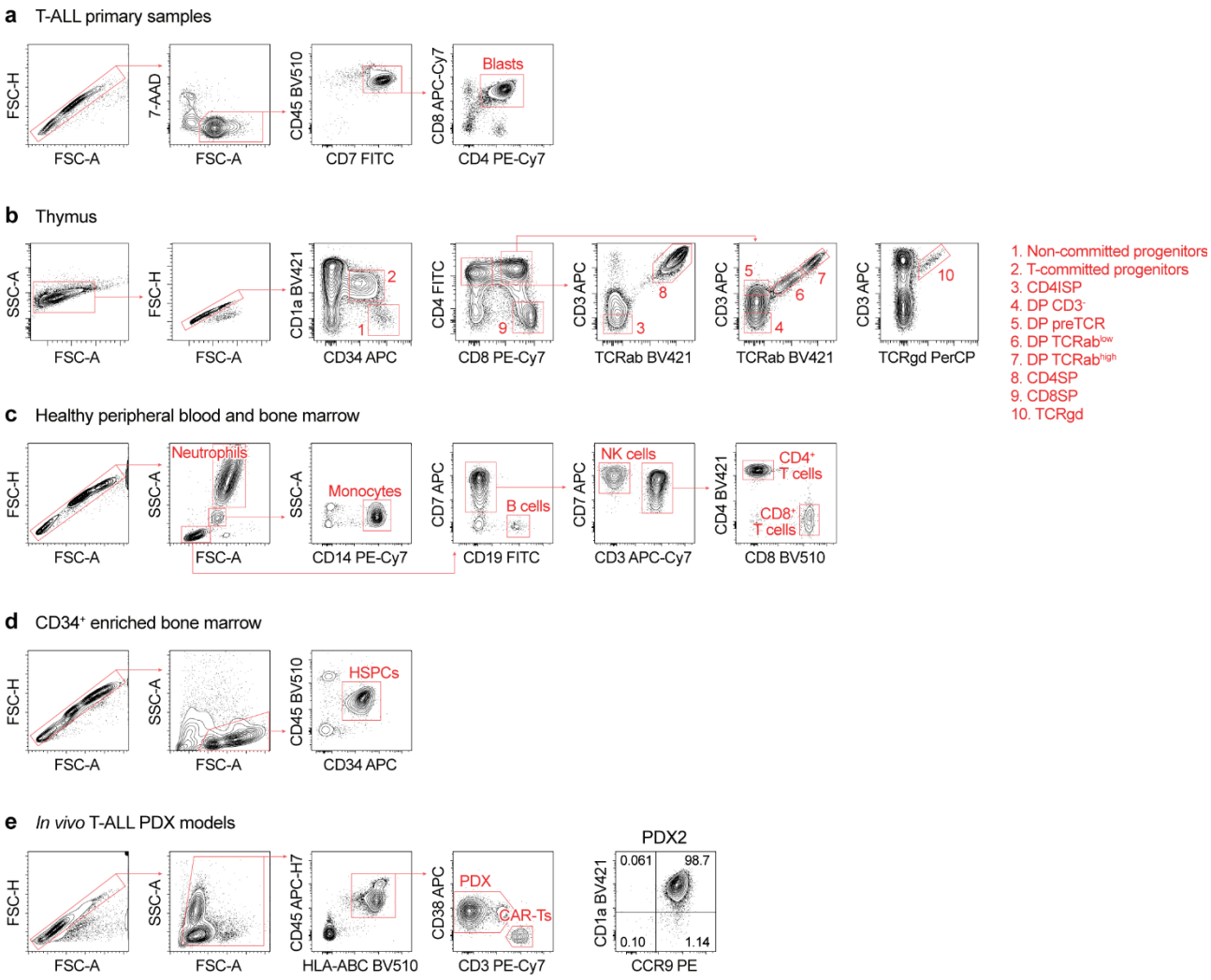

Figure S1. Gating strategies for flow cytometry analyses. (**a**) Flow cytometry gating strategies for T-ALL primary samples. Blasts were identified as $CD7^{+}CD45^{dim}$ and were further gated based on CD4 and CD8 expression to exclude healthy (single $CD4^{+}$ and single $CD8^{+}$) T cells from the analysis. (**b-d**) Flow cytometry gating strategies for the indicated cell populations within healthy thymus (**b**), PB and total BM (**c**), and MACS-enriched BM $CD34^{+}$ HSPCs (**d**). (**f**) Flow cytometry gating strategies for *in vivo* PDX assays. A representative phenotype of PDX2 is included.

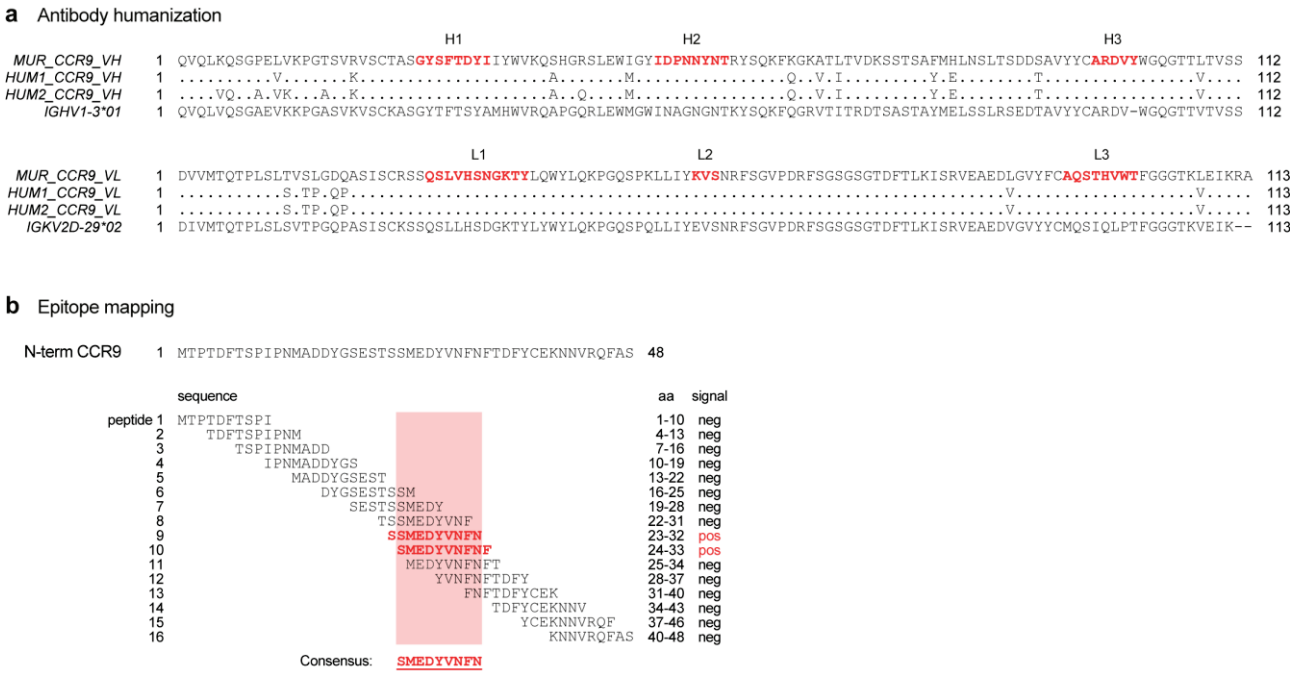

Figure S2. CCR9 binder characterization. (**a**) Protein sequence alignment of the original murine heavy (V_H) and light (V_L) chains with their humanized counterparts (H1 and H2) and the most structurally similar human immunoglobulin gene. CDRs are highlighted in red, and only mutated residues in the humanized sequences are shown. (**b**) Epitope mapping of the anti-CCR9 binder. Overlapping peptides were derived from the extracellular N-terminus of CCR9 used for mice immunization during hybridoma generation and tested for antibody binding by ELISA. The consensus sequence is indicated.

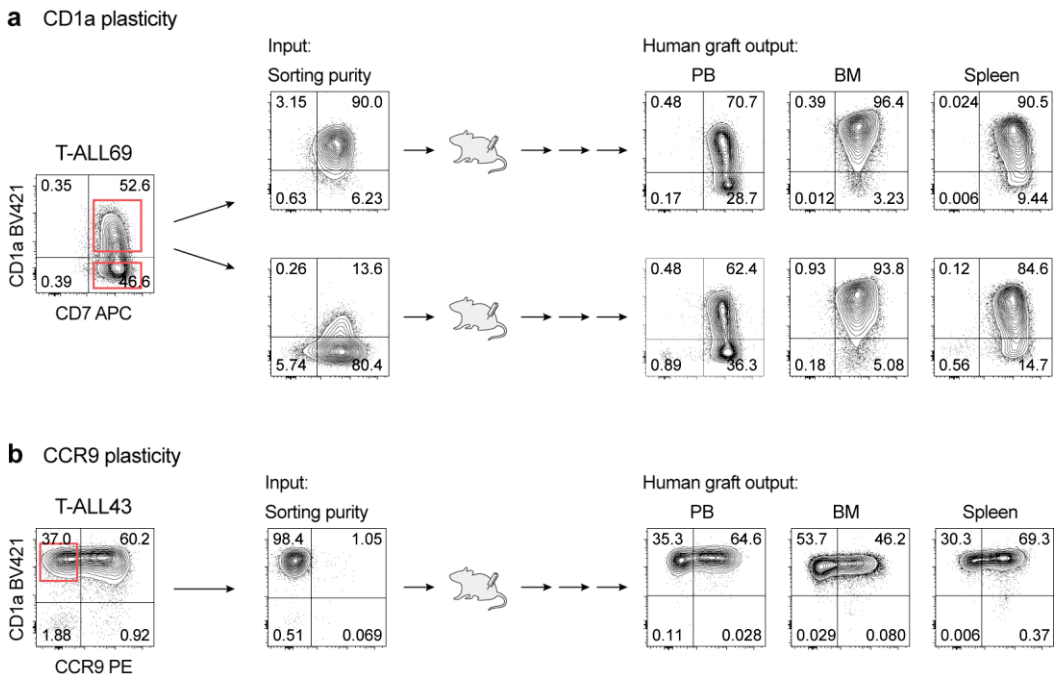

Figure S3. Expression plasticity of CD1a and CCR9. Two primary T-ALL samples with variable expression of CD1a (**a**) and CCR9 (**b**) were sorted, and the purified CD1a$^{+/-}$ or CCR9^{-} fractions (purity: 81%-98%) transplanted into NSG mice. Leukemic graft was followed up biweekly and mice were sacrificed for leukemia immunophenotyping upon detection in PB.

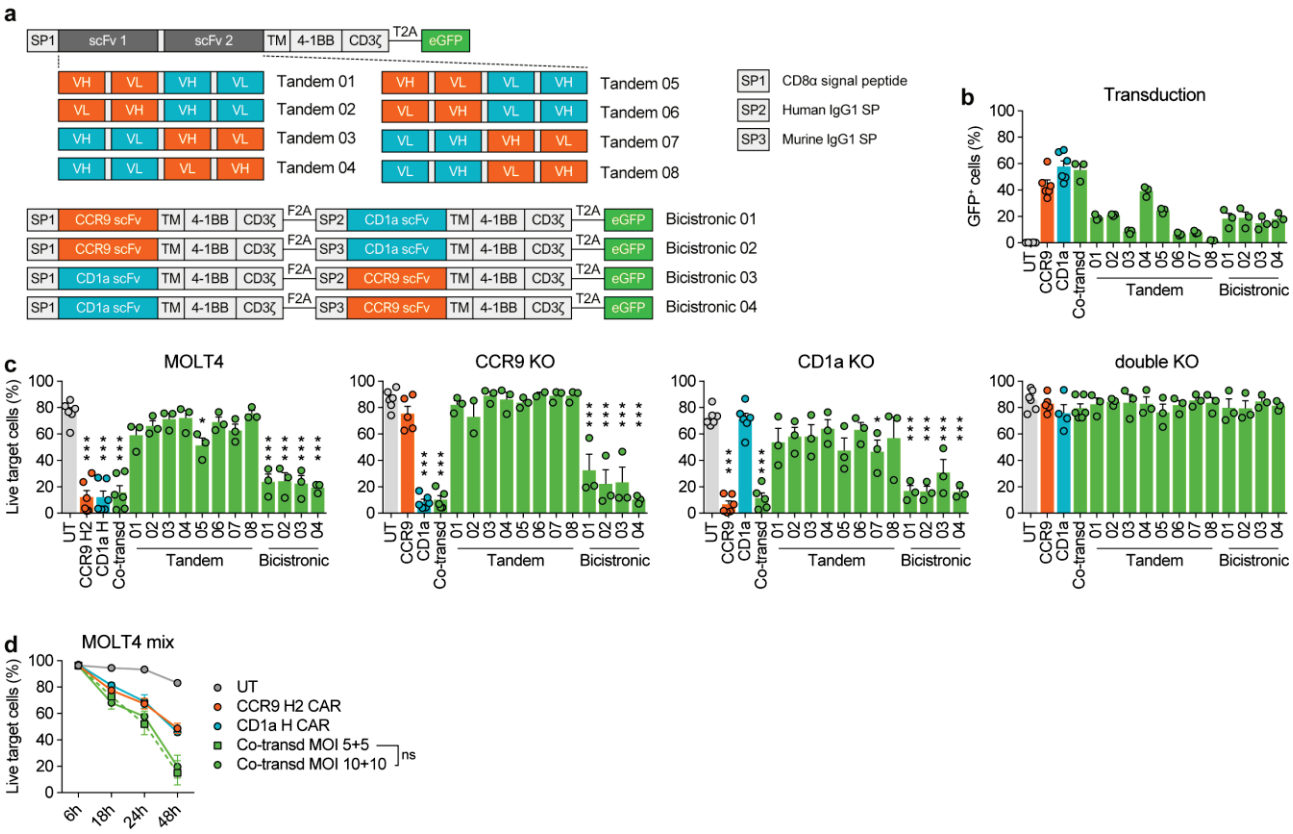

Figure S4. Different molecular strategies for dual targeting of CCR9 and CD1a with CAR-T cells. (**a**) Cartoons of all CAR constructs tested. Top panels, eight different configurations of tandem CAR constructs (CCR9-CD1a vs. CD1a-CCR9 and V_H-V_L vs. V_L-V_H). Bottom panels, four distinct configurations of bicistronic CAR constructs (CCR9-CD1a vs. CD1a-CCR9). Different signal peptides (SP) derived from CD8α (SP1), human IgG1 (SP2), and murine IgG1 (SP3) were used for bicistronic CARs. (**b**) Transduction efficiencies of single, co-transduced, tandem, and bicistronic CAR-T cells. (**c**) Cytotoxicity assays comparing the specificity and efficiency of the different single, co-transduced, tandem, and bicistronic CAR-T cells against combinatorial phenotypes of MOLT4 T-ALL cells at a 1:1 E:T ratio after 24 hours of co-culture (*n*=3-6). UT T cells were used as controls. (**d**) Time-course cytotoxicity comparing dual targeting CAR-T cells co-transduced using a MOI of 5 versus 10 for each CAR against mixed target cells at a 1:1 E:T ratio (*n*=3).

4. Discussion

Acute leukemias constitute a very heterogeneous group of hematological malignancies, which can be risk-stratified according to subtype and molecular lesions, but also factors like age at diagnosis. Still, relapse and refractory acute leukemias pose a great challenge, one in which immunotherapy offers a great opportunity.

As previously discussed, CAR-T immunotherapy has produced great results in B-ALL and other B cell malignancies like multiple myeloma, with impressive response rates[86–90]. However, CAR-T cell therapies are still at the infancy of their clinical implementation, and 50% of patients relapse within the first year of treatment, related with low CAR-T cell persistence[89,267,301]. Despite this, it is widely accepted that CAR-T cells have revolutionized cancer treatment and represent a great therapeutic tool in the treatment of B cell malignancies.

On the other hand, CAR-T therapies for AML and T-ALL have been less successful, mainly because of the on-target, off-tumor toxicities. Most commonly targeted antigens in AML are myeloablative, and their immunotherapy can only be used as a bridge to HSCT, whereas the most targeted antigens in T-ALL therapy lead to life-threatening T cell aplasia, as well as CAR-T fratricide. Another great limitation to all CAR-T therapies is the sourcing of fit T cells for CAR-T manufacturing. T cells of multi-treated patients, who undergo several chemotherapy and lymphodepleting regimens, show reduced fitness, severely limiting overall treatment efficacy[230–232,235].

The main goal of this thesis was to improve current CAR-T cell approaches in the treatment of acute leukemias, using different disease models and focusing on one incremental improvement at a time.

For the first project, we sought to employ γδ T cells, in particular DOT cells, as an allogeneic-safe, off-the-shelf effector CAR-T platform. Compared to αβ-dominated conventional CAR-T products, CAR-DOT cells are MHC-unrestricted and safe for allogeneic use, not requiring any additional engineering to prevent GvHD[302]. Several groups have now reported on the feasibility of a TCR knock out model to prevent allogeneic reaction, but it has also been reported that TCR elimination leads to decreased persistence[248], already a limitation in current CAR-T therapies. DOT cells solve the problem of allogeneicity while avoiding extra regulatory requirements concerning CRISPR/Cas9 genome editing[303].

A second benefit to the use of DOT cells over conventional αβ T cells is the expression of many NK-like cytotoxicity receptors (NKG2D, DNAM-1, NKp30, and NKp44), leading to intrinsic potent, CAR-independent anti-tumoral mechanisms. However, unlike NK cells which have also been used in adoptive cell immunotherapies, γδ T cells offer several advantages: while they share expression of many natural cytotoxicity receptors (NCRs), DOT cells do not express inhibitory KIR receptors, and critically, DOTs allow for a potent TCR-dependent activation upon CD3 stimulation, achieving very high yields from the initial low levels of γδ T cells in peripheral blood. One additional benefit to DOTs' CAR-independent activity is that they would retain their anti-tumoral function even if there were antigen-escape phenomena as a result of the CAR targeting.

DOTs resulted a particularly attractive platform for AML CAR-T immunotherapy, as they had already demonstrated anti-leukemic potential in chronic lymphocytic leukemia and AML[63,304]. Recently, the molecular mechanisms by which DOT cells are able to recognize and eliminate AML cells has been reported, with AML blasts consistently expressing high levels of multiple NCR ligands, particularly

DNAM-1 ligand PVR[305], critical for DOT cell engagement. Furthermore, finding a reliable source of allogeneic T cells for AML is critical, not only due to common lymphopenias, but also because of the exhausted phenotype of multi-treated patients' T cells has been extensively characterized in AML[230].

Our results showed increased in cytotoxic potential and overall efficacy of CD123 CAR-transduced DOT cells against AML in all experimental settings, eliminating more blasts at similar effector:target ratios *in vitro*, releasing increased levels of many key cytokines involved in immune orchestration and the amplification of the antitumor response, and controlling tumor growth in AML PDX models *in vivo*.

DOT cells exhibited limited persistence in mouse *in vivo* models, contrary to conventional αβ T cells, and requiring multiple cell infusions to efficaciously control leukemic progression. However, based on γδ T cell biology and the expansion protocol[62], we found that intraperitoneal IL-15 administration was able to increase T cell persistence in a dose dependent manner, to the extent that untransduced DOT cells were able to ablate AML progression just like CD123 CAR-DOT cells, for up to 70 days, highlighting again the revolutionary potential of γδ T cells in cancer immunotherapy.

The need for exogenous homeostatic IL-15 in our mice models to support and maintain CAR-T cell persistence is in accordance with what has been reported in the bibliography of NK cells and Vδ1$^+$ γδ T cells[306–311]. However, the relevance of IL-15 supplementation in the clinical setting is yet to be determined, as basal circulating levels in patients might be enough to sustain DOT persistence and action. Importantly, lymphodepleting regimens commonly used before CAR-T cell administration have been shown to increase IL-15 levels in patients, probably as a compensatory mechanism[312].

Importantly, and highlighting the importance of γδ T cells in cancer immunotherapy, high γδ T cell infiltration has been associated with better clinical outcomes in many different tumors (melanoma, colorectal, gastric, neck)[313–318], and γδ T cells have even been identified as the single most favorable immune cell in tumor infiltrates across 39 malignancies, including blood, brain, and solid tumors[319].

The positive impact of γδ T cells on the clinical outcome of HSCT has been extensively reported[320–323]. Meta-analysis reveals that higher numbers of γδ T cells in HSCT products associates with lower risk of disease relapse, improved survival and immune reconstitution, fewer viral infections, and no association of developing GvHD[320].

The benefits of γδ T cells extend to CAR-T therapies: the retrospective analysis of a large cohort (*n*=58) of B cell lymphoma patients receiving CD19 CAR-T immunotherapies confirm that high CAR$^+$ γδ counts are associated with a much better progression/recurrence free survival[324]. In accordance with this work, a recent paper reported two chronic lymphocytic leukemia patients that had received CD19 CAR-T cells back in 2010, and still remained disease-free over a decade later[325]. Although an obviously very limited cohort, it serves to illustrate long-term CAR-T dynamics: at earlier timepoints there is a predominant CD8$^+$ response, while at later timepoints once disease remission is achieved almost all CAR$^+$ cells are CD4$^+$, able to better orchestrate immune responses. Interestingly, in one of these two patients there is a very potent γδ T cell response, with γδ T cells reaching up to almost 50% of total CAR$^+$ cells during the first two years after administration. Although these cells were reduced to 0.5% of CAR$^+$ cells by year 7, it helps illustrate the important antitumoral function of (CAR-)γδ T cells in achieving deep responses[325].

It is because of this extensively reported antitumor capacity that there is great interest in developing new γδ T cell immunotherapies, with many trials currently exploring their efficacy in a multitude of clinical settings.

Some trials are exploring the use of unmodified Vδ2^{+} γδ T cells, in late-stage pancreatic, lung, or liver cancer[326,327]. DOT cells, using the same exact expansion protocol we have used for this project, are being tested in the treatment of AML in a clinical trial led by GammaDelta Therapeutics, later acquired by Takeda (NCT05001451).

The use of γδ T cells as the effector platform for CAR-T therapies dates back to 2004, where it was first proposed with 1st generation CD19 CARs[328]. Many groups have developed CAR-γδT therapies, although they are almost always Vδ2-based[329–338] with the exception of a couple of CAR-Vδ1 T cell products[311,339]. Our works builds on this foundation, and offers a new therapeutic option, feasible and ready-to-use with increased effectiveness in multiple models, for AML patients.

For the second project, we developed a STAb-T cell immunotherapy targeting CD1a against coT-ALL and made a side-by-side comparison with conventional CAR-T cells. These CD1a STAb-T cells produce and release CD1axCD3 bispecific T cell engagers, bridging coT-ALL blasts with effector T cells and eliciting a cytotoxic response.

Bispecific T cell engagers, or more specifically bispecific antibodies, are artificial molecules made from the antigen-binding domains of two different antibodies, used to crosslink different cell types, usually in cancer immunotherapy[340]. Most BiTEs have an anti-CD3 scFv, to recruit T cell cytotoxicity, although several BiTE formats specifically engage γδ T cells have been designed[341–349].

CD19xCD3 blinatumomab was the first FDA-approved BiTE, for the treatment of Ph^{-} R/R B-ALL, in 2014[350,351]. Blinatumomab has now become a staple of R/R B-ALL treatment, and more BiTEs have since been approved or are in advanced development for the treatment of other malignancies[352,353].

In situ secretion of BiTEs through genetic engineering of bystander cells to engage T lymphocytes has long been proposed[250–252,258,354–361], as well as innovative approaches with varied functions like immune checkpoint blockade[362], protection against HIV infection by secreted antibodies[363], and oncolytic virus-mediated tumor killing and BiTE production, to augment the antitumor response[364], even using γδ T cells as effector cells[338].

We proposed a CD1a-directed STAb-T therapy as STAb-T cells achieve similar cytotoxicity effects to CAR-Ts at much inferior effector:target ratios, as patients suffering from T cell malignancies (or any other hematological malignancy) often present with lymphopenias and the obtention of enough fit T cells to start CAR-T manufacturing can be challenging (another reason supporting the use of allogeneic effector cells)[177,232,234].

In accordance with what has already been reported for CD19^{+} B-ALL[250,252,258] and more recently for BCMA^{+} multiple myeloma[361], our CD1a STAb-T cells showed drastically increased cytotoxicity over CD1a CAR-T cells *in vitro,* due to their ability to recruit unmodified bystander T cells. The benefit of CD1a STAb-T cells in *in vivo* experiments, however, was not necessarily as marked as that observed with CD19 and BCMA.

Increased *in vivo* efficacy of CD19 STAb-T cells was due to rapid CAR-mediated down-regulation of CD19, along with surface CAR loss. STAb-T cells overcame this antigen escape mechanism, and were able to prevent disease relapses in mice: both treatments showed similar efficacies at earlier timepoints (up to day 60), but in the long-term only STAb-T cells were able to maintain remission[252].

On the other hand, common shedding of surface BCMA by myeloma cells leads to soluble BCMA proteins, that can block CAR-T cytotoxicity by saturating CAR molecules with cell-free BCMA. This phenomenon, however, had no impact on STAb-T function[361].

These two phenomena giving an advantage to STAb-T therapies—CD19 downregulation and BCMA shedding—do not happen with CD1a. This absence of evident immune escape mechanisms could explain the similar efficacy of CD1a CAR and STAb therapies *in vivo*, despite the clearly more potent and rapid *in vitro* responses of CD1a STAb-T cells.

We then propose our CD1a STAb-T therapy as an alternative to CAR-T cells for coT-ALL patients with aggressive and hyperleukocytic relapses, with limited numbers of non-leukemic effector T lymphocytes.

Finally, for the final project we aimed to identify and evaluate novel safe immunotherapeutic targets and generate an according CAR-T immunotherapy for T-ALL. We chose to focus on this disease as R/R T-ALL has a dismal prognosis, with long-term overall survivals of only 20%[111,120]. Building on CD1a immunotherapy again, we sought to find novel antigens for T-ALL to expand the applicability beyond cortical T-ALL, while maintaining safety and keeping toxicities to a minimum.

Based on previous works describing the mAb-based targeting of CCR9 for the treatment of T-ALL preclinical models[227,228], we decided to evaluate the feasibility of CCR9-directed immunotherapies. We first evaluated its specificity in a large cohort of 180 primary T-ALL samples collected from various biobanks, and found CCR9 to be heterogeneously expressed, although across all subtypes and very specific to the blast population and minimal in all relevant healthy tissues.

After the analysis of CCR9 expression, we proceeded to generate a proprietary anti-CCR9 antibody using hybridoma technology to derive its scFv for CCR9 CAR design. Because our ultimate goal was for this therapy to eventually get into clinical trials, the CCR9 CAR was humanized, to reduce immunogenicity and improve its efficacy in patients.

Proof of the relevance of this work, Maciocia and colleagues developed CCR9-directed CAR-T cells for T-ALL in a very similar work[229]. Strikingly, the same percentage of CCR9 expression was seen in both cohorts (73%). One difference between both works is the reported expression in thymocytes: Maciocia reports “low” to “somewhat higher” expression in certain thymic subsets, as opposed to the near-total expression we detected in these same subsets. This difference may be explained by the method of detection: Maciocia used quantitative PCR, while we used flow cytometry. While it is true that CCR9 surface density (mean fluorescence intensity) varies along thymocyte differentiation, all stages were undoubtedly positive.

Another difference is the sourcing of the CCR9 binder: Maciocia *et al.* used a rat-derived scFv, while we started with a mouse antibody. The fact that they use a rat antibody, as opposed to the mouse norm, is probably indicative of the difficulty of generating anti-CCR9 antibodies. Due to its structure (most of the protein is embedded in the plasma membrane) and the high homclogy of murine and human forms, it shows very low immunogenicity. In fact, in our project, only one out of almost 100 initial hybridoma subclones that initially tested positive in an ELISA screening turned out to be a true positive and could be used for scFv generation.

Importantly, most of the clinical trials currently evaluating CAR-T cells for R/R T-ALL are based on panT antigens CD7 or CD5, which are consistently expressed at high levels by >95% of T lymphoblasts (with the exception of CD5 in the case of ETP-ALL). These immunotherapies, although

applicable to virtually all T-ALL cases, come at the great expense of profound, life-threatening T cell aplasias[94,290].

CD7-targeting immunotherapies are compromised by T cell fratricide, and thus CRISPR/Cas9 gene editing and other techniques, such as ER-retention motifs, have been used to produce $CD7^{neg}$ CD7-targeting CAR-T cells. The costs of these additional genetic manipulations are prohibitive, and they also pose greater regulatory challenges, and so new strategies are being explored[202,203].

While most T cells are $CD7^{+}$, around 3-5% of circulating T cells are naturally $CD7^{-}$, and some groups have proposed the use of this small fraction to develop fratricide resistant CD7 immunotherapies, where $CD7^{+}$ T cells would be eliminated during CAR-T manufacturing[279]. Because of the small numbers of this naturally existing population, the collection of sufficient functional T cells for product manufacturing remains a challenge, even when using donor-derived T cells instead of sourcing them from the patients[262,279,278]. Furthermore, even if this prevents CAR-T fratricide, there is still the ensuing T (and NK cell) aplasia, and it is not clear whether these small numbers of surviving $CD7^{-}$ T cells are able to provide full immune protection. PanT-targeting therapies will thus require HSCT, much like CAR-T therapies for AML, not only for its GvL effect, but also to restore immunity[262].

Co-expression analysis of CCR9 and CD1a in our cohort revealed a large number of T-ALL patients with heterogeneous expression of both markers, including some cases with biclonal populations with each clone predominantly expressing a different antigen. Based on this data, and because of the expected minimal toxicity of CCR9 and CD1a targeting, we proposed a dual immunotherapy to have a single product to treat any T-ALL case, whether or not it is double positive for both antigens. We believe this dual targeting would achieve deeper responses without significantly increasing on-target/off-tumor toxicities and bypassing the need for "corrective" alloHSCT after CAR-T therapy.

Critically, we have demonstrated the plasticity of CCR9 and CD1a expression: T-ALL samples with heterogeneous expression of either CCR9 or CD1a were sorted into their respective positive and negative fractions and transplanted into mice. Regardless of which fraction was transplanted, the phenotype of the leukemic graft recapitulated that of the original primary sample, showing that there is probably some degree of natural antigen turnover. Thus, it would not be necessary to present >95% antigen expression in blasts, but a much lower threshold, as blasts that would not express either antigen at the time of CAR-T infusion would eventually upregulate it and become susceptible to CAR-T killing.

A different phenomenon to natural antigen malleability is antigen down-regulation in response to its immunotherapy. Although it could be argued that this natural turnover is a risk for antigen escape, we do not expect it to be the case for CCR9, as CCR9 has been shown to negatively correlate with the outcome of a large number of tumors and contribute to their progression[217–224], including T-ALL[225,226]. Thus, CCR9 would confer a proliferative advantage to T-ALL blasts, making its targeting particularly attractive. In fact, we have observed preclinical data showing partial down-regulation of CD1a in the residual blast populations after CD1a immunotherapy (both *in vitro* and *in vivo*), but not with CCR9.

Dual targeting has been extensively proposed for B cell malignancies, particularly CD19/CD22 for B-ALL and CD19/BCMA for multiple myeloma[263–265,298]. Dual targeting is useful when there is phenotypic heterogeneity in the target population, so as to maximize coverage, but it can also help bypass the risk of antigen down-modulation in response to immunotherapy[269]. CD19 is frequently lost after CD19-immunotherapy, be it CAR-T cells or blinatumomab, and dual targeting can mitigate this antigen escape[84,252,298].

Some phase I clinical trials have also demonstrated CD7 escape after immunotherapy in as many as 25% of patients[262]. To overcome this, dual-targeting CAR-T cells have already been proposed for T-ALL, in particular CD5/CD7 CAR-T cells[355].

Our CCR9/CD1a immunotherapy, however, is the first ever non-panT dual CAR-T immunotherapy, bypassing T cell aplasias and the requirement for salvage alloHCT, offering a therapeutic option for patients with a currently unmet clinical need and hopefully reducing treatment-derived toxicities.

CAR-T immunotherapies are still in their infancy, but their promise remains and the number of clinical trials evaluating CAR-T therapies keeps growing, aiming to offer treatment to all sorts of diseases, not just hematological malignancies: high-risk tumors[366,367], autoimmune disease[368–372], cardiovascular disease[373–376], and even HIV or fungal infections[377–381].

There are many avenues being explored for CAR-T improvement, with much room for growth. In this thesis we have explored only a few of those strategies: the use of allogeneic effector cells to shorten the time to product administration (of key importance in patients with rapidly progressing disease); the potentiation of blast killing through recruitment of bystander, unmodified T cells, and finally, offering a new unique therapy for high-risk patients of R/R T-ALL, reducing the toxicities of current gold standard CAR-T therapies.

We believe that the implementation of multiple incremental enhancements—the ones explored here and the ones being explored by multitude of groups all over the globe—will take immunotherapy to the next level, making it more effective and being moved to the first line of treatment, while hopefully reducing the costs and making it more accessible in resource-poor healthcare environments.

5. Conclusions

1. CD123 CAR-DOT cells for AML

1.1. CD123-directed CAR-DOT cells expand robustly while preserving DOT phenotype.

1.2. CD123 CAR-DOTs specifically augment cytotoxicity against AML cell lines and primary blasts *in vitro*.

1.3. Serial infusions of CD123 CAR-DOTs exhibit robust antileukemic effect *in vivo*.

1.4. Provision of IL-15 supports single-dose CD123 CAR-DOT activity *in vivo*.

2. CD1a STAb-T cells for coT-ALL

2.1. The CD1a T cell engager (CD1axCD3) binds to both CD1a and CD3 and induces specific T cell activation.

2.2. CD1a STAb-T cells induce a more potent and rapid cytotoxic responses than CD1a CAR-T cells.

2.3. CD1a STAb-T cells eliminate T-ALL cells through the granular exocytosis pathway.

2.4. Recruitment of bystander T cells provides CD1a STAb-T cells with greater *in vitro* tumor cell killing efficiency than CD1a CAR-T cells.

2.5. CD1a STAb-T cells are as effective as CD1a CAR-T cells in *in vivo* patient-derived xenograft T-ALL models.

3. CCR9/CD1a CAR-T cells for T-ALL

3.1. CCR9 is a safe and specific immunotherapeutic target for T-ALL, expressed across subtypes and absent in all relevant healthy tissues.

3.2. Murine and humanized CCR9 CAR-T cells exhibit a potent, expression-dependent cytotoxic activity against T-ALL blasts, both *in vitro* and *in vivo*.

3.3. The dual targeting of CCR9 and CD1a allows to increase the number of patients eligible for our immunotherapy without significantly increasing on-target/off-tumor toxicities.

3.4. CCR9/CD1a dual-targeting T cells retain the specificity of single targeting CAR-T cells, and are equally as effective in models with homogeneous antigen expression, *in vitro* and *in vivo*.

3.5. In short-term models with CCR9/CD1a phenotypic heterogeneity within a sample dual CAR-T cells show increased anti-leukemic ability over single-targeting CAR-T cells.

Bibliography

1. Abbas, A. K., Lichtman, A. H. & Pillai, S. *Cellular and Molecular Immunology*.
2. Silverstein, A. M. Cellular versus humoral immunology: a century-long dispute. *Nat. Immunol.* **4**, 425–428 (2003).
3. Boehm, T. & Swann, J. B. Origin and Evolution of Adaptive Immunity. *Annu. Rev. Anim. Biosci.* **2**, 259–283 (2014).
4. Flajnik, M. F. A cold-blooded view of adaptive immunity. *Nat. Rev. Immunol.* **18**, 438–453 (2018).
5. Burnet, F. M. A modification of Jerne's theory of antibody production using the concept of clonal selection. *CA. Cancer J. Clin.* **26**, 119–121 (1976).
6. Cohn, M. *et al.* Reflections on the clonal-selection theory. *Nat. Rev. Immunol.* **7**, 823–830 (2007).
7. Hoffman, R. *Hematology: Basic Principles and Practice*. (Saunders/Elsevier, Philadelphia, PA, 2013).
8. Farley, A. M. *et al.* Dynamics of thymus organogenesis and colonization in early human development. *Dev. Camb. Engl.* **140**, 2015–2026 (2013).
9. Bromley, S. K., Mempel, T. R. & Luster, A. D. Orchestrating the orchestrators: chemokines in control of T cell traffic. *Nat. Immunol.* **9**, 970–980 (2008).
10. Schulz, O., Hammerschmidt, S. I., Moschovakis, G. L. & Förster, R. Chemokines and Chemokine Receptors in Lymphoid Tissue Dynamics. *Annu. Rev. Immunol.* **34**, 203–242 (2016).
11. Dreyer, W. J. & Bennett, J. C. The molecular basis of antibody formation: a paradox. *Proc. Natl. Acad. Sci. U. S. A.* **54**, 864–869 (1965).
12. Tonegawa, S., Steinberg, C., Dube, S. & Bernardini, A. Evidence for somatic generation of antibody diversity. *Proc. Natl. Acad. Sci. U. S. A.* **71**, 4027–4031 (1974).
13. Schatz, D. G., Oettinger, M. A. & Baltimore, D. The V(D)J recombination activating gene, RAG-1. *Cell* **59**, 1035–1048 (1989).
14. Bronte, V. & Pittet, M. J. The Spleen in Local and Systemic Regulation of Immunity. *Immunity* **39**, 806–818 (2013).
15. Qi, H., Kastenmüller, W. & Germain, R. N. Spatiotemporal Basis of Innate and Adaptive Immunity in Secondary Lymphoid Tissue. *Annu. Rev. Cell Dev. Biol.* **30**, 141–167 (2014).
16. Lewis, S. M., Williams, A. & Eisenbarth, S. C. Structure and function of the immune system in the spleen. *Sci. Immunol.* **4**, eaau6085 (2019).
17. Grant, S. M., Lou, M., Yao, L., Germain, R. N. & Radtke, A. J. The lymph node at a glance – how spatial organization optimizes the immune response. *J. Cell Sci.* **133**, jcs241828 (2020).
18. Clark, M. R., Mandal, M., Ochiai, K. & Singh, H. Orchestrating B cell lymphopoiesis through interplay of IL-7 receptor and pre-B cell receptor signalling. *Nat. Rev. Immunol.* **14**, 69–80 (2014).
19. Kwak, K., Akkaya, M. & Pierce, S. K. B cell signaling in context. *Nat. Immunol.* **20**, 963–969 (2019).
20. Kurosaki, T., Shinohara, H. & Baba, Y. B cell signaling and fate decision. *Annu. Rev. Immunol.* **28**, 21–55 (2010).
21. Edelman, G. M. & Poulik, M. D. Studies on structural units of the gamma-globulins. *J. Exp. Med.* **113**, 861–884 (1961).
22. Porter, R. R. Separation and isolation of fractions of rabbit gamma-globulin containing the antibody and antigenic combining sites. *Nature* **182**, 670–671 (1958).

23. Sun, Y., Huang, T., Hammarström, L. & Zhao, Y. The Immunoglobulins: New Insights, Implications, and Applications. *Annu. Rev. Anim. Biosci.* **8**, 145–169 (2020).

24. Stanfield, R. L. & Wilson, I. A. Antibody Structure. *Microbiol. Spectr.* **2**, (2014).

25. Sanoja-Flores, L., Flores-Montero, J., Pérez-Andrés, M., Puig, N. & Orfao, A. Detection of Circulating Tumor Plasma Cells in Monoclonal Gammopathies: Methods, Pathogenic Role, and Clinical Implications. *Cancers* **12**, 1499 (2020).

26. Beers, S. A., Glennie, M. J. & White, A. L. Influence of immunoglobulin isotype on therapeutic antibody function. *Blood* **127**, 1097–1101 (2016).

27. Köhler, G. & Milstein, C. Continuous cultures of fused cells secreting antibody of predefined specificity. *Nature* **256**, 495–497 (1975).

28. Taniuchi, I. CD4 Helper and CD8 Cytotoxic T Cell Differentiation. *Annu. Rev. Immunol.* **36**, 579–601 (2018).

29. Klein, L., Robey, E. A. & Hsieh, C.-S. Central CD4+ T cell tolerance: deletion versus regulatory T cell differentiation. *Nat. Rev. Immunol.* **19**, 7–18 (2019).

30. Boehm, T. & Swann, J. B. Thymus involution and regeneration: two sides of the same coin? *Nat. Rev. Immunol.* **13**, 831–838 (2013).

31. Rossjohn, J. *et al.* T Cell Antigen Receptor Recognition of Antigen-Presenting Molecules. *Annu. Rev. Immunol.* **33**, 169–200 (2015).

32. Babbitt, B. P., Allen, P. M., Matsueda, G., Haber, E. & Unanue, E. R. Binding of immunogenic peptides to Ia histocompatibility molecules. *Nature* **317**, 359–361 (1985).

33. Adams, E. J. & Luoma, A. M. The Adaptable Major Histocompatibility Complex (MHC) Fold: Structure and Function of Nonclassical and MHC Class I–Like Molecules. *Annu. Rev. Immunol.* **31**, 529–561 (2013).

34. Stern, L. J. & Santambrogio, L. The melting pot of the MHC II peptidome. *Curr. Opin. Immunol.* **40**, 70–77 (2016).

35. Hedrick, S. M., Cohen, D. I., Nielsen, E. A. & Davis, M. M. Isolation of cDNA clones encoding T cell-specific membrane-associated proteins. *Nature* **308**, 149–153 (1984).

36. Yanagi, Y. *et al.* A human T cell-specific cDNA clone encodes a protein having extensive homology to immunoglobulin chains. *Nature* **308**, 145–149 (1984).

37. Courtney, A. H., Lo, W.-L. & Weiss, A. TCR Signaling: Mechanisms of Initiation and Propagation. *Trends Biochem. Sci.* **43**, 108–123 (2018).

38. Gaud, G., Lesourne, R. & Love, P. E. Regulatory mechanisms in T cell receptor signalling. *Nat. Rev. Immunol.* **18**, 485–497 (2018).

39. Malissen, B. & Bongrand, P. Early T cell activation: integrating biochemical, structural, and biophysical cues. *Annu. Rev. Immunol.* **33**, 539–561 (2015).

40. Chen, L. & Flies, D. B. Molecular mechanisms of T cell co-stimulation and co-inhibition. *Nat. Rev. Immunol.* **13**, 227–242 (2013).

41. Rothenberg, E. V. Programming for T-lymphocyte fates: modularity and mechanisms. *Genes Dev.* **33**, 1117–1135 (2019).

42. Ceredig, R. & Rolink, T. A positive look at double-negative thymocytes. *Nat. Rev. Immunol.* **2**, 888–897 (2002).

43. Von Boehmer, H. Unique features of the pre-T-cell receptor α-chain: not just a surrogate. *Nat. Rev. Immunol.* **5**, 571–577 (2005).

44. Carpenter, A. C. & Bosselut, R. Decision checkpoints in the thymus. *Nat. Immunol.* **11**, 666–673 (2010).

45. La Gruta, N. L., Gras, S., Daley, S. R., Thomas, P. G. & Rossjohn, J. Understanding the drivers of MHC restriction of T cell receptors. *Nat. Rev. Immunol.* **18**, 467–478 (2018).

46. Murata, S., Takahama, Y., Kasahara, M. & Tanaka, K. The immunoproteasome and thymoproteasome: functions, evolution and human disease. *Nat. Immunol.* **19**, 923–931 (2018).

47. Aifantis, I., Raetz, E. & Buonamici, S. Molecular pathogenesis of T-cell leukaemia and lymphoma. *Nat. Rev. Immunol.* **8**, 380–390 (2008).

48. Hogquist, K. A. & Jameson, S. C. The self-obsession of T cells: how TCR signaling thresholds affect fate 'decisions' and effector function. *Nat. Immunol.* **15**, 815–823 (2014).

49. Takahama, Y., Ohigashi, I., Baik, S. & Anderson, G. Generation of diversity in thymic epithelial cells. *Nat. Rev. Immunol.* **17**, 295–305 (2017).

50. Cyster, J. G. Lymphoid organ development and cell migration. *Immunol. Rev.* **195**, 5–14 (2003).

51. Sallusto, F., Lenig, D., Förster, R., Lipp, M. & Lanzavecchia, A. Two subsets of memory T lymphocytes with distinct homing potentials and effector functions. *Nature* **401**, 708–712 (1999).

52. Gattinoni, L. T memory stem cells in health and disease. *Nat. Med.* **23**, (2017).

53. Wherry, E. J. T cell exhaustion. *Nat. Immunol.* **12**, 492–499 (2011).

54. Wherry, E. J. & Kurachi, M. Molecular and cellular insights into T cell exhaustion. *Nat. Rev. Immunol.* **15**, 486–499 (2015).

55. Godfrey, D. I., Uldrich, A. P., McCluskey, J., Rossjohn, J. & Moody, D. B. The burgeoning family of unconventional T cells. *Nat. Immunol.* **16**, 1114–1123 (2015).

56. Lin, T. D. *et al.* Evolution of T cells in the cancer-resistant naked mole-rat. *Nat. Commun.* **15**, 3145 (2024).

57. Pennington, D. J., Silva-Santos, B. & Hayday, A. C. γδ T cell development — having the strength to get there. *Curr. Opin. Immunol.* **17**, 108–115 (2005).

58. Silva-Santos, B., Serre, K. & Norell, H. γδ T cells in cancer. *Nat. Rev. Immunol.* **15**, 683–691 (2015).

59. Silva-Santos, B., Mensurado, S. & Coffelt, S. B. γδ T cells: pleiotropic immune effectors with therapeutic potential in cancer. *Nat. Rev. Cancer* **19**, 392–404 (2019).

60. Gray, J. I. *et al.* Human γδ T cells in diverse tissues exhibit site-specific maturation dynamics across the life span. *Sci. Immunol.* **9**, eadn3954 (2024).

61. Vantourout, P. & Hayday, A. Six-of-the-best: unique contributions of γδ T cells to immunology. *Nat. Rev. Immunol.* **13**, 88–100 (2013).

62. Correia, D. V. *et al.* Differentiation of human peripheral blood Vδ1+ T cells expressing the natural cytotoxicity receptor NKp30 for recognition of lymphoid leukemia cells. *Blood* **118**, 992–1001 (2011).

63. Almeida, A. R. *et al.* Delta One T Cells for Immunotherapy of Chronic Lymphocytic Leukemia: Clinical-Grade Expansion/Differentiation and Preclinical Proof of Concept. *Clin. Cancer Res.* **22**, 5795–5804 (2016).

64. Döhner, H., Weisdorf, D. J. & Bloomfield, C. D. Acute Myeloid Leukemia. *N. Engl. J. Med.* **373**, 1136–1152 (2015).

65. Hunger, S. P. & Mullighan, C. G. Acute Lymphoblastic Leukemia in Children. *N. Engl. J. Med.* **373**, 1541–1552 (2015).

66. Greaves, M., Chan, L., Furley, A., Watt, S. & Molgaard, H. Lineage promiscuity in hemopoietic differentiation and leukemia. *Blood* **67**, 1–11 (1986).

67. Hurwitz, C. A. *et al.* Asynchronous antigen expression in B lineage acute lymphoblastic leukemia. *Blood* **72**, 299–307 (1988).

68. Craig, F. E. & Foon, K. A. Flow cytometric immunophenotyping for hematologic neoplasms. *Blood* **111**, 3941–3967 (2008).

69. DiGiuseppe, J. A. Acute Lymphoblastic Leukemia: Diagnosis and Detection of Minimal Residual Disease Following Therapy. *Clin. Lab. Med.* **27**, 533–549 (2007).

70. Kita, K. *et al.* Phenotypical characteristics of acute myelocytic leukemia associated with the t(8;21)(q22;q22) chromosomal abnormality: frequent expression of immature B-cell antigen CD19 together with stem cell antigen CD34. *Blood* **80**, 470–477 (1992).

71. Bene, M. C. *et al.* Proposals for the immunological classification of acute leukemias. European Group for the Immunological Characterization of Leukemias (EGIL). *Leukemia* **9**, 1783–1786 (1995).

72. Lapidot, T. *et al.* A cell initiating human acute myeloid leukaemia after transplantation into SCID mice. *Nature* **367**, 645–648 (1994).

73. Bonnet, D. & Dick, J. E. Human acute myeloid leukemia is organized as a hierarchy that originates from a primitive hematopoietic cell. *Nat. Med.* **3**, 730–737 (1997).

74. Shlush, L. I. *et al.* Identification of pre-leukaemic haematopoietic stem cells in acute leukaemia. *Nature* **506**, 328–333 (2014).

75. Sung, H. *et al.* Global Cancer Statistics 2020: GLOBOCAN Estimates of Incidence and Mortality Worldwide for 36 Cancers in 185 Countries. *CA. Cancer J. Clin.* **71**, 209–249 (2021).

76. Arber, D. A. *et al.* International Consensus Classification of Myeloid Neoplasms and Acute Leukemias: integrating morphologic, clinical, and genomic data. *Blood* **140**, 1200–1228 (2022).

77. DiNardo, C. D. & Wei, A. H. How I treat acute myeloid leukemia in the era of new drugs. *Blood* **135**, 85–96 (2020).

78. Sweeney, C. & Vyas, P. The Graft-Versus-Leukemia Effect in AML. *Front. Oncol.* **9**, 1217 (2019).

79. Styczyński, J. *et al.* Death after hematopoietic stem cell transplantation: changes over calendar year time, infections and associated factors. *Bone Marrow Transplant.* **55**, 126–136 (2020).

80. Yanada, M. *et al.* Predicting non-relapse mortality following allogeneic hematopoietic cell transplantation during first remission of acute myeloid leukemia. *Bone Marrow Transplant.* **56**, 387–394 (2021).

81. Pui, C.-H. *et al.* Childhood Acute Lymphoblastic Leukemia: Progress Through Collaboration. *J. Clin. Oncol.* **33**, 2938–2948 (2015).

82. Quijano, C. A. *et al.* Cytogenetically aberrant cells are present in the CD34+CD33-38-19- marrow compartment in children with acute lymphoblastic leukemia. *Leukemia* **11**, 1508–1515 (1997).

83. le Viseur, C. *et al.* In childhood acute lymphoblastic leukemia, blasts at different stages of immunophenotypic maturation have stem cell properties. *Cancer Cell* **14**, 47–58 (2008).

84. Bueno, C. *et al.* CD34+CD19-CD22+ B-cell progenitors may underlie phenotypic escape in patients treated with CD19-directed therapies. *Blood* **140**, 38–44 (2022).

85. Hunger, S. P. *et al.* Dasatinib with intensive chemotherapy in de novo paediatric Philadelphia chromosome-positive acute lymphoblastic leukaemia (CA180-372/COG AALL1122): a single-arm, multicentre, phase 2 trial. *Lancet Haematol.* **10**, e510–e520 (2023).

86. Maude, S. L. *et al.* Chimeric antigen receptor T cells for sustained remissions in leukemia. *N. Engl. J. Med.* **371**, 1507–1517 (2014).

87. Park, J. H. *et al.* Long-Term Follow-up of CD19 CAR Therapy in Acute Lymphoblastic Leukemia. *N. Engl. J. Med.* **378**, 449–459 (2018).

88. Myers, R. M. *et al.* Humanized CD19-Targeted Chimeric Antigen Receptor (CAR) T Cells in CAR-Naive and CAR-Exposed Children and Young Adults With Relapsed or Refractory Acute Lymphoblastic Leukemia. *J. Clin. Oncol.* **39**, 3044–3055 (2021).

89. Ortíz-Maldonado, V. *et al.* CART19-BE-01: A Multicenter Trial of ARI-0001 Cell Therapy in Patients with CD19+ Relapsed/Refractory Malignancies. *Mol. Ther.* **29**, 636–644 (2021).

90. Ortiz-Maldonado, V. *et al.* Results of ARI-0001 CART19 cell therapy in patients with relapsed/refractory CD19-positive acute lymphoblastic leukemia with isolated extramedullary disease. *Am. J. Hematol.* **97**, 731–739 (2022).

91. Cox, C. V. *et al.* Characterization of a progenitor cell population in childhood T-cell acute lymphoblastic leukemia. *Blood* **109**, 674–682 (2007).

92. Chiu, P. P. L., Jiang, H. & Dick, J. E. Leukemia-initiating cells in human T-lymphoblastic leukemia exhibit glucocorticoid resistance. *Blood* **116**, 5268–5279 (2010).

93. Gerby, B. *et al.* Expression of CD34 and CD7 on human T-cell acute lymphoblastic leukemia discriminates functionally heterogeneous cell populations. *Leukemia* **25**, 1249–1258 (2011).

94. Bayón-Calderón, F., Toribio, M. L. & González-García, S. Facts and Challenges in Immunotherapy for T-Cell Acute Lymphoblastic Leukemia. *Int. J. Mol. Sci.* **21**, 7685 (2020).

95. Litzow, M. R. & Ferrando, A. A. How I treat T-cell acute lymphoblastic leukemia in adults. *Blood* **126**, 833–841 (2015).

96. Hoelzer, D. *et al.* Successful Subtype Oriented Treatment Strategies in Adult T-All; Results of 744 Patients Treated in Three Consecutive GMALL Studies. *Blood* **114**, 324 (2009).

97. Schrappe, M. *et al.* Late MRD response determines relapse risk overall and in subsets of childhood T-cell ALL: results of the AIEOP-BFM-ALL 2000 study. *Blood* **118**, 2077–2084 (2011).

98. Leong, S. *et al.* CD1a is rarely expressed in pediatric or adult relapsed/refractory T-ALL: implications for immunotherapy. *Blood Adv.* **4**, 4665–4668 (2020).

99. Neumann, M. *et al.* Molecular subgroups of T-cell acute lymphoblastic leukemia in adults treated according to pediatric-based GMALL protocols. *Leukemia* (2024) doi:10.1038/s41375-024-02264-0.

100. Pear, W. S. *et al.* Exclusive development of T cell neoplasms in mice transplanted with bone marrow expressing activated Notch alleles. *J. Exp. Med.* **183**, 2283–2291 (1996).

101. Weng, A. P. *et al.* Activating mutations of NOTCH1 in human T cell acute lymphoblastic leukemia. *Science* **306**, 269–271 (2004).

102. Liu, Y. *et al.* The genomic landscape of pediatric and young adult T-lineage acute lymphoblastic leukemia. *Nat. Genet.* **49**, 1211–1218 (2017).

103. Belver, L. & Ferrando, A. The genetics and mechanisms of T cell acute lymphoblastic leukaemia. *Nat. Rev. Cancer* **16**, 494–507 (2016).

104. Genescà, E. & González-Gil, C. Latest Contributions of Genomics to T-Cell Acute Lymphoblastic Leukemia (T-ALL). *Cancers* **14**, 2474 (2022).

105. Teachey, D. T. & Pui, C.-H. Comparative features and outcomes between paediatric T-cell and B-cell acute lymphoblastic leukaemia. *Lancet Oncol.* **20**, e142–e154 (2019).

106. Van Vlierberghe, P. *et al.* PHF6 mutations in T-cell acute lymphoblastic leukemia. *Nat. Genet.* **42**, 338–342 (2010).

107. Van der Meulen, J. *et al.* The H3K27me3 demethylase UTX is a gender-specific tumor suppressor in T-cell acute lymphoblastic leukemia. *Blood* **125**, 13–21 (2015).

108. Schneider, N. R. *et al.* New recurring cytogenetic abnormalities and association of blast cell karyotypes with prognosis in childhood T-cell acute lymphoblastic leukemia: a pediatric oncology group report of 343 cases. *Blood* **96**, 2543–2549 (2000).

109. Ballerini, P. *et al.* Impact of genotype on survival of children with T-cell acute lymphoblastic leukemia treated according to the French protocol FRALLE-93: the effect of TLX3/HOX11L2 gene expression on outcome. *Haematologica* **93**, 1658–1665 (2008).

110. Karrman, K. *et al.* Clinical and cytogenetic features of a population-based consecutive series of 285 pediatric T-cell acute lymphoblastic leukemias: rare T-cell receptor gene rearrangements are associated with poor outcome. *Genes. Chromosomes Cancer* **48**, 795–805 (2009).

111. Teachey, D. T. & O'Connor, D. How I treat newly diagnosed T-cell acute lymphoblastic leukemia and T-cell lymphoblastic lymphoma in children. *Blood* **135**, 159–166 (2020).

112. Coustan-Smith, E. *et al.* Early T-cell precursor leukaemia: a subtype of very high-risk acute lymphoblastic leukaemia. *Lancet Oncol.* **10**, 147–156 (2009).

113. Giacomo, D. D. *et al.* 14q32 rearrangements deregulating BCL11B mark a distinct subgroup of T-lymphoid and myeloid immature acute leukemia.

114. Montefiori, L. E. *et al.* Enhancer Hijacking Drives Oncogenic *BCL11B* Expression in Lineage-Ambiguous Stem Cell Leukemia. *Cancer Discov.* **11**, 2846–2867 (2021).

115. Genescà, E. & La Starza, R. Early T-Cell Precursor ALL and Beyond: Immature and Ambiguous Lineage T-ALL Subsets. *Cancers* **14**, 1873 (2022).

116. DeAngelo, D. J. *et al.* Nelarabine induces complete remissions in adults with relapsed or refractory T-lineage acute lymphoblastic leukemia or lymphoblastic lymphoma: Cancer and Leukemia Group B study 19801. *Blood* **109**, 5136–5142 (2007).

117. Bataller, A. *et al.* Early T-cell precursor lymphoblastic leukaemia: response to FLAG-IDA and high-dose cytarabine with sorafenib after initial refractoriness. *Br. J. Haematol.* **185**, 755–757 (2019).

118. Hamilton, B. K. *et al.* Allogeneic Hematopoietic Cell Transplantation for Adult T Cell Acute Lymphoblastic Leukemia. *Biol. Blood Marrow Transplant. J. Am. Soc. Blood Marrow Transplant.* **23**, 1117–1121 (2017).

119. Sutton, R. *et al.* Persistent MRD before and after allogeneic BMT predicts relapse in children with acute lymphoblastic leukaemia. *Br. J. Haematol.* **168**, 395–404 (2015).

120. Samra, B. *et al.* Outcome of adults with relapsed/refractory T-cell acute lymphoblastic leukemia or lymphoblastic lymphoma. *Am. J. Hematol.* **95**, (2020).

121. Reismüller, B. *et al.* Long-term outcome of initially homogenously treated and relapsed childhood acute lymphoblastic leukaemia in Austria--a population-based report of the Austrian Berlin-Frankfurt-Münster (BFM) Study Group. *Br. J. Haematol.* **144**, 559–570 (2009).

122. Jain, N. *et al.* A Multicenter Phase I Study Combining Venetoclax with Mini-Hyper-CVD in Older Adults with Untreated and Relapsed/Refractory Acute Lymphoblastic Leukemia. *Blood* **134**, 3867–3867 (2019).

123. Lacayo, N. J. *et al.* Safety and Efficacy of Venetoclax in Combination with Navitoclax in Adult and Pediatric Relapsed/Refractory Acute Lymphoblastic Leukemia and Lymphoblastic Lymphoma. *Blood* **134**, 285–285 (2019).

124. Lu, B. Y. *et al.* Decitabine enhances chemosensitivity of early T-cell precursor-acute lymphoblastic leukemia cell lines and patient-derived samples. *Leuk. Lymphoma* **57**, 1938–1941 (2016).

125. Laukkanen, S. *et al.* Therapeutic targeting of LCK tyrosine kinase and mTOR signaling in T-cell acute lymphoblastic leukemia. *Blood* **140**, 1891–1906 (2022).

126. Saygin, C. *et al.* Dual Targeting of Apoptotic and Signaling Pathways in T-Lineage Acute Lymphoblastic Leukemia. *Clin. Cancer Res. Off. J. Am. Assoc. Cancer Res.* **29**, 3151–3161 (2023).

127. Bride, K. L. *et al.* Preclinical efficacy of daratumumab in T-cell acute lymphoblastic leukemia. *Blood* **131**, 995–999 (2018).

128. Ehrlich, P. Über den jetzigen Stand der Karzinomforschung. (1909).

129. Silverstein, A. M. Paul Ehrlich's Passion: The Origins of His Receptor Immunology. *Cell. Immunol.* **194**, 213–221 (1999).

130. Burnet, M. Cancer; A Biological Approach: I. The Processes Of Control. *BMJ* **1**, 779–786 (1957).

131. Burnet, F. M. The Concept of Immunological Surveillance. in *Progress in Tumor Research* (ed. Schwartz, R. S.) vol. 13 1–27 (S. Karger AG, 1970).

132. Ward, J. P., Gubin, M. M. & Schreiber, R. D. The Role of Neoantigens in Naturally Occurring and Therapeutically Induced Immune Responses to Cancer. in *Advances in Immunology* vol. 130 25–74 (Elsevier, 2016).

133. Schumacher, T. N., Scheper, W. & Kvistborg, P. Cancer Neoantigens. *Annu. Rev. Immunol.* **37**, 173–200 (2019).

134. Pearlman, A. H. *et al.* Targeting public neoantigens for cancer immunotherapy. *Nat. Cancer* **2**, 487–497 (2021).

135. Lang, F., Schrörs, B., Löwer, M., Türeci, Ö. & Sahin, U. Identification of neoantigens for individualized therapeutic cancer vaccines. *Nat. Rev. Drug Discov.* **21**, 261–282 (2022).

136. Dunn, G. P., Old, L. J. & Schreiber, R. D. The Three Es of Cancer Immunoediting. *Annu. Rev. Immunol.* **22**, 329–360 (2004).

137. Smyth, M. J., Dunn, G. P. & Schreiber, R. D. Cancer Immunosurveillance and Immunoediting: The Roles of Immunity in Suppressing Tumor Development and Shaping Tumor Immunogenicity. in *Advances in Immunology* vol. 90 1–50 (Elsevier, 2006).

138. O'Donnell, J. S., Teng, M. W. L. & Smyth, M. J. Cancer immunoediting and resistance to T cell-based immunotherapy. *Nat. Rev. Clin. Oncol.* **16**, 151–167 (2019).

139. Chen, D. S. & Mellman, I. Elements of cancer immunity and the cancer–immune set point. *Nature* **541**, 321–330 (2017).

140. Hanahan, D. & Weinberg, R. A. Hallmarks of Cancer: The Next Generation. *Cell* **144**, 646–674 (2011).

141. Linsley, P. S. *et al.* Human B7-1 (CD80) and B7-2 (CD86) bind with similar avidities but distinct kinetics to CD28 and CTLA-4 receptors. *Immunity* **1**, 793–801 (1994).

142. Freeman, G. J. *et al.* Engagement of the PD-1 immunoinhibitory receptor by a novel B7 family member leads to negative regulation of lymphocyte activation. *J. Exp. Med.* **192**, 1027–1034 (2000).

143. *Tumor Microenvironment:* vol. 1224 (Springer International Publishing, Cham, 2020).

144. Dysthe, M. & Parihar, R. Myeloid-Derived Suppressor Cells in the Tumor Microenvironment. *Adv. Exp. Med. Biol.* **1224**, 117–140 (2020).

145. Dhatchinamoorthy, K., Colbert, J. D. & Rock, K. L. Cancer Immune Evasion Through Loss of MHC Class I Antigen Presentation. *Front. Immunol.* **12**, 636568 (2021).

146. Cornel, A. M., Mimpen, I. L. & Nierkens, S. MHC Class I Downregulation in Cancer: Underlying Mechanisms and Potential Targets for Cancer Immunotherapy. *Cancers* **12**, 1760 (2020).

147. Waldman, A. D., Fritz, J. M. & Lenardo, M. J. A guide to cancer immunotherapy: from T cell basic science to clinical practice. *Nat. Rev. Immunol.* **20**, 651–668 (2020).

148. Salles, G. *et al.* Rituximab in B-Cell Hematologic Malignancies: A Review of 20 Years of Clinical Experience. *Adv. Ther.* **34**, 2232–2273 (2017).

149. Goldsmith, S. R., Foley, N. & Schroeder, M. A. Daratumumab for the treatment of multiple myeloma. *Drugs Today Barc. Spain 1998* **57**, 591–605 (2021).

150. Lambert, J. *et al.* Gemtuzumab ozogamicin for *de novo* acute myeloid leukemia: final efficacy and safety updates from the open-label, phase III ALFA-0701 trial. *Haematologica* **104**, 113–119 (2019).

151. Kantarjian, H. M. *et al.* Inotuzumab Ozogamicin versus Standard Therapy for Acute Lymphoblastic Leukemia. *N. Engl. J. Med.* **375**, 740–753 (2016).

152. Cameron, D. *et al.* 11 years' follow-up of trastuzumab after adjuvant chemotherapy in HER2-positive early breast cancer: final analysis of the HERceptin Adjuvant (HERA) trial. *Lancet Lond. Engl.* **389**, 1195–1205 (2017).

153. Rudin, C. M. *et al.* Pembrolizumab or Placebo Plus Etoposide and Platinum as First-Line Therapy for Extensive-Stage Small-Cell Lung Cancer: Randomized, Double-Blind, Phase III KEYNOTE-604 Study. *J. Clin. Oncol.* **38**, 2369–2379 (2020).

154. Provencio, M. *et al.* Perioperative Nivolumab and Chemotherapy in Stage III Non–Small-Cell Lung Cancer. *N. Engl. J. Med.* **389**, 504–513 (2023).

155. Kantarjian, H. *et al.* Blinatumomab versus Chemotherapy for Advanced Acute Lymphoblastic Leukemia. *N. Engl. J. Med.* **376**, 836–847 (2017).

156. Van Der Sluis, I. M. *et al.* Blinatumomab Added to Chemotherapy in Infant Lymphoblastic Leukemia. *N. Engl. J. Med.* **388**, 1572–1581 (2023).

157. Wagner, D. L. *et al.* Immunogenicity of CAR T cells in cancer therapy. *Nat. Rev. Clin. Oncol.* **18**, 379–393 (2021).

158. Chiu, M. L., Goulet, D. R., Teplyakov, A. & Gilliland, G. L. Antibody Structure and Function: The Basis for Engineering Therapeutics. *Antibodies* **8**, 55 (2019).

159. Sommermeyer, D. *et al.* Fully human CD19-specific chimeric antigen receptors for T-cell therapy. *Leukemia* **31**, 2191–2199 (2017).

160. Oliver-Caldés, A. *et al.* Fractionated initial infusion and booster dose of ARI0002h, a humanised, BCMA-directed CAR T-cell therapy, for patients with relapsed or refractory multiple myeloma (CARTBCMA-HCB-01): a single-arm, multicentre, academic pilot study. *Lancet Oncol.* **24**, 913–924 (2023).

161. Granot, N. & Storb, R. History of hematopoietic cell transplantation: challenges and progress. *Haematologica* **105**, 2716–2729 (2020).

162. Bacigalupo, A. *et al.* Defining the Intensity of Conditioning Regimens: Working Definitions. *Biol. Blood Marrow Transplant.* **15**, 1628–1633 (2009).

163. Southam, C. M., Brunschwig, A., Levin, A. G. & Dizon, Q. S. Effect of leukocytes on transplantability of human cancer. *Cancer* **19**, 1743–1753 (1966).

164. Weiden, P. L. *et al.* Antileukemic effect of graft-versus-host disease in human recipients of allogeneic-marrow grafts. *N. Engl. J. Med.* **300**, 1068–1073 (1979).

165. Zeiser, R. & Blazar, B. R. Acute Graft-versus-Host Disease — Biologic Process, Prevention, and Therapy. *N. Engl. J. Med.* **377**, 2167–2179 (2017).

166. Cordonnier, C. *et al.* Vaccination of haemopoietic stem cell transplant recipients: guidelines of the 2017 European Conference on Infections in Leukaemia (ECIL 7). *Lancet Infect. Dis.* **19**, e200–e212 (2019).

167. Kamboj, M. & Shah, M. K. Vaccination of the Stem Cell Transplant Recipient and the Hematologic Malignancy Patient. *Infect. Dis. Clin. North Am.* **33**, 593–609 (2019).

168. Rosenberg, S. A. *et al.* Use of tumor-infiltrating lymphocytes and interleukin-2 in the immunotherapy of patients with metastatic melanoma. A preliminary report. *N. Engl. J. Med.* **319**, 1676–1680 (1988).

169. Rosenberg, S. A. *et al.* Durable Complete Responses in Heavily Pretreated Patients with Metastatic Melanoma Using T-Cell Transfer Immunotherapy. *Clin. Cancer Res.* **17**, 4550–4557 (2011).

170. Guedan, S., Ruella, M. & June, C. H. Emerging Cellular Therapies for Cancer. *Annu. Rev. Immunol.* **37**, 145–171 (2019).

171. Gross, G., Waks, T. & Eshhar, Z. Expression of immunoglobulin-T-cell receptor chimeric molecules as functional receptors with antibody-type specificity. *Proc. Natl. Acad. Sci.* **86**, 10024–10028 (1989).

172. Eshhar, Z., Waks, T., Gross, G. & Schindler, D. G. Specific activation and targeting of cytotoxic lymphocytes through chimeric single chains consisting of antibody-binding domains and the gamma or zeta subunits of the immunoglobulin and T-cell receptors. *Proc. Natl. Acad. Sci.* **90**, 720–724 (1993).

173. Maher, J., Brentjens, R. J., Gunset, G., Rivière, I. & Sadelain, M. Human T-lymphocyte cytotoxicity and proliferation directed by a single chimeric TCRζ /CD28 receptor. *Nat. Biotechnol.* **20**, 70–75 (2002).

174. Sterner, R. C. & Sterner, R. M. CAR-T cell therapy: current limitations and potential strategies. *Blood Cancer J.* **11**, 69 (2021).

175. Majzner, R. G. & Mackall, C. L. Tumor Antigen Escape from CAR T-cell Therapy. *Cancer Discov.* **8**, 1219–1226 (2018).

176. Wat, J. & Barmettler, S. Hypogammaglobulinemia After Chimeric Antigen Receptor (CAR) T-Cell Therapy: Characteristics, Management, and Future Directions. *J. Allergy Clin. Immunol. Pract.* **10**, 460–466 (2022).

177. Amini, L. *et al.* Preparing for CAR T cell therapy: patient selection, bridging therapies and lymphodepletion. *Nat. Rev. Clin. Oncol.* **19**, 342–355 (2022).

178. Turtle, C. J. *et al.* CD19 CAR–T cells of defined CD4+:CD8+ composition in adult B cell ALL patients. *J. Clin. Invest.* **126**, 2123–2138 (2016).

179. Lee, D. W. *et al.* ASTCT Consensus Grading for Cytokine Release Syndrome and Neurologic Toxicity Associated with Immune Effector Cells. *Biol. Blood Marrow Transplant.* **25**, 625–638 (2019).

180. Jain, M. D., Smith, M. & Shah, N. N. How I Treat Refractory CRS and ICANS Following CAR T-cell Therapy. *Blood* blood.2022017414 (2023) doi:10.1182/blood.2022017414.

181. Si, S. & Teachey, D. T. Spotlight on Tocilizumab in the Treatment of CAR-T-Cell-Induced Cytokine Release Syndrome: Clinical Evidence to Date. *Ther. Clin. Risk Manag.* **16**, 705–714 (2020).

182. Wijewarnasuriya, D., Bebernitz, C., Lopez, A. V., Rafiq, S. & Brentjens, R. J. Excessive Costimulation Leads to Dysfunction of Adoptively Transferred T Cells. *Cancer Immunol. Res.* **8**, 732–742 (2020).

183. Gill, S. *et al.* Preclinical targeting of human acute myeloid leukemia and myeloablation using chimeric antigen receptor–modified T cells. *Blood* **123**, 2343–2354 (2014).

184. Kenderian, S. S. *et al.* CD33-specific chimeric antigen receptor T cells exhibit potent preclinical activity against human acute myeloid leukemia. *Leukemia* **29**, 1637–1647 (2015).

185. Baroni, M. L. *et al.* 41BB-based and CD28-based CD123-redirected T-cells ablate human normal hematopoiesis in vivo. *J. Immunother. Cancer* **8**, e000845 (2020).

186. Bataller Torralba, A. *et al.* Design and in Vitro Evaluation of a CAR-T Prototype (ARI-0003) Targeting CD123 for Acute Myeloid Leukemia. *Blood* **138**, 4799–4799 (2021).

187. Taussig, D. C. Hematopoietic stem cells express multiple myeloid markers: implications for the origin and targeted therapy of acute myeloid leukemia. *Blood* **106**, 4086–4092 (2005).

188. He, X. *et al.* Bispecific and split CAR T cells targeting CD13 and TIM3 eradicate acute myeloid leukemia. *Blood* **135**, 713–723 (2020).

189. Lynn, R. C. *et al.* High-affinity FRβ-specific CAR T cells eradicate AML and normal myeloid lineage without HSC toxicity. *Leukemia* **30**, 1355–1364 (2016).

190. Jetani, H. *et al.* CAR T-cells targeting FLT3 have potent activity against FLT3–ITD+ AML and act synergistically with the FLT3-inhibitor crenolanib. *Leukemia* **32**, 1168–1179 (2018).

191. Niswander, L. M. *et al.* Potent preclinical activity of FLT3-directed chimeric antigen receptor T-cell immunotherapy against *FLT3*-mutant acute myeloid leukemia and *KMT2A*-rearranged acute lymphoblastic leukemia. *Haematologica* **108**, 457–471 (2022).

192. Danylesko, I. *et al.* Remission of acute myeloid leukemia with t(8;21) following CD19 CAR T-cells. *Leukemia* **34**, 1939–1942 (2020).

193. Venditti, A. *et al.* Prognostic relevance of the expression of Tdt and CD7 in 335 cases of acute myeloid leukemia. *Leukemia* **12**, 1056–1063 (1998).

194. Lu, Y. *et al.* Naturally selected CD7 CAR-T therapy without genetic editing demonstrates significant antitumour efficacy against relapsed and refractory acute myeloid leukaemia (R/R-AML). *J. Transl. Med.* **20**, 600 (2022).

195. Hu, Y. *et al.* Genetically modified CD7-targeting allogeneic CAR-T cell therapy with enhanced efficacy for relapsed/refractory CD7-positive hematological malignancies: a phase I clinical study. *Cell Res.* **32**, 995–1007 (2022).

196. Kim, M. Y. *et al.* Genetic Inactivation of CD33 in Hematopoietic Stem Cells to Enable CAR T Cell Immunotherapy for Acute Myeloid Leukemia. *Cell* **173**, 1439-1453.e19 (2018).

197. Casirati, G. *et al.* Epitope editing enables targeted immunotherapy of acute myeloid leukaemia. *Nature* **621**, 404–414 (2023).

198. Wellhausen, N. *et al.* Epitope base editing CD45 in hematopoietic cells enables universal blood cancer immune therapy. *Sci. Transl. Med.* **15**, eadi1145 (2023).

199. Ruella, M. *et al.* Induction of resistance to chimeric antigen receptor T cell therapy by transduction of a single leukemic B cell. *Nat. Med.* **24**, 1499–1503 (2018).

200. Alcantara, M., Tesio, M., June, C. H. & Houot, R. CAR T-cells for T-cell malignancies: challenges in distinguishing between therapeutic, normal, and neoplastic T-cells. *Leukemia* **32**, 2307–2315 (2018).

201. Mamonkin, M., Rouce, R. H., Tashiro, H. & Brenner, M. K. A T-cell–directed chimeric antigen receptor for the selective treatment of T-cell malignancies. *Blood* **126**, 983–992 (2015).

202. Gomes-Silva, D. *et al.* CD7-edited T cells expressing a CD7-specific CAR for the therapy of T-cell malignancies. *Blood* **130**, 285–296 (2017).

203. Png, Y. T. *et al.* Blockade of CD7 expression in T cells for effective chimeric antigen receptor targeting of T-cell malignancies. *Blood Adv.* **1**, 2348–2360 (2017).

204. Maciocia, P. M. *et al.* Targeting the T cell receptor β-chain constant region for immunotherapy of T cell malignancies. *Nat. Med.* **23**, 1416–1423 (2017).

205. Ferrari, M. *et al.* Structure-guided engineering of immunotherapies targeting TRBC1 and TRBC2 in T cell malignancies. *Nat. Commun.* **15**, 1583 (2024).

206. Burger, R., Hansen-Hagge, T. E., Drexler, H. G. & Gramatzki, M. Heterogeneity of T-acute lymphoblastic leukemia (T-ALL) cell lines: suggestion for classification by immunophenotype and T-cell receptor studies. *Leuk. Res.* **23**, 19–27 (1999).

207. Niehues, T. *et al.* A classification based on T cell selection-related phenotypes identifies a subgroup of childhood T-ALL with favorable outcome in the COALL studies. *Leukemia* **13**, 614–617 (1999).

208. van Grotel, M. *et al.* Prognostic significance of molecular-cytogenetic abnormalities in pediatric T-ALL is not explained by immunophenotypic differences. *Leukemia* **22**, 124–131 (2008).

209. Sánchez-Martínez, D. *et al.* Fratricide-resistant CD1a-specific CAR T cells for the treatment of cortical T-cell acute lymphoblastic leukemia. *Blood* **133**, 2291–2304 (2019).

210. Maciocia, P. M. & Pule, M. A. Anti-CD1a CAR T cells to selectively target T-ALL. *Blood* **133**, 2246–2247 (2019).

211. Wurbel, M.-A. *et al.* The chemokine TECK is expressed by thymic and intestinal epithelial cells and attracts double- and single-positive thymocytes expressing the TECK receptor CCR9. *Eur. J. Immunol.* **30**, 262–271 (2000).

212. Youn, B. S., Kim, C. H., Smith, F. O. & Broxmeyer, H. E. TECK, an efficacious chemoattractant for human thymocytes, uses GPR-9-6/CCR9 as a specific receptor. *Blood* **94**, 2533–2536 (1999).

213. Zaballos, Á., Gutiérrez, J., Varona, R., Ardavín, C. & Márquez, G. Cutting Edge: Identification of the Orphan Chemokine Receptor GPR-9-6 as CCR9, the Receptor for the Chemokine TECK. *J. Immunol.* **162**, 5671–5675 (1999).

214. Bemark, M. *et al.* Limited clonal relatedness between gut IgA plasma cells and memory B cells after oral immunization. *Nat. Commun.* **7**, 12698 (2016).

215. Kunkel, E. J. *et al.* Lymphocyte CC Chemokine Receptor 9 and Epithelial Thymus-expressed Chemokine (TECK) Expression Distinguish the Small Intestinal Immune Compartment: Epithelial Expression of Tissue-specific Chemokines as an Organizing Principle in Regional Immunity.

216. Wendland, M. *et al.* CCR9 is a homing receptor for plasmacytoid dendritic cells to the small intestine. *Proc. Natl. Acad. Sci.* **104**, 6347–6352 (2007).

217. Zhang, Z. *et al.* CCR9 as a prognostic marker and therapeutic target in hepatocellular carcinoma. *Oncol. Rep.* **31**, 1629–1636 (2014).

218. Zhang, Z. *et al.* CCL25/CCR9 Signal Promotes Migration and Invasion in Hepatocellular and Breast Cancer Cell Lines. *DNA Cell Biol.* **35**, 348–357 (2016).

219. Shen, X. *et al.* CC Chemokine Receptor 9 Enhances Proliferation in Pancreatic Intraepithelial Neoplasia and Pancreatic Cancer Cells. *J. Gastrointest. Surg.* **13**, 1955–1962 (2009).

220. Gupta, P. *et al.* CCR9/CCL25 expression in non-small cell lung cancer correlates with aggressive disease and mediates key steps of metastasis. *Oncotarget* **5**, 10170–10179 (2014).

221. Zhong, Y. *et al.* Expression of CC chemokine receptor 9 predicts poor prognosis in patients with lung adenocarcinoma. *Diagn. Pathol.* **10**, 101 (2015).

222. Amersi, F. F. *et al.* Activation of CCR9/CCL25 in Cutaneous Melanoma Mediates Preferential Metastasis to the Small Intestine. *Clin. Cancer Res.* **14**, 638–645 (2008).

223. Singh, S. Expression and histopathological correlation of CCR9 and CCL25 in ovarian cancer. *Int. J. Oncol.* (2011) doi:10.3892/ijo.2011.1059.

224. Chen, H. *et al.* Intratumoral delivery of CCL25 enhances immunotherapy against triple-negative breast cancer by recruiting CCR9 $^{+}$ T cells. *Sci. Adv.* **6**, eaax4690 (2020).

225. Mirandola, L. *et al.* Notch1 regulates chemotaxis and proliferation by controlling the CC-chemokine receptors 5 and 9 in T cell acute lymphoblastic leukaemia. *J. Pathol.* **226**, 713–722 (2012).

226. Annels, N. E. Possible link between unique chemokine and homing receptor expression at diagnosis and relapse location in a patient with childhood T-ALL. *Blood* **103**, 2806–2808 (2004).

227. Chamorro, S. *et al.* Antitumor effects of a monoclonal antibody to human CCR9 in leukemia cell xenografts. *mAbs* **6**, 1000–1012 (2014).

228. Somovilla-Crespo, B. *et al.* 92R Monoclonal Antibody Inhibits Human CCR9+ Leukemia Cells Growth in NSG Mice Xenografts. *Front. Immunol.* **9**, 77 (2018).

229. Maciocia, P. M. *et al.* Anti-CCR9 chimeric antigen receptor T cells for T-cell acute lymphoblastic leukemia. *Blood* **140**, 25–37 (2022).

230. Noviello, M. *et al.* Bone marrow central memory and memory stem T-cell exhaustion in AML patients relapsing after HSCT. *Nat. Commun.* **10**, 1065 (2019).

231. Das, R. K., Vernau, L., Grupp, S. A. & Barrett, D. M. Naïve T-cell Deficits at Diagnosis and after Chemotherapy Impair Cell Therapy Potential in Pediatric Cancers. *Cancer Discov.* **9**, 492–499 (2019).

232. Das, R. K., O'Connor, R. S., Grupp, S. A. & Barrett, D. M. Lingering effects of chemotherapy on mature T cells impair proliferation. *Blood Adv.* **4**, 4653–4664 (2020).

233. McGuirk, J. *et al.* Building blocks for institutional preparation of CTL019 delivery. *Cytotherapy* **19**, 1015–1024 (2017).

234. Allen, E. S. *et al.* Autologous lymphapheresis for the production of chimeric antigen receptor T cells. *Transfusion (Paris)* **57**, 1133–1141 (2017).

235. Shah, N. N. *et al.* CD4/CD8 T-Cell Selection Affects Chimeric Antigen Receptor (CAR) T-Cell Potency and Toxicity: Updated Results From a Phase I Anti-CD22 CAR T-Cell Trial. *J. Clin. Oncol. Off. J. Am. Soc. Clin. Oncol.* **38**, 1938–1950 (2020).

236. *Natural Killer Cells*. vol. 395 (Springer International Publishing, Cham, 2016).

237. Sebestyen, Z., Prinz, I., Déchanet-Merville, J., Silva-Santos, B. & Kuball, J. Translating gammadelta (γδ) T cells and their receptors into cancer cell therapies. *Nat. Rev. Drug Discov.* **19**, 169–184 (2020).

238. Kabelitz, D., Serrano, R., Kouakanou, L., Peters, C. & Kalyan, S. Cancer immunotherapy with γδ T cells: many paths ahead of us. *Cell. Mol. Immunol.* **17**, 925–939 (2020).

239. Wang, H. *et al.* Costimulation of γδTCR and TLR7/8 promotes Vδ2 T-cell antitumor activity by modulating mTOR pathway and APC function. *J. Immunother. Cancer* **9**, e003339 (2021).

240. Nishimoto, K. P. *et al.* Allogeneic CD20-targeted γδ T cells exhibit innate and adaptive antitumor activities in preclinical B-cell lymphoma models. *Clin. Transl. Immunol.* **11**, e1373 (2022).

241. Ruella, M. & Kenderian, S. S. Next-Generation Chimeric Antigen Receptor T-Cell Therapy: Going off the Shelf. *BioDrugs* **31**, 473–481 (2017).

242. Cooper, M. L. *et al.* An "off-the-shelf" fratricide-resistant CAR-T for the treatment of T cell hematologic malignancies. *Leukemia* **32**, 1970–1983 (2018).

243. Rasaiyaah, J., Georgiadis, C., Preece, R., Mock, U. & Qasim, W. TCRαβ/CD3 disruption enables CD3-specific antileukemic T cell immunotherapy. *JCI Insight* **3**, e99442, 99442 (2018).

244. Qasim, W. *et al.* Molecular remission of infant B-ALL after infusion of universal TALEN gene-edited CAR T cells. *Sci. Transl. Med.* **9**, eaaj2013 (2017).

245. Eyquem, J. *et al.* Targeting a CAR to the TRAC locus with CRISPR/Cas9 enhances tumour rejection. *Nature* **543**, 113–117 (2017).

246. Mansilla-Soto, J. *et al.* HLA-independent T cell receptors for targeting tumors with low antigen density. *Nat. Med.* **28**, 345–352 (2022).

247. Maldonado-Pérez, N. *et al.* Efficacy and safety of universal (TCRKO) ARI-0001 CAR-T cells for the treatment of B-cell lymphoma. *Front. Immunol.* **13**, 1011858 (2022).

248. Stenger, D. *et al.* Endogenous TCR promotes in vivo persistence of CD19-CAR-T cells compared to a CRISPR/Cas9-mediated TCR knockout CAR. *Blood* **136**, 1407–1418 (2020).

249. Blanco, B., Compte, M., Lykkemark, S., Sanz, L. & Alvarez-Vallina, L. T Cell-Redirecting Strategies to 'STAb' Tumors: Beyond CARs and Bispecific Antibodies. *Trends Immunol.* **40**, 243–257 (2019).

250. Velasquez, M. P. *et al.* T cells expressing CD19-specific Engager Molecules for the Immunotherapy of CD19-positive Malignancies. *Sci. Rep.* **6**, 27130 (2016).

251. Liu, X. *et al.* Improved anti-leukemia activities of adoptively transferred T cells expressing bispecific T-cell engager in mice. *Blood Cancer J.* **6**, e430 (2016).

252. Blanco, B. *et al.* Overcoming CAR-Mediated CD19 Downmodulation and Leukemia Relapse with T Lymphocytes Secreting Anti-CD19 T-cell Engagers. *Cancer Immunol. Res.* **10**, 498–511 (2022).

253. Mukherjee, M., Mace, E. M., Carisey, A. F., Ahmed, N. & Orange, J. S. Quantitative Imaging Approaches to Study the CAR Immunological Synapse. *Mol. Ther.* **25**, 1757–1768 (2017).

254. Davenport, A. J. *et al.* Chimeric antigen receptor T cells form nonclassical and potent immune synapses driving rapid cytotoxicity. *Proc. Natl. Acad. Sci.* **115**, (2018).

255. Watanabe, K., Kuramitsu, S., Posey, A. D. & June, C. H. Expanding the Therapeutic Window for CAR T Cell Therapy in Solid Tumors: The Knowns and Unknowns of CAR T Cell Biology. *Front. Immunol.* **9**, 2486 (2018).

256. Offner, S., Hofmeister, R., Romaniuk, A., Kufer, P. & Baeuerle, P. A. Induction of regular cytolytic T cell synapses by bispecific single-chain antibody constructs on MHC class I-negative tumor cells. *Mol. Immunol.* **43**, 763–771 (2006).

257. Kouhestani, D. *et al.* Variant signaling topology at the cancer cell–T-cell interface induced by a two-component T-cell engager. *Cell. Mol. Immunol.* **18**, 1568–1570 (2021).

258. Ramírez-Fernández, Á. *et al.* Synapse topology and downmodulation events determine the functional outcome of anti-CD19 T cell-redirecting strategies. *OncoImmunology* **11**, 2054106 (2022).

259. Topp, M. S. *et al.* Long-term follow-up of hematologic relapse-free survival in a phase 2 study of blinatumomab in patients with MRD in B-lineage ALL. *Blood* **120**, 5185–5187 (2012).

260. Topp, M. S. *et al.* Phase II trial of the anti-CD19 bispecific T cell-engager blinatumomab shows hematologic and molecular remissions in patients with relapsed or refractory B-precursor acute lymphoblastic leukemia. *J. Clin. Oncol. Off. J. Am. Soc. Clin. Oncol.* **32**, 4134–4140 (2014).

261. Grupp, S. A. *et al.* Durable Remissions in Children with Relapsed/Refractory ALL Treated with T Cells Engineered with a CD19-Targeted Chimeric Antigen Receptor (CTL019). *Blood* **126**, 681 (2015).

262. Tan, Y. *et al.* Long-term follow-up of donor-derived CD7 CAR T-cell therapy in patients with T-cell acute lymphoblastic leukemia. *J. Hematol. Oncol.J Hematol Oncol* **16**, 34 (2023).

263. Amrolia, P. J. *et al.* Phase I Study of AUTO3, a Bicistronic Chimeric Antigen Receptor (CAR) T-Cell Therapy Targeting CD19 and CD22, in Pediatric Patients with Relapsed/Refractory B-Cell Acute Lymphoblastic Leukemia (r/r B-ALL): Amelia Study. *Blood* **134**, 2620 (2019).

264. Hossain, N. *et al.* Phase I Experience with a Bi-Specific CAR Targeting CD19 and CD22 in Adults with B-Cell Malignancies. *Blood* **132**, 490 (2018).

265. Schultz, L. M. *et al.* Phase 1 Study of CD19/CD22 Bispecific Chimeric Antigen Receptor (CAR) Therapy in Children and Young Adults with B Cell Acute Lymphoblastic Leukemia (ALL). *Blood* **132**, 898 (2018).

266. Yang, J. *et al.* A Feasibility and Safety Study of CD19 and CD22 Chimeric Antigen Receptors-Modified T Cell Cocktail for Therapy of B Cell Acute Lymphoblastic Leukemia. *Blood* **132**, 277 (2018).

267. Gardner, R. A. *et al.* Intent-to-treat leukemia remission by CD19 CAR T cells of defined formulation and dose in children and young adults. *Blood* **129**, 3322–3331 (2017).

268. Huang, L. *et al.* CAR22/19 Cocktail Therapy for Patients with Refractory/Relapsed B-Cell Malignancies. *Blood* **132**, 1408 (2018).

269. Brillembourg, H. *et al.* The role of chimeric antigen receptor T cells targeting more than one antigen in the treatment of B-cell malignancies. *Br. J. Haematol.* (2024) doi:10.1111/bjh.19348.

270. Wilkie, S. *et al.* Dual targeting of ErbB2 and MUC1 in breast cancer using chimeric antigen receptors engineered to provide complementary signaling. *J. Clin. Immunol.* **32**, 1059–1070 (2012).

271. Kloss, C. C., Condomines, M., Cartellieri, M., Bachmann, M. & Sadelain, M. Combinatorial antigen recognition with balanced signaling promotes selective tumor eradication by engineered T cells. *Nat. Biotechnol.* **31**, 71–75 (2013).

272. Choe, J. H. *et al.* SynNotch-CAR T cells overcome challenges of specificity, heterogeneity, and persistence in treating glioblastoma. *Sci. Transl. Med.* **13**, eabe7378 (2021).

273. Hyrenius-Wittsten, A. *et al.* SynNotch CAR circuits enhance solid tumor recognition and promote persistent antitumor activity in mouse models. *Sci. Transl. Med.* **13**, eabd8836 (2021).

274. Vora, A. *et al.* Treatment reduction for children and young adults with low-risk acute lymphoblastic leukaemia defined by minimal residual disease (UKALL 2003): a randomised controlled trial. *Lancet Oncol.* **14**, 199–209 (2013).

275. Marks, D. I. *et al.* T-cell acute lymphoblastic leukemia in adults: clinical features, immunophenotype, cytogenetics, and outcome from the large randomized prospective trial (UKALL XII/ECOG 2993). *Blood* **114**, 5136–5145 (2009).

276. Fielding, A. K. *et al.* Outcome of 609 adults after relapse of acute lymphoblastic leukemia (ALL); an MRC UKALL12/ECOG 2993 study. *Blood* **109**, 944–950 (2007).

277. Diorio, C. *et al.* Cytosine base editing enables quadruple-edited allogeneic CART cells for T-ALL. *Blood* **140**, 619–629 (2022).

278. Pan, J. *et al.* Donor-Derived CD7 Chimeric Antigen Receptor T Cells for T-Cell Acute Lymphoblastic Leukemia: First-in-Human, Phase I Trial. *J. Clin. Oncol.* **39**, 3340–3351 (2021).

279. Lu, P. *et al.* Naturally selected CD7 CAR-T therapy without genetic manipulations for T-ALL/LBL: first-in-human phase 1 clinical trial. *Blood* **140**, 321–334 (2022).

280. Hu, Y. *et al.* Sequential CD7 CAR T-Cell Therapy and Allogeneic HSCT without GVHD Prophylaxis. *N. Engl. J. Med.* **390**, 1467–1480 (2024).

281. Ramos, C. A. *et al.* Clinical and immunological responses after CD30-specific chimeric antigen receptor–redirected lymphocytes. *J. Clin. Invest.* **127**, 3462–3471 (2017).

282. Shi, J. *et al.* CAR T cells targeting CD99 as an approach to eradicate T-cell acute lymphoblastic leukemia without normal blood cells toxicity. *J. Hematol. Oncol.J Hematol Oncol* **14**, 162 (2021).

283. Jiménez-Reinoso, A. *et al.* Efficient preclinical treatment of cortical T cell acute lymphoblastic leukemia with T lymphocytes secreting anti-CD1a T cell engagers. *J. Immunother. Cancer* **10**, e005333 (2022).

284. Velasco-Hernandez, T. *et al.* Efficient elimination of primary B-ALL cells in vitro and in vivo using a novel 4-1BB-based CAR targeting a membrane-distal CD22 epitope. *J. Immunother. Cancer* **8**, e000896 (2020).

285. Lefranc, M.-P. Antibody Informatics: IMGT, the International ImMunoGeneTics Information System. *Microbiol. Spectr.* **2**, (2014).

286. Dull, T. *et al.* A Third-Generation Lentivirus Vector with a Conditional Packaging System. *J. Virol.* **72**, 8463–8471 (1998).

287. THE TABULA SAPIENS CONSORTIUM. The Tabula Sapiens: A multiple-organ, single-cell transcriptomic atlas of humans. *Science* **376**, eabl4896 (2022).

288. Prieto, C. *et al.* NG2 antigen is involved in leukemia invasiveness and central nervous system infiltration in MLL-rearranged infant B-ALL. *Leukemia* **32**, 633–644 (2018).

289. Rehe, K. *et al.* Acute B lymphoblastic leukaemia-propagating cells are present at high frequency in diverse lymphoblast populations. *EMBO Mol. Med.* **5**, 38–51 (2013).

290. Scherer, L. D., Brenner, M. K. & Mamonkin, M. Chimeric Antigen Receptors for T-Cell Malignancies. *Front. Oncol.* **9**, 126 (2019).

291. Fleischer, L. C., Spencer, H. T. & Raikar, S. S. Targeting T cell malignancies using CAR-based immunotherapy: challenges and potential solutions. *J. Hematol. Oncol.J Hematol Oncol* **12**, 141 (2019).

292. Roosen, J., Oosterlinck, W. & Meyns, B. Routine thymectomy in congenital cardiac surgery changes adaptive immunity without clinical relevance. *Interact. Cardiovasc. Thorac. Surg.* **20**, 101–106 (2015).

293. Torfadottir, H. *et al.* Evidence for extrathymic T cell maturation after thymectomy in infancy. *Clin. Exp. Immunol.* **145**, 407–412 (2006).

294. Keshav, S. & Wendt, E. CCR9 antagonism: potential in the treatment of Inflammatory Bowel Disease. *Clin. Exp. Gastroenterol.* 119 (2015) doi:10.2147/CEG.S48305.

295. Trivedi, P. J. *et al.* Intestinal CCL25 expression is increased in colitis and correlates with inflammatory activity. *J. Autoimmun.* **68**, 98–104 (2016).

296. Walters, M. J. *et al.* Characterization of CCX282-B, an orally bioavailable antagonist of the CCR9 chemokine receptor, for treatment of inflammatory bowel disease. *J. Pharmacol. Exp. Ther.* **335**, 61–69 (2010).

297. Feagan, B. G. *et al.* Randomised clinical trial: vercirnon, an oral CCR9 antagonist, vs. placebo as induction therapy in active Crohn's disease. *Aliment. Pharmacol. Ther.* **42**, 1170–1181 (2015).

298. Zanetti, S. R. *et al.* A novel and efficient tandem CD19- and CD22-directed CAR for B cell ALL. *Mol. Ther. J. Am. Soc. Gene Ther.* **30**, 550–563 (2022).

299. Perriello, V. M. *et al.* IL-3-zetakine combined with a CD33 costimulatory receptor as a dual CAR approach for safer and selective targeting of AML. *Blood Adv.* **7**, 2855–2871 (2023).

300. Brown, C. E. *et al.* Off-the-shelf, steroid-resistant, IL13Rα2-specific CAR T cells for treatment of glioblastoma. *Neuro-Oncol.* **24**, 1318–1330 (2022).

301. Finney, O. C. *et al.* CD19 CAR T cell product and disease attributes predict leukemia remission durability. *J. Clin. Invest.* **129**, 2123–2132 (2019).

302. Handgretinger, R. & Schilbach, K. The potential role of γδ T cells after allogeneic HCT for leukemia. *Blood* **131**, 1063–1072 (2018).

303. Doudna, J. A. The promise and challenge of therapeutic genome editing. *Nature* **578**, 229–236 (2020).

304. Di Lorenzo, B. *et al.* Broad Cytotoxic Targeting of Acute Myeloid Leukemia by Polyclonal Delta One T Cells. *Cancer Immunol. Res.* **7**, 552–558 (2019).

305. Mensurado, S. *et al.* CD155/PVR determines acute myeloid leukemia targeting by Delta One T cells. *Blood* **143**, 1488–1495 (2024).

306. Becker-Hapak, M. K. *et al.* A Fusion Protein Complex that Combines IL-12, IL-15, and IL-18 Signaling to Induce Memory-Like NK Cells for Cancer Immunotherapy. *Cancer Immunol. Res.* **9**, 1071–1087 (2021).

307. Soldierer, M. *et al.* Genetic Engineering and Enrichment of Human NK Cells for CAR-Enhanced Immunotherapy of Hematological Malignancies. *Front. Immunol.* **13**, 847008 (2022).

308. Aryee, K.-E. *et al.* Enhanced development of functional human NK cells in NOD-scid-IL2rgnull mice expressing human IL15. *FASEB J. Off. Publ. Fed. Am. Soc. Exp. Biol.* **36**, e22476 (2022).

309. Schober, R. *et al.* Multimeric immunotherapeutic complexes activating natural killer cells towards HIV-1 cure. *J. Transl. Med.* **21**, 791 (2023).

310. Abeynaike, S. A. *et al.* Human Hematopoietic Stem Cell Engrafted IL-15 Transgenic NSG Mice Support Robust NK Cell Responses and Sustained HIV-1 Infection. *Viruses* **15**, 365 (2023).

311. Makkouk, A. *et al.* Off-the-shelf Vδ1 gamma delta T cells engineered with glypican-3 (GPC-3)-specific chimeric antigen receptor (CAR) and soluble IL-15 display robust antitumor efficacy against hepatocellular carcinoma. *J. Immunother. Cancer* **9**, e003441 (2021).

312. Dudley, M. E. *et al.* Adoptive Cell Therapy for Patients With Metastatic Melanoma: Evaluation of Intensive Myeloablative Chemoradiation Preparative Regimens. *J. Clin. Oncol.* **26**, 5233–5239 (2008).

313. Meraviglia, S. *et al.* Distinctive features of tumor-infiltrating γδ T lymphocytes in human colorectal cancer. *OncoImmunology* **6**, e1347742 (2017).

314. Wang, J. *et al.* Tumor-infiltrating γδT cells predict prognosis and adjuvant chemotherapeutic benefit in patients with gastric cancer. *Oncoimmunology* **6**, e1353858 (2017).

315. Donia, M., Ellebaek, E., Andersen, M. H., Straten, P. T. & Svane, I. M. Analysis of Vδ1 T cells in clinical grade melanoma-infiltrating lymphocytes. *Oncoimmunology* **1**, 1297–1304 (2012).

316. Lu, H. *et al.* High Abundance of Intratumoral γδ T Cells Favors a Better Prognosis in Head and Neck Squamous Cell Carcinoma: A Bioinformatic Analysis. *Front. Immunol.* **11**, 573920 (2020).

317. Zhao, N. *et al.* Intratumoral γδ T-Cell Infiltrates, Chemokine (C-C Motif) Ligand 4/Chemokine (C-C Motif) Ligand 5 Protein Expression and Survival in Patients With Hepatocellular Carcinoma. *Hepatol. Baltim. Md* **73**, 1045–1060 (2021).

318. Lien, S. C. *et al.* Tumor reactive γδ T cells contribute to a complete response to PD-1 blockade in a Merkel cell carcinoma patient. *Nat. Commun.* **15**, 1094 (2024).

319. Gentles, A. J. *et al.* The prognostic landscape of genes and infiltrating immune cells across human cancers. *Nat. Med.* **21**, 938–945 (2015).

320. Arruda, L. C. M., Gaballa, A. & Uhlin, M. Impact of γδ T cells on clinical outcome of hematopoietic stem cell transplantation: systematic review and meta-analysis. *Blood Adv.* **3**, 3436–3448 (2019).

321. Lamb, L. S. *et al.* Increased Frequency of TCRγδ+ T Cells in Disease-Free Survivors Following T Cell-Depleted, Partially Mismatched, Related Donor Bone Marrow Transplantation for Leukemia. *J. Hematother.* **5**, 503–509 (1996).

322. Godder, K. *et al.* Long term disease-free survival in acute leukemia patients recovering with increased γδ T cells after partially mismatched related donor bone marrow transplantation. *Bone Marrow Transplant.*

323. Mathioudaki, A. *et al.* The remission status of AML patients after allo-HCT is associated with a distinct single-cell bone marrow T-cell signature. *Blood* **143**, 1269–1281 (2024).

324. Guerrero-Murillo, M. *et al.* Integrative single-cell multi-omics of CD19-CARpos and CARneg T cells suggest drivers of immunotherapy response in B-cell neoplasias. Preprint at https://doi.org/10.1101/2024.01.23.576878 (2024).

325. Melenhorst, J. J. *et al.* Decade-long leukaemia remissions with persistence of CD4+ CAR T cells. *Nature* **602**, 503–509 (2022).

326. Lin, M. *et al.* Irreversible electroporation plus allogenic Vγ9Vδ2 T cells enhances antitumor effect for locally advanced pancreatic cancer patients. *Signal Transduct. Target. Ther.* **5**, 215 (2020).

327. Xu, Y. *et al.* Allogeneic Vγ9Vδ2 T-cell immunotherapy exhibits promising clinical safety and prolongs the survival of patients with late-stage lung or liver cancer. *Cell. Mol. Immunol.* **18**, 427–439 (2021).

328. Rischer, M. *et al.* Human gammadelta T cells as mediators of chimaeric-receptor redirected anti-tumour immunity. *Br. J. Haematol.* **126**, 583–592 (2004).

329. Deniger, D. C. *et al.* Bispecific T-cells Expressing Polyclonal Repertoire of Endogenous γδ T-cell Receptors and Introduced CD19-specific Chimeric Antigen Receptor. *Mol. Ther.* **21**, 638–647 (2013).

330. Harrer, D. C. *et al.* RNA-transfection of γ/δ T cells with a chimeric antigen receptor or an α/β T-cell receptor: a safer alternative to genetically engineered α/β T cells for the immunotherapy of melanoma. *BMC Cancer* **17**, 551 (2017).

331. Capsomidis, A. *et al.* Chimeric Antigen Receptor-Engineered Human Gamma Delta T Cells: Enhanced Cytotoxicity with Retention of Cross Presentation. *Mol. Ther.* **26**, 354–365 (2018).

332. Xiao, L. *et al.* Large-scale expansion of Vγ9Vδ2 T cells with engineered K562 feeder cells in G-Rex vessels and their use as chimeric antigen receptor–modified effector cells. *Cytotherapy* **20**, 420–435 (2018).

333. Ang, W. X. *et al.* Electroporation of NKG2D RNA CAR Improves Vγ9Vδ2 T Cell Responses against Human Solid Tumor Xenografts. *Mol. Ther. - Oncolytics* **17**, 421–430 (2020).

334. Fleischer, L. C. *et al.* Non-signaling Chimeric Antigen Receptors Enhance Antigen-Directed Killing by γδ T Cells in Contrast to αβ T Cells. *Mol. Ther. - Oncolytics* **18**, 149–160 (2020).

335. Rozenbaum, M. *et al.* Gamma-Delta CAR-T Cells Show CAR-Directed and Independent Activity Against Leukemia. *Front. Immunol.* **11**, 1347 (2020).

336. Wallet, M. A. *et al.* Induced Pluripotent Stem Cell-Derived Gamma Delta CAR-T Cells for Cancer Immunotherapy. *Blood* **138**, 2771 (2021).

337. Li, H.-K. *et al.* A Novel Allogeneic Rituximab-Conjugated Gamma Delta T Cell Therapy for the Treatment of Relapsed/Refractory B-Cell Lymphoma. *Cancers* **15**, 4844 (2023).

338. Becker, S. A. *et al.* Enhancing the effectiveness of γδ T cells by mRNA transfection of chimeric antigen receptors or bispecific T cell engagers. *Mol. Ther. Oncolytics* **29**, 145–157 (2023).

339. Ferry, G. M. *et al.* A Simple and Robust Single-Step Method for CAR-Vδ1 γδT Cell Expansion and Transduction for Cancer Immunotherapy. *Front. Immunol.* **13**, 863155 (2022).

340. Mack, M., Riethmüller, G. & Kufer, P. A small bispecific antibody construct expressed as a functional single-chain molecule with high tumor cell cytotoxicity. *Proc. Natl. Acad. Sci.* **92**, 7021–7025 (1995).

341. Oberg, H.-H. *et al.* Novel bispecific antibodies increase γδ T-cell cytotoxicity against pancreatic cancer cells. *Cancer Res.* **74**, 1349–1360 (2014).

342. Seidel, U. J. E. *et al.* γδ T Cell-Mediated Antibody-Dependent Cellular Cytotoxicity with CD19 Antibodies Assessed by an Impedance-Based Label-Free Real-Time Cytotoxicity Assay. *Front. Immunol.* **5**, 618 (2014).

343. Oberg, H.-H. *et al.* γδ T cell activation by bispecific antibodies. *Cell. Immunol.* **296**, 41–49 (2015).

344. Schiller, C. B. *et al.* CD19-specific triplebody SPM-1 engages NK and γδ T cells for rapid and efficient lysis of malignant B-lymphoid cells. *Oncotarget* **7**, 83392–83408 (2016).

345. de Bruin, R. C. G. *et al.* A bispecific nanobody approach to leverage the potent and widely applicable tumor cytolytic capacity of Vγ9Vδ2-T cells. *Oncoimmunology* **7**, e1375641 (2017).

346. Hoeres, T. *et al.* Improving Immunotherapy Against B-Cell Malignancies Using γδ T-Cell-specific Stimulation and Therapeutic Monoclonal Antibodies. *J. Immunother. Hagerstown Md 1997* **42**, 331–344 (2019).

347. de Weerdt, I. *et al.* A Bispecific Single-Domain Antibody Boosts Autologous Vγ9Vδ2-T Cell Responses Toward CD1d in Chronic Lymphocytic Leukemia. *Clin. Cancer Res. Off. J. Am. Assoc. Cancer Res.* **27**, 1744–1755 (2021).

348. de Weerdt, I. *et al.* A Bispecific Antibody Antagonizes Prosurvival CD40 Signaling and Promotes Vγ9Vδ2 T cell-Mediated Antitumor Responses in Human B-cell Malignancies. *Cancer Immunol. Res.* **9**, 50–61 (2021).

349. Ganesan, R. *et al.* Selective recruitment of γδ T cells by a bispecific antibody for the treatment of acute myeloid leukemia. *Leukemia* **35**, 2274–2284 (2021).

350. Przepiorka, D. *et al.* FDA Approval: Blinatumomab. *Clin. Cancer Res.* **21**, 4035–4039 (2015).

351. Blinatumomab Approval Expanded Based on MRD. *Cancer Discov.* **8**, OF3–OF3 (2018).

352. Wei, J., Yang, Y., Wang, G. & Liu, M. Current landscape and future directions of bispecific antibodies in cancer immunotherapy. *Front. Immunol.* **13**, 1035276 (2022).

353. Fenis, A., Demaria, O., Gauthier, L., Vivier, E. & Narni-Mancinelli, E. New immune cell engagers for cancer immunotherapy. *Nat. Rev. Immunol.* (2024) doi:10.1038/s41577-023-00982-7.

354. Cochlovius, B. *et al.* Treatment of Human B Cell Lymphoma Xenografts with a CD3 × CD19 Diabody and T Cells. *J. Immunol.* **165**, 888–895 (2000).

355. Compte, M. *et al.* Inhibition of tumor growth in vivo by in situ secretion of bispecific anti-CEA x anti-CD3 diabodies from lentivirally transduced human lymphocytes. *Cancer Gene Ther.* (2007).

356. Compte, M. *et al.* Factory neovessels: engineered human blood vessels secreting therapeutic proteins as a new drug delivery system. *Gene Ther.* **17**, 745–751 (2010).

357. Aliperta, R. *et al.* Bispecific antibody releasing-mesenchymal stromal cell machinery for retargeting T cells towards acute myeloid leukemia blasts. *Blood Cancer J.* **5**, e348–e348 (2015).

358. Iwahori, K. *et al.* Engager T cells: a new class of antigen-specific T cells that redirect bystander T cells. *Mol. Ther. J. Am. Soc. Gene Ther.* **23**, 171–178 (2015).

359. Pang, X. *et al.* Treatment of Human B-Cell Lymphomas Using Minicircle DNA Vector Expressing Anti-CD3/CD20 in a Mouse Model. *Hum. Gene Ther.* **28**, 216–225 (2017).

360. Zhang, X. *et al.* Mesenchymal stromal cells as vehicles of tetravalent bispecific Tandab (CD3/CD19) for the treatment of B cell lymphoma combined with IDO pathway inhibitor D-1-methyl-tryptophan. *J. Hematol. Oncol.J Hematol Oncol* **10**, 56 (2017).

361. Díez-Alonso, L. *et al.* Engineered T cells secreting anti-BCMA T cell engagers control multiple myeloma and promote immune memory in vivo. *Sci. Transl. Med.* **16**, eadg7962 (2024).

362. Rafiq, S. *et al.* Targeted delivery of a PD-1-blocking scFv by CAR-T cells enhances anti-tumor efficacy in vivo. *Nat. Biotechnol.* **36**, 847–856 (2018).

363. Balazs, A. B. *et al.* Antibody-based protection against HIV infection by vectored immunoprophylaxis. *Nature* **481**, 81–84 (2012).

364. Speck, T. *et al.* Targeted BiTE Expression by an Oncolytic Vector Augments Therapeutic Efficacy Against Solid Tumors. *Clin. Cancer Res.* **24**, 2128–2137 (2018).

365. Dai, Z. *et al.* T cells expressing CD5/CD7 bispecific chimeric antigen receptors with fully human heavy-chain-only domains mitigate tumor antigen escape. *Signal Transduct. Target. Ther.* **7**, 85 (2022).

366. Flugel, C. L. *et al.* Overcoming on-target, off-tumour toxicity of CAR T cell therapy for solid tumours. *Nat. Rev. Clin. Oncol.* **20**, 49–62 (2023).

367. Baker, D. J., Arany, Z., Baur, J. A., Epstein, J. A. & June, C. H. CAR T therapy beyond cancer: the evolution of a living drug. *Nature* **619**, 707–715 (2023).

368. Ellebrecht, C. T. *et al.* Reengineering chimeric antigen receptor T cells for targeted therapy of autoimmune disease. *Science* **353**, 179–184 (2016).

369. Kansal, R. *et al.* Sustained B cell depletion by CD19-targeted CAR T cells is a highly effective treatment for murine lupus. *Sci. Transl. Med.* **11**, eaav1648 (2019).

370. Jin, X. *et al.* Therapeutic efficacy of anti-CD19 CAR-T cells in a mouse model of systemic lupus erythematosus. *Cell. Mol. Immunol.* **18**, 1896–1903 (2021).

371. Baker, D. J. & June, C. H. CAR T therapy extends its reach to autoimmune diseases. *Cell* **185**, 4471–4473 (2022).

372. Mackensen, A. *et al.* Anti-CD19 CAR T cell therapy for refractory systemic lupus erythematosus. *Nat. Med.* **28**, 2124–2132 (2022).

373. Kakarla, S. *et al.* Antitumor effects of chimeric receptor engineered human T cells directed to tumor stroma. *Mol. Ther. J. Am. Soc. Gene Ther.* **21**, 1611–1620 (2013).

374. Wang, L.-C. S. *et al.* Targeting fibroblast activation protein in tumor stroma with chimeric antigen receptor T cells can inhibit tumor growth and augment host immunity without severe toxicity. *Cancer Immunol. Res.* **2**, 154–166 (2014).

375. Aghajanian, H. *et al.* Targeting cardiac fibrosis with engineered T cells. *Nature* **573**, 430–433 (2019).

376. Rurik, J. G. *et al.* CAR T cells produced in vivo to treat cardiac injury. *Science* **375**, 91–96 (2022).

377. Mitsuyasu, R. T. *et al.* Prolonged survival and tissue trafficking following adoptive transfer of CD4zeta gene-modified autologous CD4(+) and CD8(+) T cells in human immunodeficiency virus-infected subjects. *Blood* **96**, 785–793 (2000).

378. Leibman, R. S. *et al.* Supraphysiologic control over HIV-1 replication mediated by CD8 T cells expressing a re-engineered CD4-based chimeric antigen receptor. *PLoS Pathog.* **13**, e1006613 (2017).

379. Campos-Gonzalez, G., Martinez-Picado, J., Velasco-Hernandez, T. & Salgado, M. Opportunities for CAR-T Cell Immunotherapy in HIV Cure. *Viruses* **15**, 789 (2023).

380. Kumaresan, P. R. *et al.* Bioengineering T cells to target carbohydrate to treat opportunistic fungal infection. *Proc. Natl. Acad. Sci. U. S. A.* **111**, 10660–10665 (2014).

381. Seif, M. *et al.* CAR T cells targeting Aspergillus fumigatus are effective at treating invasive pulmonary aspergillosis in preclinical models. *Sci. Transl. Med.* **14**, eabh1209 (2022).

Annex

Other publications in immunotherapy

blood®
Brief Report

IMMUNOBIOLOGY AND IMMUNOTHERAPY

CD155/PVR determines acute myeloid leukemia targeting by Delta One T cells

Sofia Mensurado,[1,*] Carolina Condeço,[1,*] Diego Sánchez-Martínez,[2-5] Sara Shirley,[1] Rui M. L. Coelho,[1] Néstor Tirado,[2,3] Meritxell Vinyoles,[2,3] Rafael Blanco-Domínguez,[1] Leandro Barros,[1] Beatriz Galvão,[1] Noélia Custódio,[1] Maria Gomes da Silva,[6] Pablo Menéndez,[2,3,7,8,†] and Bruno Silva-Santos[1,†]

[1]Instituto de Medicina Molecular João Lobo Antunes, Faculdade de Medicina, Universidade de Lisboa, Lisbon, Portugal; [2]Josep Carreras Leukaemia Research Institute, Department of Biomedicine, School of Medicine, University of Barcelona, Barcelona, Spain; [3]Red Española de Terapias Avanzadas, Instituto de Salud Carlos III, Redes de Investigación Cooperativa Orientadas a Resultados en Salud (RD21/0017/0029), Madrid, Spain; [4]Aragon Health Research Institute, Centro de Investigación Biomédica en Red en Enfermedades Infecciosas, Instituto de Salud Carlos III, Zaragoza, Spain; [5]Aragon I+D Foundation, Zaragoza, Spain; [6]Instituto Português de Oncologia Francisco Gentil, Lisbon, Portugal; [7]Centro de Investigación Biomédica en Red-Oncología, Instituto de Salud Carlos III, Barcelona, Spain; and [8]Institució Catalana de Recerca i Estudis Avançats, Barcelona, Spain

KEY POINTS

- **The NK receptor ligands, PVR and B7-H6, are required for AML cell recognition and immunological synapse formation with DOT cells.**
- **PVR expression predicts primary AML sample targeting by cytotoxic DOT cells.**

Relapsed or refractory acute myeloid leukemia (AML) remains a major therapeutic challenge. We have recently developed a Vδ1$^+$ γδ T cell–based product for adoptive immunotherapy, named Delta One T (DOT) cells, and demonstrated their cytolytic capacity to eliminate AML cell lines and primary blasts in vitro and in vivo. However, the molecular mechanisms responsible for the broad DOT-cell recognition of AML cells remain poorly understood. Here, we dissected the role of natural killer (NK) cell receptor ligands in AML cell recognition by DOT cells. Screening of multiple AML cell lines highlighted a strong upregulation of the DNAM-1 ligands, CD155/pulmonary vascular resistance (PVR), CD112/nectin-2, as well as the NKp30 ligand, B7-H6, in contrast with NKG2D ligands. CRISPR-mediated ablation revealed key nonredundant and synergistic contributions of PVR and B7-H6 but not nectin-2 to DOT-cell targeting of AML cells. We further demonstrate that PVR and B7-H6 are critical for the formation of robust immunological synapses between AML and DOT cells. Importantly, PVR but not B7-H6 expression in primary AML samples predicted their elimination by DOT cells. These data provide new mechanistic insight into tumor targeting by DOT cells and suggest that assessing PVR expression levels may be highly relevant to DOT cell–based clinical trials.

Introduction

Acute myeloid leukemia (AML) remains an unmet medical need, given its relatively high incidence and morbidity and mortality rates because of chemotherapy resistance and relapse in the absence of breakthrough therapies.[1] In contrast to B-cell malignancies, in which adoptive autologous chimeric antigen receptor (CAR) T-cell therapies have delivered impressive rates of complete responses and changed clinical practice,[2] AML remains a major challenge for current immunotherapies, especially because of on-target off-tumor effects on vital healthy myeloid progenitor cells that share expression of targetable antigens like CD33 or CD123, thus promoting a life-threatening myeloablation.[3] By contrast, nonengineered lymphocytes, although likely less potent, may preserve their ability to distinguish AML cells from healthy progenitors, thus avoiding severe myeloablation. Such is the case of Delta One T (DOT) cells, a cell therapy product based on Vδ1$^+$ γδ T cells,[4-6] which display robust cytotoxic potency against multiple AML cell lines and samples from patients with primary AML, including chemotherapy-resistant AML cells, while sparing normal CD33$^+$ or CD123$^+$ myeloid cells and progenitor cells.[7] Moreover, we recently showed that, although requiring a higher effector-to-target ratio to achieve equivalent AML elimination compared with CD123 CAR-transduced DOT cells, nonengineered DOT cells were able to control AML growth in patient-derived xenografts.[8] This is highly relevant because DOT cells have been evolved into an allogeneic cellular product that is being tested in patients with AML (ClinicalTrials.gov identifier: NCT05886491).

On the path to a DOT cell–based treatment for AML, a fundamental question urges: how do DOT cells recognize AML cells, that is, which molecules on the surface of AML cells are essential for efficient cytotoxic targeting by DOT cells? We previously reported a striking T-cell receptor (TCR) polyclonality of DOT-cell products, and a very limited impact of anti-TCRVδ1 antibody blockade on AML targeting by DOT cells.[7] In contrast, we have clearly demonstrated that DOT cells upregulate multiple natural killer (NK) cell receptors (NKR), especially NKp30,

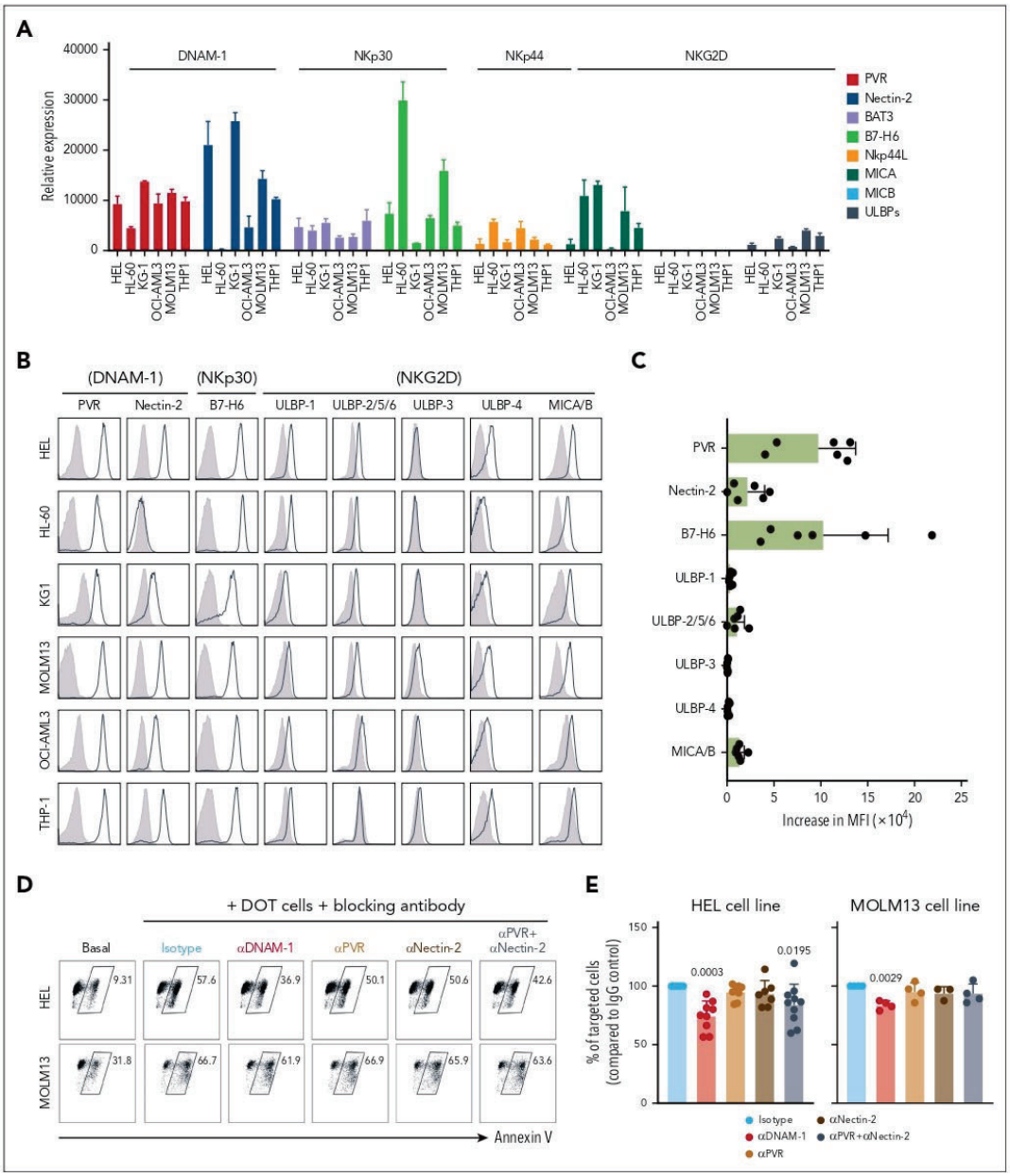

Figure 1. The DNAM-1 ligand, CD155/ PVR is required for DOT-cell targeting of AML cell lines. (A) Gene expression of ligands for DNAM-1, NKp30, NKp44, and NKG2D receptors in a panel of AML cell lines; results are normalized to the housekeeping genes *GUSB* and *PSM6*. (B) Protein expression of ligands for DNAM-1, NKp30, NKp44, and NKG2D receptors in a panel of AML cell lines; gray histograms represent isotype; black lines represent sample. (C) Summary of flow cytometry data depicted in panel B. Data represented as mean fluorescence intensity (MFI) increase relative to isotype control. (D) Representative flow cytometry plots of killing assay performed in the absence (basal) or presence of DOT cells that were previously incubated with blocking antibodies for the proteins indicated. (E) Summary of killing assays performed against HEL (left) and MOLM13 (right) cell lines. Results are normalized to the percentage of tumor cells targeted in the condition in which DOT cells are incubated with isotype control antibodies. Each dot represents a different DOT-cell donor. Data were generated in ≥3 independent experiments. (F) Flow cytometry plots depicting the phenotype of MOLM13 cell lines modified via CRISPR–CRISPR-associated protein 9 editing. (G) Summary of killing assays performed against the indicated KO cell lines, compared with the mock-transfected cell line. Each dot represents a different DOT-cell donor. Data were generated in >3 independent experiments. (H) Schematic representation of the experimental design of competitive killing assays. (I) Summary of killing assays performed against the indicated KO HEL cell lines in a competitive setting, compared with the mock-transfected cell line. Each dot represents a different DOT-cell donor. Data were generated in 3 independent experiments. Statistical analysis was performed using 1-sample *t* test (hypothetical value: 100). WT, wild type.

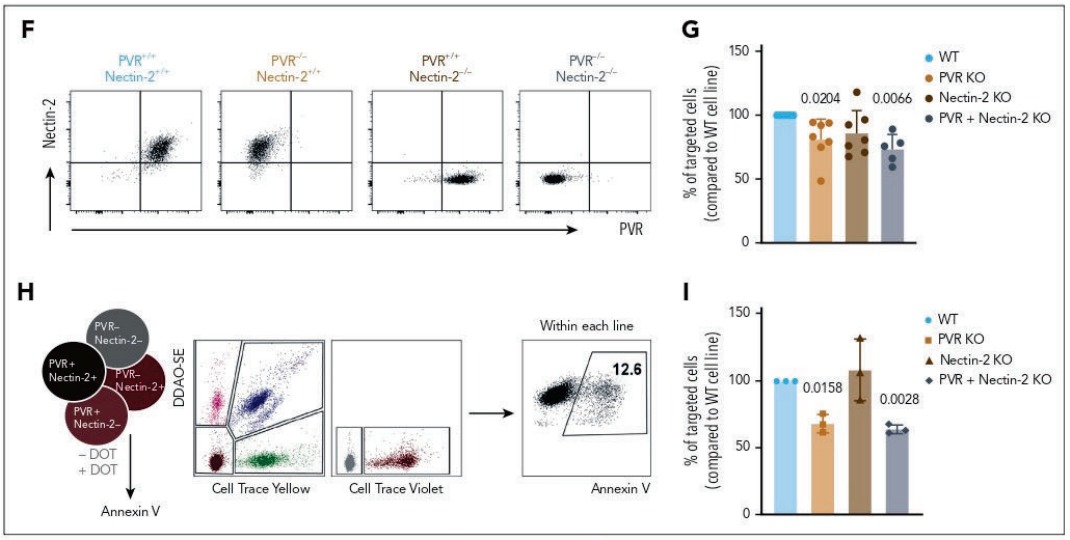

Figure 1 (continued)

NKG2D, and DNAM-1, when compared with ex vivo Vδ1$^+$ γδ T cells.[4,5] Building on these foundations, here we hypothesized that the broad reactivity of DOT cells against AML cells is NKR mediated and thus dependent on the expression of key counter NKR ligands on AML cells, which we set out to identify.

Study design

Ethics

Primary AML cells were obtained from diagnostic bone marrow or peripheral blood samples, after informed consent and institutional review board approval, in accordance with the Declaration of Helsinki.

DOT cells, AML samples, and cell lines

DOT cells were analyzed for their NKR phenotype, as well as for the expression of TIGIT and CD96, by flow cytometry (supplemental Figure 1, available on the *Blood* website). In this study we used DOT cells with <10% of TIGIT$^+$ cells. Primary AML samples were used either fresh or cryopreserved, upon a 2-hour incubation after thawing in RPMI 1640 supplemented with 20% fetal bovine serum, 1% penicillin/streptomycin, 100 μg/mL of stem cell factor and FMS-like tyrosine kinase 3, and 20 μg/mL of thrombopoetin. The source and culture media of AML cell lines are summarized in supplemental Table 1. Genetic deletion of pulmonary vascular resistance (PVR) gene, nectin-2, and B7-H6 was performed by cloning the guide RNAs (supplemental Table 2) into the PX459 plasmid (Addgene), as previously described.[9] Cells were electroporated using Neon Transfection System (1300 V, 20 ms, 2 pulses). Knockout (KO) cells were sorted via fluorescence-activated cell sorting based on protein expression. Analysis of ligand expression was performed using the antibodies provided in supplemental Table 3, upon incubation with Fc receptor inhibitor. A given AML sample was considered positive for a specific ligand when the difference in percentage of positive cells between the test and isotype control samples was >5%. Messenger RNA from AML cells was isolated, reverse transcribed, and quantified, as previously described.[10] Primer sequences are summarized in supplemental Table 2.

AML cell targeting

For killing assays, AML cell lines or primary samples were stained with a dye and washed before coincubation with DOT cells at an effector-to-target ratio of 5:1, for 3 or 24 hours, in the presence of 100 ng/mL of interleukin-15 (Peprotech). For blocking experiments, cells were preincubated for 15 minutes at 4°C with blocking antibodies (supplemental Table 3). Cells were stained with annexin V and analyzed in an LSR Fortessa (BD Biosciences) and data analyzed with FlowJo software (Tree Star). For imaging experiments, cells were stained with different dyes for 10 minutes at room temperature before coincubation; then fixed with 1.5% paraformaldehyde and stained for phalloidin during the permeabilization step (phosphate-buffered saline + 0.1% Triton X-100 + 2% fetal bovine serum). Before acquisition in Amnis ImageStreamX (Luminex), 4′,6-diamidino-2-phenylindole was added. Results were analyzed using IDEAS software. Details of concentrations are provided in supplemental Table 3.

Statistical analysis

Individual values, mean, and standard error of the mean are plotted. The statistical tests used, and significant *P* values are indicated in each figure.

Results and discussion

To study NKR-ligand expression on a panel of AML cell lines (supplemental Table 1), we quantified both messenger RNA

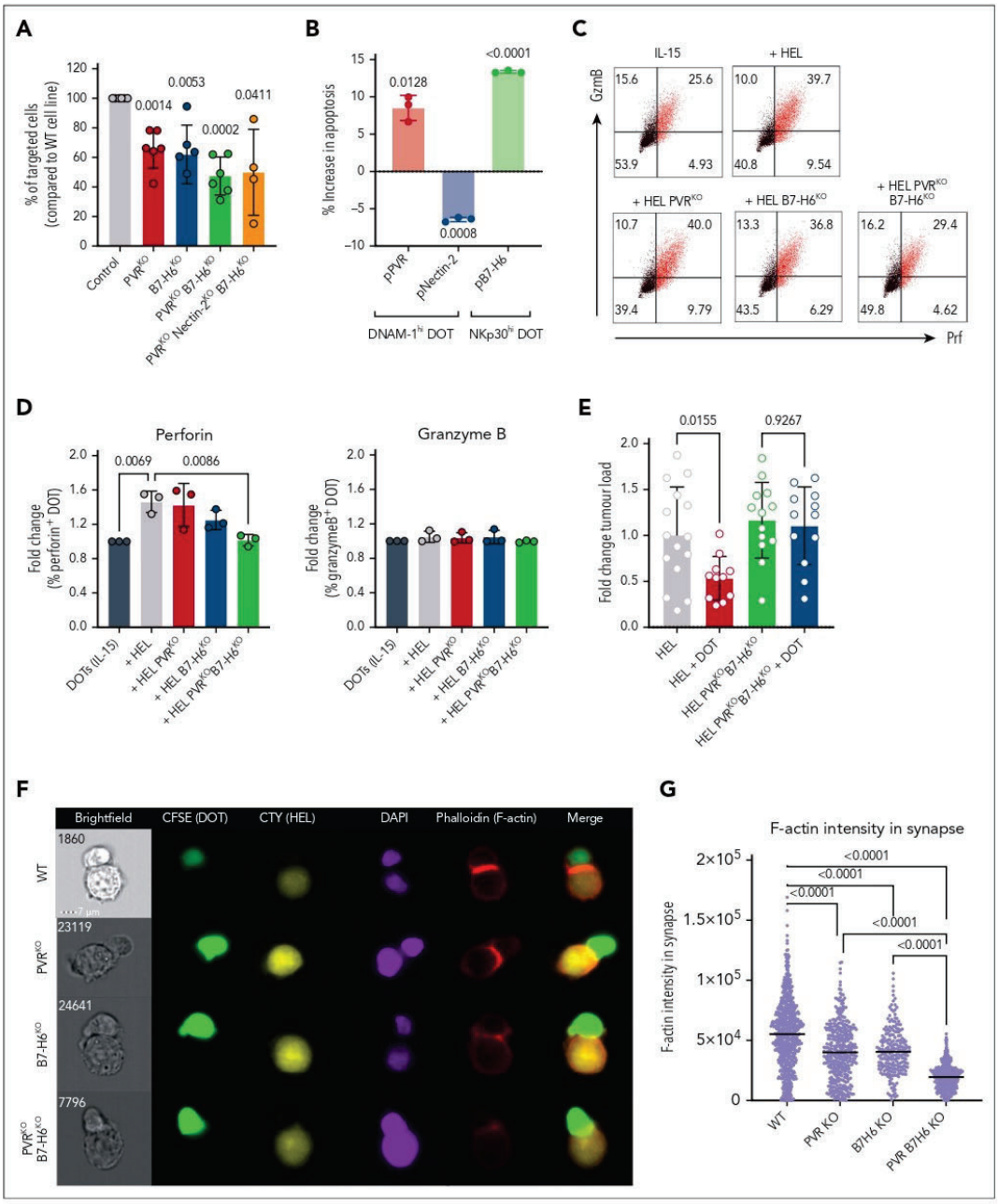

Figure 2. PVR and B7-H6 are essential for formation of robust immunological synapses between DOT cells and AML cells. (A) Summary of killing assays performed against the indicated KO HEL cell lines, compared with the mock-transfected cell line. Each dot represents a different DOT-cell donor. Data were generated in 3 independent experiments. (B) Killing assay performed against the mouse breast cancer cell line E0771 previously transfected to express human PVR, nectin-2, or B7-H6 compared with the mock-transfected cell line. DOT cells were selected for high expression of the respective counterreceptors (DNAM-1 or NKp30). Each dot represents a technical replicate. Data were generated in 2 independent experiments. (C) Representative flow cytometry plots of granzyme B (GzmB) and perforin (Prf) expression on DOT cells, when in contact with different cell lines or in the presence of interleukin-15 (IL-15) only. (D) Summary of the flow cytometry data depicted in panel C. Each dot represents a DOT-cell donor. Data were generated in 2 independent experiments. (E) Tumor load in the blood of a xenograft model of AML. Immunodeficient NSG-HuIL-15 mice were engrafted with control or PVR/B7-H6 double-KO HEL (luciferase positive) cell lines. Mice were treated with DOT cells intravenously or left untreated. Three weeks after tumor injection, mice

(Figure 1A) and surface protein (Figure 1B) levels and found a marked upregulation of PVR and B7-H6, which contrasted with milder expression of nectin-2 and very low NKG2D ligands (Figure 1A-C). We first focused on DNAM-1 and its ligands, PVR and nectin-2, emerging players in tumor immunology,[11] previously shown to be important for Vδ2$^+$ γδ T-cell responses to liver or brain cancers.[12-14] We used blocking antibodies in 3-hour killing assays against HEL or MOLM13 AML cells, and found a 20% to 30% decrease in DOT-cell cytotoxicity upon DNAM-1 neutralization (Figure 1D-E). However, because ligand blockade failed to reproduce this effect, we used a more stringent methodology, CRISPR–CRISPR-associated protein 9 gene editing, to knock out each or both ligands (Figure 1F). Upon coincubation with DOT cells, we found lower targeting (compared with mock transduced) of PVR KO but not nectin-2 KO MOLM13 cells, whereas the double KO behaved similarly to PVR KO cells (Figure 1G). We then designed competitive killing assays in the presence of all the edited HEL lines labeled with different fluorescent dyes (Figure 1H). Consistently, PVR KO (and double KO) but not nectin-2 KO AML cells were ~40% less targeted than control HEL cells (Figure 1I).

Next, we inquired the role of the NKp30 ligand, B7-H6.[15] We observed a reduction (compared with mock-transduced HEL cells) in B7-H6 KO killing by DOT cells, plus an additive effect (to 60% loss in reactivity) in PVR/ B7-H6 double-KO cells (Figure 2A). To complement these loss-of-function experiments, we ectopically expressed PVR, nectin-2, or B7-H6 in murine E0771 tumor cells, given their natural lack of expression of these human ligands (supplemental Figure 2). Upon coincubation with DOT cells selected for high expression of DNAM-1 or NKp30, we found that ectopic PVR and B7-H6 but not nectin-2 conferred susceptibility to DOT-cell targeting (Figure 2B). To gain further mechanistic insight, we analyzed cytotoxic molecule expression and formation of immune synapses between DOT cells and AML cells. We observed perforin induction on DOT cells upon coincubation with HEL cells, which was fully dependent on the presence of both PVR and B7-H6 (Figure 2C-D). Importantly, imaging synapse formation (via F-actin staining) also showed its synergistic dependence on PVR and B7-H6 (Figure 2F-G), thus strengthening the importance of these 2 ligands in AML cell line recognition by DOT cells. To validate these findings in vivo, we transplanted the KO cell lines into NOD scid gamma (NSG)-HuIL-15 transgenic mice and observed that the absence of PVR and B7-H6 impaired tumor clearance by DOT cells (Figure 2E).

Finally, we investigated the impact of NKR ligands on DOT-cell targeting of primary AML cells. Unlike AML cell lines (Figure 1B), primary AML showed variable levels of PVR, nectin-2, and B7-H6, and mostly lacked NKG2D ligand expression (Figure 3A; supplemental Figure 3A-B). This led us to segregate the patient samples into those that expressed (n = 9) or did not express (n = 4) any of the 3 ligands (Figure 3B), and to demonstrate clearly distinct extents of DOT-cell cytotoxicity (Figure 3C). By focusing on each of the ligands, we found PVR and nectin-2, which followed similar expression patterns (Figure 3B), but not B7-H6 or NKG2D ligands to predict DOT-cell cytotoxicity (Figure 3D; supplemental Figure 3C) with significant receiver operating characteristic curves (area under the curve, >0.75; Figure 3E; supplemental Figure 3D). Moreover, we found that incubation of DOT cells with AML samples that express PVR led to an upregulation of CD69 (Figure 3F), a T-cell activation marker, corroborating that PVR expression promotes DOT-cell activation. Altogether, our data indicate that PVR uniquely combines functional relevance, as assessed by genetic manipulation in AML cell lines, with predictive capacity with patient-derived AML samples, and we thus propose that its expression should be considered as a potential biomarker of response to Vδ1/DOT cell–based therapies in AML.

From a conceptual point of view, this study highlights the potential of NKRs to provide broad innate sensing mechanisms to T-cell products, such as DOT cells, for adoptive immunotherapy. This is especially relevant for diseases like AML in which it is difficult to define a safe CAR T-cell antigen, and even in B-cell malignancies, in which target antigen loss can drive relapses that limit the 1-year progression-free survival rates to 50%.[16,17] Furthermore, the high DNAM-1 expression on DOT cells may be important to compensate for the decreased DNAM-1 expression in endogenous, and functionally impaired, NK cells of patients with AML.[18] Furthermore, DOT cells display the key advantages over NK cells of lacking the expression of inhibitory killer cell immunoglobulin-like receptors[5] and the additional activation via the TCR, allowing for high yields during in vitro expansion protocols.

In contrast, T-cell dysfunctionality or exhaustion has also been demonstrated in patients with relapsed AML,[19] as well as in patients with B-cell leukemia/lymphoma treated with autologous CAR T cells.[20] This favors allogeneic T cells, which are neither affected by cancer nor chemotherapy, and may be further boosted in vitro, alike DOT cells.[5] Moreover, by being major histocompatibility/human leukocyte antigen independent, DOT cells are particularly well suited for allogeneic use, without need of genetic edition of the endogenous TCR, as for αβ T cells,[21] to prevent graft-versus-host disease.[22] Importantly, DOT cells are derived from peripheral blood Vδ1$^+$ γδ T cells, which were shown to correlate with long-term disease-free survival of patients with leukemia after allogeneic hematopoietic stem cell transplantation,[23] and were recently associated with a CD19 CAR T-cell expansion in a patient with chronic lymphocytic leukemia who was disease free 10 years after treatment.[24] We therefore expect DOT cells to constitute a distinctive platform for adoptive immunotherapy of AML and potentially other hematological (and solid) malignancies.

Figure 2 (continued) were euthanized and tumor load in the blood was quantified by luminescence. Data were generated in 2 independent experiments. (F) Representative images of image-flow cytometry data of immunological synapses established between DOT cells and different HEL cell lines. (G) Quantification of filamentous actin (F-actin) signal within the area of interaction between the DOT cell and the tumor cell. Data are representative of 2 independent experiments. Statistical analysis was performed using 1-sample *t* test (hypothetical value: 100 for panel A, or 0 for panel B), 1-way analysis of variance followed by Šidák multiple comparisons test for panel E, or Kruskal-Wallis test followed by Dunn multiple comparisons test for panels D and G. WT, wild type.

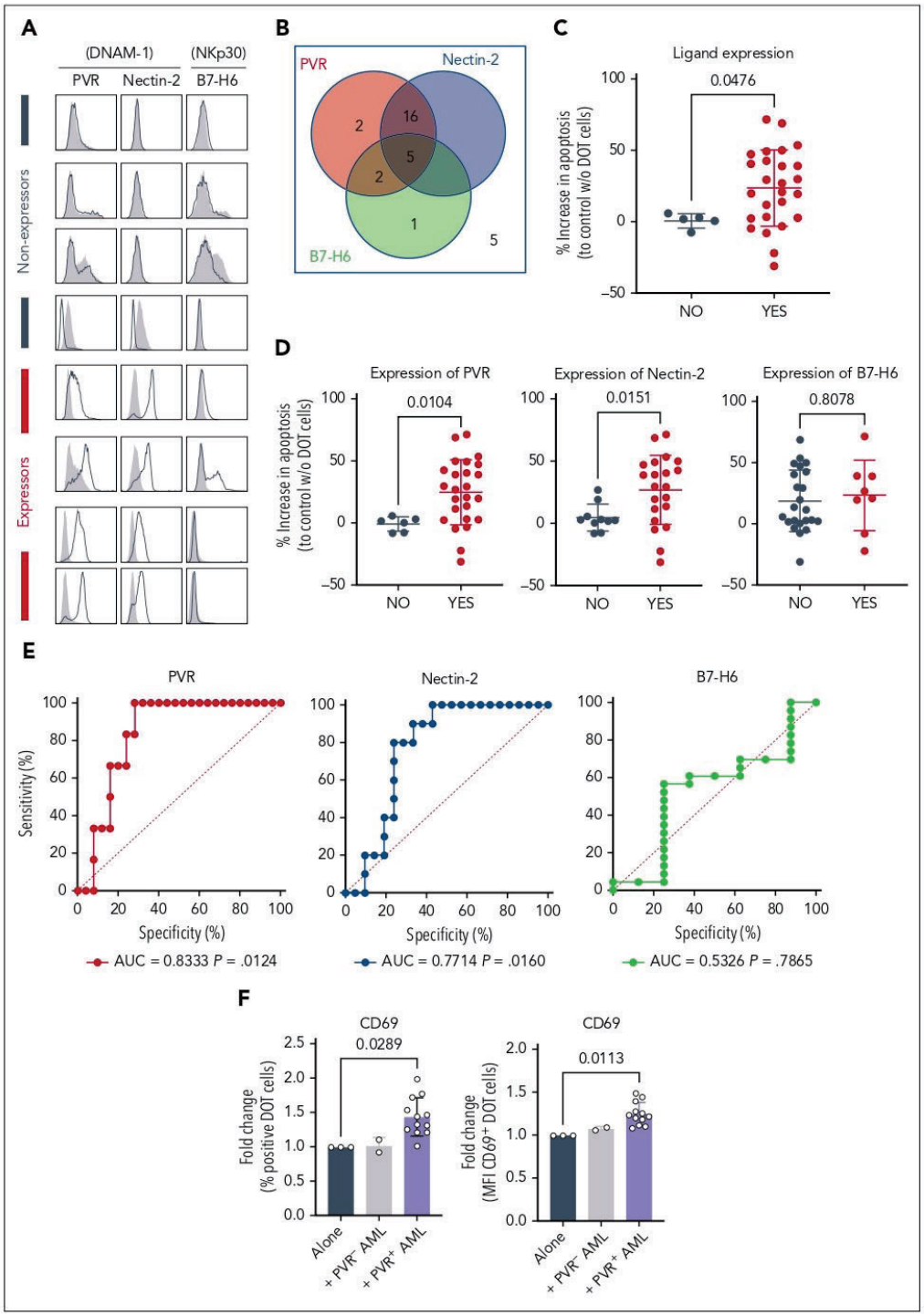

Figure 3.

Figure 3. Expression of PVR but not B7-H6 predicts cytotoxic targeting of primary AML samples by DOT cells. (A) Representative flow cytometry histograms of the expression of PVR, nectin-2, and B7-H6. Each row depicts a different AML sample donor. Gray histograms, isotype; black lines, sample. (B) Distribution of PVR, nectin-2, and B7-H6 expression on all primary AML samples analyzed. (C) Targeting of primary AML samples by DOT cells based on the expression of 1 of 3 ligands shown in panels A-B. (D) Targeting of primary AML samples by DOT cells based on the expression of PVR, nectin-2, or B7-H6. (E) Receiver operating characteristic curves that illustrate the predictive ability of the expression of each of the depicted ligand(s) to discriminate whether primary AML samples are targeted by DOT cells. (F) Fold change of percentage of $CD69^+$ cells (left) or CD69 MFI (right) on DOT cells that were cultured alone, or in the presence of PVR^- or PVR^+ primary AML samples. Each dot represents a different DOT cell/AML combination. Statistical analysis was performed using the Mann-Whitney *U* test for panels C-D, and Kruskal-Wallis followed by Dunn multiple comparisons test for panel E. AUC, area under the curve; w/o, without.

Acknowledgments

The authors thank André Simões, Daniel V. Correia, Simão Rocha, Natacha Gonçalves-Sousa and the Flow Cytometry, Bioimaging and Rodent Facilities of Instituto de Medicina Molecular João Lobo Antunes for their technical support and assistance. The authors also thank the patients, and their families, for donating AML samples.

The authors acknowledge financing by national funds through Fundação para a Ciência e a Tecnologia, I.P. (PTDC/MED-ONC/6829/2020, DOI: 10.54499/PTDC/MED-ONC/6829/2020 to B.S.-S. and L.B.; and 2021.01953.CEECIND, DOI: 10.54499/2021.01953.CEECIND/CP1673/CT0007 to S.M.). The authors also acknowledge funding from Takeda Development Center Americas, Inc (B.S.-S., S.M., C.C., and R.B.-D.); "la Caixa" Foundation (ID 100010434, under agreement LCF/PR/HR19/52160011 [B.S.-S. and P.M.]); "Ayudas Merck de Investigación" from Health Merck Foundation; grant PID2022-136554OA-I00 funded by MICIU/AEI 10.13039/501100011033 and the European Regional Development Fund (ERDF)/EU (D.S.-M.); Centres de Recerca de Catalunya/Generalitat de Catalunya and Fundació Josep Carreras-Obra Social la Caixa for core support; the Spanish Ministry of Economy and Competitiveness/European Union NextGenerationEU (grants CPP2021-008508 and CPP2022-009759); and the scientific foundation of the Spanish Association Against Cancer (grants AECC,PRYGN234975MENE and PRYGN211192BUEN) to P.M.

Authorship

Contribution: S.M. and C.C. performed most of the experiments and analyzed the data; D.S.-M., S.S., R.M.L.C., N.T., and M.V. contributed to the generation of k cell lines; S.S., R.M.L.C., R.B.-D., and L.B. assisted in some experiments and provided critical feedback; B.G., N.C., and M.G.d.S. supplied primary AML samples; B.S.-S., S.M., and P.M. designed the study and wrote the manuscript; and D.S.-M. and R.B.-D. revised the manuscript.

Conflict-of-interest disclosure: B.S.-S., S.M., C.C., and R.B.-D. received funding from a sponsored research agreement with Takeda Development Center Americas, Inc, Lexington, MA. P.M. is cofounder of One-Chain ImmunoTherapeutics, a spin-off from the Josep Carreras Leukemia Research Institute, Barcelona, Spain. The remaining authors declare no competing financial interests.

ORCID profiles: S.M., 0000-0002-5157-0033; C.C., 0000-0002-5046-4685; D.S.-M., 0000-0003-4605-5325; S.S., 0000-0001-9420-6058; R.M.L.C., 0000-0003-3199-2199; N.T., 0000-0001-8352-2194; M.V., 0000-0003-1906-4701; R.B.-D., 0000-0003-2448-8699; L.B., 0000-0002-7339-9994; B.G., 0000-0002-0249-9285; N.C., 0000-0001-9230-9870; M.G.d.S., 0000-0002-6993-2450; P.M., 0000-0001-9372-1007; B.S.-S., 0000-0003-4141-9302.

Correspondence: Sofia Mensurado, Instituto de Medicina Molecular João Lobo Antunes, Avenida Prof Egas Moniz, 1649-028 Lisbon, Portugal; email: sofiamensurado@medicina.ulisboa.pt; and Bruno Silva-Santos, Instituto de Medicina Molecular João Lobo Antunes, Avenida Prof Egas Moniz, 1649-028 Lisbon, Portugal; email: bssantos@medicina.ulisboa.pt.

Footnotes

Submitted 19 October 2023; accepted 25 January 2024; prepublished online on *Blood* First Edition 16 February 2024. https://doi.org/10.1182/blood.2023022992.

*S.M. and C.C. contributed equally to this study.

†P.M. and B.S.-S. contributed equally to this study.

Data are available on request from corresponding authors, Sofia Mensurado (sofiamensurado@medicina.ulisboa.pt) and Bruno Silva-Santos (bssantos@medicina.ulisboa.pt).

The online version of this article contains a data supplement.

There is a *Blood* Commentary on this article in this issue.

The publication costs of this article were defrayed in part by page charge payment. Therefore, and solely to indicate this fact, this article is hereby marked "advertisement" in accordance with 18 USC section 1734.

REFERENCES

1. DiNardo CD, Wei AH. How I treat acute myeloid leukemia in the era of new drugs. *Blood*. 2020;135(2):85-96.
2. June CH, O'Connor RS, Kawalekar OU, Ghassemi S, Milone MC. CAR T cell immunotherapy for human cancer. *Science*. 2018;359(6382):1361-1365.
3. Wei W, Yang D, Chen X, Liang D, Zou L, Zhao X. Chimeric antigen receptor T-cell therapy for T-ALL and AML. *Front Oncol*. 2022;12:967754.
4. Correia DV, Fogli M, Hudspeth K, da Silva MG, Mavilio D, Silva-Santos B. Differentiation of human peripheral blood Vδ1+ T cells expressing the natural cytotoxicity receptor NKp30 for recognition of lymphoid leukemia cells. *Blood*. 2011;118(4):992-1001.
5. Almeida AR, Correia DV, Fernandes-Platzgummer A, et al. Delta One T cells for immunotherapy of chronic lymphocytic leukemia: clinical-grade expansion/differentiation and preclinical proof of concept. *Clin Cancer Res*. 2016;22(23):5795-5804.
6. Mensurado S, Blanco-Domínguez R, Silva-Santos B. The emerging roles of γδ T cells in cancer immunotherapy. *Nat Rev Clin Oncol*. 2023;20(3):178-191.
7. Di Lorenzo B, Simões AE, Caiado F, et al. Broad cytotoxic targeting of acute myeloid leukemia by polyclonal Delta One T cells. *Cancer Immunol Res*. 2019;7(4):552-558.
8. Sánchez Martínez D, Tirado N, Mensurado S, et al. Generation and proof-of-concept for allogeneic CD123 CAR-Delta One T (DOT) cells in acute myeloid leukemia. *J Immunother Cancer*. 2022;10(9):e005400.
9. Joung J, Konermann S, Gootenberg JS, et al. Genome-scale CRISPR-Cas9 knockout and transcriptional activation screening. *Nat Protoc*. 2017;12(4):828-863.
10. Mensurado S, Rei M, Lança T, et al. Tumor-associated neutrophils suppress pro-tumoral IL-17+ γδ T cells through induction of oxidative stress. *PLoS Biol*. 2018;16(5):e2004990.
11. Conner M, Hance KW, Yadavilli S, Smothers J, Waight JD. Emergence of the CD226 axis in cancer immunotherapy. *Front Immunol*. 2022;13:914406.
12. Toutirais O, Cabillic F, Le Friec G, et al. DNAX accessory molecule-1 (CD226) promotes human hepatocellular carcinoma cell lysis by Vgamma9Vdelta2 T cells. *Eur J Immunol*. 2009;39(5):1361-1368.

13. Choi H, Lee Y, Park SA, et al. Human allogenic γδ T cells kill patient-derived glioblastoma cells expressing high levels of DNAM-1 ligands. *Oncoimmunology*. 2022; 11(1):2138152.

14. Wang X, Mou W, Han W, et al. Diminished cytolytic activity of γδ T cells with reduced DNAM-1 expression in neuroblastoma patients. *Clin Immunol*. 2019; 203:63-71.

15. Brandt CS, Baratin M, Yi EC, et al. The B7 family member B7-H6 is a tumor cell ligand for the activating natural killer cell receptor NKp30 in humans. *J Exp Med*. 2009;206(7): 1495-1503.

16. Gardner RA, Finney O, Annesley C, et al. Intent-to-treat leukemia remission by CD19 CAR T cells of defined formulation and dose in children and young adults. *Blood*. 2017; 129(25):3322-3331.

17. Maude SL, Laetsch TW, Buechner J, et al. Tisagenlecleucel in children and young adults with B-cell lymphoblastic leukemia. *N Engl J Med*. 2018;378(5):439-448.

18. Sanchez-Correa B, Gayoso I, Bergua JM, et al. Decreased expression of DNAM-1 on NK cells from acute myeloid leukemia patients. *Immunol Cell Biol*. 2012;90(1): 109-115.

19. Noviello M, Manfredi F, Ruggiero E, et al. Bone marrow central memory and memory stem T-cell exhaustion in AML patients relapsing after HSCT. *Nat Commun*. 2019; 10(1):1065.

20. Finney OC, Brakke HM, Rawlings-Rhea S, et al. CD19 CAR T cell product and disease attributes predict leukemia remission durability. *J Clin Invest*. 2019;129(5): 2123-2132.

21. Stenger D, Stief TA, Kaeuferle T, et al. Endogenous TCR promotes in vivo persistence of CD19-CAR-T cells compared to a CRISPR/Cas9-mediated TCR knockout CAR. *Blood*. 2020;136(12): 1407-1418.

22. Liu P, Liu M, Lyu C, et al. Acute graft-versus-host disease after humanized anti-CD19-CAR T therapy in relapsed B-ALL patients after allogeneic hematopoietic stem cell transplant. *Front Oncol*. 2020;10: 573822.

23. Godder KT, Henslee-Downey PJ, Mehta J, et al. Long term disease-free survival in acute leukemia patients recovering with increased gammadelta T cells after partially mismatched related donor bone marrow transplantation. *Bone Marrow Transplant*. 2007;39(12):751-757.

24. Melenhorst JJ, Chen GM, Wang M, et al. Decade-long leukaemia remissions with persistence of CD4(+) CAR T cells. *Nature*. 2022;602(7897):503-509.

Zanetti SR, Velasco-Hernandez T, et al. A novel and efficient tandem CD19- and CD22-directed CAR for B cell ALL. Mol Ther (2022)

Molecular Therapy
Original Article

A novel and efficient tandem CD19- and CD22-directed CAR for B cell ALL

Samanta Romina Zanetti,[1,15] Talia Velasco-Hernandez,[1,2,15] Francisco Gutierrez-Agüera,[1,2] Víctor M. Díaz,[1,3,4] Paola Alejandra Romecín,[1,2] Heleia Roca-Ho,[1] Diego Sánchez-Martínez,[1,2] Néstor Tirado,[1,2] Matteo Libero Baroni,[1] Paolo Petazzi,[1,2] Raúl Torres-Ruiz,[1,2,5] Oscar Molina,[1,2] Alex Bataller,[1,6] José Luis Fuster,[2,7] Paola Ballerini,[8] Manel Juan,[2,9] Irmela Jeremias,[10,11] Clara Bueno,[1,2,12] and Pablo Menéndez[1,2,12,13,14]

[1]Josep Carreras Leukemia Research Institute, School of Medicine, University of Barcelona, Carrer Casanova 143, 4° floor, Barcelona 08036, Spain; [2]RICORS-TERAV, ISCIII, Madrid, Spain; [3]OneChain Immunotherapeutics S.L., Barcelona, Spain; [4]Faculty of Medicine and Health Sciences, International University of Catalonia, Sant Cugat del Vallès 08195, Spain; [5]Centro Nacional de Investigaciones Oncológicas, Madrid 28029, Spain; [6]Department of Hematology, Hospital Clínic de Barcelona, Barcelona 08036, Spain; [7]Sección de Oncohematología Pediátrica, Hospital Virgen de Arrixaca, Murcia 30120, Spain; [8]Department of Pediatric Hemato-oncology, Hospital Armand Trousseau, Paris 75012, France; [9]Department of Immunology, Hospital Clínic de Barcelona and Hospital Sant Joan de Déu, Barcelona 08950, Spain; [10]Department of Apoptosis in Hematopoietic Stem Cells, Helmholtz Center Munich, German Center for Environmental Health (HMGU), Munich 85764, Germany; [11]Department of Pediatrics, Dr von Hauner Children's Hospital, LMU, Munich 80337, Germany; [12]CIBER-ONC, ISCIII, Barcelona, Spain; [13]Department of Biomedicine, School of Medicine, University of Barcelona, Barcelona 08036, Spain; [14]Institució Catalana de Recerca i Estudis Avançats (ICREA), Barcelona, Spain

CD19-directed chimeric antigen receptor (CAR) T cells have yielded impressive response rates in refractory/relapse B cell acute lymphoblastic leukemia (B-ALL); however, most patients ultimately relapse due to poor CAR T cell persistence or resistance of either CD19$^+$ or CD19$^-$ B-ALL clones. CD22 is a pan-B marker whose expression is maintained in both CD19$^+$ and CD19$^-$ relapses. CD22-CAR T cells have been clinically used in B-ALL patients, although relapse also occurs. T cells engineered with a tandem CAR (Tan-CAR) containing in a single construct both CD19 and CD22 scFvs may be advantageous in achieving higher remission rates and/or preventing antigen loss. We have generated and functionally validated using cutting-edge assays a 4-1BB-based CD22/CD19 Tan-CAR using in-house-developed novel CD19 and CD22 scFvs. Tan-CAR-expressing T cells showed similar *in vitro* expansion to CD19-CAR T cells with no increase in tonic signaling. CRISPR-Cas9-edited B-ALL cells confirmed the bispecificity of the Tan-CAR. Tan-CAR was as efficient as CD19-CAR *in vitro* and *in vivo* using B-ALL cell lines, patient samples, and patient-derived xenografts (PDXs). Strikingly, the robust antileukemic activity of the Tan-CAR was slightly more effective in controlling the disease in long-term follow-up PDX models. This Tan-CAR construct warrants a clinical appraisal to test whether simultaneous targeting of CD19 and CD22 enhances leukemia eradication and reduces/delays relapse rates and antigen loss.

INTRODUCTION

B cell acute lymphoblastic leukemia (B-ALL) is an aggressive hematologic malignancy characterized by the clonal expansion of CD19$^+$ B cell precursors.[1] B-ALL is the most common malignancy in children, and although less prevalent in adults, it is associated with an unfavorable prognosis.[2] Although >90% of patients achieve complete remission after first-line treatment, the prognosis of those with refractory/relapse (R/R) B-ALL is dismal, with a 5-year overall survival of <20%.[2,3]

Adoptive transfer of T cells engineered to express artificial chimeric antigen receptors (CARs) targeting tumor cell surface-associated antigens (Ag) represents a revolutionary approach in cancer immunotherapy.[4] CD19 represents the ideal CAR T cell therapy for B-ALL, because it is homogeneously expressed on malignant cells, its off-target expression is limited to normal B cells, and CD19-CAR T cell-mediated B cell aplasia is easily manageable clinically through the administration of gamma-immunoglobulins (γ-Igs).[5] CD19-CAR T cells have revolutionized the treatment of R/R B-ALL with complete response rates of ∼80%–90%; however, 40%–60% of patients treated with CD19-targeted immunotherapy still relapse after 1 year.[3,6] Two major types of relapse have been distinguished[7–10]: relapse that remains CD19$^+$, typically linked to poor T cell function or loss of CAR T cell persistence, and relapse CD19$^-$, in which the disease recurs with loss of CD19, representing a novel "stem cell origin-related" mechanism of tumor escape.

Received 12 January 2021; accepted 25 August 2021;
https://doi.org/10.1016/j.ymthe.2021.08.033.

[15]These authors contributed equally

Correspondence: Samanta Romina Zanetti, Josep Carreras Leukemia Research Institute, School of Medicine, University of Barcelona, Carrer Casanova 143, 4° floor, Barcelona 08036, Spain.
E-mail: samzanetti@gmail.com
Correspondence: Talia Velasco-Hernández, Josep Carreras Leukemia Research Institute, School of Medicine, University of Barcelona, Carrer Casanova 143, 4° floor, Barcelona 08036, Spain.
E-mail: tvelasco@carrerasresearch.org
Correspondence: Pablo Menéndez, Josep Carreras Leukemia Research Institute, School of Medicine, University of Barcelona, Carrer Casanova 143, 4° floor, Barcelona 08036, Spain.
E-mail: pmenendez@carrerasresearch.org

Another promising target for CAR T cell therapy in B-ALL is CD22. CD22 is a pan B cell surface Ag expressed in most cases of B-ALL.[11] CD22-targeted immunotherapy has been developed and tested in several studies,[12–15] and the results from initial clinical trials in children with either $CD19^+$ or $CD19^-$ R/R B-ALL are promising, but relapses are also common[12,14] and are in a proportion of patients associated with a downregulation of CD22 expression.[12] R/R B-ALL thus remains clinically challenging.

To overcome leukemia immunoediting during CAR T cell therapy for the treatment of B-ALL, compensatory strategies such as dual-Ag or multi-Ag targeting by CARs will likely be needed.[10,16] One potential strategy to reduce immunological pressure over a single Ag and to offset tumor Ag-loss relapse involves generating T cells with one CAR molecule containing two different binding domains in tandem (Tan-CAR),[17] which appears to enhance the potency and antitumor activity *in vivo* when compared with single CARs.[18–20] Several clinical trials exploring combinatorial anti-CD19 and anti-CD22 strategies are under way to optimize response rates and reduce the risk of leukemic cell escape to CAR T cell therapy in B-ALL.[17,21]

We have developed, characterized, and functionally validated a 4-1BB-based CD22/CD19 Tan-CAR using in-house-developed novel CD19 and CD22 monoclonal antibodies (mAbs). Here, we report a specific and efficient *in vitro* and *in vivo* elimination of B-ALL cell lines, primary B-ALL cells, and B-ALL patient-derived xenografts (PDXs) cells with our Tan-CAR construct that is on par with CD19-CAR, but is slightly more effective *in vivo* in controlling the disease in long-term follow-up B-ALL PDXs.

RESULTS

Generation and expression of CD22/CD19 Tan-CARs on human T cells

We sought to evaluate a strategy to reduce immunological pressure over a single Ag (CD19) in B-ALL by modifying T cells with one CAR molecule containing both CD19- and CD22-binding domains, generating a CD22/CD19 Tan-CAR. To compare the effectiveness of the CD22/CD19 Tan-CAR and CD19-CAR, we designed two second-generation Tan-CARs: a short (S) and a long (L) version (Figure 1A). We used a proprietary anti-CD22 single-chain fragment variable (scFv)[15] and a clinically validated anti-CD19 scFv.[22–25] Constructs S and L differ only in the length of the flexible linker sequence connecting the anti-CD22 scFv and anti-CD19 scFv (Figure 1A). We maintained the original linkers between the VH and VL domains from each single CAR. The hinge, transmembrane (TM), and signaling domains were identical for CD19-CAR and Tan-CARs constructs, each encoding a CD8-derived hinge and TM domain, a 4-1BB signaling domain, and a CD3ζ-derived signaling domain. As an experimental control, we used an "empty" CD8TM-4-1BB-CD3ζ CAR construct without a scFv (Mock-CAR) (Figure 1A). To assess the transduction efficiency and to track the CAR expression, we incorporated a GFP reporter gene after a 2A ribosomal skip sequence at the C-terminal of the CAR sequence.

Human T cells were activated as described in the Method details section, and successful T cell activation was determined 48 h later by measuring CD25 and CD69 expression by fluorescence-activated cell sorting (FACS) and by observing the formation of activated T cell clusters with light microscopy (Figure 1B). T cells were transduced with CAR-expressing lentivectors and expanded in the presence of interleukin-7 (IL-7) and IL-15.[7,15,24,26,27] The results showed that the transduction efficiency of Tan-CARs was lower than that of the Mock-CAR or CD19-CAR (Figure 1C). Expression of Mock- and CD19-CARs on the surface of transduced T cells ranged from 30% to 50%, whereas the expression of Tan(S)-CAR ranged from 5% to 26% and Tan(L)-CAR ranged from 1% to 13%. Of note, retroviral infection substantially increased the transduction efficiencies of T cells with the Tan(S)-CAR to ~30%–40% (Figures S2A–S2C), facilitating the clinical translation of this Tan(S)-CAR. All CAR T cells had an identical proliferative capacity and expanded 200-fold over a 15-day period, with the exception of the Tan(L)-CAR, which expanded 50% less (Figure 1C). CAR transduction efficiency in human T cells was analyzed by FACS using GFP reporter expression, and CAR expression was detected on the surface of transduced T cells using an anti-scFv antibody (Figure 1D). To verify that both scFvs were intact, we incubated CAR T cells with human recombinant CD19-Fc protein or CD22-HisTag protein. Both Tan-CAR constructs retained the ability to bind CD19 and CD22 Ags, but Tan(L)-CAR showed a slightly lower binding on the surface. As expected, CD19-CAR bound to CD19-Fc but not CD22-HisTag. Mock-CAR surface expression was detected using an anti-HisTag antibody (Figures 1D and 1E). Binding of Tan-CARs to recombinant CD22 was similar to that observed for the single CD22-CAR.[15] The expression of all CARs could be easily detected in both $CD4^+$ and $CD8^+$ T cells (Figure 1F). These observations were reproduced in CAR T cells generated from n = 5 healthy donors (HDs). In addition, we analyzed the vector copy number (VCN) of the CAR vector (provirus) in the T cells. We found 6–7 proviral copies genome integrated in Mock-CAR and CD19-CAR, whereas for Tan(S)-CAR up to an average of 12 proviral copies were found per transduced cell, indicating a proper genome integration of the Tan(S)-CAR vector into the T cells (Figure 1G). Finally, kinetics of T cell volume of the CAR T cells together with analysis of the expression of activation (CD69 and CD25), differentiation (CCR7, CD27, and CD45RO), and inhibition (LAG3, TIM3, and PD-1) markers on the indicated CAR T cells throughout the 21-day *in vitro* expansion revealed no differences in tonic signaling of the different CARs as compared to activated untransduced T cells (Figure S3). In all subsequent experiments, we normalized the rates of transduction efficiency between vectors by diluting with non-transduced T cells to functionally compare CAR T cells with equal transduction rates.

CD22/CD19 Tan-CAR T cells display a highly efficient and bispecific cytotoxicity

We next evaluated and compared the antileukemic activity of Tan-CARs by measuring the cytotoxicity and secretion of pro-inflammatory cytokines against B-ALL cell lines *in vitro*. Both Tan(S)-CAR and Tan(L)-CAR displayed a comparable massive cytotoxicity activity against SEM and NALM6 cell lines after 48 h, at a 1:1

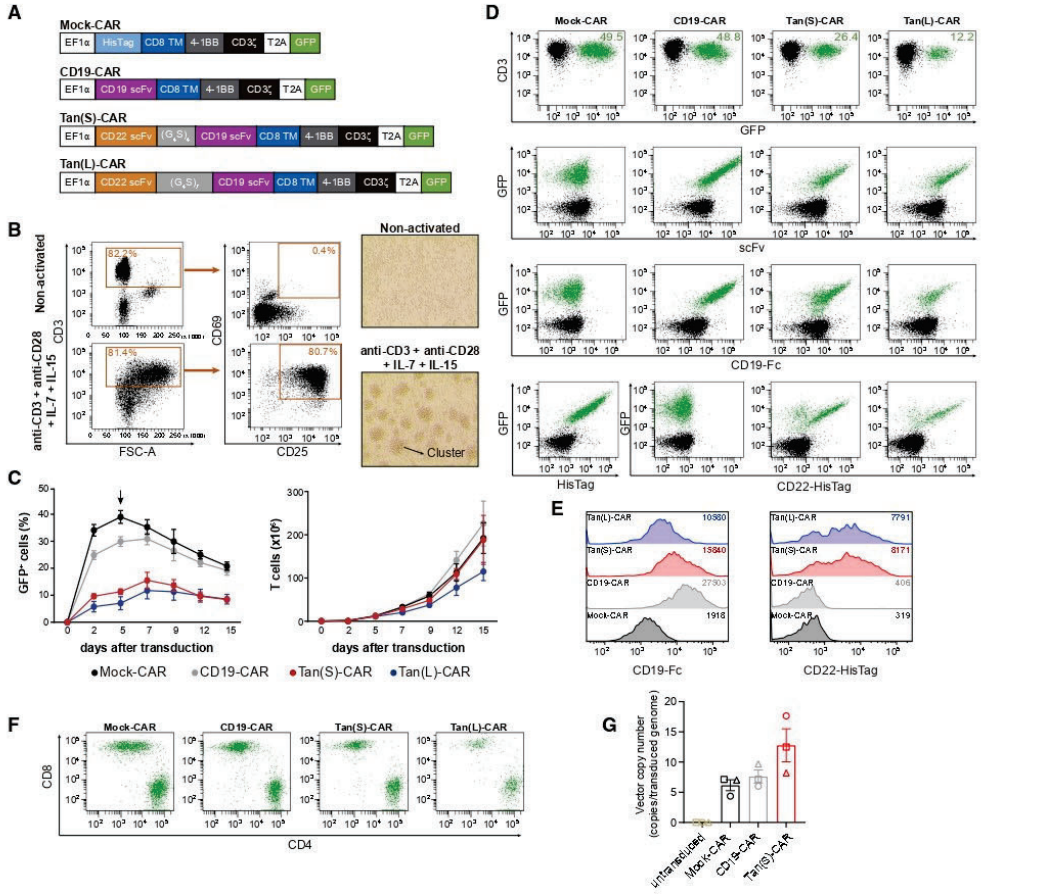

Figure 1. Generation, transduction, expansion, and detection of Tan-CAR T cells

(A) Scheme of the CAR constructs used: (S) and (L) denote short -$(G_4S)_4$- and long -$(G_4S)_7$- size for the inter-scFv linker, respectively. (B) T cell activation after 48-h exposure to anti-CD3/CD28, plus IL-7 and IL-15 evaluated by CD25 and CD69 expression by FACS (left panel) and by light microscopy analysis of activated T cell clusters (right panel, magnification ×40) (n = 5). (C) Transduction efficiency (left panel) and expansion (right panel) of activated T cells transduced with the indicated CARs (n = 5). The arrow represents the time of CAR T cell harvesting for CAR detection in the surface of T cells. (D) Representative flow cytometry plots of CAR expression on human T cells detected as GFP$^+$ (top panels), anti-scFv (second row), CD19-Fc/anti-Fc-PE (third row), and anti-HisTag-APC or CD22-HisTag/anti-HisTag-APC (bottom row). CAR-transduced T cells are shown in green. (E) Representative CD19 and CD22 mean fluorescence intensity (MFI) quantification by FACS of the GFP$^+$ CAR T cells shown in (D). MFI values are indicated in the upper right corner. (F) Representative CAR detection on human CD4$^+$ and CD8$^+$ T cells. (G) VCN representing the number of integrated copies of the provirus (CAR vector) per transduced genome. Each symbol represents a different donor (n = 3). See also Figure S2.

effector:target (E:T) ratio (Figure 2A). Of note, Tan(S)-CAR had a slightly stronger activity than Tan(L)-CAR against SEM cells at a lower E:T ratio (Figure 2B). Both Tan-CARs produced equivalent amounts of IL-2, interferon γ (IFN-γ), and tumor necrosis factor α (TNF-α) (Figure 2C). This, together with the lower expansion of Tan(L)-CAR (Figure 1C), made us choose the Tan(S)-CAR for subsequent experiments.

To test the bispecific functionality of Tan(S)-CAR T cells, we generated CRISPR/Cas9-edited CD19-knockout (KO), CD22-KO, and DO-KO SEM cells, and validated the expression of CD19 and CD22 in each cell line by FACS (Figure 2D). We then used the resulting transgenic SEM cells in cytotoxicity assays with CD19-CAR and Tan(S)-CAR. Results using single CD22-CAR T cells are shown in Velasco-Hernandez et al. [15] As shown in Figures 2E and 2F,

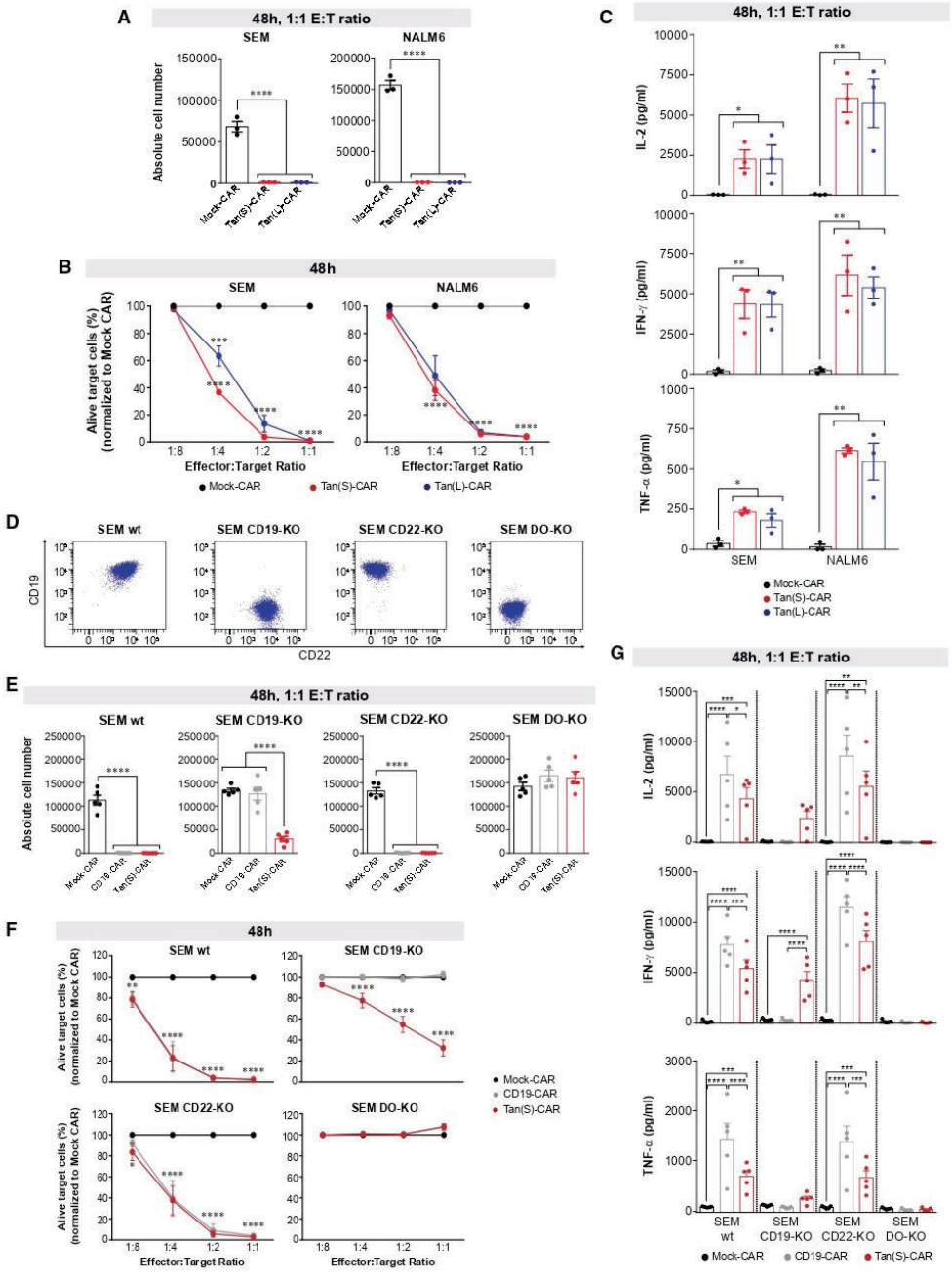

(legend on next page)

CD19-CAR and Tan(S)-CAR T cells eliminated wild-type (WT) and CD22-KO SEM cells, but not DO-KO SEM cells. In addition, Tan(S)-CAR T cells also eliminated CD19-KO SEM cells, suggesting that Tan(S)-CAR T cells specifically eliminate both $CD19^+CD22^-$ and $CD19^-CD22^+$ leukemic cells.

We next surveyed cytokine secretion (at a 1:1 ratio) after 48 h. Of note, the production of pro-inflammatory cytokines by Tan(S)-CAR T cells was significantly lower than that of CD19-CAR T cells (when exposed to $CD19^+$ target cells: SEM WT and SEM CD22-KO; Figure 2G). Neither CD19-CAR nor Tan(S)-CAR T cells secreted pro-inflammatory cytokines in co-culture with SEM DO-KO cells. Also, cytokine levels were undetectable in the Mock-CAR group regardless of the phenotype of the target cells (Figure 2G). Collectively, Tan(S)-CAR T cells recognize both Ags and display bispecific *in vitro* cytotoxicity activity on par with that of CD19-CAR T cells.

Tan(S)-CAR T cells are as efficient as CD19-CAR T cells *in vivo*

We next determined the *in vivo* activity of Tan(S)-CAR T cells in two xenograft mouse models with different aggressiveness based on either NALM6 (Figures 3A–3E) or SEM (Figures 3F–3I) B-ALL cell lines. NALM6-Luc^+ or SEM-Luc^+ cells were intratibially (i.t.) injected into NSG mice (n = 6/group), followed 4 days later by CAR T cells at 15% of transduction. A schematic of the experimental design is shown in Figure 3A. Mice were followed up weekly by bioluminescence imaging (BLI). Analysis showed that Tan(S)-CAR T cells and CD19-CAR T cells had equivalent activity against NALM6 (Figures 3B and 3C) and SEM (Figures 3F and 3G) growth in NSG mice, whereas mice treated with Mock-CAR failed to control the disease. Mice were sacrificed at day 14 ("highly aggressive" NALM6) and 35 ("less aggressive" SEM), and bone marrow (BM) and peripheral blood (PB) were collected and analyzed by FACS for the detection of residual leukemic cells and the presence of T cells (Figures 3D, 3E, 3H, and 3I). Mice treated with Mock-CAR showed a massive expansion of leukemic cells, whereas mice treated with either CD19-CAR T or Tan(S)-CAR T cells showed leukemic eradication accompanied by circulating T cells. Targeting CD19 and CD22 simultaneously does not compromise *in vivo* the antileukemic efficacy of the Tan(S)-CAR.

Tan(S)-CAR T cells and CD19-CAR T cells efficiently eliminate primary and PDX B-ALL cells *in vitro*

We next tested the function of Tan(S)-CAR and CD19-CAR T cells after co-culture with three human primary B-ALL samples and three PDX samples of B-ALL that exhibit distinct expression levels of target Ags (Figures 4A and 4B; Table 1). Notably, T cells transduced with either Tan(S)-CAR or CD19-CAR showed equivalent cytotoxicity activity (Figures 4C and 4D) and production of IFN-γ and TNF-α (Figures 4E and 4F). Of note, however, a significantly higher production of IL-2 was consistently observed with Tan(S)-CAR (Figures 4E and 4F) and does not correlate with a differential T cell proliferation (Figure 4G), suggesting a functional advantage of the Tan(S)-CAR over the single CD19-CAR. In a more clinically applicable setting, PB-derived T cells from a B-ALL patient (patient 4 [Pt#4]) were used as effector cells. Magnetic-activated cell sorting (MACS)-sorted $CD3^+$ T cells were activated, transduced with either Mock-CAR or Tan(S)-CAR, and exposed for 24 h to both autologous B-ALL $CD19^+$ blasts and SEM cells (2:1 ratio). B-ALL patient-derived T cells were efficiently transduced, with similar levels to healthy donor-derived T cells (Figure 4H), and effectively and specifically eliminated both autologous $CD19^+$ blasts and allogenic SEM cells (Figure 4I).

Simultaneous targeting of CD22 and CD19 Ags controls the disease in long-term follow-up B-ALL PDXs

To further explore the *in vivo* activity of Tan(S)-CAR versus CD19-CAR T cells, we used clinically relevant PDX models of B-ALL. NSG mice (n = 5–9/group) were intravenously (i.v.) transplanted with 0.5×10^6 B-ALL cells (PDX#3) or 1×10^6 B-ALL cells (PDX#4), and CAR T cells were infused when B-ALL engraftment was detectable in BM (day 17 for PDX#3 or day 31 for PDX#4). A schematic of the experimental design is shown in Figure 5A. One day before CAR T cell infusion, the leukemic ($CD19^+CD22^+CD10^+$) engraftment was determined in the PB and BM, and mice were subsequently randomized based on BM leukemic burden to receive i.v. 5×10^6 Mock-CAR, CD19-CAR, or Tan(S)-CAR T cells. Leukemic burden and CAR T cell persistence was monitored in PB biweekly by FACS. BM aspirates were FACS analyzed when Mock-treated mice were sacrificed (week 4) and at the endpoint (week 13). As expected, mice treated with Mock-CAR T cells succumbed quickly to the disease, and had to be sacrificed with >40% and >80% of the leukemic graft in PB and BM, respectively (Figure 5B). By contrast, CD19-CAR and Tan(S)-CAR T cells were both capable of controlling the disease by eliminating leukemic cells in BM within 4 weeks after CAR T cell infusion (Figure 5B). For the PDX#4 model, disease recurrence was followed up biweekly from week 4 (minimal residual disease negativity [MRD−]) to week 13, when many mice had to be sacrificed because termination criteria had been reached. Six weeks after CAR T cell infusion, circulating leukemic cells began to emerge in mice treated with CD19-CAR, and both leukemic burden and the number of relapsing mice (>1% blasts in BM or >0.1% in PB)

Figure 2. Robust antileukemic efficacy and specificity of both Tan(S)- and Tan(L)-CAR T cells *in vitro*

(A and B) Absolute number (A) and percentage (B) of alive target cells (SEM or NALM6) after 48-h incubation with the indicated CAR T cells and E:T ratios. Results in (B) are normalized to Mock-CAR data. PBMCs from n = 3 independent HDs. (C) Production of the pro-inflammatory cytokines IL-2, IFN-γ, and TNF-α by CAR T cells after 48-h exposure to SEM or NALM6 target cells at 1:1 E:T ratio. PBMCs from n = 3 independent HDs. (D) Different CD22/CD19 combinatorial phenotypes of CRISPR/Cas9-edited SEM cells. (E and F) Absolute number (E) and percentage (F) of alive target cells after 48-h incubation with the indicated CAR T cells and E:T ratios. Results in (F) are normalized to Mock-CAR data. PBMCs from n = 5 independent HDs. (G) Production of IL-2, IFN-γ, and TNF-α by the indicated CAR T cells after 48-h exposure to the indicated phenotypes of SEM cells (n = 5). Data are shown as means ± SEMs. $^*p < 0.05$, $^{**}p < 0.01$, $^{***}p < 0.001$, $^{****}p < 0.0001$; 1-way ANOVA with the Tukey post hoc test. See also Figures S1 and S3.

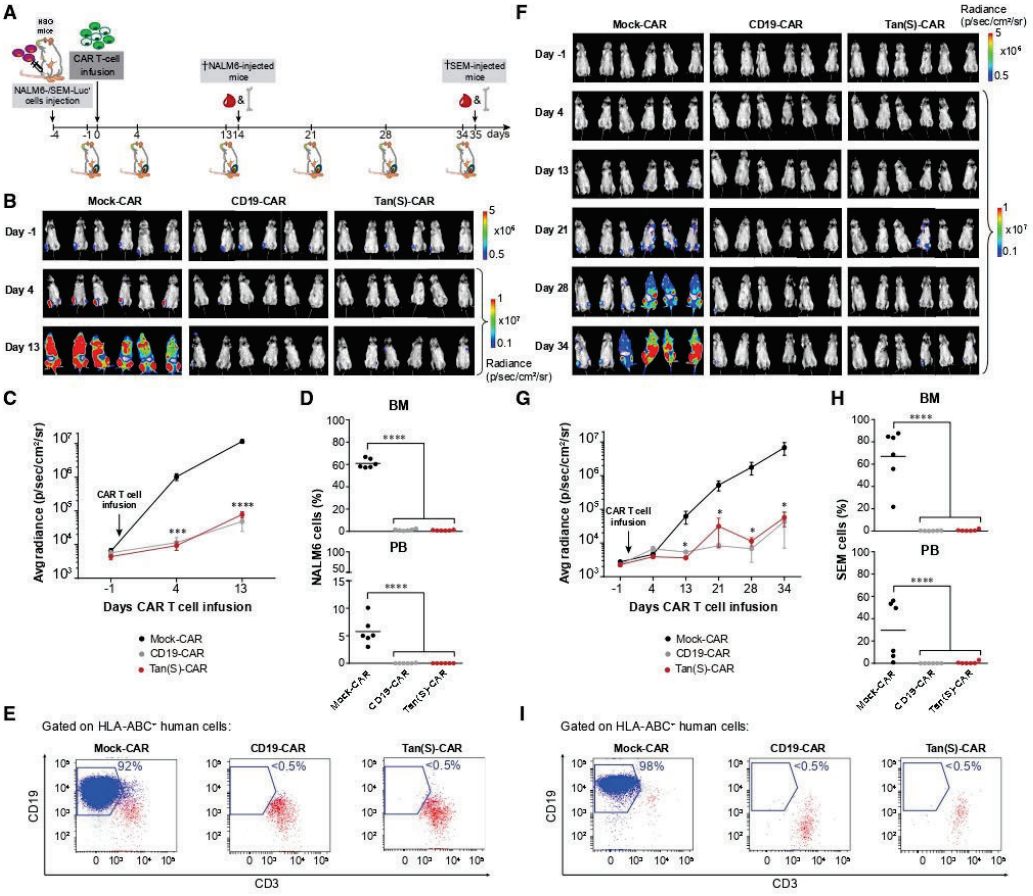

Figure 3. Tan(S)-CAR T cells are as efficient as CD19-CAR T cells *in vivo* using both NALM6 and SEM B-ALL cell lines

(A) Scheme of the experimental design. NSG mice (n = 6/group) were intra-BM transplanted with 1 × 10^5 Luc-expressing NALM6 or SEM cells. Four days later, 4 × 10^6 Mock-CAR, CD19-CAR, or Tan(S)-CAR T cells were i.v. injected. Leukemic burden was monitored weekly by BLI. Mice were sacrificed and FACS analyzed for leukemic burden and T cell persistence when Mock-treated mice were fully leukemic by BLI. (B) IVIS imaging of NALM6 leukemic burden monitored by BLI at the indicated time points. (C) Average radiance quantification (p/sec/cm^2/sr) for NALM6 at the indicated time points. (D) NALM6 leukemic burden quantified by FACS in BM and PB at sacrifice of mice treated with Mock-CAR, CD19-CAR, and Tan(S)-CAR, respectively. Each dot represents a mouse. (E) Representative FACS plots showing NALM6 cells (blue) and T cell persistence (red) in BM at sacrifice of mice treated with Mock-CAR, CD19-CAR, and Tan(S)-CAR, respectively. (F–I) Identical analysis to (B)–(E) for SEM target cells. Data are shown as means ± SEMs. *p < 0.05, ***p < 0.001, ****p < 0.0001; 1-way ANOVA with the Tukey post hoc test.

increased over time in this group of CD19-CAR-treated mice (Figure 5C). In contrast, leukemic cells in PB were observed in only one mouse treated with Tan(S)-CAR 13 weeks after CAR T cell infusion (Figure 5C). Importantly, T cell persistence in PB was observed throughout the 13 weeks for both CAR-19 and Tan(S)-CAR T cells (Figure 5C). Accordingly, the disease-free survival (DFS) for Tan(S)-CAR-treated mice at week 13 was double that of CD19-CAR-treated mice (86% versus 43%; p = 0.08; Figure 5D). Detailed BM analysis at the endpoint confirmed that 4 of 7 (57%) of the CD19-CAR-treated mice and only 1 of 7 (14%) of the Tan(S)-CAR-treated mice presented leukemic cells (>1%) (Figure 5E). Of note, FACS analysis of the BM revealed a diminished expression of CD19 in some cells in 1 of 4 mice (25%) that relapsed after CD19-CAR T cell infusion (Figure 5E). Our pre-clinical results suggest that simultaneous targeting of CD22 and CD19 may have a longer therapeutic effect in B-ALL patients.

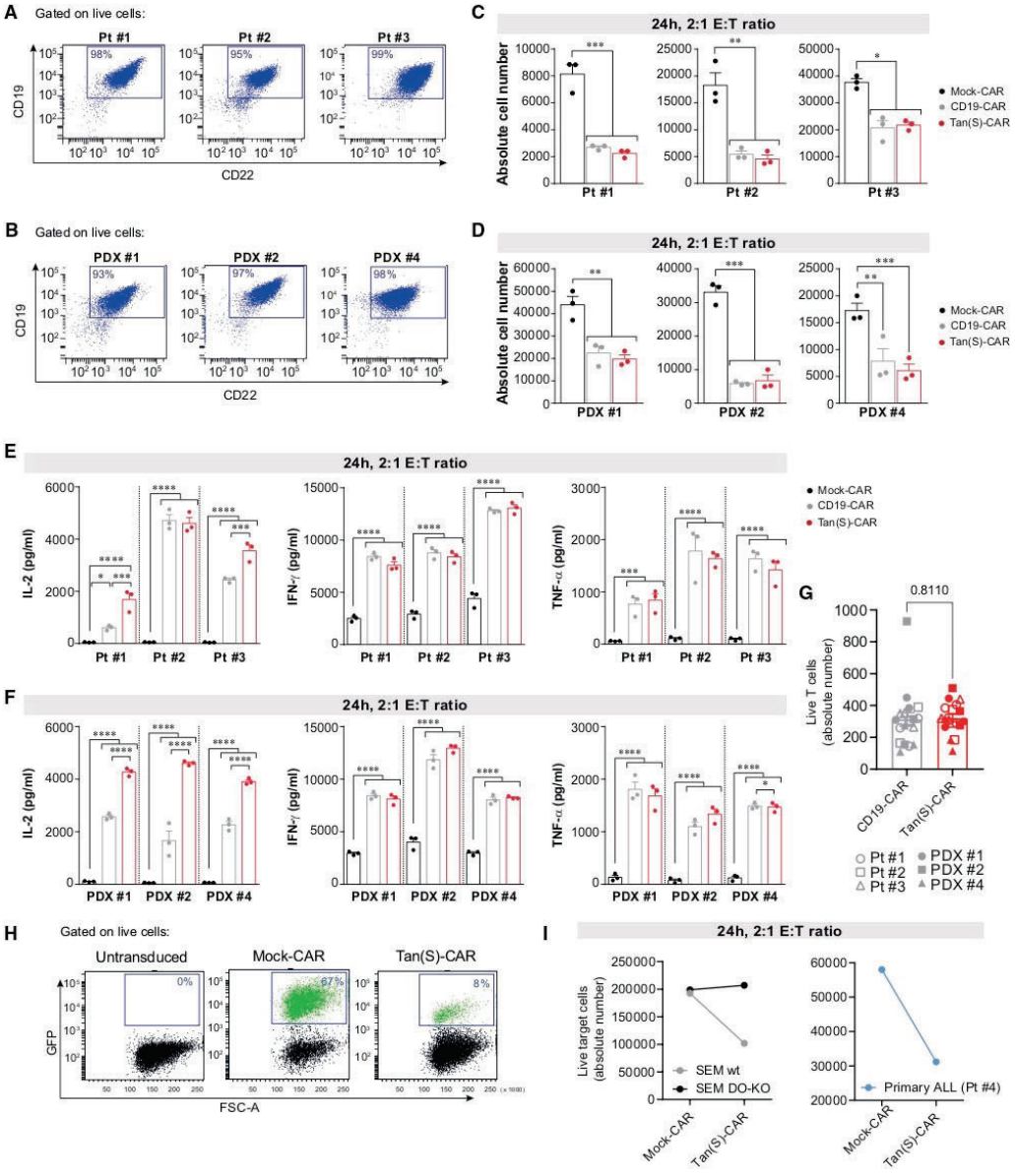

Figure 4. Tan(S)-CAR T cells eliminate primary and PDX B-ALL cells *in vitro*

(A and B) CD22 and CD19 FACS expression in primary B-ALL blasts (n = 3) (A) and B-ALL PDX cells (n = 3) (B). (C and D) Absolute number of live primary B-ALL blasts (C) and B-ALL PDX cells (D) after 24-h incubation with the indicated CAR T cells at 2:1 E:T ratio. (E and F) Production of the pro-inflammatory cytokines IL-2, IFN-γ, and TNF-α by the indicated CAR T cells after 24-h exposure to either primary B-ALL blasts (E) or B-ALL PDX cells (F) at 2:1 E:T ratio. PBMCs from n = 3 independent HDs. (G) Absolute number

(legend continued on next page)

Finally, to explore further the *in vivo* bispecificity of the Tan(S)-CAR in a clinically relevant model of CD19 or CD22 resistance, we next assessed the ability of the Tan(S)-CAR to control $CD19^{-}CD22^{+}$ and $CD19^{+}CD22^{-}$ B-ALL cells *in vivo*. We used both SEM CD19-KO and SEM CD22-KO as well as $CD19^{-}$ primary B-ALL cells from a patient relapsed after CD19-CAR treatment (Pt#5). Tan(S)-CAR T cells fully controlled the *in vivo* growth of SEM CD22-KO and partially that of SEM CD19-KO (Figures 6A and 6B). Strikingly, we observed a fully eradication of the *in vivo* growth of $CD19^{-}CD22^{+}$ primary B-ALL cells (Figure 6C) in mice infused with Tan(S)-CAR and CD22-CAR T cells (Figure 6D). The experiment was terminated at day 49 due to graft-versus-host disease associated with a high number of human T cells in PB and BM (data not shown). These results demonstrate the *in vivo* bispecificity of the Tan(S)-CAR presented in this work, positioning it as an effective asset for clinical translation.

DISCUSSION

CD19-CAR T cells have produced unprecedented results in multiple clinical trials.[6,28] However, only one CD19-CAR T cell product is currently approved in Europe and the United States for the treatment of R/R B-ALL in patients younger than 25 years old, tisagenlecleucel (Kymriah). The long-term follow-up of CD19-CAR-treated patients shows that the durability of the response is limited and relapse rates are ~50% after 12–18 months.[6,8,28] Relapse is likely not unique to therapeutic approaches targeting CD19, as it was also observed with other agents targeting CD22.[12,14] Poor CAR T cell persistence and/or leukemic cell resistance resulting from Ag loss or modulation are among the most common limitations of single targeted CAR T cell therapies,[9,17] and guide the search for innovative CAR T cell approaches.

Activation and exponential expansion of CAR T cells following infusion are essential for successful clinical responses.[29,30] In fact, leukemia recurrence after CAR T cell therapy, especially when occurring a few months after achieving initial complete response, is often associated with limited CAR T cell persistence. Accordingly, strategies to improve CAR T cell persistence independently of the CAR T cell design and manufacturing process are being tested clinically.[29,30] Early relapse with Ag^{+} disease and loss of CAR T cell persistence presents a potential opportunity for the reinfusion of CAR T cells. However, later relapses are frequently associated with either loss of the target Ag or biological resistance to the CD19-directed CAR. Established mechanisms of the loss of CD19 expression include alternative splicing, low Ag density, epitope masking, interruption in the transport of CD19 to the cell surface, and cell lineage switching.[9,10,17] Of note, rather than a complete Ag loss, partial Ag loss due to downregulation has been reported in patients treated with CD22-CAR T cells.[12]

CAR T cells against single Ags are likely insufficient for effective and durable (years) long-term antileukemic responses due to CAR-mediated immune pressure and patient-specific intrinsic vulnerabilities to CAR resistance. Of note, previous administration of inotuzumab ozogamicin, a toxic-conjugated anti-CD22 mAb clinically used to induce complete remission in relapsing B-ALL patients, has been suggested to limit/impair the subsequent expansion of autologous CD19-CAR T cells.[31] For this reason, CAR constructs incorporating multi-Ag targeting are being investigated to allow simultaneous co-targeting of more than a single Ag, extending the activity of CAR T cells to several phenotypic subpopulations of the disease. This can be achieved by (1) generating two or more T cell products, each one expressing different CARs and infusing them together or sequentially (co-administration); (2) using a bicistronic vector that encodes two different CARs on the same cell (bicistronic CAR T cells); (3) simultaneously engineering T cells with two different CAR constructs (co-transduction), which will generate three CAR T subsets consisting of dual and single CAR-expressing cells; or (4) encoding two Ag-recognizing scFvs on the same chimeric protein using a single vector (Tan-CAR T cells), which will mediate T cell activation in response to either one of the two target Ags.[17] Importantly, there is evidence that pooled infusions of single CARs are inferior to Tan-CARs or dual CARs in preclinical models,[20,32] and that Tan-CARs can induce additive cytokine secretion upon encounter of both targets simultaneously, boosting antitumor efficacy with an enhancement of the immune synapse.[20]

In B cell malignancies, targeting pan-B Ags beyond CD19, such as CD20 and CD22, has the advantage of low cumulative risk of on-target off-tumor toxicity. In this line, two preclinical studies with bispecific CARs for B-ALL—CD22/CD19-CAR or CD20/CD19-CAR—have reported *in vitro* and *in vivo* eradication of PDX or primary B-ALL cells.[12,33] Based on this encouraging preclinical data, several clinical trials with Tan-CARs are under way for B-ALL.[9,21] Preliminary data from a Phase I clinical trial with a CD22/CD19-CAR demonstrate that CD22/CD19-CAR T cell therapy is safe and mediates a robust antileukemic activity in patients with R/R B-ALL; however, relapse occurred in three of six enrolled patients: two patients as $CD19^{+}CD22^{+}$ and one patient as $CD19^{-}CD22^{low}$.[34] Follow-up data on clinical trials with different Tan-CARs are still limited, but in the future, they will help inform whether dual-Ag-targeted approaches are sufficient to prevent/delay disease relapse and whether targeting more than one Ag will be an effective strategy for enhancing clinical outcomes.

Developing functional multitargeted constructs is no easy task, as acknowledged by Qin and colleagues.[35] In our drive to improve CD19-CAR T cell therapy for B-ALL, we developed a Tan-CAR to simultaneously target CD19 and CD22 based on our proprietary single-CAR constructs and the clinical validation of our

of live T cells after 24-h incubation with the indicated primary B-ALL blasts or B-ALL PDX cells at 2:1 E:T ratio. (H and I) Autologous cytotoxicity experiment. Representative FACS plots of CAR T cells produced from MACS-sorted T cells from the PB of a B-ALL patient (Pt #4) showing the transduction efficiency at day 6 (H). Absolute number of live SEM cells (left panel) or live primary B-ALL blasts from the same patient (patient 4) after 24-h incubation with the Tan(S)-CAR T cells at 2:1 E:T ratio (I). Data are shown as means ± SEMs. $^{*}p < 0.05$, $^{**}p < 0.01$, $^{***}p < 0.001$; 2-way ANOVA with the Tukey post hoc test.

Table 1. Clinical and biological features of the primary B-ALL samples used in this study

Sample	Molecular	Disease stage	Blasts, %	Age, years	Gender	CD19 MFI	CD22 MFI
Pt#1	ETV6/RUNX1	diagnosis	90	12	female	9,749	3,848
Pt#2	ETV6/RUNX1	diagnosis	96	5	male	22,826	7,570
Pt#3	ETV6/RUNX1	diagnosis	97	2	male	12,104	3,581
Pt#4	NUP214-ABL1	diagnosis	95	24	male	+	+
Pt#5	PAX5-MLLT3	relapse after CD19-CAR T cell therapy and alloSCT	92	31	male	–	+
PDX#1	high-hyperdiploid	relapse	97	3.5	male	14,963	7,881
PDX#2	low-hypodiploid	diagnosis	97	12	male	25,459	15,192
PDX#3	TCF3-PBX1	diagnosis	98	7	female	4,510	2,028
PDX#4	high-hyperdiploid	diagnosis	92	2.5	male	15,554	6,167

alloSCT, allogenic stem cell transplantation; MFI, mean fluorescence intensity.

CD19-CAR.[15,22–25] We compared two versions of Tan-CARs *in vitro* and we observed that both had similar antileukemic activity and cytokine production. However, transduction efficiencies with the Tan-CAR carrying a longer scFv linker (Tan(L)-CAR) were lower due to size constraints, and T cells transduced with this Tan(L)-CAR displayed a lower proliferation; therefore, the Tan(S)-CAR was selected for further characterization and comparison with CD19-CAR. The different functionality between the structure of our Tan(S)-CAR and those LoopTan-CARs previously reported by Qin et al.[35] may respond to a distinct VH/VL combination, scFv order, length and flexibility/rigidity of the linkers, and extracellular spacer length, which have all been suggested to affect the expression and the activity/potency of Tan-CAR constructs.[33,35,36] In addition, another not minor difference may be the nature of our CD22 scFv that is unique in targeting a distal membrane epitope of CD22.[15] Further configurational studies will reveal the functional differences among the distinct Tan-CARs available.

Demonstration of the ability to bind/recognize target Ags by both scFvs in our Tan(S)-CAR was achieved using human recombinant CD19 and CD22 proteins. *In vitro* pro-inflammatory cytokine release and cytotoxicity activity also established Tan-CAR functionality. Moreover, our results indicate that the Tan(S)-CAR performs as well as the CD19-CAR *in vitro* and *in vivo* against both B-ALL cell lines and patient leukemic cells. Although previous preclinical studies suggested that both scFvs may act synergistically,[18–20] this was not observed in the present study, which concurs with the previous study by Qin and colleagues,[35] suggesting that this effect may be dependent on the Ag/epitope targeted or the affinity/avidity of the scFvs. Similar to Qin and colleagues,[35] our Tan(S)-CAR displayed a potency/efficacy comparable to that of the single CD19-CAR, but slightly less potent/efficient than the single CD22-CAR.[15] An encouraging observation is that the current Tan(S)-CAR seems more effective *in vivo* than a CD19-CAR in controlling the disease in a long-term follow-up B-ALL PDX model. Whether the superior ability of the Tan(S)-CAR to produce IL-2 in the presence of B-ALL primary samples and B-ALL PDXs contributes to this observation needs further investigation. These data fit well with a study by Schneider and colleagues,[36] who observed that a higher ability to produce IL-2 leads to better antileukemia CAR activity in NSG mice. These data indicate that our Tan(S)-CAR warrants a clinical appraisal to test whether simultaneous targeting of CD19 and CD22 Ags offers more durable clinical responses with reduced risk of Ag loss than the standard-of-care CD19-CAR approach. In addition, the excellent performance of the Tan(S)-CAR *in vitro* and *in vivo* also positions them as promising assets for clinical translation.

MATERIALS AND METHODS

Reagents, drugs, and antibodies

Advanced DMEM, IMDM, RPMI-1640, L-glutamine, penicillin/streptomycin (P/S), and insulin-transferrin-selenium (ITS) were purchased from GIBCO/Invitrogen (Waltham, MA, USA). StemSpan serum-free expansion medium (SFEM) was purchased from STEMCELL Technologies (Vancouver, Canada). Phosphate-buffered saline was purchased from Merck Life Science SL (Darmstadt, Germany). Human (h) stem cell factor (SCF), hFMS-like tyrosine kinase 3 ligand (FLT3-L), hIL-3, hIL-7, and hIL-15 were purchased from Miltenyi Biotec (Bergisch Gladbach, Germany). Fetal bovine serum (FBS) was purchased from Sigma-Aldrich (St. Louis, MO, USA). Anti-CD3 (OKT3) and anti-CD28 (CD28.2) mAbs, 7-amino-actinomycin D (7-AAD), and fluorescein isothiocyanate (FITC)-, phycoerythrin (PE)-, peridin chlorophyll (PerCP)-, allophycocyanin (APC)-, phycoerythrin/cyanine7 (PE/Cy7)-, Brilliant Violet 421 (BV421)-, and BV510-conjugated mAbs specific for human CD3 (SK7), CD19 (HIB19), CD22 (HIB22), CD10 (HI10a), CD13 (WM15), CD45 (HI30), HLA-ABC (G46-2.6), CD25 (M-A251), CCR7 (150503), CD27 (L128), CD45RO (UCHL1), LAG3 (T47-530), TIM3 (7D3), PD-1 (MIH4), and isotype-matched negative control mAbs, were purchased from BD Biosciences (Franklin Lakes, NJ, USA), CD69 (REA824) from Miltenyi Biotec, and anti-His (J095G46) from BioLegend (San Diego, CA, USA).

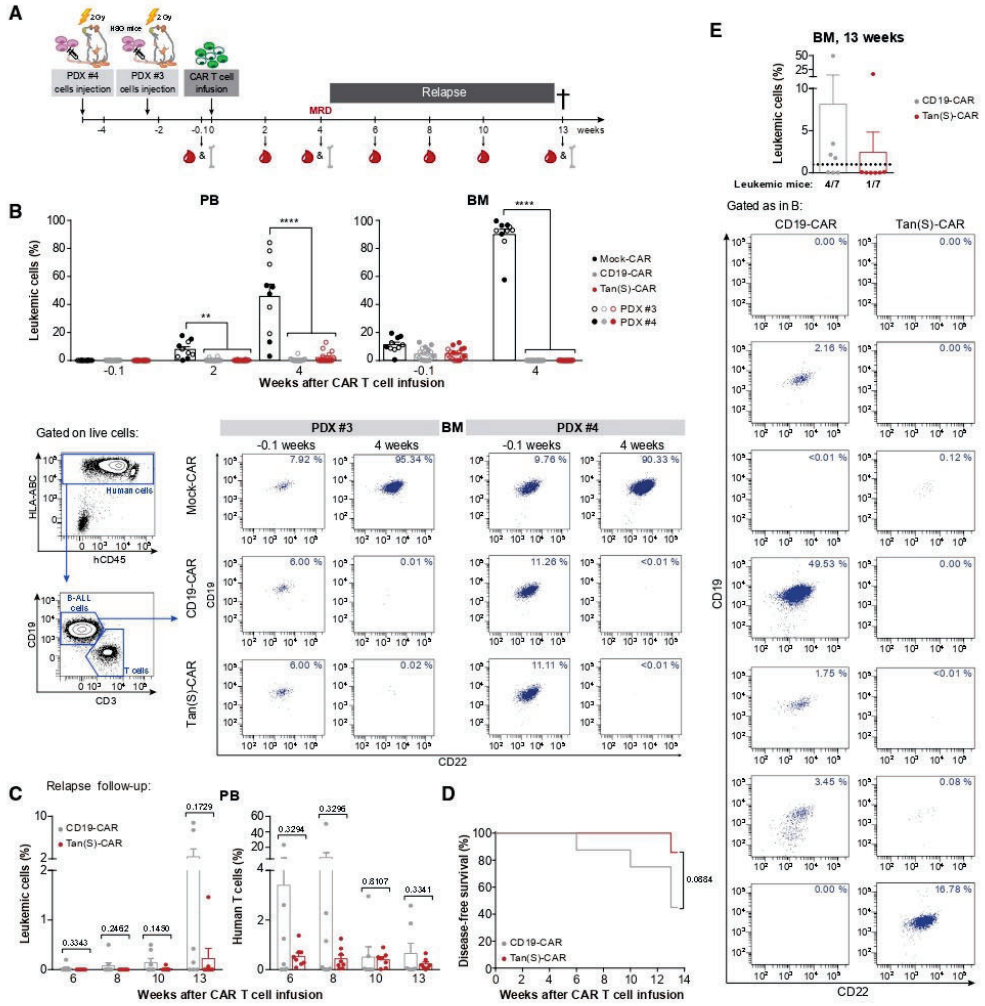

Figure 5. Tan(S)-CAR is very effective in controlling the disease in a long-term follow-up B-ALL PDX model

(A) Scheme showing the experimental design. NSG mice (n = 5–9/group) were i.v. transplanted with 0.5×10^6 or 1×10^6 of B-ALL cells from PDX#3 or PDX#4, respectively. Upon B-ALL engraftment detectable in BM, mice were randomized, and 5×10^6 Mock-CAR, CD19-CAR, or Tan(S)-CAR T cells were i.v. injected. Leukemic burden and CAR T cell persistence was monitored in PB biweekly by FACS. BM aspirates were FACS analyzed when Mock-treated mice were sacrificed (week 4) and at the endpoint (week 13). (B) Upper panels, leukemic burden in PB and BM at the indicated time points after CAR T cell infusion. Bottom panels, representative BM FACS analysis showing CD19 and CD22 expression for both PDXs before CAR T cell infusion (1 day before CAR T cell infusion [−0.1]) and at the time Mock-treated mice were sacrificed (week 4). The gating strategy is shown on the left. Indicated percentages are referred to the total live single cells in each sample. The complete gating strategy is shown in Figure S1B. (C) Follow-up at the indicated time points after CAR T cell infusion of leukemic progression/relapse (left panel) and persistent T cells (right panel) of CD19-CAR-treated versus Tan(S)-CAR-treated mice transplanted with PDX#4 (n = 7 mice/group). (D) DFS curves for CD19-CAR-treated versus Tan(S)-CAR-treated mice transplanted with PDX#4. The log-rank (Mantel-Cox) test was used to calculate significance. (E) Leukemic burden at sacrifice/endpoint (week 13 after CAR T cell infusion) in BM from CD19-CAR-treated versus Tan(S)-CAR-treated mice transplanted with PDX#4 (n = 7 mice/group). A mouse is considered in relapse when the percentage of blasts in BM is >1% (horizontal dotted line) or >0.1% in PB. Each dot represents a mouse. The bottom panels show the expression of CD19 and CD22 by FACS analysis of B-ALL cells for each independent CD19-CAR-treated and Tan(S)-CAR-treated mouse. Indicated percentages are referred to the total live single cells in each sample. The complete gating strategy is shown in Figure S1B. Data are shown as means ± SEMs. $^{**}p < 0.01$, $^{***}p < 0.001$, $^{****}p < 0.0001$; 1-way ANOVA with the Tukey post hoc test. See also Figure S1.

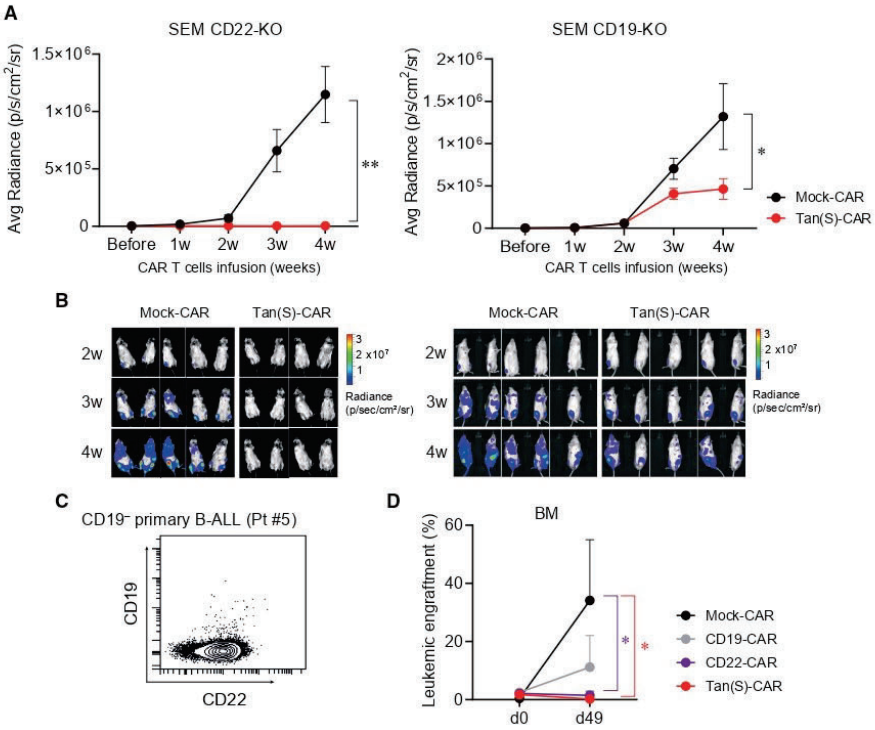

Figure 6. *In vivo* bispecificity of Tan(S)-CAR T cells

(A) Average radiance quantification (p/sec/cm^2/sr) from mice transplanted with SEM CD22-KO (n = 4–5/group) or SEM CD19-KO (n = 9–10/group) at the indicated time points after Mock- or Tan(S)-CAR T cell infusion. Data from n = 2 independent experiments. (B) Representative BLIs of SEM CD22-KO- and SEM CD19-KO-transplanted mice from week 2 to week 4 after CAR T cell infusion. (C) CD19 and CD22 expression of the CD19$^-$CD22$^+$ blasts from the B-ALL patient (Pt#5) used for the *in vivo* bispecificity experiment. (D) NSG mice (n = 6/group) were i.v. transplanted with 1 × 10^6 of CD19$^-$CD22$^+$ B-ALL cells (Pt#5). Upon detectable B-ALL engraftment in BM, mice were randomized to receive 5 × 10^6 Mock-CAR, CD19-CAR, CD22-CAR, or Tan(S)-CAR T cells. The leukemic burden in BM before CAR T cell infusion (day 0) and at endpoint of the experiment (day 49) is shown. Data are shown as means ± SEMs. *$p < 0.05$, **$p < 0.01$, 2-way ANOVA (mixed-effects model) with Šídáks multiple comparisons test.

Cell lines

The B-ALL cell lines SEM and NALM6 were obtained from the DSMZ cell line bank (Braunschweig, Germany). Luciferase (Luc)/GFP-expressing NALM6 cells were kindly provided by Prof. R.J. Brentjens (Memorial Sloan Kettering Cancer Center, NY, USA). Stable Luc-expressing SEM cell lines were generated with the lentiviral pUltra-Chili-Luc backbone (Addgene #48688) using a spinfection (centrifugation) protocol, as previously described.[37] Briefly, 1 × 10^6 cells were seeded on a 6-well plate with 1.2 mL viral supernatant. Plates were then centrifuged at 900 × *g* for 1 h at 28°C, after which the plate was placed in an incubator at 37°C for 3 h and fresh media was added. Cells were incubated for an additional 48 h after a medium exchange. Finally, cherry-positive cells were isolated by FACS (>99% purity) and luminescence was checked. CD19-KO, CD22-KO, and double-KO (DO-KO) SEM cells were generated by CRISPR-mediated genome editing. Briefly, 200,000 cells were electroporated (Neon transfector, ThermoFisher Scientific, Waltham, MA, USA) with a Cas9 protein/tracrRNA/crRNA complex (IDT, Coralville, IA, USA). Two guides were designed for each gene: CD19-exon 2.1 CAGGCCTGGGAATCCACATG and CD19-exon 14.1 AGAACA TGGATAATCCCGAT and CD22-exon 3.2 TCAATGACAGTGGT CAGCTG and CD22-exon 9 CAGGTGTAGTGGGAGACGGG. Cells were allowed to recover after electroporation, and CD19$^-$ or CD22$^-$ cells were isolated by FACS sorting (>99% purity).[15]

Human samples

PB mononuclear cells (PBMCs) were isolated from buffy coats of HDs by Ficoll-Hypaque gradient centrifugation (GE Healthcare, Chicago, IL, USA).[38] Buffy coats were obtained from the Catalan Blood and Tissue Bank upon institutional review board approval (HCB/2018/0030). BM aspirates were obtained from five B-ALL patients (Table 1). Human samples were obtained after written informed consent

the reappearance of blasts in either PB (>0.1%) or BM (>1%) after complete remission.

Statistical analysis

Data were plotted as means ± SEMs. One-way analysis of variance with Tukey's post hoc test was used unless stated otherwise. All of the analyses were performed with Prism software, version 8.0 (GraphPad Prism Software, San Diego, CA, USA).

SUPPLEMENTAL INFORMATION

Supplemental information can be found online at https://doi.org/10.1016/j.ymthe.2021.08.033.

ACKNOWLEDGMENTS

We thank Dr. Meritxell Vinyoles for technical support and Dr. Maksim Mamonkin, who kindly provided the SFG retroviral backbone. We thank CERCA/Generalitat de Catalunya and Fundació Josep Carreras-Obra Social la Caixa for core support. Financial support for this work was obtained from the European Research Council (CoG-2014-646903, PoC-2018-811220), the Spanish Ministry of Economy and Competitiveness (SAF2016-80481R, PID2019-108160RB-I00), the Health Institute Carlos III (ISCIII/FEDER, PI17/01028, PI20/00822, to C.B.), the Fundación Uno entre Cienmil, the Obra Social La Caixa (LCF/PR/HR19/52160011), the Leo Messi Foundation, and the "Heroes hasta la médula" initiative to P.M. S.R.Z. and T.V.-H. were supported by Marie Skłodowska Curie Fellowships (GA795833 and GA792923, respectively). D.S.-M. and R.T.-R. were supported by postdoctoral fellowships from ISCIII (Sara Borrell) and the Spanish Association against Cancer (AECC), respectively.

AUTHOR CONTRIBUTIONS

S.R.Z. conceived the study, designed and performed the experiments, analyzed and interpreted the data, prepared the figures, and wrote the manuscript. T.V.-H. designed and performed the experiments, analyzed and interpreted the data, prepared the figures, and wrote the manuscript. F.G.-A., V.M.D., P.A.R., H.R.-H., D.S.-M., N.T., M.L.B., P.P., and R.T.-R. performed the experiments. O.M., A.B., J.L.F., P.B., M.J., and I.J. provided the human primary samples and PDXs. C.B. supported the study technically and financially. P.M. conceived the study, designed the experiments, interpreted the data, wrote the manuscript, and financially supported the study.

DECLARATION OF INTERESTS

S.R.Z., T.V.-H., F.G.-A., D.S.-M., and P.M. are inventors of a CD22scFv pending European patent (file no. 20382175.6). P.M. is the co-founder of OneChain Immunotherapeutics (OCI). V.M.D. is employed by OCI.

REFERENCES

1. Katz, A.J., Chia, V.M., Schoonen, W.M., and Kelsh, M.A. (2015). Acute lymphoblastic leukemia: an assessment of international incidence, survival, and disease burden. Cancer Causes Control *26*, 1627–1642.
2. Gavralidis, A., and Brunner, A.M. (2020). Novel Therapies in the Treatment of Adult Acute Lymphoblastic Leukemia. Curr. Hematol. Malig. Rep. *15*, 294–304.
3. Capitini, C.M. (2018). CAR-T immunotherapy: how will it change treatment for acute lymphoblastic leukemia and beyond? Expert Opin. Orphan Drugs *6*, 563–566.
4. Waldman, A.D., Fritz, J.M., and Lenardo, M.J. (2020). A guide to cancer immunotherapy: from T cell basic science to clinical practice. Nat. Rev. Immunol. *20*, 651–668.
5. Scheuermann, R.H., and Racila, E. (1995). CD19 antigen in leukemia and lymphoma diagnosis and immunotherapy. Leuk. Lymphoma *18*, 385–397.
6. Rafei, H., Kantarjian, H.M., and Jabbour, E.J. (2019). Recent advances in the treatment of acute lymphoblastic leukemia. Leuk. Lymphoma *60*, 2606–2621.
7. Aldoss, I., Bargou, R.C., Nagorsen, D., Friberg, G.R., Baeuerle, P.A., and Forman, S.J. (2017). Redirecting T cells to eradicate B-cell acute lymphoblastic leukemia: bispecific T-cell engagers and chimeric antigen receptors. Leukemia *31*, 777–787.
8. Ruella, M., and Maus, M.V. (2016). Catch Me If You Can: Leukemia Escape after CD19-Directed T Cell Immunotherapies. Comput. Struct. Biotechnol. J. *14*, 357–362.
9. Shah, N.N., and Fry, T.J. (2019). Mechanisms of resistance to CAR T cell therapy. Nat. Rev. Clin. Oncol. *16*, 372–385.
10. Song, M.K., Park, B.B., and Uhm, J.E. (2019). Resistance Mechanisms to CAR T-Cell Therapy and Overcoming Strategy in B-Cell Hematologic Malignancies. Int. J. Mol. Sci. *20*, E5010.
11. Nitschke, L. (2009). CD22 and Siglec-G: B-cell inhibitory receptors with distinct functions. Immunol. Rev. *230*, 128–143.
12. Fry, T.J., Shah, N.N., Orentas, R.J., Stetler-Stevenson, M., Yuan, C.M., Ramakrishna, S., Wolters, P., Martin, S., Delbrook, C., Yates, B., et al. (2018). CD22-targeted CAR T cells induce remission in B-ALL that is naive or resistant to CD19-targeted CAR immunotherapy. Nat. Med. *24*, 20–28.
13. Haso, W., Lee, D.W., Shah, N.N., Stetler-Stevenson, M., Yuan, C.M., Pastan, I.H., Dimitrov, D.S., Morgan, R.A., FitzGerald, D.J., Barrett, D.M., et al. (2013). Anti-CD22-chimeric antigen receptors targeting B-cell precursor acute lymphoblastic leukemia. Blood *121*, 1165–1174.
14. Pan, J., Niu, Q., Deng, B., Liu, S., Wu, T., Gao, Z., Liu, Z., Zhang, Y., Qu, X., Zhang, Y., et al. (2019). CD22 CAR T-cell therapy in refractory or relapsed B acute lymphoblastic leukemia. Leukemia *33*, 2854–2866.
15. Velasco-Hernandez, T., Zanetti, S.R., Roca-Ho, H., Gutierrez-Aguera, F., Petazzi, P., Sánchez-Martínez, D., Molina, O., Baroni, M.L., Fuster, J.L., Ballerini, P., et al. (2020). Efficient elimination of primary B-ALL cells in vitro and in vivo using a novel 4-1BB-based CAR targeting a membrane-distal CD22 epitope. J. Immunother. Cancer *8*, e000896.
16. Navai, S.A., and Ahmed, N. (2016). Targeting the tumour profile using broad spectrum chimaeric antigen receptor T-cells. Biochem. Soc. Trans. *44*, 391–396.
17. Shah, N.N., Maatman, T., Hari, P., and Johnson, B. (2019). Multi Targeted CAR-T Cell Therapies for B-Cell Malignancies. Front. Oncol. *9*, 146.
18. Grada, Z., Hegde, M., Byrd, T., Shaffer, D.R., Ghazi, A., Brawley, V.S., Corder, A., Schönfeld, K., Koch, J., Dotti, G., et al. (2013). TanCAR: A Novel Bispecific Chimeric Antigen Receptor for Cancer Immunotherapy. Mol. Ther. Nucleic Acids *2*, e105.
19. Hegde, M., Corder, A., Chow, K.K., Mukherjee, M., Ashoori, A., Kew, Y., Zhang, Y.J., Baskin, D.S., Merchant, F.A., Brawley, V.S., et al. (2013). Combinational targeting offsets antigen escape and enhances effector functions of adoptively transferred T cells in glioblastoma. Mol. Ther. *21*, 2087–2101.
20. Hegde, M., Mukherjee, M., Grada, Z., Pignata, A., Landi, D., Navai, S.A., Wakefield, A., Fousek, K., Bielamowicz, K., Chow, K.K., et al. (2016). Tandem CAR T cells targeting HER2 and IL13Rα2 mitigate tumor antigen escape. J. Clin. Invest. *126*, 3036–3052.
21. Zhao, J., Song, Y., and Liu, D. (2019). Clinical trials of dual-target CAR T cells, donor-derived CAR T cells, and universal CAR T cells for acute lymphoid leukemia. J. Hematol. Oncol. *12*, 17.
22. Castella, M., Boronat, A., Martín-Ibáñez, R., Rodríguez, V., Suñé, G., Caballero, M., Marzal, B., Pérez-Amill, L., Martín-Antonio, B., Castaño, J., et al. (2018). Development of a Novel Anti-CD19 Chimeric Antigen Receptor: A Paradigm for an Affordable CAR T Cell Production at Academic Institutions. Mol. Ther. Methods Clin. Dev. *12*, 134–144.
23. Castella, M., Caballero-Baños, M., Ortiz-Maldonado, V., González-Navarro, E.A., Suñé, G., Antoñana-Vidósola, A., Boronat, A., Marzal, B., Millán, L., Martín-

in accordance with the Declaration of Helsinki. All of the experimental studies were approved by the institutional review board of the Ethics Committee on Clinical Research of the Clinic Hospital of Barcelona (HCB/2017/0781).

CD19-CAR and CD22/CD19 Tan-CAR vector, lentiviral production, T cell transduction, activation, and expansion

CAR Ag-binding domain (scFv) sequences were derived from the mouse hybridoma A3B1 for CD19[22,23,25] and hCD22.7 for CD22.[15] We used a clinically validated pCCL second-generation lentiviral CD19-CAR backbone, which contains the A3B1 scFv, the hinge and human CD8 TM domain, and human 4-1BB and CD3ζ endodomains.[22–24,26,27] Two second-generation lentiviral bispecific, tandem CD22/CD19-CARs were designed and referred to as Tan(S)- and Tan(L)-CARs; these included the hCD22.7 scFv and the A3B1 scFv linked in sequence by a flexible $(glycine_4serine)_{4-7}$ interchain linker, followed by the hinge and the human CD8 TM domain and the human 4-1BB and CD3ζ endodomains. Constructs S and L differ only in the length of the flexible interchain linker sequence connecting the anti-CD22 scFv and the anti-CD19 scFv (Figure 1A). An identical lentiviral vector with the CD8 TM-4-1BB-CD3ζ domains linked to a His-Tag (Mock-CAR) was used as an experimental control.[15] All of the CARs were fused to a GFP reporter gene by a 2A ribosomal skip sequence (T2A) at the C-terminal CAR sequence, for tracing the transduction efficiency and CAR expression.

CAR-expressing viral particles pseudotyped with VSV-G were generated by the transfection of HEK293T cells with pCCL, VSV-G, and psPAX2 vectors using polyethylenimine (Polysciences Inc., Warrington, PA, USA). Supernatants were collected at 48 and 72 h after transfection and concentrated by ultracentrifugation following the standard procedure. T cells were activated by plate coating with anti-CD3 and anti-CD28 mAbs (1 μg/mL) in complete RPMI medium for 2 days, and were then transduced with a CAR-expressing lentivirus at a multiplicity of infection of 10 in the presence of hIL-7 and hIL-15 (10 ng/mL).[15,24,26,27] T cells from a B-ALL patient were purified using anti-hCD3 magnetic beads (Miltenyi Biotec) by AutoMACs according to the manufacturer's instructions. T cells were expanded in complete RPMI medium plus hIL-7 and hIL-15 for up to 5–7 days. CAR transduction efficiency in T cells was analyzed by FACS. Vector copy number (VCN) was determined by quantitative PCR using Light Cycler 480 SYBRGreen I Master (Roche, Basel, Switzerland), as in Ortiz-Maldonado et al.[25] Briefly, pairs of primers were designed against GATA2 (control gene, GATA2_F: 5′tggcgcacaactacatggaa3′; GATA2_R: 5′cgagtcgaggtgattgaagaaga3′) and WPRE sequence (part of the provirus WPRE_F: 5′gtcctttcca tggctgctc3′; WPRE_R: 5′ccgaagggacgtagcaga3′). Absolute quantification method was used to determine the VCN/genome. VCN results were adjusted to the percentage of transduction of each CAR determined by FACS analysis. The same cassettes of CD19-CAR and Tan(S)-CAR were cloned into the SFG retroviral backbone kindly provided by Dr. Maksim Mamonkin, and retrovirus production and transduction were performed following standard procedures.[39]

CAR surface detection

Cell surface expression of Mock-CAR was confirmed by binding to anti-His-APC. Cell surface expression of the CD19-CAR and Tan-CARs was confirmed by binding to an AffiniPure $F(ab')_2$ fragment goat anti-mouse IgG (H+L)-APC and an anti-human IgG (H+L)-PE (both from Jackson ImmunoResearch, Westgrove, PA, USA) after prior incubation with human recombinant CD19-Fc (R&D Systems, Abingdon, UK). Tan-CARs were also confirmed by binding to an anti-His-APC after prior incubation with human recombinant CD22-His (ThermoFisher Scientific).

In vitro CAR T cell cytotoxicity assays and cytokine release determination

Target cells (B-ALL cell lines, primary B-ALL cells, and B-ALL PDXs cells; 1×10^5 target cells/well) were incubated with Mock-, CD19-, or Tan-CAR T cells at different E:T ratios for the indicated time periods. Cell lines were cultured in complete RPMI medium and primary cells/PDXs were cultured in StemSpan SFEM supplemented with 20% heat-inactivated FBS, P/S, ITS, hSCF (100 ng/mL), hFLT3-L (100 ng/mL), hIL-3 (10 ng/mL), and hIL-7 (10 ng/mL). At each time point, cells were collected, washed, and stained with anti-CD3, anti-CD19, anti-CD10, and anti-CD22 mAbs, and 7-AAD. CAR T cell-mediated cytotoxicity was determined by analyzing the residual living ($7\text{-AAD}^-\text{CD3}^-\text{GFP}^-\text{CD10}^+$) target cells at each time point and E:T ratio (Figure S1A). BD TruCount absolute count tubes (BD Biosciences) were used for absolute cell counting. The quantification of IL-2, IFN-γ, and TNF-α was measured by enzyme-linked immunosorbent assay (ELISA) using the OptEIA Human ELISA Kit (BD Biosciences) on supernatants harvested after 1–2 days of co-culture at a 1:1 E:T ratio. ELISA determinations were performed in triplicate.

In vivo CAR T cell-mediated cytotoxicity assay with B-ALL cell lines and PDX samples

Ten-week-old non-obese diabetic (NOD) Cg-$Prkdc^{scid}$ $Il2rg^{tm1Wjl}$/SzJ (NSG) mice (The Jackson Laboratory, Bar Harbor, ME, USA) were bred and housed under pathogen-free conditions. Animal experimentation procedures were approved by the local ethics committee (HRH-17-0029-P1). For B-ALL cell lines, NSG mice were i.t. injected with 1×10^5 of either NALM6-Luc^+ cells or SEM-Luc^+ cells[24], followed 4 days later by an i.v. infusion of 4×10^6 CAR T cells. Mice were followed up weekly by BLI using an *in vivo* imaging system (IVIS, Lumina III; Perkin-Elmer, Waltham, MA, USA). Mice were sacrificed at day 14 (NALM6-injected mice) and day 35 (SEM-injected mice), and PB and BM samples were collected and analyzed by FACS to assess leukemic burden and CAR T cell persistence.

For PDXs, $0.5–1.0 \times 10^6$ PDX B-ALL cells were i.v. injected in sublethally irradiated (2 Gy) NSG mice, followed by i.v. infusion of 5×10^6 CAR T cells at the indicated time points. B-ALL engraftment was monitored in PB every other week, and BM aspirates were analyzed 4 weeks after CAR T cell infusion and at sacrifice by FACS. MRD− was defined as <0.1% BM blasts (identified as $CD45^+$HLA-ABC^+ $CD3^-GFP^-CD10^+$ by FACS) (Figure S1B). Relapse was defined as

Antonio, B., et al. (2020). Point-Of-Care CAR T-Cell Production (ARI-0001) Using a Closed Semi-automatic Bioreactor: Experience From an Academic Phase I Clinical Trial. Front. Immunol. *11*, 482.

24. Zanetti, S.R., Romecin, P.A., Vinyoles, M., Juan, M., Fuster, J.L., Cámos, M., Querol, S., Delgado, M., and Menendez, P. (2020). Bone marrow MSC from pediatric patients with B-ALL highly immunosuppress T-cell responses but do not compromise CD19-CAR T-cell activity. J. Immunother. Cancer *8*, e001419.

25. Ortiz-Maldonado, V., Rives, S., Castella, M., Alonso-Saladrigues, A., Benitez-Ribas, D., Caballero-Banos, M., Baumann, T., Cid, J., Garcia-Rey, E., Llanos, C., et al. (2021). CART19-BE-01: A Multicenter Trial of ARI-0001 Cell Therapy in Patients with CD19(+) Relapsed/Refractory Malignancies. Mol. Ther. *29*, 636–644.

26. Baroni, M.L., Sanchez Martinez, D., Gutierrez Aguera, F., Roca Ho, H., Castella, M., Zanetti, S.R., Velasco Hernandez, T., Diaz de la Guardia, R., Castaño, J., Anguita, E., et al. (2020). 41BB-based and CD28-based CD123-redirected T-cells ablate human normal hematopoiesis in vivo. J. Immunother. Cancer *8*, e000845.

27. Sánchez-Martínez, D., Baroni, M.L., Gutierrez-Agüera, F., Roca-Ho, H., Blanch-Lombarte, O., González-García, S., Torrebadell, M., Junca, J., Ramírez-Orellana, M., Velasco-Hernández, T., et al. (2019). Fratricide-resistant CD1a-specific CAR T cells for the treatment of cortical T-cell acute lymphoblastic leukemia. Blood *133*, 2291–2304.

28. Sermer, D., and Brentjens, R. (2019). CAR T-cell therapy: Full speed ahead. Hematol. Oncol. *37* (*Suppl 1*), 95–100.

29. Maude, S.L., Frey, N., Shaw, P.A., Aplenc, R., Barrett, D.M., Bunin, N.J., Chew, A., Gonzalez, V.E., Zheng, Z., Lacey, S.F., et al. (2014). Chimeric antigen receptor T cells for sustained remissions in leukemia. N. Engl. J. Med. *371*, 1507–1517.

30. Nie, Y., Lu, W., Chen, D., Tu, H., Guo, Z., Zhou, X., Li, M., Tu, S., and Li, Y. (2020). Mechanisms underlying CD19-positive ALL relapse after anti-CD19 CAR T cell therapy and associated strategies. Biomark. Res. *8*, 18.

31. Baruchel, A., Krueger, J., Balduzzi, A., Bittencourt, H., Moerloose, B.D., Peters, C., Bader, P., Buechner, J., Boissel, N., Hiramatsu, H., et al. (2020). Tisagenlecleucel for pediatric/young adult patients with relapsed/refractory B-cell acute lymphoblastic leukemia: preliminary report of B2001X focusing on prior exposure to blinatumomab and inotuzumab, https://eha25-eha.web.indrina.com/abstracts/page/list/5db0358bf4d01d313c664553/programelement/5eb52c8d5275843e2bdece84.

32. Ruella, M., Barrett, D.M., Kenderian, S.S., Shestova, O., Hofmann, T.J., Perazzelli, J., Klichinsky, M., Aikawa, V., Nazimuddin, F., Kozlowski, M., et al. (2016). Dual CD19 and CD123 targeting prevents antigen-loss relapses after CD19-directed immunotherapies. J. Clin. Invest. *126*, 3814–3826.

33. Martyniszyn, A., Krahl, A.C., André, M.C., Hombach, A.A., and Abken, H. (2017). CD20-CD19 Bispecific CAR T Cells for the Treatment of B-Cell Malignancies. Hum. Gene Ther. *28*, 1147–1157.

34. Dai, H., Wu, Z., Jia, H., Tong, C., Guo, Y., Ti, D., Han, X., Liu, Y., Zhang, W., Wang, C., et al. (2020). Bispecific CAR-T cells targeting both CD19 and CD22 for therapy of adults with relapsed or refractory B cell acute lymphoblastic leukemia. J. Hematol. Oncol. *13*, 30.

35. Qin, H., Ramakrishna, S., Nguyen, S., Fountaine, T.J., Ponduri, A., Stetler-Stevenson, M., Yuan, C.M., Haso, W., Shern, J.F., Shah, N.N., and Fry, T.J. (2018). Preclinical Development of Bivalent Chimeric Antigen Receptors Targeting Both CD19 and CD22. Mol. Ther. Oncolytics *11*, 127–137.

36. Schneider, D., Xiong, Y., Wu, D., Nölle, V., Schmitz, S., Haso, W., Kaiser, A., Dropulic, B., and Orentas, R.J. (2017). A tandem CD19/CD20 CAR lentiviral vector drives on-target and off-target antigen modulation in leukemia cell lines. J. Immunother. Cancer *5*, 42.

37. Rodriguez-Perales, S., Torres-Ruiz, R., Suela, J., Acquadro, F., Martin, M.C., Yebra, E., Ramirez, J.C., Alvarez, S., and Cigudosa, J.C. (2016). Truncated RUNX1 protein generated by a novel t(1;21)(p32;q22) chromosomal translocation impairs the proliferation and differentiation of human hematopoietic progenitors. Oncogene *35*, 125–134.

38. Zanetti, S.R., Ziblat, A., Torres, N.I., Zwirner, N.W., and Bouzat, C. (2016). Expression and Functional Role of α7 Nicotinic Receptor in Human Cytokine-stimulated Natural Killer (NK) Cells. J. Biol. Chem. *291*, 16541–16552.

39. Gomes-Silva, D., Srinivasan, M., Sharma, S., Lee, C.M., Wagner, D.L., Davis, T.H., Rouce, R.H., Bao, G., Brenner, M.K., and Mamonkin, M. (2017). CD7-edited T cells expressing a CD7-specific CAR for the therapy of T-cell malignancies. Blood *130*, 285–296.

YMTHE, Volume *30*

Supplemental Information

A novel and efficient tandem CD19- and CD22-directed CAR for B cell ALL

Samanta Romina Zanetti, Talia Velasco-Hernandez, Francisco Gutierrez-Agüera, Víctor M. Díaz, Paola Alejandra Romecín, Heleia Roca-Ho, Diego Sánchez-Martínez, Néstor Tirado, Matteo Libero Baroni, Paolo Petazzi, Raúl Torres-Ruiz, Oscar Molina, Alex Bataller, José Luis Fuster, Paola Ballerini, Manel Juan, Irmela Jeremias, Clara Bueno, and Pablo Menéndez

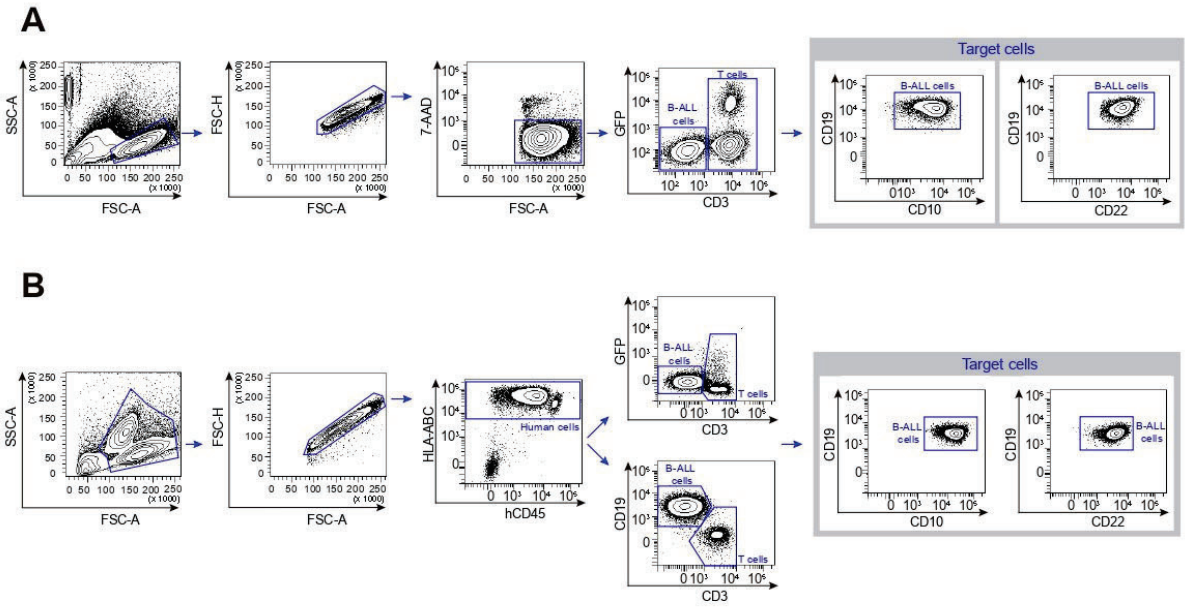

Figure S1. Flow cytometry gating strategies. A) Flow cytometry gating strategy used to analyse *in vitro* CAR T cell cytotoxicity. Doublets were removed from the analysis. Live target cells were identified as 7-AAD^{-}CD3^{-}GFP^{-}CD10^{+}. Then, within this population of cells, we studied the expression of CD19 and CD22. **B)** Flow cytometry gating strategy used to analyse *in vivo* CAR T cell cytotoxicity. Doublets were removed from the analysis. Live target cells were identified as CD45^{+}HLA-ABC^{+}CD3^{-}GFP^{-}CD10^{+}. Then, within this population of cells, we studied the expression of CD10 and CD22. Human T cells were identified as CD45^{+}HLA-ABC^{+}CD3^{+}.

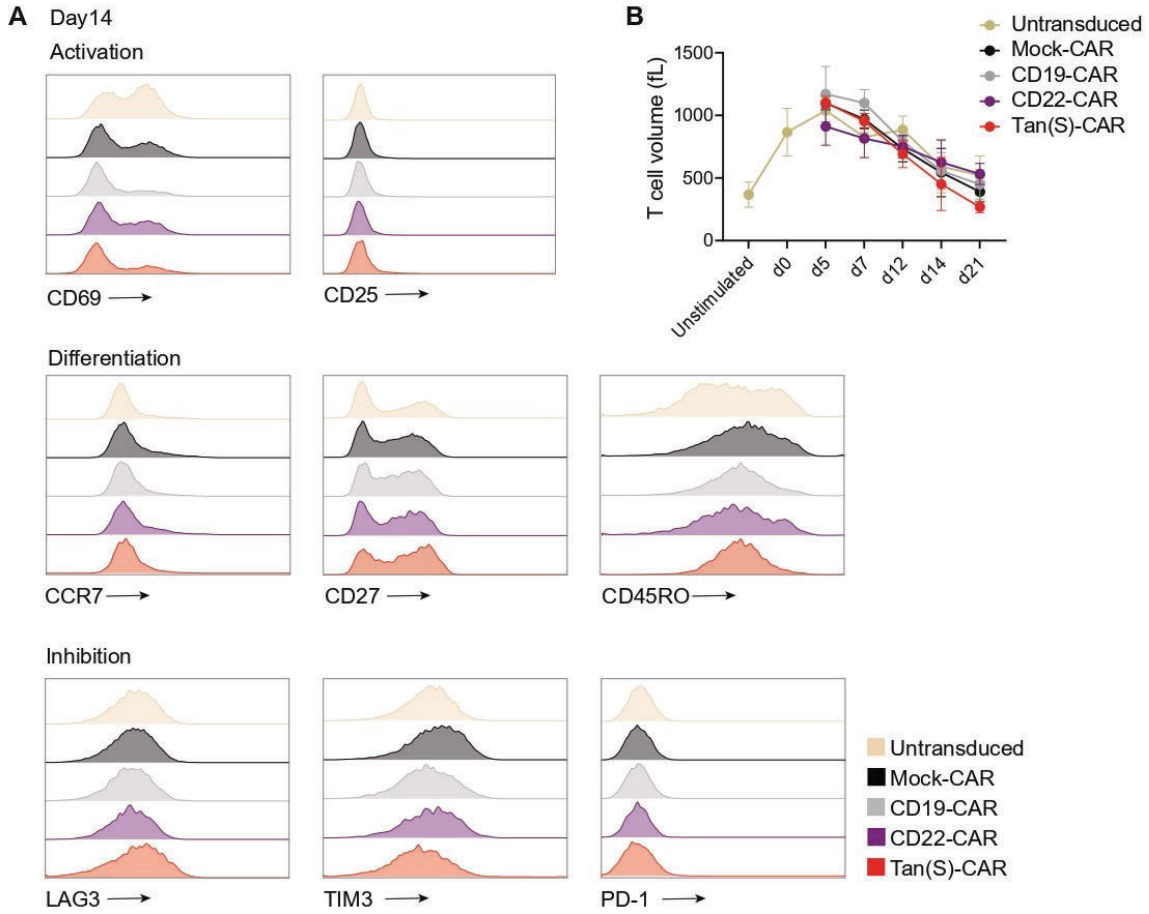

Figure S3. Tan(S)-CAR shows no increased tonic signaling than single CARs, Mock or untransduced T cells. A) Tonic signaling of the CAR T cells was determined by analysing the expression of activation (CD69 and CD25), differentiation (CCR7, CD27 and CD45RO) and inhibition (LAG3, TIM3 and PD-1) markers on the indicated CAR T cells throughout *in vitro* expansion (day 7, day 14 and day 21). Representative FACS histograms of the expression of these markers at day 14 are shown. **B)** Kinetics of T cell volume of the CAR T cells throughout the 21-day *in vitro* expansion. (PBMCs from n=3 independent healthy donors). No significant differences were found among the different CAR T cells using two-way ANOVA with the Tukey *post hoc* multiple comparisons test.

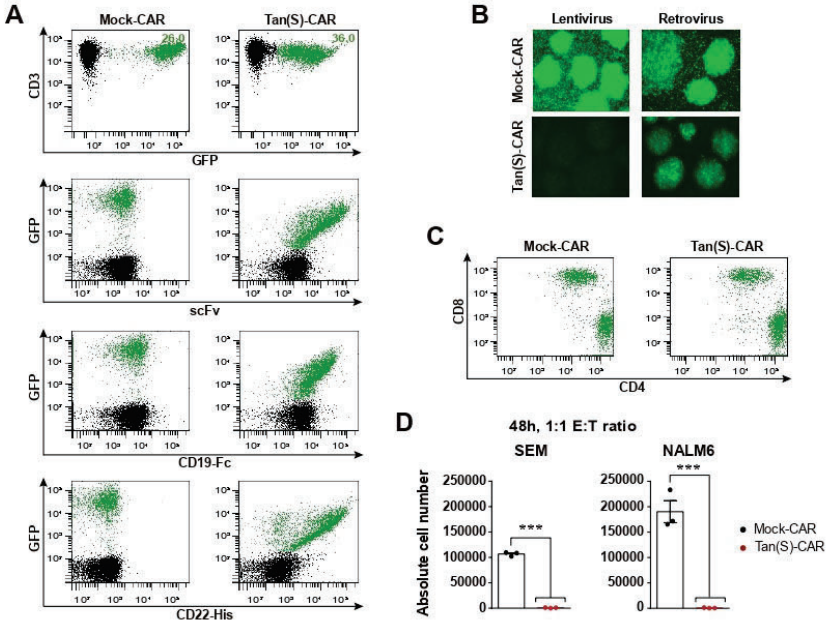

Figure S2. Detection and *in vitro* antileukemic efficacy of Tan(S)-CAR T cells transduced with retrovirus. A) Representative FACS plots of CAR expression on human T cells detected as GFP$^+$ (top panels), anti-scFv (second row), CD19-Fc/anti-Fc-PE (third row), and CD22-HisTag/anti-HisTag-APC (bottom row). CAR-transduced T cells are shown in green. Mock-CAR depicts T cells transduced with the GFP-SFG vector. **B)** Fluorescence microscope images of CAR T cells cultures depicting the GFP expression of T cells transduced with the corresponding lentivirus or retrovirus. **C)** Representative CAR detection on human CD4$^+$ and CD8$^+$ T cells. **D)** Absolute number of live target cells (SEM or NALM6) after 48 h incubation with the indicated CAR T cells at 1:1 E:T ratio (PBMCs from n=3 independent HD). Data are shown as mean ± SEM ***p<0.001; 2-tailed unpaired Student's t-test.

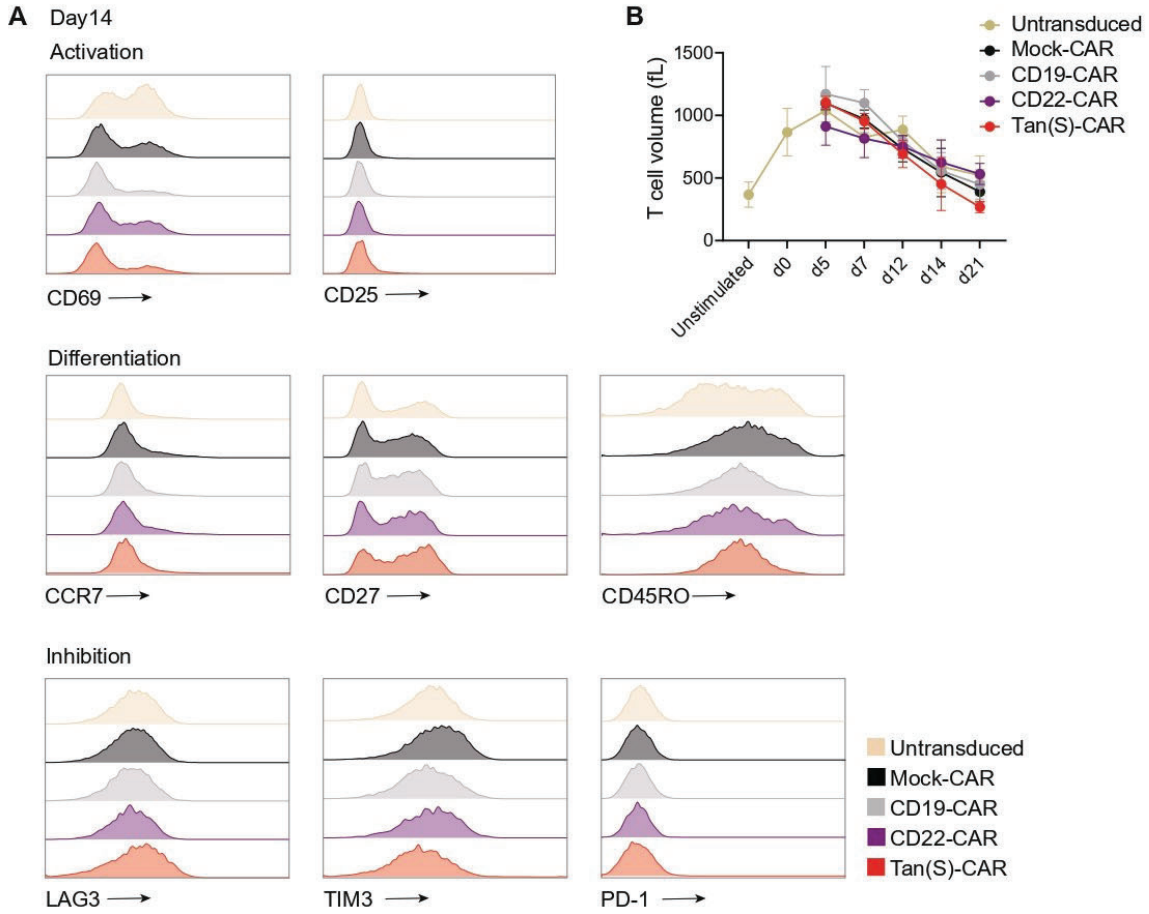

Figure S3. Tan(S)-CAR shows no increased tonic signaling than single CARs, Mock or untransduced T cells. A) Tonic signaling of the CAR T cells was determined by analysing the expression of activation (CD69 and CD25), differentiation (CCR7, CD27 and CD45RO) and inhibition (LAG3, TIM3 and PD-1) markers on the indicated CAR T cells throughout *in vitro* expansion (day 7, day 14 and day 21). Representative FACS histograms of the expression of these markers at day 14 are shown. **B)** Kinetics of T cell volume of the CAR T cells throughout the 21-day *in vitro* expansion. (PBMCs from n=3 independent healthy donors). No significant differences were found among the different CAR T cells using two-way ANOVA with the Tukey *post hoc* multiple comparisons test.

Sánchez-Martínez D, et al. Enforced sialyl-Lewis-X (sLeX) display in E-selectin ligands by exofucosylation is dispensable for CD19-CAR T-cell activity and bone marrow homing. *Clin Transl Med* (2021)

Received: 22 September 2020 | Revised: 22 December 2020 | Accepted: 28 December 2020 | Published online: 23 February 2021

DOI: 10.1002/ctm2.280

CLINICAL AND TRANSLATIONAL MEDICINE

WILEY

RESEARCH ARTICLE

Enforced sialyl-Lewis-X (sLeX) display in E-selectin ligands by exofucosylation is dispensable for CD19-CAR T-cell activity and bone marrow homing

Diego Sánchez-Martínez[1] | **Francisco Gutiérrez-Agüera**[1] | **Paola Romecin**[1] | **Meritxell Vinyoles**[1] | **Marta Palomo**[1] | **Néstor Tirado**[1] | **Samanta Romina Zanetti**[1] | **Manel Juan**[2] | **Michela Carlet**[3,4] | **Irmela Jeremias**[3,4] | **Pablo Menéndez**[1,5,6,7]

[1] Department of Biomedicine, Josep Carreras Leukemia Research Institute, School of Medicine, University of Barcelona, Barcelona, Spain

[2] Servei d'Immunologia, Hospital Clínic de Barcelona, Barcelona, Spain

[3] Department of Apoptosis in Hematopoietic Stem Cells, Helmholtz Center Munich, German Center for Environmental Health (HMGU), Munich, Germany

[4] Department of Pediatrics, Dr von Hauner Children's Hospital, LMU, Munich, Germany

[5] Department of Biomedicine, School of Medicine, University of Barcelona, Barcelona, Spain

[6] Centro de Investigación Biomédica en Red-Oncología (CIBERONC), Instituto de Salud Carlos III, Madrid, Spain

[7] Institució Catalana de Recerca i Estudis Avançats (ICREA), Barcelona, Spain

Correspondence
Dr. Pablo Menéndez and Diego Sánchez-Martínez, Department of Biomedicine, Josep Carreras Leukemia Research Institute, School of Medicine, University of Barcelona, Barcelona, Spain.
Email: pmenendez@carrerasresearch.org; dsanchez@carrerasresearch.org

Graphical Abstract

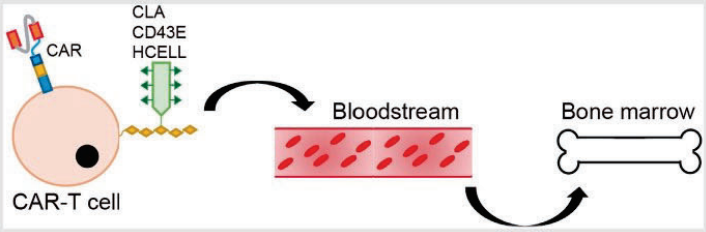

Glyco-engineered enforced sialofucosylation of E-selectin ligands was dispensable for CD19-CAR T-cell activity and BM homing in multiple xenograft models, thus representing an unnecessary strategy for CD19-CAR T-cell therapy

Received: 22 September 2020 | Revised: 22 December 2020 | Accepted: 28 December 2020 | Published online: 23 February 2021

DOI: 10.1002/ctm2.280

CLINICAL AND TRANSLATIONAL MEDICINE

WILEY

RESEARCH ARTICLE

Enforced sialyl-Lewis-X (sLeX) display in E-selectin ligands by exofucosylation is dispensable for CD19-CAR T-cell activity and bone marrow homing

Diego Sánchez-Martínez[1] | **Francisco Gutiérrez-Agüera**[1] | **Paola Romecin**[1] | **Meritxell Vinyoles**[1] | **Marta Palomo**[1] | **Néstor Tirado**[1] | **Samanta Romina Zanetti**[1] | **Manel Juan**[2] | **Michela Carlet**[3,4] | **Irmela Jeremias**[3,4] | **Pablo Menéndez**[1,5,6,7]

[1] Department of Biomedicine, Josep Carreras Leukemia Research Institute, School of Medicine, University of Barcelona, Barcelona, Spain

[2] Servei d'Immunologia, Hospital Clínic de Barcelona, Barcelona, Spain

[3] Department of Apoptosis in Hematopoietic Stem Cells, Helmholtz Center Munich, German Center for Environmental Health (HMGU), Munich, Germany

[4] Department of Pediatrics, Dr von Hauner Children's Hospital, LMU, Munich, Germany

[5] Department of Biomedicine, School of Medicine, University of Barcelona, Barcelona, Spain

[6] Centro de Investigación Biomédica en Red-Oncología (CIBERONC), Instituto de Salud Carlos III, Madrid, Spain

[7] Institució Catalana de Recerca i Estudis Avançats (ICREA), Barcelona, Spain

Correspondence
Dr. Pablo Menéndez and Diego Sánchez-Martínez, Department of Biomedicine, Josep Carreras Leukemia Research Institute, School of Medicine, University of Barcelona, Barcelona, Spain.
Email: pmenendez@carrerasresearch.org; dsanchez@carrerasresearch.org

Funding information
European Research Council, Grant/Award Numbers: CoG-2014–646903, PoC-2018-811220; Spanish Ministry of Economy and Competitiveness, Grant/Award Numbers: MINECO, SAF2016-80481R, SAF2019-108160R; Fundacion Uno entre Cienmil; "la Caixa" Foundation, Grant/Award Number: LCF/PR/HR19/52160011; Spanish Association against cancer (AECC, Semilla 2019)

Abstract

CD19-directed chimeric antigen receptors (CAR) T cells induce impressive rates of complete response in advanced B-cell malignancies, specially in B-cell acute lymphoblastic leukemia (B-ALL). However, CAR T-cell-treated patients eventually progress due to poor CAR T-cell persistence and/or disease relapse. The bone marrow (BM) is the primary location for acute leukemia. The rapid/efficient colonization of the BM by systemically infused CD19-CAR T cells might enhance CAR T-cell activity and persistence, thus, offering clinical benefits. Circulating cells traffic to BM upon binding of tetrasaccharide sialyl-Lewis X (sLeX)-decorated E-selectin ligands (sialofucosylated) to the E-selectin receptor expressed in the vascular endothelium. sLeX-installation in E-selectin ligands is achieved through an *ex vivo* fucosylation reaction. Here, we sought to characterize the basal and cell-autonomous display of sLeX in CAR T-cells activated using different cytokines, and to assess whether exofucosylation of E-selectin ligands improves CD19-CAR T-cell activity and BM homing. We report that cell-autonomous sialofucosylation (sLeX display) steadily increases in culture- and *in vivo*-expanded CAR T cells, and that, the cytokines used during T-cell activation influence both the degree of such endogenous sialofucosylation and the CD19-CAR T-cell efficacy and persistence *in vivo*. However, glycoengineered

enforced sialofucosylation of E-selectin ligands was dispensable for CD19-CAR T-cell activity and BM homing in multiple xenograft models regardless the cytokines employed for T-cell expansion, thus, representing a dispensable strategy for CD19-CAR T-cell therapy.

KEYWORDS
BM homing, CAR T-cells, E-selectin ligands, exofucosylation

1 | INTRODUCTION

Immunotherapy has revolutionized cancer treatment. Adoptive cell immunotherapy using T cells genetically redirected to a tumor-specific antigen by chimeric antigen receptors (CAR) has induced impressive rates of complete response in advanced B-cell malignancies, especially in B-cell acute lymphoblastic leukemia (B- ALL).[1,2] Unfortunately, however, CAR T-cell-treated patients eventually progress due to either poor CAR T-cell persistence and/or disease relapse. Common limitations associated to CD19-CAR T-cell treatment, but extendable to other CARs are: (i) failure to achieve complete remission, (ii) relapse with potential antigen loss, (iii) cytokine release syndrome (CRS) and related toxicities, and (iv) existence of multi-treated patients not eligible for CAR T-cell therapy due to low counts of T cells.[3–5]

In the clinical practice, adoptive cell therapies are systemically infused via the bloodstream. However, the bone marrow (BM) is the primary location for acute leukemia initiation and maintenance.[6–8] Anatomically, the BM microenvironment confers cellular interactions and signals promoting leukemia initiation, maintenance and progression, as well as drug resistance of leukemic cells.[9] Current challenges associated to CAR T-cell treatment in acute leukemia patients might be partially overcome by a rapid and effective CAR T-cell redirection to the BM. In fact, efficient seeding of systematically infused CAR T cells in the leukemic BM might enhance CAR T-cell activity and persistence, eventually providing key clinical benefits associated to the potential reduction of the CAR T-cell dose infused, namely less procedure-related toxicities, lower production costs, and broader patient's inclusion criteria.

Although several mechanisms regulate the homing of circulating cells to the BM,[10–12] the ability of circulating cells to traffic to the BM initially relies on their robust adherence to the E-selectin receptor (CD62E) displayed in the vascular endothelium (VE). Adhesive interactions between the E-selectin receptor and its cognate ligand, tetrasaccharide sialyl-Lewis X (sLeX), displayed on circulating cells dictate adherence of circulating cells to the VE, the first step of such biological process.[8] Cell binding activity to E-selectin receptor is specifically exerted by the sialofucosylated E-selectin ligands CLA, CD43E, and HCELL resulting from the sLeX instalment (α-2,3-sialic acid and α-1,3-fucose binding determinants on *N*-glycans) in the native E-selectin ligands PSGL1, CD43, and CD44, respectively.[13,14] Of note, native E-selectin ligands can be converted into sLeX-displaying (sialofucosylated) E-selectin ligands through a straightforward glycan engineering approach involving minimal *ex vivo* cellular manipulation based on a α-1,3-fucosyltransferase enzymatic reaction and guanosine diphosphate-fucose (GDP-fucose) substrate.[15–17] Such exofucosylation reaction was previously shown to endow BM homing abilities to hematopoietic stem/progenitors cells (HSPCs), mesenchymal stem/stromal cells (MSCs), and immune cells.[15,18,19]

Here, using CD19-CAR T cells as a working model, we sought (i) to characterize the basal/cell-autonomous display of sLeX in CAR T-cells activated with either IL-2 or IL-7/IL-15, and (ii) to assess whether exofucosylation of E-selectin ligands to enforce sLeX display improves CD19-CAR T-cell activity and BM homing. Our results revealed that cell-autonomous sialofucosylation steadily augments in culture- and *in vivo*-expanded CAR T cells, and that the type of cytokines used during T-cell activation influences both the cell surface display of sLeX in CD19-CAR T cells and the CD19-CAR T-cell efficacy and persistence *in vivo*. However, enforced sLeX display in E-selectin ligands by exofucosylation was dispensable for both CD19-CAR T-cell activity and BM homing, regardless the cytokines employed for T-cell expansion. Collectively, glycoengineered sLeX display in CAR T-cells systemically administered is a dispensable strategy for improved CAR T-cell function.

2 | RESULTS

2.1 | Cell-autonomous and exofucosylation-enforced expression of sLeX in CD19-CAR T cells

T cells from peripheral blood (PB) of healthy donors (n = 5) were activated using CD3/CD28 plus either IL-2 or IL-7/

IL-15 and transduced on day 2 with CD19-CAR-expressing lentivectors (Figure 1A). The levels of sialofucosylation (sLeX display in cell surface) were analyzed by FACS on CAR T cells over the 9-day activation/expansion period using the HECA452 MoAb, which recognizes sLeX.[20] Basal expression of sLeX (HECA452+) was found in approximately 31 ± 5% of T cells at day 0 (Figure 1B). Interestingly, *in vitro* T-cell activation/expansion led to a cell-autonomous gradual increase in sLeX-expressing CAR T cells (Figure 1B). Of note, IL-7/IL-15 activation consistently rendered higher frequency of sialofucosylated (HECA452+) CAR T cells than IL-2-based activation (75 ± 7% vs 50 ± 5% at day 9; Figure 1B), in a T-cell proliferation/expansion independent manner (Figure 1C). Using a well-established FTVII-based exofucosylation reaction[17] (Figure 1D), 100% of culture-expanded CAR T cells became HECA452+ within 48 h, regardless the cytokines used during T-cell activation (Figure 1E). Western Blot (WB) analysis using E-selectin-Ig immunoprecipitates clearly identified CD43 (CD43E), and partially PSGL1 (CLA), as the E-selectin ligands carrying sLeX in exofucosylated CAR T cells (Figure 1F). We next analyzed the phenotype of the expanded T cells using a CCR7 and CD45RA staining, and found that neither the cytokines used nor the exofucosylation reaction affected the T-cell phenotype (TN, TCM, TEFF/EM, TEMRA) upon 9 days of expansion (Figure 1G). Collectively, although the cytokines used for T-cell activation influence the level of sLeX display in CAR T cells, cell-autonomous sialofucosylation gradually increases in culture-expanded CAR T cells, with up to 80% of CAR T cells being endogenously fucosylated at the end of the *in vitro* expansion.

2.2 | Exofucosylation enhances neither cytotoxic activity nor homing of CAR T cells *in vitro*

We first prompted to analyze *in vitro* the cytotoxic activity of exofucosylated CD19-CAR T cells. The cytotoxicity and specificity of both BT- (control) and FTVII-treated (sialofucosylated) CD19-CAR T cells were identical in *in vitro* assays against CD19+ (NALM6, SEM) and CD19- (Jurkat) cell lines at multiple effector:target ratios (Figure 2A). We next investigated the potential of exofucosylated CD19-CAR T cells to migrate through TNF-α-stimulated Human Umbilical Vein Endothelial Cells (HUVEC) monolayers using standard *in vitro* transwell migration assays (Figure 2B). As expected, the expression of both E-selectin receptor and VCAM-1, a key vascular cell adhesion molecule, was upregulated in HUVEC cells upon TNF-α stimulation, thus, mimicking an activated microvasculature environment[21,22] (Figure 2B, right panels). Regardless the cytokines used for T-cell activation, exofucosylation rendered HECA452 expression in 100% of the FTVII-treated CD19-CAR T cells while not affecting the expression of the VLA-4, the putative VCAM-1 ligand, confirming the specificity of the FTVII treatment (Figure 2C). BT- and FTVII-treated CD19 CAR T cells (upper chamber) showed identical migratory capacity toward target cells (bottom chamber) through either nonstimulated or TNF-α-stimulated HUVEC monolayers (Figure 2D), which translated into identical cytotoxicity of target cells by the migrating CAR T cells, in 24 h assays (Figure 2E). Taken together, enforced exofucosylation of CD19-CAR T cells enhances neither cytotoxicity nor homing *in vitro*.

2.3 | Exofucosylation enhances neither homing to BM/spleen nor activity/persistence of CAR T cells *in vivo*

We next assessed whether enforcing sLeX display by exofucosylation promotes rapid migration of CD19 CAR T cells to BM and spleen. A sum of 3×10^6 BT- or FTVII-treated CD19-CAR T cells were i.v. infused in NSG mice previously intra-BM transplanted with CD19+ target cells, and the ability of CD19-CAR T cells to colonize the BM and spleen was analyzed as early as 24 and 72 h after (Supporting information Figure S1A). In line with the *in vitro* data, similar numbers of BT- and FTVII-treated CAR T cells were found in PB and BM 24 and 72 h (Figure S1B) after CAR T-cell infusion, regardless the cytokines used during T-cell stimulation. These data suggest that, at least as a "stand-alone" strategy, exofucosylation of CAR T cells does not speed-up CD19-CAR T-cell colonization of BM.

We next investigated whether exofucosylation endows CD19-CAR T cells with an enhanced cytotoxic activity or prolonged persistence. Three *in vivo* models using differentially aggressive targets cells were employed (Figures 3 and 4). A sum of 3×10^6 of IL-2-expanded BT- or FTVII-treated CD19-CAR T cells from different donors were i.v. infused in NSG mice 3, 7, or 14 days after transplantation of Luc-expressing NALM6 (Figure 3A), SEM (Figure 3B), or B-ALL PDX (n = 2, Figure 4A), respectively. BT- or FTVII-treated CD19-CAR T cells were equally effective in controlling the leukemia overtime, regardless the target cells used (Figures 3C, D and 4B). FACS analysis of residual target cells at sacrifice revealed identical cytotoxic activity of both BT- or FTVII-treated CD19-CAR T cells in controlling NALM6 (Figure 3E), SEM (Figure 3F), and PDX B-ALL (Figure 4C) cells in PB, BM, and spleen. In addition, endpoint analysis of CAR T cells revealed no persistence advantage of FTVII-treated effector CAR T cells in PB, BM, and spleen (Figures 3G, H and 4D). We then infused limiting doses of BT- and FTVII-treated CAR T

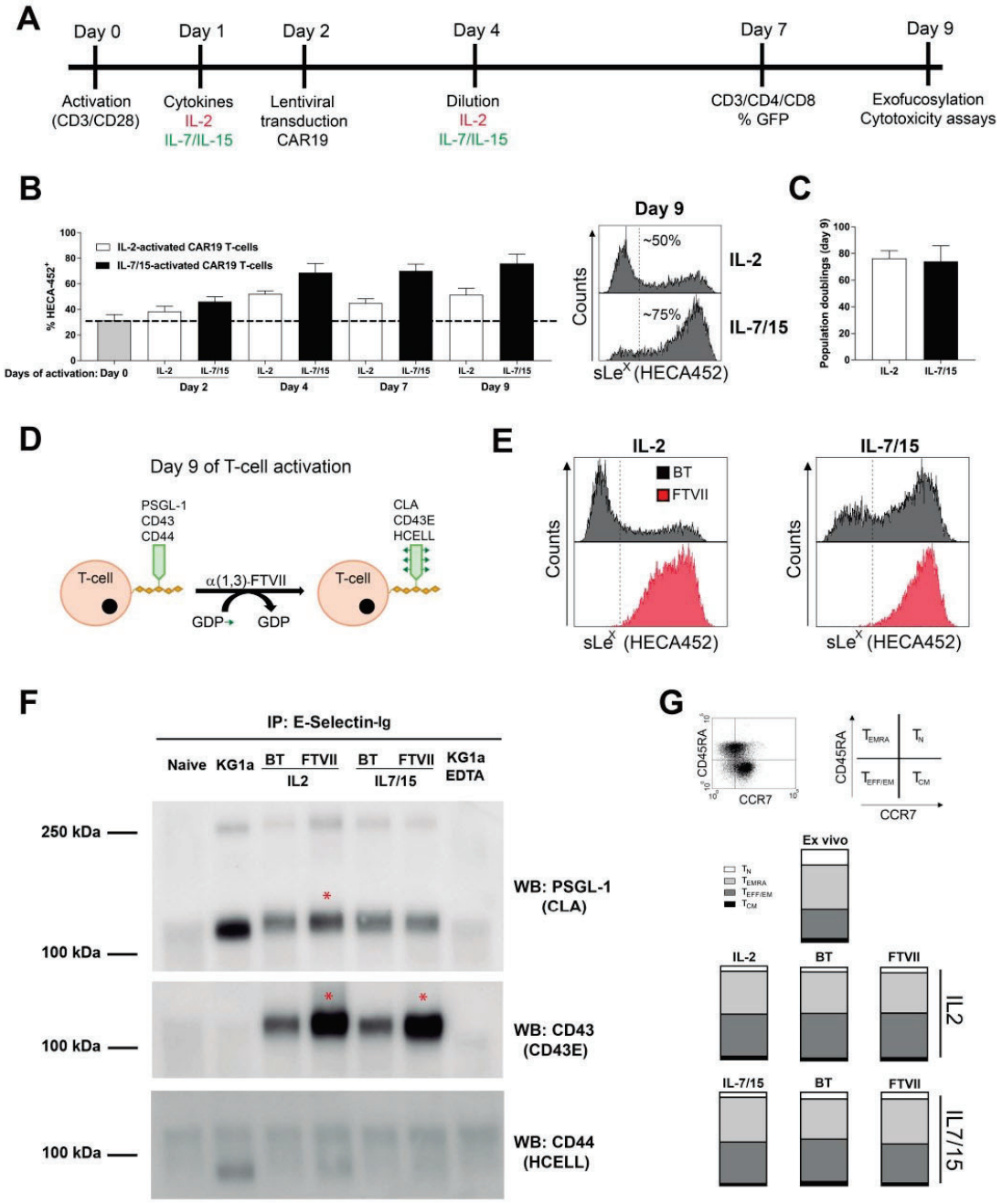

FIGURE 1 Cell-autonomous and enforced expression of sLeX in CAR T cells. (A) Experimental design and timing of *ex vivo* CAR T-cell activation, transduction and exofucosylation. (B) Basal expression and *in vitro* regulation of sLeX (detected by HECA452 MoAb) at the indicated time points in IL-2- or IL-7/IL-15-activated T cells (n = 5 independent donors). Horizontal dotted line depicts the basal expression of HECA452 before T- cell activation. Right panels, representative FACS analysis of sLeX (HECA452) at the end of the activation protocol. Vertical dotted lines represent the isotype staining. (C) Very similar T-cell expansion at the end (day 9) of the *in vitro* culture protocol under

cells (in the SEM model) to more accurately assess whether FTVII-treatment may provide an improved *in vivo* cytotoxic activity of CAR T cells when administered in limited numbers, and found that exofucosylation did not endow CAR T cells with an improved antileukemia effects regardless the cell dose infused (Supporting information Figure S2). We finally measured the frequency of sialofucosylated (HECA452+) CAR T cells in both BM and PB at sacrifice of the B-ALL PDX models, and found identical levels (~80%) of sLeX display in both BT- and FTVII-treated CAR T cells (Figure 4E), further indicating cell-autonomous sialofucosylation of *in vivo*-expanded CAR T cells.

Of note, the results from these three *in vivo* models were fully reproduced with IL-7/IL-15-activated/expanded CAR T cells (Supporting information Figure S3), further validating that glycoengineered sLeX display in CAR T cells is dispensable for CAR T-cell activity and persistence, regardless the cytokines used during T-cell stimulation. However, regardless enforced exofucosylation of CAR T cells, IL-2-expanded CD19-CAR T-cells displayed a better control of the disease coupled to a higher T-cell persistence than IL-7/IL-15-expanded CD19 CAR T cells in all the *in-vivo* leukemia models used (NALM6, SEM, and PDXs, Figures 3 and 4 versus Supporting information Figure S3).

3 | DISCUSSION

CAR T-cell therapy has been acclaimed as a revolution in cancer treatment following the impressive results in hematological B-cell malignancies, especially in refractory/relapse B-ALL. However, despite the impressive response rates, CD19-directed adoptive cell immunotherapy is on its infancy, and unfortunately, a large proportion of CD19-CAR T-cell-treated patients eventually progress due to either poor CAR T-cell persistence and/or disease relapse.[23,24] Indeed, many studies in the coming years are expected to seed light into key molecular and cellular immunological mechanisms underlying CAR T-cell biology.[25] Furthermore, CAR T cells for solid tumors are lagging behind in part because the need to circumvent the physical barriers of the tumor architecture such as subverted tumor vasculature, impediments of CAR T-cell trafficking, and immunesuppressive microenvironment.[26] Similarly, the primary location for acute leukemogenesis is the BM, and the BM microenvironment provides leukemic cells with cellular interactions and signals promoting leukemia initiation, progression, and chemoresistance.[6–9] However, CAR T cells in patients suffering from acute leukemias are systemically infused via the bloodstream.

Practically all cellular therapies systemically administered to treat hematological malignancies such as transplantation of unmodified or gene therapy-modified HSPCs,[27] or infusion of donor unmodified immune cells rely on efficient seeding in the leukemic BM.[28] Similarly, cell therapy based on MSCs for graft-versus-host disease or inflammatory conditions also rely on successful MSC trafficking/homing to the damaged tissue.[29,30] Here, we have hypothesized that CAR T-cell immunotherapies (CD19-CAR as a working model) in acute leukemia patients may also benefit from a rapid and effective redirection of effector cells to BM. Efficient seeding of infused CAR T cells in the leukemic BM might enhance their activity and persistence, eventually providing many clinical benefits associated to the potential reduction in the CAR T-cell dose to be infused, namely less CRS, lower production costs, and broader patientt's inclusion criteria. Previous studies from several laboratories have suggested that enforced expression *ex vivo* of E-selectin ligands (exofucosylation) leads to transendothelial migration of systemically administered HSPCs, MSCs, and T cells at E-selectin-expressing endothelial beds.[16,19,31–33] Here, we have addressed the role of cell-autonomous and enforced sialofucosylation (sLeX display) in E-selectin ligands in the cytotoxic activity and homing ability of systemically administered CD19 CAR T cells. Taking advantage of state-of-the-art *in vitro* assays as well as short- and long-term *in vivo* xenograft models using several B-ALL cell lines and PDXs, our FACS and biochemical data revealed that cell-autonomous sialofucosylation steadily increases in culture- and *in vivo*-expanded CAR T cells. In contrast, a study by Mondal et al. has recently shown that *in vitro*-expanded CAR T cells do not exhibit sLeX expression/E-selectin binding capacity.[34] One may attribute such differences to the use of different scFvs, T-cell activation conditions, biological differences of the

both IL-2- and IL-7/IL-15-activation conditions. (D) Cartoon of the *ex vivo* exofucosylation reaction using fucosyltransferase-VII (FTVII) and GDP-fucose. Exofucosylation of PSGL-1, CD43, and CD44 generates the corresponding glycomodified E-selectin ligands CLA, CD43E, and HCELL, respectively. (E) Representative FACS analysis of sLeX (HECA452) expression in IL-2- or IL-7/IL-15-activated T cells after buffer-(BT) or FTVII-treatment (n = 5). (F) Western blot analysis of E-selectin reactive glycoproteins in naïve T cells, KG1a cells (positive control), and BT or FTVII-treated CAR T cells. E-selectin-Ig immunoprecipitated (IP) glycoproteins from BT or FTVII-treated CAR T cells were blotted against (PSGL-1, CD43, and CD44). Representative image of n = 3 independent donors. (G) Top panels, a representative FACS plot depicting how TN, TCM, TEFF/EM, TEMRA T-cell subsets were identified using a CCR7 and CD45RA staining. Bottom panels, relative proportion of TN, TCM, TEFF/EM, TEMRA cell subsets after IL-2- versus IL-7/IL-15-based T-cell activation or after exofucosylation (FTVII- versus buffer treatment)

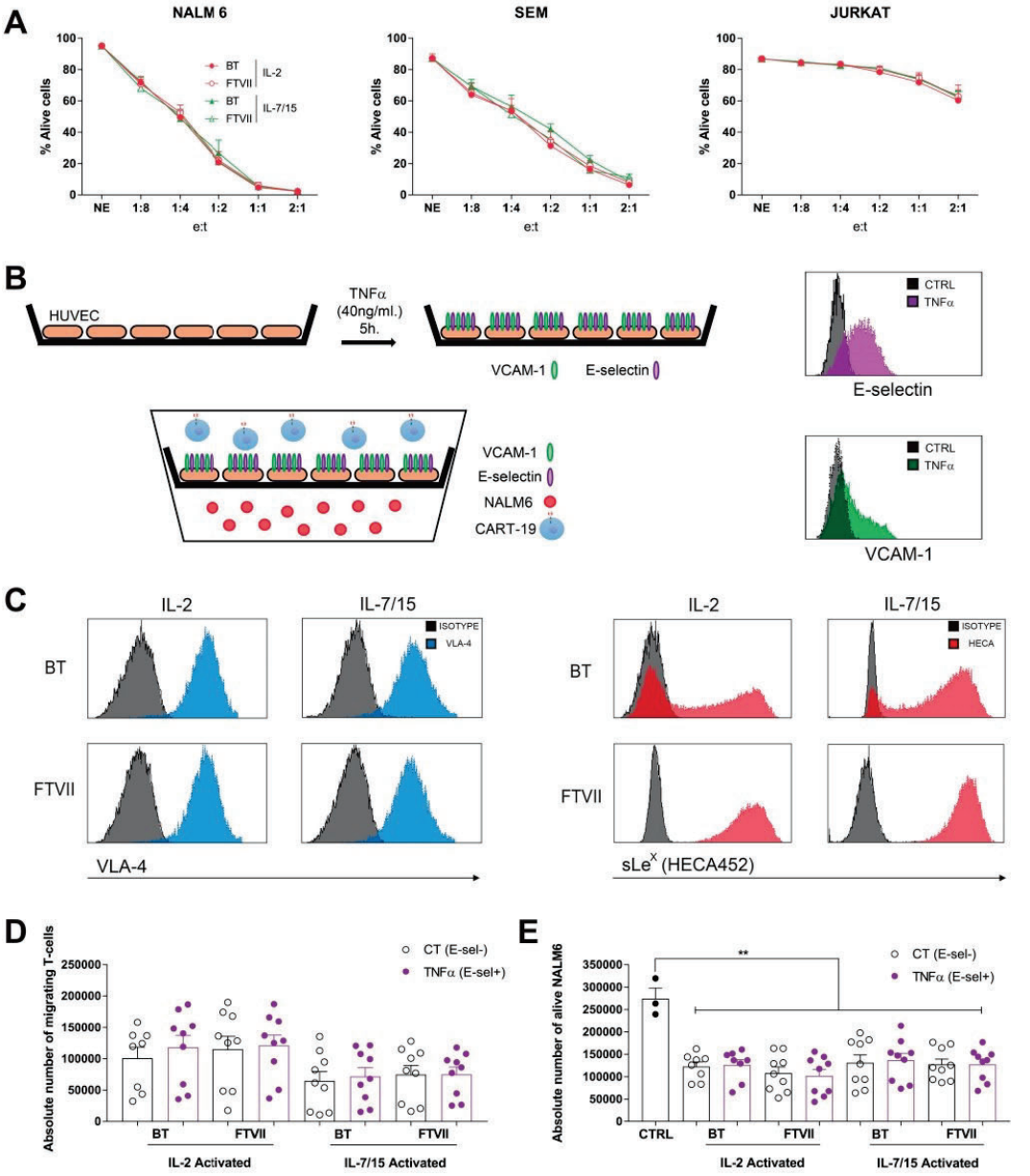

FIGURE 2 Exofucosylation enhances neither *in vitro* cytotoxicity nor homing of CAR T-cells on TNF-α-activated HUVEC cells. (A) IL-2- and IL-7/IL-15-activated CAR T cells were BT- or FTVII-treated before *in vitro* exposure (24 h) to NALM6, SEM, and Jurkat at the indicated Effector:Target ratio. The alive (7-AAD-) eFluor 670+ target cells were determined by FACS (n = 3, independent donors). (B) Cartoon depicting the transwell assay using HUVEC monolayers for analysis of CAR T-cell (upper) migration toward target cells (bottom). HUVECs were stimulated with TNF-α-stimulated for 4 h for expression of VCAM-1 and E-selectin expression (right panels). (C) Representative FACS of the expression of the VCAM-1 ligand VLA-4 (left panels) and the exofucosylated E-selectin ligands (sLeX/HECA452-expressing, right panels) in IL-2- and IL-7/IL-15-activated CAR T cells after BT- or FTVII treatment (n = 3). (D,E) Absolute number of migrating BT- or FTVII-treated CAR T cells (D) and alive (7ADD-) target cells (E) quantified in the bottom chamber after 24 h (n = 6 donors in three independent experiments). CAR T cells were activated either with IL-2 or IL-7/IL-15. The assays were performed using unstimulated or TNF-α-stimulated HUVECs. $^{*}P < .05$, $^{**}P < .01$, $^{***}P < .001$

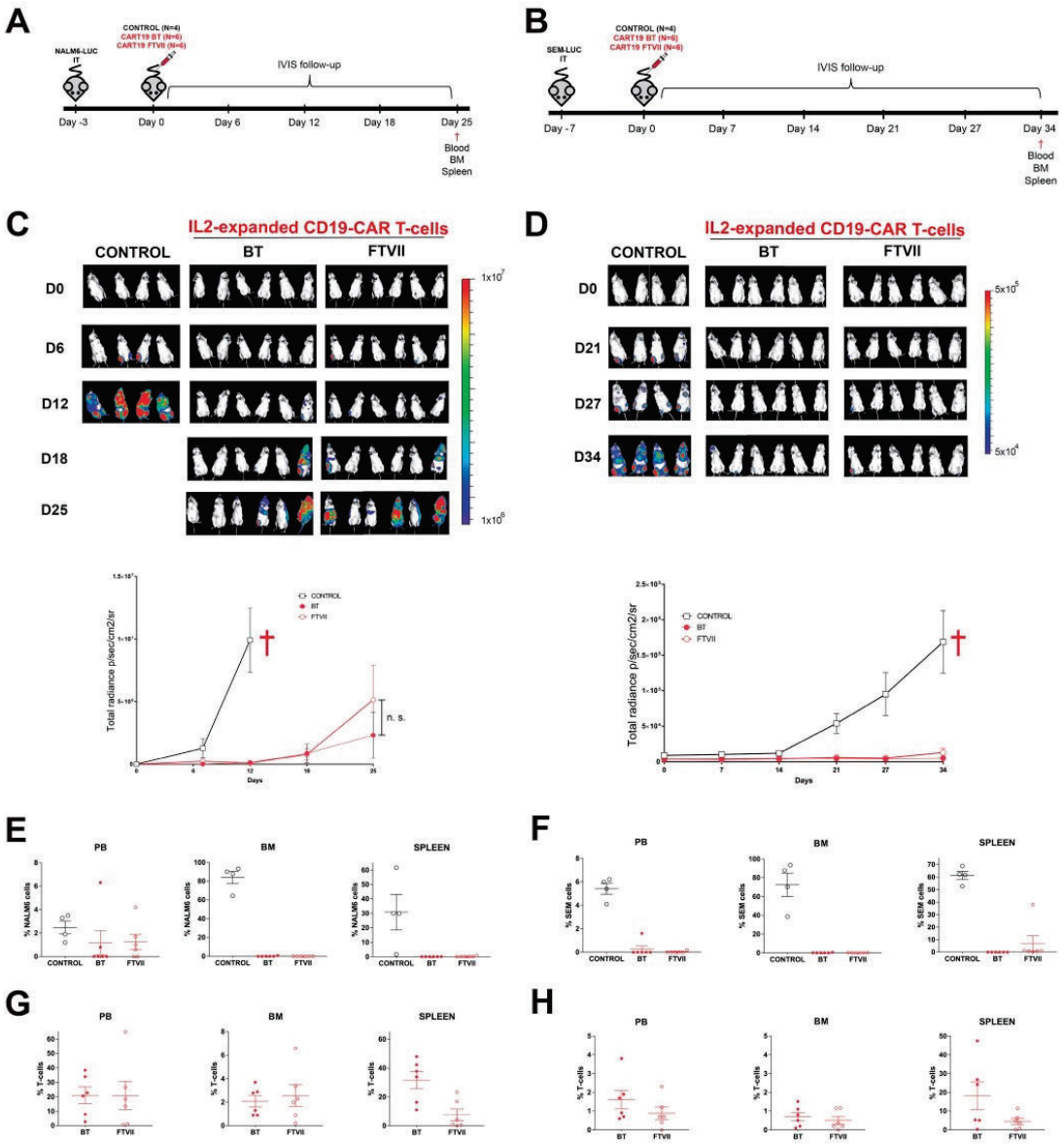

FIGURE 3 Exofucosylation is dispensable for CAR T-cell activity and BM homing in both NALM6 and SEM *in vivo* models. (A,B) Schematic of CAR T-cell activity and homing using NALM6 (A) or SEM (B) as target cells. NSG mice (n = 6 per group) intra-BM transplanted with 1 × 105 Luc-expressing NALM6 cells were i.v. infused 72 h later with 3×10^6 BT- or FTVII-treated CAR T cells. NALM6/SEM engraftment was followed weekly by bioluminescence. Target cell and T-cell engraftment was FACS analyzed in PB, BM, and spleen at sacrifice (for NALM6, day +12 for Mock T cells and day +25 for CAR T-cells; SEM, day +34). (C,D) IVIS imaging of NALM6 (C) and SEM (D) tumor burden monitored by BLI at the indicated time points. Bottom panels, total radiance quantification (p/s/cm2/sr) at the indicated time points. †: sacrifice. (E,F) NALM6 (E) and SEM (F) engraftment in PB, BM, and spleen at sacrifice in control mice (Mock T-cells), BT- and FTVII- treated CAR T-cells. (G,H) Persisting CAR T cells in PB, BM, and spleen at sacrifice in control mice, BT-, and FTVII-treated CAR T cells in the NALM6 (G) and SEM (H) model

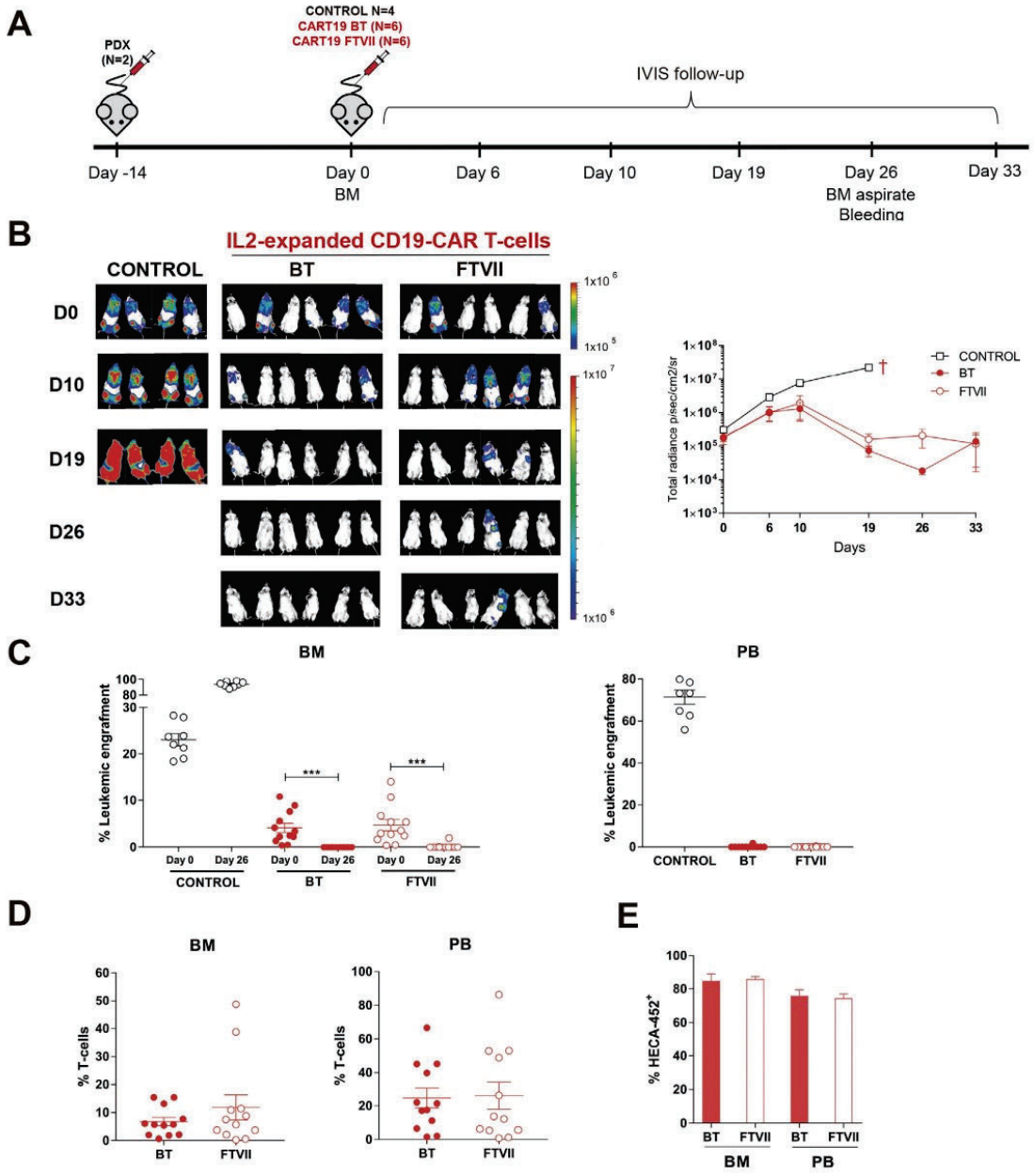

FIGURE 4 Exofucosylation is dispensable for CAR T-cell activity and BM homing in B-ALL PDX models. (A) Schematic of CAR T-cell activity and homing experiment using two independent B-ALL PDX (n = 2). NSG mice (n = 6 per group) were i.v. transplanted with 5×10^5 Luc-expressing PDX cells and 3×10^6 BT- or FTVII-treated 3×10^6 CAR T-cells were i.v. infused 14 days later, after engraftment was determined by FACS. Mice were distributed equally in each group. PDX engraftment was followed weekly by BLI. Tumor burden and T-cell engraftment was analyzed in PB and BM at sacrifice (day +33). (B) IVIS imaging of tumor burden monitored by BLI at the indicated time points. Right panel, total radiance quantification (p/s/cm2/sr) at the indicated time points. †: sacrifice. (C) Tumor burden in PB and BM at sacrifice in control (Mock T-cells) mice, BT- and FTVII-treated CAR T cells. (D) Persisting CAR T cells in PB and BM at sacrifice in control mice, BT-, and FTVII-treated CAR T-cells. (E) Expression of sLeX (HECA452) in BT- and FTVII-treated CAR T cells circulating in PB and present in BM at sacrifice

donor T-cells employed (HLA haplotypes, age, comorbilities), etc. We have systematically compared side-by-side IL-2- versus IL-7/IL-15-based T-cell activation conditions, concluding that the cytokines used for T-cell activation influence the degree of cell-autonomous sLeX expression in CAR T cells. However, regardless of the cytokines used for T-cell activation, cell-autonomous sLeX expression/E-selectin binding capacity gradually increased in culture- and *in vivo*-expanded CAR T cells. Moreover, identical levels of sLeX expression/sialofucosylation were observed in *in vitro*-expanded CAR+ and CAR-T cells, suggesting a CAR-independent cell-autonomous sialofucosylation of activated culture-expanded T cells (data not shown).

Our results using multiple *in vitro* and *in vivo* xenograft models revealed that further enforced sLeX-installation in E-selectin ligands improves neither the cytotoxic activity nor BM/spleen homing of vascularly administered CD19-CAR T cells, regardless of the cytokines used for T-cell activation. Of note, the T-cell phenotype was not altered by either the cytokines used for T-cell expansion or the exofucosylation reaction. This is in line with the reported cell-autonomous steady sialofucosylation of *in vitro* culture-expanded CAR T cells prior to *in vivo* infusion. Furthermore, the frequency of HECA452+ CAR T cells was found very similar in xenografts infused with either BT- or FTVII-treated CAR T cells, suggesting that cell-autonomous sialofucosylation of T cells *in vivo* seems sufficient for proper *in vivo* effector function. A major difference between our experimental design and that by Mondal et al. is that, in our study, CAR T cells were infused in NSG mice previously transplanted with CD19+ target cells, thus, making our *in vivo* model more informative. It should be noted that CAR T cells are not expected to migrate or persist in BM or spleen in the absence of target antigen. Therefore, our xenograft models permit a physiologically more relevant *in vivo* assessment of (i) the trafficking ability of the infused exofucosylated CAR T cells in the presence of target antigen-expressing leukemic niches, and (ii) the cytotoxic activity of exofucosylated CAR T cells. In a different adoptive immunotherapy context, tumor infiltrated lymphocytes (TILs) have been recently reported to display an increased *in vivo* but also *in vitro* cytotoxic activity upon exofucosylation, suggesting that the enhanced sLeX expression seemed important for the target cell recognition.[35] Furthermore, the mechanisms for activation/expansion and target cell recognition of TILs clearly differ from those from CAR T cells, further explaining such experimental discrepancies between the distinct effector cells used for adoptive cell immunotherapies. Of note, regardless enforced exofucosylation of CAR T cells, IL-2-expanded CD19-CAR T cells showed a better control of the disease coupled to a higher T-cell persistence than IL7-/IL-15-expanded CD19-CAR T cells in all the *in-vivo* leukemia models employed in the present study (NALM6, SEM, and PDXs), suggesting that adequate T-cell expansion protocols may benefit the manufacturing and clinical outcome of CAR T cells. Collectively, our results support that the cytokines used during T-cell activation influence both the degree of cell-autonomous sialofucosylation and the CD19-CAR T-cell efficacy and persistence *in vivo*. However, at least as a "stand-alone" strategy, glycoengineered exosialofucosylation of E-selectin ligands seems dispensable for CD19-CAR T-cell activity and BM homing in multiple xenograft models regardless of cytokines employed for T-cell expansion. Which and how alternative cellular and molecular mechanisms regulate the migration of circulating CAR T-cells to BM needs to be explored in further studies.

4 | MATERIALS AND METHODS

4.1 | CD19-CAR vector, lentiviral production, T-cell transduction, activation and expansion

Our clinically validated pCCL lentiviral second-generation CD19CAR backbone containing a human CD8 transmembrane (TM) domain, human 4-1BB and CD3z endodomains, and a T2A-GFP cassette has been reported elsewhere.[36,37] CAR-expressing viral particles pseudotyped with VSV-G were generated in 293T cells using standard polyethylenimine transfection protocols, and were concentrated by ultracentrifugation as described elsewhere.[38] Viral titers were consistently in the range of 10^8 TU/mL. Peripheral blood mononuclear cells (PBMCs) were isolated from buffy coats from healthy volunteers by using Ficoll–Hypaque gradient centrifugation. Buffy coats were obtained from the Barcelona Blood and Tissue Bank upon institutional review board approval (HCB/2018/0030). T cells were plate-bound activated with anti-CD3 and anti-CD28 antibodies for 2 days and then transduced with CAR-expressing lentivirus (multiplicity of infection = 10) in the presence of either interleukin-2 (IL-2, 50 UI/mL, Mitenyi Biotec) or IL-7 and IL-15 (10 ng/mL, Mitenyi Biotec).[38] Proper CAR expression, T-cell activation, and expansion was confirmed at the end of the activation period, as previously described.[38]

4.2 | Exofucosylation reaction

CD19-CAR T cells expanded for 9 days either with IL-2- or IL-7/IL-15 were treated on Hanks' Balanced Salt solution (0.1% human serum albumin and 10 mM HEPES)

with GDP-fucose (Biosynth Carbosynth, Compton, UK) and FTVII (RD Systems). One million cells were incubated in 20 μL of buffer containing 1 mM of GDP-fucose and 70 μg/mL of purified FTVII enzyme at 37°C for 1 h as previously detailed.[17] Control cells were incubated in the same solution but without FTVII/GDP-fucose (buffer-treated [BT] cells). After the enzymatic reaction, cells were always washed twice with PBS before downstream experiments.

4.3 | E-selectin-Ig immunoprecipitation

CAR T-cell lysates were prepared using lysis buffer containing 150 mM NaCl, 50 mM Tris-HCI (pH 7.4), 2% Nonidet P-40, 2 mM CaCl2, and protease and phosphatase inhibitor cocktails (Roche). When indicated, 5 mM EDTA was added to the lysis buffer as negative control condition. A sum of 5×10^6 cells were pelleted per condition, washed with PBS, and lysed in 500 μL of lysis buffer. Cell lysates were incubated on ice for 15 min and centrifuged at 12 000 *g* for 10 min. Cell lysates were then precleared overnight using protein G-agarose beads (Roche) and incubated for 2 h at 4°C with 3 μg of murine E-selectin-human Fc chimera ("E-Ig," R&D Systems), as described.[17] Agarose beads were then washed twice with lysis buffer, and immunoprecipitated glycoproteins were collected by boiling the beads in the presence of 2-mercaptoethanol in Laemmli loading buffer. For western blot (WB) analysis, immunoprecipitates were resolved on a 7.5% SDS-PAGE gel (Bio-Rad Laboratories) and then transferred onto a polyvinylidene difluoride (PVDF) membrane (Bio-Rad). The membrane was then blocked with blocking reagent (Chemiluminescence Western Blotting Kit, Roche), and incubated with monoclonal antibodies (MoAb) against PSGL1 (clone KPL1, BD), CD43 (clone IG10, BD), and CD44 (clone 2C5, R&D). Protein bands were detected by chemiluminescence using Lumi-Light substrate (Chemiluminescence Western Blotting Kit).

4.3.1 | *In vitro* cytotoxicity assays

Luciferase (Luc)/GFP-expressing-NALM6 cells were kindly provided by Prof. RJ Brentjens (MSKCC, NY). SEM were generated by retroviral transduction and GFP-based FACS-selection.[39] Jurkat were purchased from DSMZ. Target cells were labeled with 3 μM eFluor670 (eBioscience) and incubated with BT- and CD19-CAR T cells at different Effector:Target (E:T) ratios. CAR T-cell-mediated cytotoxicity was determined by analyzing the residual alive (7-AAD-) eFluor670+ target cells after 24 h CAR T-cell exposure.

4.4 | HUVEC transwell assays

HUVEC were maintained in EGM-2 Endothelial Cell Growth Medium-2 BulletKit (Lonza, Cultek SLU), as previously described.[40] Early passage HUVECs were plated on 24-well Transwell plates (5 μm polycarbonate membrane, 6.5 mm insert), and stimulated with 40 ng/mL of TNF-α (R&D) for 4 h at 37°C to activate cell surface expression of E-selectin and VCAM-1.17 A sum of 2×10^5 of each NALM6 cells and BT- or FTVII-treated CAR T cells were seeded in the bottom and upper chamber, respectively. Twenty-four hours later, the absolute number of alive (7AAD-) NALM6 and CAR T cells present in the bottom chamber were quantified using Trucount tubes (BD Biosciences).[38]

4.5 | *In vivo* NALM6, SEM, and B-ALL patient-derived xenograft (PDX) models

Six- to twelve-week-old nonobese diabetic NOD.Cg-Prkdc^{scid} Il2rg^{tm1Wjl}/SzJ (NSG) mice (Jackson Laboratory) were bred and housed under pathogen-free conditions in the animal facility of the Barcelona Biomedical Research Park (PRBB). All *in vivo* experimental procedures were performed in compliance with the institutional animal care committee of the PRBB (DAAM7393). Briefly, irradiated (2 Gy) mice (5-6/condition) were intra-BM or i.v. transplanted with Luc/GFP-expressing SEM (1×10^5), NALM6 (1×10^5), or B-ALL PDX (5×10^5, PDX-50/PDX-265) cells and then i.v. infused with 3×10^6 BT- or FTVII-treated CD19-CAR T cells when engraftment was detectable. An *in vivo* experiment was performed with SEM cells where decreasing doses (2×10^6, 1×10^6, 0.5×10^6, 0.2×10^6) of BT- or FTVII-treated CD19-CAR T cells were infused. Both IL-2- and IL-7/IL-15-based CAR T-cell activation protocols were used. Tumor burden was monitored weekly by bioluminescence (BLI) using the Xenogen IVIS 50 Imaging System (Perkin Elmer).[38] Tumor burden (HLA-ABC+CD45+CD19+CD22+CD3-) and CAR T-cell persistence (HLA-ABC+CD45+CD3+GFP+) were also quantified by FACS at sacrifice in BM, PB, and spleen.

4.6 | FACS analysis

Cell staining and FACS analysis were performed as extensively described[38] using a FACSCanto-II flow cytometer equipped with FACSDiva software (BDBioscience). Briefly, 0.5×10^5 total cells recovered from *in vitro* or *in vivo* assays were stained in PBS + 2%FBS with the following MoAb: HECA-452 (CLA)-BV421, CD62/E-Selectin-APC, CD49d/VLA-4-PE, VCAM-1-APC, HLA-ABC-PE, CD45-BV421, CD3-PerCP, CD45RA-AmCyan, CCR7-PE,

CD22-APC, and CD19-BV421. IgG1-APC, IgG1-PE, and Rat IgM-BV421 were used as isotype controls. All MoAb were purchased from BD Biosciences. Supporting information Figures S1B and S4 show the gating strategies for T-cell analysis.

4.7 | Statistical analysis

Data are shown always from at least three individual donors. At least five animals were used per condition. *P*-values were calculated by an unpaired two-tailed Student's *t-test* using Prism software (GraphPad).

ACKNOWLEDGMENTS

We are indebted to Juan José Rodríguez-Sevilla and PM's lab members for their technical feedback and constructive discussions.

We thank CERCA Programme / Generalitat de Catalunya and Fundacio Josep Carreras-Obra Social la Caixa for their institutional support. The research leading to these results has received funding from the European Research Council (CoG-2014–646903, PoC-2018-811220), the Spanish Ministry of Economy and Competitiveness (MINECO, SAF2016-80481R and SAF2019-108160R), the Fundacion Uno entre Cienmil, "la Caixa" Foundation (ID 100010434) under the agreement LCF/PR/HR19/52160011, and the Spanish Association against cancer (AECC, Semilla 2019) to PM. DSM is partially supported by a Sara Borrell fellowship from the Instituto de Salud Carlos III. MV is partially supported by a Juan de la Cierva fellowship from the MINECO. SRZ was supported by Marie Sklodowska Curie Fellowship. PM is an investigator of the Spanish Cell Therapy cooperative network (TERCEL).

AUTHOR CONTRIBUTIONS

Study conception and design: DSM, PM.

Experimentation: DSM, FGA, PR, MV, MC, NT.

Data analysis and interpretation: FGA, DSM, PM.

Technical and primary sample contribution: MP, SRZ, IJ, MJ.

Manuscript writing: DSM, PM.

CONFLICT OF INTEREST

The authors have nothing to disclose.

APPROVAL AND CONSENT TO PARTICIPATE

This study was IRB-approved by the Barcelona Clinic Hospital Ethics Committee (HCB/2019/0450). All *in vivo* procedures were approved by the Animal Care Committee of The Barcelona Biomedical Research Park (HRH-17-0029-P1).

AVAILABILITY OF DATA AND MATERIAL

The datasets and materials generated in this study are available from the corresponding author on reasonable request.

ORCID

Diego Sánchez-Martínez https://orcid.org/0000-0003-4605-5325

REFERENCES

1. Humphries C. Adoptive cell therapy: honing that killer instinct. *Nature*. 2013;504(7480):S13-15.
2. Maude SL, Frey N, Shaw PA, et al. Chimeric antigen receptor T cells for sustained remissions in leukemia. *N Engl J Med*. 2014;371(16):1507-1517.
3. Majzner RG, Mackall CL. Tumor antigen escape from CAR T-cell therapy. *Cancer Discov*. 2018;8(10):1219-1226.
4. Brentjens RJ, Riviere I, Park JH, et al. Safety and persistence of adoptively transferred autologous CD19-targeted T cells in patients with relapsed or chemotherapy refractory B-cell leukemias. *Blood*. 2011;118(18):4817-4828.
5. Kochenderfer JN, Dudley ME, Feldman SA, et al. B-cell depletion and remissions of malignancy along with cytokine-associated toxicity in a clinical trial of anti-CD19 chimeric-antigen-receptor-transduced T cells. *Blood*. 2012;119(12):2709-2720.
6. Chiarini F, Lonetti A, Evangelisti C, et al. Advances in understanding the acute lymphoblastic leukemia bone marrow microenvironment: from biology to therapeutic targeting. *Biochim Biophys Acta*. 2016;1863(3):449-463.
7. Duarte D, Hawkins ED, Lo Celso C. The interplay of leukemia cells and the bone marrow microenvironment. *Blood*. 2018;131(14):1507-1511.
8. Tabe Y, Konopleva M. Advances in understanding the leukaemia microenvironment. *Br J Haematol*. 2014;164(6):767-778.
9. Meads MB, Hazlehurst LA, Dalton WS. The bone marrow microenvironment as a tumor sanctuary and contributor to drug resistance. *Clin Cancer Res*. 2008;14(9):2519-2526.
10. Alvarez P, Carrillo E, Velez C, et al. Regulatory systems in bone marrow for hematopoietic stem/progenitor cells mobilization and homing. *Biomed Res Int*. 2013;2013:312656.
11. Jin H, Aiyer A, Su J, et al. A homing mechanism for bone marrow-derived progenitor cell recruitment to the neovasculature. *J Clin Invest*. 2006;116(3):652-662.
12. Sackstein R, Schatton T, Barthel SR. T-lymphocyte homing: an underappreciated yet critical hurdle for successful cancer immunotherapy. *Lab Invest*. 2017;97(6):669-697.
13. Sarkar AK, Rostand KS, Jain RK, Matta KL, Esko JD. Fucosylation of disaccharide precursors of sialyl LewisX inhibit selectin-mediated cell adhesion. *J Biol Chem*. 1997;272(41):25608-25616.
14. Merzaban JS, Burdick MM, Gadhoum SZ, et al. Analysis of glycoprotein E-selectin ligands on human and mouse marrow cells enriched for hematopoietic stem/progenitor cells. *Blood*. 2011;118(7):1774-1783.
15. Robinson SN, Thomas MW, Simmons PJ, et al. Fucosylation with fucosyltransferase VI or fucosyltransferase VII improves cord blood engraftment. *Cytotherapy*. 2014;16(1):84-89.

16. Sackstein R. Fulfilling Koch's postulates in glycoscience: hCELL, GPS and translational glycobiology. *Glycobiology*. 2016;26(6):560-570.
17. Silva M, Fung RKF, Donnelly CB, Videira PA, Sackstein R. Cell-specific variation in E-selectin ligand expression among human peripheral blood mononuclear cells: implications for immunosurveillance and pathobiology. *J Immunol*. 2017;198(9):3576-3587.
18. Parmar S, Liu X, Najjar A, et al. Ex vivo fucosylation of third-party human regulatory T cells enhances anti-graft-versus-host disease potency in vivo. *Blood*. 2015;125(9):1502-1506.
19. Sackstein R, Merzaban JS, Cain DW, et al. Ex vivo glycan engineering of CD44 programs human multipotent mesenchymal stromal cell trafficking to bone. *Nat Med*. 2008;14(2):181-187.
20. Wagers AJ, Stoolman LM, Craig R, Knibbs RN, Kansas GS. An sLex-deficient variant of HL60 cells exhibits high levels of adhesion to vascular selectins: further evidence that HECA-452 and CSLEX1 monoclonal antibody epitopes are not essential for high avidity binding to vascular selectins. *J Immunol*. 1998;160(10):5122-5129.
21. Haraldsen G, Kvale D, Lien B, Farstad IN, Brandtzaeg P. Cytokine-regulated expression of E- selectin, intercellular adhesion molecule-1 (ICAM-1), and vascular cell adhesion molecule-1 (VCAM-1) in human microvascular endothelial cells. *J Immunol*. 1996;156(7):2558-2565.
22. Scott DW, Patel RP. Endothelial heterogeneity and adhesion molecules *N*-glycosylation: implications in leukocyte trafficking in inflammation. *Glycobiology*. 2013;23(6):622-633.
23. Cheng J, Zhao L, Zhang Y, et al. Understanding the mechanisms of resistance to CAR T-cell therapy in malignancies. *Front Oncol*. 2019;9:1237.
24. Shah NN, Fry TJ. Mechanisms of resistance to CAR T cell therapy. *Nat Rev Clin Oncol*. 2019;16(6):372-385.
25. Benmebarek MR, Karches CH, Cadilha BL, Lesch S, Endres S, Kobold S. Killing mechanisms of chimeric antigen receptor (CAR) T cells. *Int J Mol Sci*. 2019;20(6).
26. Fuca G, Reppel L, Landoni E, Savoldo B, Dotti G. Enhancing chimeric antigen receptor T-cell efficacy in solid tumors. *Clin Cancer Res*. 2020.
27. Grant ML, Bollard CM. Cell therapies for hematological malignancies: don't forget non-gene-modified T cells. *Blood Rev*. 2018;32(3):203-224.
28. Majhail NS, Farnia SH, Carpenter PA, et al. Indications for autologous and allogeneic hematopoietic cell transplantation: guidelines from the American Society for blood and marrow transplantation. *Biol Blood Marrow Transplant*. 2015;21(11):1863-1869.
29. Ullah M, Liu DD, Thakor AS. Mesenchymal stromal cell homing: mechanisms and strategies for improvement. *iScience*. 2019;15:421-438.
30. Godoy JAP, Paiva RMA, Souza AM, Kondo AT, Kutner JM, Okamoto OK. Clinical Translation of mesenchymal stromal cell therapy for graft versus host disease. *Front Cell Dev Biol*. 2019;7:255.
31. Dykstra B, Lee J, Mortensen LJ, et al. Glycoengineering of E-selectin ligands by intracellular versus extracellular fucosylation differentially affects osteotropism of human mesenchymal stem cells. *Stem Cells*. 2016;34(10):2501-2511.
32. Thankamony SP, Sackstein R. Enforced hematopoietic cell E- and L-selectin ligand (HCELL) expression primes transendothelial migration of human mesenchymal stem cells. *Proc Natl Acad Sci USA*. 2011;108(6):2258-2263.
33. Silva M, Videira PA, Sackstein R. E-Selectin ligands in the human mononuclear phagocyte system: implications for infection, inflammation, and immunotherapy. *Front Immunol*. 2017;8:1878.
34. Mondal N, Silva M, Castano AP, Maus MV, Sackstein R. Glycoengineering of chimeric antigen receptor (CAR) T-cells to enforce E-selectin binding. *J Biol Chem*. 2019;294(48):18465-18474.
35. Alatrash G, Qiao N, Zhang M, et al. Fucosylation enhances the efficacy of adoptively transferred antigen-specific cytotoxic T lymphocytes. *Clin Cancer Res*. 2019;25(8):2610-2620.
36. Castella M, Boronat A, Martin-Ibanez R, et al. Development of a novel anti-CD19 chimeric antigen receptor: a paradigm for an affordable CAR T-cell production at academic institutions. *Mol Ther Methods Clin Dev*. 2019;12:134-144.
37. Delgado J, Caballero-Banos M, Ortiz-Maldonado V, et al. Chimeric antigen receptor T cells targeting CD19 and ibrutinib for chronic lymphocytic leukemia. *Hemasphere*. 2019;3(2):e174.
38. Sanchez-Martinez D, Baroni ML, Gutierrez-Aguera F, et al. Fratricide-resistant CD1a-specific CAR T cells for the treatment of cortical T-cell acute lymphoblastic leukemia. *Blood*. 2019;133(21):2291-2304.
39. Recasens-Zorzo C, Cardesa-Salzmann T, Petazzi P, et al. Pharmacological modulation of CXCR4 cooperates with BET bromodomain inhibition in diffuse large B-cell lymphoma. *Haematologica*. 2019;104:778-788.
40. Jaffe EA, Nachman RL, Becker CG, Minick CR. Culture of human endothelial cells derived from umbilical veins. Identification by morphologic and immunologic criteria. *J Clin Invest*. 1973;52(11):2745-2756.

SUPPORTING INFORMATION

Additional supporting information may be found online in the Supporting Information section at the end of the article.

How to cite this article: Sánchez-Martínez D, Gutiérrez-Agüera F, Romecin P, et al. Enforced sialyl-Lewis-X (sLeX) display in E-selectin ligands by exofucosylation is dispensable for CD19-CAR T-cell activity and bone marrow homing. *Clin Transl Med*. 2021;11:e280. https://doi.org/10.1002/ctm2.280